

National Academy of Sciences of Ukraine
Institute of Physics NAS of Ukraine
Taras Shevchenko National University of Kyiv
Odesa I. I. Mechnikov National University
Junior Academy of Sciences of Ukraine
Ukrainian Physical Society

*In commemoration of 85th birthday
of Professor Galyna Puchkovska*

SPECTROSCOPY OF MOLECULES AND CRYSTALS

Book of Abstracts
of XXIV Galyna Puchkovska International School-
Seminar

Dedicated to 90th anniversary of the Institute of Physics of
the National Academy of Sciences of Ukraine

August 25-30, 2019
Odesa, Ukraine

The Book of Abstracts was approved for publication by the Scientific Council of the Institute of Physics of the National Academy of Sciences of Ukraine (Protocol No. 4 of 18.04.2019)

The Book contains abstracts of reports presented at XXIVth Galyna Puchkovska International School-Seminar “Spectroscopy of Molecules and Crystals” (25-30 August, 2019, Odesa, Ukraine). The abstracts cover recent advances in theoretical and experimental spectroscopy of crystalline and amorphous solids, liquid crystals, biological objects and polymers, nanosystems, thin films, surface and intermolecular interactions. Non-linear optical phenomena, computer simulation, as well as state-of-the-art spectroscopic instrumentation and methods are included. Abstracts are published as received from the authors.

УДК 531:535 (063)

В збірнику представлені тези доповідей XXIV Міжнародної Школи-семінару імені Галини Пучковської “Спектроскопія молекул і кристалів” (25-30 серпня 2019 р., м. Одеса, Україна). В тезах викладено нові результати досліджень з основних напрямків сучасної теоретичної і експериментальної спектроскопії неметалічних кристалів, аморфних речовин, рідких кристалів, полімерів і біологічних об’єктів, нанорозмірних систем, тонких плівок, поверхні і міжмолекулярної взаємодії. Також розглянуто такі напрямки як нелінійно-оптичні явища, комп’ютерне моделювання, нові прилади та методи спектральних досліджень.

Тези надруковано в авторському поданні.

COMMITTEES

HONORARY PRESIDENT

Henryk Ratajczak (Polish Academy of Sciences, Wroclaw)

ORGANIZING COMMITTEE

CO-CHAIRS

L. Yatsenko (Institute of Physics, NAS of Ukraine)

V. Pogorelov (Taras Shevchenko National University of Kyiv)

SECRETARY of XXIV ISSMC

Natalia Berezovska (Ukraine)

INTERNATIONAL SCIENTIFIC COMMITTEE

O. Adiguzel (Turkey), V. Balevicius (Lithuania), M. Bondar (Ukraine), L. Bulavin (Ukraine), G. Chikvaidze (Latvia), N. Davydova (Ukraine), I. Dmitruk (Ukraine), D. Dorohoi (Romania), G. Dovbeshko (Ukraine), M. Drozd (Poland), A. Jumabaev (Uzbekistan), A. Naumenko (Ukraine), A. Negriyko (Ukraine), G. Pitsevich (Belarus), M. Strzhemechny (Ukraine), A. Verbitsky (Ukraine), V. Yashchuk (Ukraine)

LOCAL ORGANIZING COMMITTEE

CO-CHAIRS

Iryna Doroshenko

Tamara Bezrodna

Yaroslav Lepikh

*T. Gavrilko, I. Gnatyuk, V. Gotsulsky, O. Doroshenko,
V. Kravchenko, Yu. Kurioz, O. Kerita, T. Mykytyuk,
V. Nesprava, V. Reznichenko, V. Shymanovska, A. Vasylieva*

CONTENTS

Foreword	7
1. LECTURES	9
2. MOLECULES	25
3. CRYSTALS	55
4. LIQUID CRYSTALS	91
5. BIOMOLECULES AND POLYMERS	101
6. NANOOBJECTS	127
7. SURFACES AND FILMS	169
8. THEORY	187
9. METHODS AND APPLICATIONS	199
10. AUTHOR INDEX	217

Dear Participants
of XXIV Galyna Puchkovska International School-Seminar
“Spectroscopy of Molecules and Crystals”

dedicated to 90th anniversary of the Institute of Physics of
the National Academy of Sciences of Ukraine

The Institute of Physics of the National Academy of Sciences of Ukraine had celebrated its 90th anniversary on January 22, 2019. The Institute was founded in 1929 and was headed by his first director, academician Oleksandr G. Goldman. Nowadays, the Institute is a world known academic organization in Ukraine. Five other independent research institutes of the National Academy of Sciences of Ukraine have emerged from the Institute of Physics over the years, namely: the Institute of Metal Physics (1945), the Institute of Semiconductor Physics (1960), the Institute of Theoretical Physics (1966), the Institute for Nuclear Research (1970), and the Institute of Applied Optics (1994).

First of all, our Institute is widely known in the world for its five scientific discoveries:

- cold electron emission from an island metal film under the passage of electric current (P.G. Borziak, O.G. Sarbei, R.D. Fedorovich);
- multiplex splitting of nondegenerated molecular terms in crystals (O.S. Davydov);
- multi-valued anisotropy of electrical conductivity of semiconductors in strong electric fields (O.G. Sarbei, Z.S. Gribnikov, V.V. Mitin, M. Asche, K. Helmar);
- additional light waves (Pekar waves) propagation in crystals (S.I. Pekar);
- combined resonance in crystals (E.Y. Rashba).

The Institute of Physics is proud not only of these discoveries, but also by its well-known scientific schools in the fields of optics and spectroscopy of nonmetallic crystals, nonlinear optics and laser physics, physical electronics, and solid state theory.

For all 90 years of its history, the Institute of Physics has become a leading scientific organization in the field of physical research in Ukraine. Among the most important achievements of the Institute it is worth mentioning the following:

- for the first time, academician V.Ye. Lashkaryov discovered and investigated the *p-n* transition in semiconductors, the primary structure that underlies the work of most semiconductor devices;

- for the first time, the principle of direct transformation of thermal energy into electric at thermoelectric radiation was discovered;
- for the first time, the term "polaron" was introduced, which is now widely used in the scientific world;
- the Institute took an active part in the Soviet Nuclear Project, namely in the research work focused on creation of a gas centrifuge for the efficient separation of uranium isotopes. It happened that the staff of the Institute directly participated in the development of one of the first models of gas centrifuge. Not all the facts linking our Institute with the Soviet Nuclear Project are made public so far, but we highly value the outstanding role of academician O.I. Leipunsky in the history of the Institute, who was at the beginning of this project.

Known for its unique versatility, the Institute of Physics continues active scientific activities with a wide involvement of international scientific organizations and young scientists aiming to multiply its great advances for the next decade.

Being organized by the Institute of Physics in 1973 as regular biennial international scientific meeting, Galyna Puchkovska International School-Seminar "Spectroscopy of Molecules and Crystals" turned into one of the most known in Ukraine. Every time, it brings together about a two hundred of famous scientists from different countries – Ukraine, Poland, Lithuania, USA, Germany, Spain, Sweden, Romania, Belarus, Uzbekistan, Turkey, etc. The wide scope of the School-Seminar covers all fields of spectroscopy including its theoretical aspects, molecular dynamics and molecular interactions, spectroscopy of molecular crystals, semiconductors, nanostructured systems, polymers and biological systems, as well as applied and computational methods. The organization of such conferences is of great importance for scientific community since it gives an opportunity to Ukrainian and foreign scientists from different fields of research to discuss various aspects of spectroscopy and to enter into new common research projects.

I hope that XXIV ISSSMC will help you to join the efforts for strengthening international scientific cooperation and for the development of new effective technologies for the benefit of our rapidly changing world.

Wishing you a successful work at the conference,

On behalf of the International Scientific Committee

Mykhailo Bondar

Corresponding Member of NASU

Director of the Institute of Physics NASU

1

Lectures

Structure and Stability of Gas Adsorption Complexes in Porous Solids as Studied by IR Spectroscopy – An Overview of Recent Developments

C.O. Arean*

Department of Chemistry, University of the Balearic Islands, Palma, Spain

**Corresponding author: co.arean@uib.es*

Gas adsorption (physisorption) in porous solids, which will be typified by zeolites and metal-organic frameworks, is currently being used in such industrial processes as oxygen and nitrogen separation from air, sweetening of natural gas and purification of hydrogen produced from steam reforming of hydrocarbons, to name only a few examples. Other (prospective) applications include indoor air purification (in submarines and crewed spacecraft) and the use of gas adsorbents for alternative (hydrogen or methane) fuel delivery in the transportation sector. Frequently, the gas adsorbing units are operated in a transient mode, which involves alternating gas adsorption-desorption cycles referred to as temperature swing (TSA) or pressure swing (PSA) adsorption, depending on the strategy being used for regenerating the porous adsorbent. Whichever the case, improvement of the adsorbent should be aimed at increasing (differential) gas adsorption capacity while keeping the gas-solid interaction energy small enough to curb the cost of adsorbent regeneration. To that endeavour, precise knowledge of the structure and stability of the gas adsorption complex is of paramount importance, and that is also the case when considering adsorbents for gas storage and delivery.

For such a purpose, classical infrared spectroscopy can give valuable structural information, derived from analysis of the wavenumber shifts undergone by meaningful vibrational modes of the adsorbed molecule, and from the (relative) intensity of the corresponding IR absorption bands; but determination of the gas-solid interaction energy is out of reach unless other complementary technique is also used. Nevertheless, implementation of the variable-temperature IR spectroscopic method [1,2] can give direct access to both, structural characterization and (simultaneously) determination of the enthalpy change (ΔH^0) involved in the gas adsorption process. Recent developments in this field will be highlighted and discussed in the context of practical application.

[1]. E. Garrone, C.O. Arean, Chem. Soc. Rev. 2005, 34, 846.

[2]. C.O. Arean, Ukr. J. Phys. 2018, 63, 538.

New Iridium(III) Metal-Organic Complexes in Solutions: Linear Photophysics and Femtosecond Nonlinear Optical Spectroscopy

M.V. Bondar^{1*}, S. Tofighi², P. Zhao², R.M. O'Donnell³, J. Shi³,
P.Y. Zavalij⁴, D.J. Hagan², E.W. Van Stryland²

¹ Institute of Physics, Prospect Nauki, 46, Kyiv-28, 03028, Ukraine

² CREOL, College of Optics and Photonics, University of Central Florida, Orlando, FL 32816, USA

³ US Army Research Laboratory, Adelphi, Maryland 20783, USA

⁴ Department of Chemistry and Biochemistry, University of Maryland, College Park, Maryland 20742, USA

**Corresponding author: mike_bondar@iop.kiev.ua*

The linear photophysical properties, ultrafast relaxation processes in the excited electronic state, and two-photon absorption (2PA) spectra of new metal-organic Ir(III) complexes are reported. The steady-state and time-resolved spectral properties of these new metal-organic compounds revealed the electronic nature of the absorption bands, and their photoluminescence emission shows both fluorescence and phosphorescence processes occurring simultaneously in liquid solution at room temperature. This unusual behaviour was explained by a dual-minimum potential surface of the excited electronic state resulting in two independent fluorescence and phosphorescence emission channels. The degenerate 2PA spectra were obtained by open aperture Z-scans under femtosecond excitation, and maxima values of 2PA cross sections up to ~350 GM were shown. The processes of ultrafast relaxation in the metal-organic structures were investigated by femtosecond transient absorption pump-probe spectroscopy, and the characteristic times for triplet formation were determined to be in the range 0.5-2 ps in a nonpolar medium. Potential applications of the linear photophysical and nonlinear optical properties of these newly synthesized Ir(III) complexes, along with the dual-minimum potential surface of the excited electronic states were analysed.

Photophysics and Spectroscopy Modulated by Excitation Energy in Condensed Media

A.P. Demchenko^{1,2}

¹ Palladin Institute of Biochemistry, NASU, Kyiv, Ukraine

² Yuri Fedkovych National University, Chernivtsi, Ukraine

**Corresponding author: aledem@ukr.net*

Common measurements of fluorescence emission involve recording the signal averaged over population of excited emitters. In contrast, spectroscopy of single molecules uses the advancements of microscopy to collect the signal from single emitter via many excitation-emission steps. Meantime, in condensed dielectric media there is a possibility to provide selection by the energy of excitation light of sub-population of emitters, for which the interaction energy with the environment differs from the mean value. This possibility appears due to inhomogeneous broadening of spectra and can be realized for such photoselection when the molecular dynamics averaging selected and non-selected states is slower or comparable in rate to the fluorescence lifetime. The measurements in time domain and applications of dynamic fluorescence quenchers, variations of temperature and pressure provide many possibilities for these observations. It was found that the photoselected species demonstrate quite different behavior from that of mean of population. The first observation of Gregorio Weber on the failure of Förster excitation energy transfer in frozen concentrated dye solutions [1] started the sequence of Red-Edge effects [2, 3]. Forming a new vision of structural disorder and molecular dynamics in condensed media, these effects were consistently explained based on a new paradigm that accounts for statistical distribution of fluorescence emitters on their interaction energy with the environment leading to static or dynamic inhomogeneous broadening of spectra. The present author has discovered the Red-Edge effects in intramolecular electron transfer and proton transfer reactions [4] and suggested to use their recording for studying the dynamics in condensed media, including protein molecules and biological membranes. Meantime, many ideas on observation and application of these effects remain unrealized. They will be discussed.

- [1]. G. Weber. Fluorescence-polarization spectrum and electronic-energy transfer in tyrosine, tryptophan and related compounds // Biochem J. – 1960. – V. 75. – N. 2. – p. 335.
- [2]. A.P. Demchenko. The Red-Edge effects: 30 years of exploration // Luminescence. – 2002. – V. 17. – N. 1. – p. 19-42.
- [3]. A.P. Demchenko. Site-selective Red-Edge effects // Methods in Enzymology. – 2008. – V. 450. – p. 59-78.
- [4]. A.P. Demchenko, A.I. Sytnik. Site-selectivity in excited-state reactions in solutions // J. Phys. Chem. – 1991. – V. 95. N. 25. – p. 10518-10524.

Do the 2D Graphene Type Nanoparticles Destroy Amyloid Fibrils Formation in Living Systems?

G.I. Dovbeshko^{*}, I.O. Polovyi , O.P. Gnatyuk

Institute of Physics, Prospect Nauki, 46, Kyiv-28, 03028, Ukraine

^{*}*Corresponding author: martinelli@gmail.com*

Last years an application of 2D graphene types nanoparticles for medical goals is intensively discussed [1-2]. Here we review our experimental and literature data of last years on usage of 2D WS₂, MoS₂, graphene and carbon nanotubes as a possible inductor or inhibitor of amyloid fibrils. Amyloid fibrils are known as highly ordered non-covalent protein aggregates formed in tissues of living organisms which correlate with various pathologies: oncology, Alzheimer's and Parkinson's diseases, other neurodegenerative disorders, neuropathic amyloidosis, etc. [1-4]. Clinical symptoms usually do not appear until the last stages of these diseases, which most often occur in middle or old age. More than 20 types of proteins can form amyloids *in vivo*, which are localized in the extracellular as well as intracellular space. The formation mechanism study of fibrils and clarification of the relationship between the fibrils appearance and the disease occurrence, as well as the development of prevention methods are an important tasks. Amyloid fibrils are formed as result of irreversible conformational transitions characterized by an increased amount of antiparallel β -sheets under the influence of external conditions: temperature, pH, component concentrations etc. [2,4]. Hen egg white lysozyme (HEWL) was used as model for amyloid formation. For characterization of amyloids we used FTIR spectroscopy, confocal and AFM microscopy, luminescence methods. The results obtained showed that the same type of 2D nanoparticles are able to partially inhibit amyloid fibril formation, do not influence the amyloid aggregation, and increase fibril aggregation for different protocols for modeling process.

The work was supported by projects: HORIZON 2020 project "Asymmetry of biological membrane: theoretical, experimental and applied aspects" (690853-assymcurv-H2020-MSCA-RISE-2015/H2020-MSCA-RISE-2015); NATO 98 5291, Ukrainian project "Development of 2D materials and "smart" sensors for medical and biological purposes" 11/1 2018; Joint Polish-Ukrainian Projects (2018-2020).

- [1]. Xie L., Lin D., Luo Y, Li H., Yang Xi, and Wei G. Effects of Hydroxylated Carbon Nanotubes on the Aggregation of A β 16–22 Peptides: A Combined Simulation and Experimental Study // Biophysical Journal. — 2014. — V. 107. — p. 1930 – 1938.
- [2]. Olenchuk M.V., Gnatyuk O.P., Dovbeshko G.I., Polovyi I.O., Karakhim S.O. Do carbon nanotubes inhibit or cause amyloid fibrils formation? // Biophysical Bulletin. — 2019. — V. 41. — p. 49 – 60.
- [3]. Du S., Wang Q., Yang X., Wang K., Liu L., Li Q., Li Z. Acceleration of Hen Egg White Lysozyme Amyloid Fibrillation by Single- or Few-Layer Molybdenum Disulfide Nanosheets. // Journal of Nanoscience and Nanotechnology. — 2017. — V. 17. – N. 5. – p. 2892 – 2898.
- [4]. Li M., Zhao A., Dong K., Li W, Ren J, and Qu X., Chemically Exfoliated WS₂ nanosheets Can Efficiently Inhibit Amyloid β -Peptide Aggregation and Use for Photothermal Treatment of Alzheimer's Disease // Nano Research. — 2015. — V. 8. – p. 3216 – 3227.

Photoluminescent and Electroluminescent Properties of Organic Donor-Acceptor Molecular Materials

J.V. Grazulevicius^{1*}, G. Grybauskaite-Kaminskiene¹, N. Kukhta¹,
R. Pashazadeh¹, E. Skuodis¹, A. Tomkeviciene¹, D. Volyniuk¹,
J. Simokaitiene¹, K. Ivaniuk², P. Stakhira², R. Keruckiene¹, J. Keruckas¹

¹ Department of Polymer Chemistry and Technology, Kaunas University of Technology, Kaunas, Lithuania

² Lviv Polytechnic National University, S. Bandera 12, 79013 Lviv, Ukraine

**Corresponding author: juozas.grazulevicius@ktu.lt*

Luminescent properties of molecular materials containing donor and acceptor moieties recently synthesized at the laboratories of the presenting author will be reported.

Derivative of 3-(trifluoromethyl)benzonitrile and 3,3'-bicarbazole was found to exhibit both TADF and exciplex-forming properties [1]. Warm-white OLED based on this material showed external quantum efficiency (EQE) of ca. 20%.

The derivative of acridan and dicyanobenzene was found to be efficient TADF-emitter exhibiting both thermally activated delayed fluorescence and aggregation induced emission enhancement. Green OLED fabricated using this emitter exhibited maximum current, power efficiency and EQE of 68 cd/m², 62 lm/W and 22.5 %, respectively [2].

A series of carbazole-quinoxaline-carbazole derivatives exhibiting TADF and mechanochromic luminescence properties were synthesized and studied. Green-blue to green-yellow TADF OLEDs fabricated by solution processing demonstrated EQE up to 10.9% and luminance of 16760 cd m⁻² [3].

By utilization of the derivatives cyanophenyl and di-tert-butylcarbazolyl substituted triphenylbenzene with the different substitution pattern as host and guest of the emissive layer, deep-blue OLED based on triplet-triplet annihilation with EQE of 14.1% were fabricated [4].

This research was funded by the European Social Fund according to the activity 'Improvement of researchers' qualification by implementing world-class R&D projects' of Measure No. 09.3.3-LMT-K-712.

[1]. G. Grybauskaite-Kaminskiene et al. J. Mater. Chem. C, 2018, 6, 1543.

[2]. E. Skuodis, Org. Electron., 2018, 63, 29.

[3]. R. Pashazadeh, J. Phys. Chem. Lett., 2018, 9, 1172.

[4]. Kukhta N. et al. J. Phys. Chem. Lett., 2017, 8, 6199.

Optoelectronic Properties of Hybrid Organic-Inorganic Perovskite Films

A. Kadashchuk^{1,2*}

¹ Photoactivity Department, Institute of Physics of NASU, Kyiv, Ukraine

² Large Area Electronics, IMEC, Leuven, Belgium

**Corresponding author: kadash@iop.kiev.ua*

Solution processed organometallic hybrid perovskites have emerged as a successful material for a range of optoelectronic devices, such as light emitting diodes (LEDs), lasers and photodetectors. These materials possess excellent optical and electronic properties such as the bandgap tunable through perovskite chemical composition, high charge-carrier mobility and long carrier diffusion length, lightweight and mechanical flexibility. Another merit lies in the processing from solutions using such methods as spin coating or inkjet printing at room temperature; these processes potentially allow for a low-cost and low-temperature device fabrication well compatible with flexible plastic substrates. Perovskite light emitting diodes (PeLEDs) have recently reached external quantum efficiencies (EQE) over 21%. The remarkable progress of these devices is mainly made via controlling the defect states responsible for non-radiative recombination. This resulted in a photoluminescence quantum efficiency (PLQE) >70% in perovskite thin films.

Further improvement of the efficiency and stability of hybrid perovskite-based devices requires a deeper understanding of their intrinsic photophysical properties and nature of defects. In particular, an accurate picture of the density of states associated to traps and energetic disorder in such films is important as these have a direct influence on charge-carrier mobility, lifetime, and diffusion length. In this work we report on temperature-dependent photoexcitation dynamics and charge carrier trapping studied in several novel hybrid perovskite materials depending on perovskite film quality. We found that perovskite chemical composition, annealing temperature and film crystallinity has a strong impact on the trap depth and trap concentration in films under investigations. We further demonstrate a clear correlation between optoelectronic device performance, crystallization dynamics in spin-coated perovskite films and trap densities in them. We also compare optoelectronic performance of 3D and 2D mixed-halide perovskite films and identify charge trapping centers in them. These results indicate that the charge trapping spectroscopy can provide valuable information about formation of crystal defects and the associated charge-carrier traps in hybrid perovskite semiconductors.

Bridging the Gap between Dispersed Nanoparticles and Low Solubility Dopants in Liquid Crystal Media

L.N. Lisetski

Institute for Scintillation Materials of NAS of Ukraine, Kharkiv, Ukraine

Corresponding author: lisetski@isma.kharkov.ua

Introduction of non-mesogenic dopants (NMD) into nematic and cholesteric liquid crystal (LC) matrices has long been known to modify their mesomorphic characteristics, as well as optical and electrophysical properties. From another side, in recent years dispersions of nanoparticles (NP) of different nature in LCs have become a base for creation of composite LC nanomaterials. These two classes of LC systems, though different in their physico-chemical nature (real solutions and colloidal dispersions, respectively), have certain similarities on the level of molecular models and mechanisms of affecting LC properties.

A review of literature data and analysis of recent results on LC+NP and LC+NMD systems obtained in our laboratory is presented. The NPs used include carbon nanotubes, exfoliated platelets of organomodified laponite, metal oxides etc. Several substances of biological origin were used as NMDs, including flavonoids (e.g., quercetin) and amino acids. The main techniques used were temperature-dependent optical transmission in the nematic and isotropic phases, as well as selective reflection spectra in the cholesteric phase. It was found that quercetin molecules could form nano-sized aggregates in LC media, with their behavior largely similar to laponite NPs.

In cholesteric matrices, both of steroid and non-steroid nature (induced cholesterics), selective reflection spectra at temperatures close to isotropic transition were found to be highly sensitive to both NMD of low solubility and NPs, which opens possibilities to used CLC systems as sensor materials.

The proposed models of supramolecular arrangement in the systems studied were in agreement with optical microphotographs and differential scanning calorimetry (DSC) data obtained in parallel experiments.

Scanning Tunneling Microscopy of Organic Monolayers on Atomically Flat Surfaces

A.A. Marchenko*

Institute of Physics, National Academy of Sciences of Ukraine, Kyiv, Ukraine

**Corresponding author: marchenko_alexandr@yahoo.com*

Highly ordered organic films deposited on the solid surface are the subject of intense experimental and theoretical researches. In this talk the results of systematic STM-investigations of self-assembled monolayers of different organic compounds (*n*-alkanes, organic acids, *n*-alkanethiols, liquid crystals, fullerenes and organosilanes) on atomically flat surfaces will be presented. The results were obtained using scanning tunneling microscope (“NT MDT” and “Molecular Imaging”) adapted to the liquid environment. The highly oriented pyrolytic graphite and reconstructed Au(111) surfaces were used as the substrates. The observed structures are discussed in terms of molecule-molecule and molecule-substrate interactions. The main attention will be focused on possible applications of obtained nanostructures for design of externally controlled interfaces, molecular matrixes for selective adsorption, electroluminescence devices and devices for nanotribology.

Pulsed Pumping Reveals Spectacular Perovskite Electroluminescence Dynamics

R. Gegevičius¹, M. Franckevičius¹, J. Chmeliov¹, W. Tress²,
A. Fakharuddin³, A. Kadashchuk⁴, V. Gulbinas^{1*}

¹ Department of Molecular Compound Physics, Center for Physical Sciences and Technology, Saulėtekio Avenue 3, LT-10257 Vilnius, Lithuania

² Laboratory of Photomolecular Science, ISIC, Swiss Federal Institute of Technology (EPFL), CH-1015 Lausanne, Switzerland

³ IMEC, Kapeldreef 75, 3001, Leuven, Belgium

⁴ Institute of Physics, National Academy of Sciences of Ukraine, Prospect Nauky 46, 03028 Kyiv, Ukraine

**Corresponding author: vidmantas.gulbinas@ftmc.lt*

Metal halide perovskites initially emerged as effective materials for solar cells. Currently, they are also attempted to use for other devices such as photodetectors, light emitting diodes, lasers. High performance of both photovoltaic and electroluminescent devices requires low non-radiative recombination losses. This requirement is obvious for electroluminescence devices. In case of solar cells, the nonradiative recombination limits the carrier lifetime and thus the open circuit voltage. Such losses in perovskites strongly depend on the carrier traps, which are also partly related to the mobile ions and vacancies, causing I-V hysteresis of solar cells and influencing the performance of other optoelectronic devices, such as photodetectors and LEDs. Consequently the electroluminescence efficiency gives no straightforward information about the perovskite quality, but depends in a complex way on many material and device parameters.

To gain deeper insight into the electroluminescence properties we have investigated electroluminescence time evolution in perovskite solar cells and LEDs under constant and pulsed voltage conditions. The electroluminescence revealed complex evolution dynamics strongly dependent on the electrical pulse duration and voltage, as well as on the pulse train application duration. We demonstrate the appearance of a high-intensity short electroluminescence peak (overshoot pulse) immediately after termination of the electrical pulse. We propose a model accounting for the spatial electron and hole distribution inside perovskite layer as well as accumulation of mobile ions explaining the complex electroluminescence dynamics both on fast (microseconds) and slow (seconds) time scales. The generation of a giant overshoot pulse suggests a simple way to achieve high-pulsed electroluminescence intensity with a low current density, which opens new prospects towards optical gain and implementation of electrically pumped lasers.

Optical Properties of ZnO: Bulk vs. Nano

G.Yu. Rudko

V.Ye. Lashkaryov Institute of Semiconductor Physics NAS of Ukraine, Kyiv, Ukraine

Corresponding author: g.yu.rudko@gmail.com

Acute interest in ZnO is caused by its potential to become a key technological material due to the perspectives for building ZnO-based transparent electronics and optoelectronics. ZnO is a direct band semiconductor with wide band gap (3.3 eV), thus it does not absorb light in the visible range and is suitable for the fabrication of transparent optoelectronic devices. ZnO is assumed to be a promising alternative to indium tin oxide (ITO), which, in view of upcoming indium shortage, puts the material into the focus of researchers' attention. Exciton binding energy in ZnO is extremely high; thus this solid is assumed to be a better candidate for UV light emitting devices than more convenient GaN because of lower generation thresholds and higher emission efficiency. Due to non-central symmetry of its lattice, ZnO is highly piezoelectric; therefore, it is also a good choice for building electromechanically coupled sensors and transducers. Among other characteristics the high thermal conductivity and radiation resistance, bio-safety and biocompatibility also attract a lot of interest. However, development of ZnO-based electronics is still impeded by poor p-type conductivity of ZnO. At present there are no reliable technological processes for wide production of highly conductive p-ZnO. Moreover, even n-type ZnO demonstrates lower carriers mobility and thermal conductivity than GaN. All the above advantages and challenges make ZnO one of the most intensively studied materials nowadays.

Low-dimensional ZnO, in turn, is a fantastic material because of huge variety of shapes ranging from usual quantum dots and rods to nano-flowers, nano-snowflakes and tetrapods. All these morphological forms of low-dimensional ZnO demonstrate various remarkable physical and chemical properties distinctive from the bulk analogue.

The present report reviews the attractive optical properties of bulk ZnO and their applications in comparison with the properties of nano-ZnO. All aspects, including absorption of light, luminescence and Raman scattering as well as applications in building LEDs and lasers are discussed. Special attention is paid to the original results on light-emitting properties of colloidal ZnO nanoparticles stabilized by polymers and to nanoparticles synthesized within the nano-pores of mesoporous silica matrices, the so-called molecular sieves. Due to different morphology, size and arrangement of pores the latter provide a possibility to obtain the ordered arrays of ZnO quantum dots with different ordering types, which can be interesting for building nanoparticles-based photonic crystals.

From Time-Resolved Measurements of Liquid Crystals, via Imaging of Biopolymer Blends and Light-Fiber Coupled Polymerization Monitoring to the Detection of Fraud by Handheld Instruments: A Journey through Non-Routine Applications of Vibrational Spectroscopy

H.W. Siesler

Department of Physical Chemistry/University of Duisburg-Essen, Essen, Germany

Corresponding author: hw.siesler@uni-due.de

The increasing demand for product quality improvement and production rationalization in the chemical, polymer, pharmaceutical, food, and agricultural industries has induced a significant renaissance of the vibrational spectroscopic techniques of Raman, mid-infrared (IR), and near-infrared (NIR) spectroscopy. Thus, these techniques have emerged over the last decade – in combination with imaging accessories, light-fiber optics, and chemometric evaluation procedures – as extremely powerful methods for industrial quality control, and process monitoring [1,2]. Specifically, the NIR wavelength gap between the visible and the IR region, which has over a long period been lying idle, has eventually also been filled with life and is now used according to its real potential [3].

However, the principal aim of this presentation are not discussions of the three techniques for routine quality control problems, but rather to demonstrate with the help of selected examples their exceptional potential for challenging research applications in material science. Thus, by using the step-scan technique the electric-field induced switching mechanism of liquid crystals can be studied by IR spectroscopy in the micro-second time-domain. With the help of focal-plane array detectors and fast scanning techniques detailed insights into the phase-separation behavior of biopolymer blends on the micro/nanometer scale can be achieved by IR and Raman imaging investigations. Light-fiber coupled Raman spectroscopy has provided important information on the styrene-butadiene-styrene triblock-polymerization and finally it will be demonstrated how the miniaturization of NIR spectrometers will revolutionize in the near future the every-day life of a new non-expert user community [4].

- [1]. H.W. Siesler. Vibrational Spectroscopy. In: Saleem Hashmi (ed.), Reference Module in Materials Science and Materials Engineering. Oxford: Elsevier; 2016. pp. 1-51.
- [2]. E. Grotheer, C. Vogel, O. Kolomiets, U. Hoffmann, M. Unger and H. W. Siesler. FT-IR and NIR Spectroscopic Imaging: Principles, Practical Aspects and Applications in Materials and Pharmaceutical Sciences. In: Infrared and Raman Spectroscopic Imaging, (R. Salzer and H. W. Siesler, eds.), 2nd ed., WILEY-VCH, Weinheim, Germany (2014).
- [3]. H.W. Siesler, Y. Ozaki, S. Kawata and H.M. Heise (eds.), Near-Infrared Spectroscopy, Wiley-VCH, Weinheim, Germany (2002).
- [4]. H. Yan and H.W. Siesler. Handheld Raman, Mid-Infrared and Near-Infrared Spectro-meters: State-of-the-Art Instrumentation and Useful Applications, Spectroscopy, 33 (11), 6-16 (2018).

Models and Mechanisms of Reversible Regulation of Photosynthetic Light Harvesting

L. Valkunas*

Molecular Compounds Physics Department, Center for Physical Sciences and Technology, Sauletekio Ave. 3, 10257 Vilnius, Lithuania and Institute of Chemical Physics, Vilnius university, Sauletekio Ave. 9-III, 10222 Vilnius, Lithuania

**Corresponding author: leonas.valkunasl@ff.vu.lt*

Photosynthesis is one of the most important processes performed by living beings that sustain life on our planet. At low light, it exhibits an unprecedented quantum efficiency: over 90% of the absorbed photons reach reaction center and initiate charge separation. However, at strong sunlight the photosynthetic light-harvesting antenna switches into a photoprotective mode, thus avoiding over-excitation and the concomitant photodamage. On a molecular level, safe dissipation of the excess absorbed light energy occurs via non-photochemical quenching (NPQ)—the feedback mechanism that reversibly activates within seconds or minutes in response to the naturally occurring illumination variations. First experimentally observed as chlorophyll (Chl) fluorescence (FL) quenching in isolated thylakoids, NPQ was later detected in the intact isolated chloroplasts and leaves. However, complex heterogeneous organisation and multiple processes, simultaneously occurring within the thylakoid membrane, have been strongly impeding the directional study of the natural NPQ under *in vivo* conditions. Instead, artificially produced photosynthetic antenna, like aggregates of purified solubilised major light-harvesting complexes (LHCII) [1] or natural membranes-mimicking liposomes with the embedded LHCII [2], have been widely and deeply surveyed. Nevertheless, it has never been shown directly that FL quenching observed in these artificial systems underlies natural NPQ in thylakoid membranes. Here we present high-resolution time-resolved FL measurements on the dark and light-adapted thylakoid membranes, performed over a broad temperature range. We show that their spectral response perfectly matches that observed in our recent study on the artificial LHCII aggregates [1], thus demonstrating for the first time that the latter *in vitro* system preserves all the properties of natural photoprotection. The model describing the mechanism of NPQ based on these fluorescence data and on the single molecule spectroscopy measurements of liposomes [2] and mutants of the light-harvesting complexes [3].

- [1]. J. Chmeliov, A. Gelzinis, E. Songaila, R. Augulis, C. D. P. Duffy, A. V. Ruban, L. Valkunas, *Nature Plants* 2, 16045 (2016).
- [2]. M. Tutkus, P. Akhtar, J. Chmeliov, F. Görföl, G. Trinkunas, P. H. Lambrev, L. Valkunas, *Langmuir* 34, 14410-14418 (2018).
- [3]. M. Tutkus, J. Chmeliov, D. Rutkauskas, A.V. Ruban, L. Valkunas, *J. Phys. Chem. Lett.* 8, 5898-5906 (2017).

Peculiarities of Electronic and Vibronic Excitations Transfer in Organic Media and Hybrid Nanosystems. Some Fundamental and Applied Problems

V.M. Yashchuk^{*1}, M.Yu. Losytskyy¹, Yu.P. Piryatinski²,
I.V. Lebedyeva³, O.M. Navozenko¹

¹ Faculty of Physics, Taras Shevchenko National University of Kyiv, Kyiv, Ukraine

² Institute of Physics, NAS of Ukraine, Kyiv, Ukraine

³ Faculty of Mechanics and Mathematics, Taras Shevchenko National University of Kyiv, Kyiv, Ukraine

**Corresponding author: yashchukvaleriy@gmail.com*

The results of investigations of electronic excitation energy transfer in organic media and hybrid nanosystems were reviewed, examined and analyzed. Particularly, the mechanisms of elementary jumps of singlet and triplet excitons between π -electron-containing molecules or groups are regarded. The traditional point of view is that elementary jumps of singlet excitations are realized due to Forster mechanism, while triplet-triplet jumps occur by Dexter mechanism. It was shown that such traditional scheme is not correct in general case. The results of experimental evaluation of elementary electronic excitations jump values were examined and discussed.

The data that prove the fact of vibronic excitations transfer along vinyl aromatic macromolecules were also regarded and analyzed, as well as approaches to evaluations of the value of critical length of vibronic excitons jump.

The applied problems connected with presented above topics were also regarded. Particularly, the pathways of excitation energy transfer were studied in hybrid nanosystems developed as sensitizers for X-ray photodynamic therapy. Such nanosystems contained polystyrene nanoparticles with encapsulated diphenyloxazole and attached photosensitizer chlorin e_6 . Excitation energy transfer from polystyrene to diphenyloxazole and further to chlorin e_6 was shown. Another nanosystem studied was composed of cerium fluoride nanoparticles doped with terbium ions and attached photosensitizer chlorin e_6 . Both direct (from cerium to chlorin e_6) and terbium-mediated pathways of excitation energy transfer were demonstrated. Efficiency of excitation energy transfer were estimated and peculiarities of this process for the studied nanosystems were discussed.

2

Molecules

Surprising Properties of Alcohols from the Methanol Homologous Series and Thermodynamic Properties of Alcohols and Water on Their Coexistence Curves

V.E. Chechko^{1,2}, V.Ya. Gotsulskiy^{*2,3}, N.P. Malomuzh²

¹ Scientific-Research Institute of Physics, Odessa I.I. Mechnikov National University, Ukraine

² Department of Theoretical Physics, Odessa I.I. Mechnikov National University, Odessa, Ukraine

³ Department of General Physics and Physics of Thermoenergetical and Chemical Processes, Odessa I. I. Mechnikov National University, Odessa, Ukraine

**Corresponding author: vygot@onu.edu.ua*

In this paper, nontrivial properties of thermodynamic quantities for normal alcohols from the methanol series, such as densities, the critical and triple point temperatures, as well as their ratios, optical [1] and dielectric polarizabilities are analyzed. More specifically, the nature of mutual relationships between them at the same temperatures for alcohols with different sequence numbers in the methanol series is studied. It is shown that the non-monotonic character of the temperature dependence of the alcohol densities is violated not ethanol, as it seems at the first view, but methanol. Similarly the critical temperature of the latter removes from the quasi-linear dependence formed by the critical temperatures of alcohols with higher sequence number. Simple linear dependences for electronic and effective static polarizabilities of alcohol molecules are established. The transverse and longitudinal components of the polarizability tensor for alcohol molecules are found. It is proved that the dipole moments of the closest neighbors in the alcohols are anticorrelated, that is testifies, that they tend to establish in opposite directions.

The thermodynamic properties of water and alcohols of the methanol series on their coexistence curves (CCs) are analyzed [2]. The main attention is focused on the behavior of their specific volumes per molecule and the evaporation heats. We show that the special normalization of these quantities and standard normalization of temperature leads to the similarity of their temperature dependencies on their CCs. And what is more, they are similar to the temperature dependencies for argon. It means that the behavior of the specific volume and the evaporation heat are determined by the averaged interparticle potentials which have the argon-like structure. Small deviations from argon-like dependence are carefully studied. We suppose that these small deviations are caused by the weak angular correlations created by H-bond interactions and should be connected with the main characteristics of H-bond network that is the averaged number of H-bonds per molecule. A method for determination of the last is developed.

- [1]. V. E. Chechko, V. Ya Gotsulskiy, N .P. Malomuzh. The Role of Two-Particle Effects in the Behavior of Refraction of Single-Component Liquids and Two-Component Solutions/ Optics and Spectroscopy. – 2016. – V. 120. – p. 615 – 621.
- [2]. V. E. Chechko, V. Ya Gotsulskiy, N .P. Malomuzh. Surprising thermodynamic properties of alcohols and water on their coexistence curves//Journal of Molecular Liquids. - 2018 – V. 272.-p.590 – 596.

Study of Soft Vibrations and Splitting of Degenerate Vibrations in the Series of Substituted Aromatic Molecules

N.E. Kornienko*, O.N. Korniienko, Ya.K. Gorban

Taras Shevchenko National University of Kyiv, Kyiv, Ukraine

*Corresponding author: nikkorn@univ.kiev.ua

The special role of aromatic compounds is associated with their use as dyes, drugs, liquid crystals, solvents, and others. Cyclic molecules (CM), the basis of DNA, chlorophyll, blood gem, are also part of oil and coal. The report based on the results of quantum chemical calculations (QCC) for the family of substituted benzene and experimental vibrational spectra (VS) (IR + Raman) revealed soft molecular oscillations (SMO), resonant interactions of fundamental oscillations (RIFO) and for the first time studied spectral regularities splitting frequencies $\Delta\nu_E(\nu)$ of degenerate vibrations in C_6H_6 . QCC were carried out using the Gaussian 09 program, the B3LYP density functional and basis sets 6-31g (2df, p) and cc-pVDZ. The substitution rows of hydrogen atoms C_6H_5X , ($X = D, T, F, Cl, Br, OH, CN, CH_3, NH_2, COH, NO_2$) and o,m,p- $C_6H_4X_2$; as well as carbon atoms C_5YH_6 ($Y = {}^{13}C, {}^{14}C, Si, Ge$) and fragments $C-H$ C_5H_5Z ($Z = {}^{13}C, {}^{14}C, {}^{14}N, {}^{15}N, B, O, Si, P, S, Al, Ge$) were studied. For these series of molecules, it is important to lower the symmetry from D_{6h} in C_6H_6 to C_{2v} , D_{2h} or C_s . In this connection, all inactive vibrations of C_6H_6 , $A_{2g}(\nu_3)$, $B_{2g}(\nu_4, \nu_5)$, $B_{1u}(\nu_{12}, \nu_{13})$ and $B_{2u}(\nu_{14}, \nu_{15})$ become active in VS and splitting of 10 degenerate vibrations of the $E_{1,2g}$ и $E_{1,2u}$ types occur. To identify the vibrations, we used data on their activities in the IR and Raman spectra, the correspondence of the symmetry types of the vibrations with decreasing symmetry, and also the analysis of vibrational waveform. Found a special sensitivity of a series of “silent” vibrations even to isotope substitution $H \rightarrow D, T$ - in C_6H_5D and C_6H_5T , the frequency ν_{13} to decrease by 809 and 1142 cm^{-1} . The SMO ν_{13} , ν_{15} , ν_{12} , ν_4 and ν_{16B} frequencies in C_6H_5X molecule series, ($X = D, T, F, Cl, Br$) decrease by 1961, 922, 341, 253, and 246 cm^{-1} respectively. It is significant that the intensity of SMO in VS is anomalously strongly increased as a result of the redistribution of electron density, which explains the key role of CM in the existence of life, medicine and production. At proximity of SMO frequencies and more stable vibrations of ν_8 , ν_{19} , ν_9 and ν_{18} , RIFO appears. In the case of RIFO, in contrast to Fermi resonances, the intensities of both vibrations in VS increase and a significantly larger frequency detuning is permissible. Substituted molecules have been established for which maximum values of $\Delta\nu_E$ splitting are observed in the region of low, medium or high frequencies. SMO can be a model of soft modes in phase transitions in ferroelectrics.

Rigid-Non-Rigid Transition in the Hydrogen Trioxide Molecule Predicted by the Calculation of its Torsional Spectrum at the CCSD(T)/cc-pVQZ Level of Theory

G.A. Pitsevich*, A.E. Malevich, A.A. Ostyakov

Department of Physical Optics, Belarusian State University, Minsk, Belarus

*Corresponding author: pitsevich@bsu.by

The hydrogen trioxide molecule (HOOOH) is a very interesting object. The molecule can exist in the *trans*- and *cis*- conformations. The first one belongs to the C_2 point group symmetry, while the second one – to the C_s point group. Both conformers as well as transition state of the molecule are represented in Fig. 1.



Fig. 1. *Trans*- and *cis*-conformers (in the left and in the center) as well as transition state (in the right) of the hydrogen trioxide molecule.

In addition, the *trans*- and *cis*-conformers can exist in two equivalent configurations which can be obtained from represented in Fig. 1 by changing on opposite directions of the both hydroxyl groups. Although one might assume that both conformers of the molecule should live their own lives, calculations of the torsion spectra of the molecule clearly indicate that this is not the case. We were able to find that the $C_{2v}(M)$ molecular symmetry group joints all properties of the both conformers. Moreover, $C_{2v}(M)$ group allows us to classify the spatial and spin wave functions, as well as all the scalar and vector characteristics of the analyzed molecule. Besides these transformations of the torsional coordinates under $C_{2v}(M)$ symmetry elements were found too. 2D PES as well as 2D surfaces of the kinematic coefficients and dipole moment vector were calculated at the CCSD(T)/cc-pVQZ level of theory. Then 2D vibrational Schrödinger equation was obtained and solved using DVR method. The energy of the stationary torsional levels and torsional wave functions were found as well as tunneling frequencies for the *trans*- and *cis*- conformers. Torsional spectra of the both conformers were calculated at different temperatures. The complex dynamic of torsional vibrations was also analyzed too.

Conformational Behavior of Highly Flexible Molecules Isolated in Inert Gas Matrices: Case of Alanyl-Glycine Dipeptide

S.G. Stepanian^{*1}, A.Yu. Ivanov¹, L. Adamowicz²

¹ B. Verkin Institute for Low Temperature Physics and Engineering, National Academy of Sciences of Ukraine, Kharkiv, Ukraine

² Department of Chemistry and Biochemistry, University of Arizona, 85721 Tucson AZ, USA

**Corresponding author: stepanian@ilt.kharkov.ua*

Conformational structure of L-alanylglycine (L-AG) dipeptide and its deuterio analog (N,N,N,O-tetradeutero-L-AG) isolated in argon matrices was determined using the FTIR spectroscopy and quantum-mechanical calculations. The L-AG molecule is highly flexible due to the presence of six internal rotational degrees of freedom and thus may adopt the numerous conformations. To determine the most stable conformers it was necessary to identify all possible conformers and determine their relative energies. We used two different approaches to search for the L-AG conformers. The first approach was an exhaustive scanning of the potential energy surface of the molecule. The second approach was to generate a large number of random starting structures of the molecule, followed by full optimization of each structure. The starting values of each of the six dihedral angles for the initial geometry were chosen randomly in the range from 0° to 360°. Totally 4000 initial structures were generated and optimized at the B3LYP/aug-cc-pVDZ level of theory. Totally 183 L-AG conformers were located. They were reoptimized at the MP2/aug-cc-pVDZ level of theory and finally the relative Gibbs free energies of the conformers were calculated at the CCSD(T)/CBS level. Calculated IR spectra of the most stable conformers were used to analyze the experimental FTIR spectra of L-AG and deuterated L-AG isolated in argon matrixes. Analysis of the obtained data allowed us to determine the conformational composition of L-AG and estimate the population of conformers in matrix samples. The effect of UV irradiation on the population of conformers was also determined. A computer simulation of the most stable conformers embedded in an fcc argon crystal was also carried out using the M06-2X density functional. This allowed us to determine the effect of the matrix environment on the structure, relative stability, and IR spectral characteristics of the conformers.

This work was supported by the National Academy of Sciences of Ukraine (Grants No. 07-01-18/19 and 0117U002287).

Polymorphism and its Manifestation in the IR Spectra of 2-Phenol-o-Cresol

J. Baran¹, N.A. Davydova^{2*}, M. Drozd¹, V.Ya. Reznichenko²,
E.A. Ponezha³

¹ Institute of Low Temperature and Structure Research, PAS, Wrocław, Poland

² Institute of Physics, NASU, Kyiv, Ukraine

³ Institute for Theoretical Physics, NASU, Kyiv, Ukraine

*Corresponding author: davydova@iop.kiev.ua

Polymorphism, the ability of a compound to crystallize in different forms, is, no doubt, important phenomenon in solid state physics. However, equally important is the study of structure - property relationships in polymorphs.

The single-crystal structure of 2-phenol-o-cresol was reported in [1]. It is build up of hydrogen-bonded tetramers of molecules and is presented in the

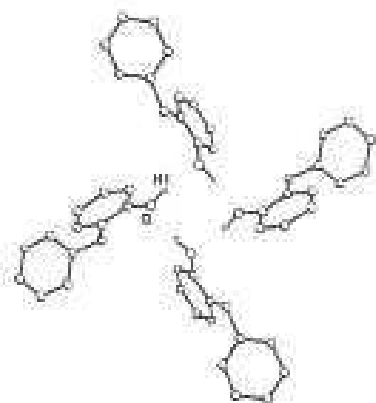


figure. Here we will monitor the hydrogen-oxygen (OH) stretch vibrations in the wide temperature range of the IR transmittance spectrum. IR spectra of 2-phenol-o-cresol as a liquid film between *KBr* plates were recorded on a FTIR spectrometer in the 400–4000 cm^{-1} range. We have shown that 2-phenol-o-cresol has two metastable phases: α , which melts at 290.2 K, and β , which melts at 296.7 K. The first time we have received the IR spectra of

the metastable polymorphs α and β . The metastable polymorph β was obtained by transforming the metastable phase α at 291 K. Based on a comparison of the obtained IR spectra of 2-phenol-o-cresol with those obtained previously for 2-biphenylmethanol [2, 3] we made the assumption that the structure of the metastable polymorphs consists of hydrogen-bonded chains of 2-phenol-o-cresol molecules.

[1]. J.C. Bryan, L.H. Delmau, J.B. Nicholas, L.M. Rogers, R.D. Rogers, B.A. Moyer // Structural Chemistry. – 1999. – V. 10. – p. 187-203.

[2]. L.M. Babkov, J. Baran, N.A. Davydova, K.E. Uspenskiy // J. Mol. Struct. – 2006. – V. 792-793. – p. 68.

[3]. L.M. Babkov, N.A. Davydova, K.E. Uspenskiy // Journal of Structural Chemistry – 2008. – V. 49. – p. 421.

The Excited Dipole Methods of Some Azo-Benzene Molecules Estimated by a Variational Method

D.O. Dorohoi^{*1}, A.C. Morosanu¹, D. Babusca¹, C. Cheptea²

¹Alexandru Ioan Cuza University of Iasi, Faculty of Physics, Iasi, Romania

²Grigore T. Popa University of Medicine and Pharmacy of Iasi, Department of Biomedical Sciences, Iasi, Romania

**Corresponding author: danadorohoi@yahoo.com*

There are some methods for estimating the excited state dipole moments of the spectrally active molecules. A part of them use the solvent influence on both emission and absorption spectra and allow to estimate the dipole moments in the electronic states responsible for the electronic bands appearance. They are applicable for dilute solutions (in which the specific interactions are neglectable), but are insufficient for estimating the angle between the dipole moments in the electronic states of transitions. In order to determine three parameters: the dipole moments and the angle between them, there are necessary some supplementary information obtained in quantum chemical molecular calculations using special programs. Unfortunately, the quantum mechanical calculations are usually developed for isolated molecules. Only a few solutions are studied in quantum mechanics due to the difficulty in expressing the solute-solvent and solvent –solvent interactions.

A great number of articles are based on these theories developed individually by McRae, Bakhshiev, Kawschi, Abe and so one. These theories consider only the influence of the universal interactions on the wavenumbers in the maximum of the electronic bands, neglecting the influence of the quasi-chemical bonds. Information obtained in solvatochromic studies are more efficient. Linear dependence between the wavenumbers in the maxima of the electronic absorption band and the solvent parameters describing both universal and specific interactions give the magnitude of each type of interactions. The regression coefficients can be used in estimating the dipole moment in excited state of electronic transition if the ground state dipole moment of spectrally active molecule is known from other evaluations. In variational method applied to electronic absorption bands one varies the angle between the dipole moments and one calculates the excited state dipole moment and the polarizability for the virtual values of this angle. One considers that the electronic transition takes place when the polarizability in the excited state equalizes the ground state polarizability.

In this paper we compare the values obtained in the mentioned theories in order to obtain information about the precision and the applicability of the variation method for the case of some studied azo-benzene derivatives.

Spectral Study of Intermolecular Interactions in Polar Solutions

D. Babusca, A.C. Morosanu, D.G. Dimitriu, D.O. Dorohoi*

Alexandru Ioan Cuza University of Iasi, Faculty of Physics, Iasi, Romania

**Corresponding author: danadorohoi@yahoo.com*

Three polar molecules belonging to cycloimmonium class are studied by spectral means from the point of view of their interactions with solvent molecules. As polar molecules, cycloimmonium ylids interact with solvents by universal interactions, especially by orientation-induction forces, while as nucleophilic agents they can participate to specific interactions by proton changes with hydroxy molecules.

In this paper, a method for separation the contribution of the universal and specific interactions based on the frequency shifts in electronic absorption spectra is applied to the diluted solutions. In concentrations of 10^{-3} - 10^{-4} Mol/L, cycloimmonium ylids interact only with the solvent molecules; the reciprocal interactions can be neglected due to the very small distance between ylid molecules.

In the graphs showing the dependence of the wavenumber in the maximum of ylid visible electronic absorption band and the solvent electric permittivity, the points are separated near two curves, one containing only points representing the protic solvents and one contains only the a-protic solvents. The distance between the two curves can be considered as being proportional to the strength of the specific interactions between ylid and protic molecules of solvents.

The contribution of each type of interactions in the studied solutions is finally established by a multilinear regression applied to solvatochromic data.

The universal interactions are prevalent in the a-protic solvents, while that specific become predominant in the ylid solutions with protic solvents.

Aminoacid Derivatives Containing Rest of 1,2,4-Triazole-3,4-Disubstituted with Potential Antitumoral Activity

D. Babusca, A.C. Morosanu, D.G. Dimitriu, D.O. Dorohoi*

Alexandru Ioan Cuza University of Iasi, Faculty of Physics, Romania

**Corresponding author: danadorohoi@yahoo.com*

Three polar molecules belonging to cycloimmonium class are studied by spectral means from the point of view of their interactions with solvent molecules. As polar molecules, cycloimmonium ylids interact with solvents by universal interactions, especially by orientation-induction forces, while as nucleophilic agents they can participate to specific interactions by proton changes with hydroxy molecules.

In this paper, a method for separation the contribution of the universal and specific interactions based on the frequency shifts in electronic absorption spectra is applied to the diluted solutions. In concentrations of 10^{-3} - 10^{-4} Mol/L, cycloimmonium ylids interact only with the solvent molecules; the reciprocal interactions can be neglected due to the very small distance between ylid molecules.

In the graphs showing the dependence of the wavenumber in the maximum of ylid visible electronic absorption band and the solvent electric permittivity, the points are separated near two curves, one containing only points representing the protic solvents and one contains only the a-protic solvents. The distance between the two curves can be considered as being proportional to the strength of the specific interactions between ylid and protic molecules of solvents.

The contribution of each type of interactions in the studied solutions is finally established by a multilinear regression applied to solvatochromic data. The universal interactions are prevalent in the a-protic solvents, while that specific become predominant in the ylid solutions with protic solvents.

Hydrogen-bonded Water Clusters in Calcium Hydroxyapatite

I. Doroshenko*, A. Vasylieva, O. Doroshenko, P. Teselko

Taras Shevchenko National University of Kyiv, Ukraine

**Corresponding author: dori11@ukr.net*

Hydroxyapatites are widely applied in implantology, orthopedic and periodontal surgery, drug carriers or bone regeneration [1 - 3]. A special place in these applications occupies calcium hydroxyapatite ($\text{Ca}_{10}(\text{PO}_4)_6(\text{OH})_2$), which shows close similarity to the mineral of hard tissues (bone, enamel, dentin, etc.) and therefore has high biocompatibility with them [3].

Several samples of calcium hydroxyapatite crystals were studied by means of Raman and infrared absorption spectroscopy. The presence of small water clusters in nanostructured calcium hydroxyapatite was shown [4]. The spectral bands of water dimer, tetramer, hexamer and several surface O–H and P–O–H modes were resolved at $2900\text{--}3900\text{ cm}^{-1}$ and assigned comparing with the spectra of water in low-temperature argon matrix [5] and in a hydrophobic solvent CCl_4 .

- [1]. R.Z. Le Geros, J.P. Le Geros, Hydroxyapatite, in: T. Kokubo (Ed.), Bioceramics and their Clinical Applications, Woodhead Publishing, Cambridge 2008, pp. 367–394.
- [2]. R.Z. Le Geros, Calcium Phosphates in Oral Biology and Medicine, Karger, Basel, 1991.
- [3]. P.W. Brown, B. Constantz (Eds.), Hydroxyapatite and Related Materials, CRC Press, 1994.
- [4]. K. Kristinaitytė, L. Dagys, J. Kausteklis, V. Klimavicius, I. Doroshenko, V. Pogorelov, N.R. Valevičienė, V. Balevicius. NMR and FTIR studies of clustering of water molecules: from low-temperature matrices to nano-structured materials used in innovative medicine // Journal of Molecular Liquids. – 2017. - V. 235. - P. 1-6.
- [5]. V. Pogorelov, I. Doroshenko, G. Pitsevich, V. Balevicius, V. Sablinskas, B. Krivenko, L.G.M. Pettersson. From clusters to condensed phase – FT IR studies of water // Journal of Molecular Liquids. – 2017. - V. 235. – P. 7-10.

Manifestation of Oscillatory Movements in the Spectra of Raman Scattering of Light in Some Aromatic Fluids

B. Eshchanov^{*1}, Sh. Otajonov², G. Mukhamedov¹, O. Karpova³

¹ Department of Science, Chirchik State Pedagogical Institute, Chirchik, Uzbekistan

² Department of Photonics, National University of Uzbekistan, Tashkent, Uzbekistan

³ Laboratory for Advanced Studies, Turin Polytechnic University in Tashkent, Tashkent, Uzbekistan

**Corresponding author: bakhodir.eshchanov@gmail.com*

Oscillatory spectroscopy is one of the most informative experimental methods for studying the liquid state of substances. Using oscillatory spectroscopy allows to obtain information about the structure of liquids and the presence of relatively long-lived intermolecular complexes and associates in them as well as to study the molecular dynamics. Intermolecular interactions (IMI) in liquids causes a change in the force constant interatomic bonds in molecules. The change in the intramolecular force constants under the influence of the IMI in a liquid leads to a change in the scattering cross sections in the Raman spectra of light (RSL) and the results of studies in molecules in liquid aromatic hydrocarbons, such as bromobenzene, dioxane and toluene are presented in this work.

A characteristic difference in the optical spectra of polyatomic molecules from ones of atomic molecules is that in all molecules consisting of no less than three atoms, the motion is more complex than that in atoms. That is, along with the motion of electrons, the oscillatory (periodic changes relative to the location of the nuclei) and rotational (periodic changes in orientation) movements of the molecule play the important role.

Our results showed that not every branching or other structural feature of the molecules, repeated in a number of similar compounds, leads to the appearance of characteristic lines in their spectra. Only some specific groups of atoms or bonds (in some cases, individual atoms and bonds) have characteristic lines in the RSL.

If there are several identical characteristic structural elements in the molecule under study, then the frequencies of the characteristic lines belonging to them in many cases coincide. As a consequence, the intensities of the corresponding lines are proportional to the number of such structural elements. This phenomenon is well illustrated by the example of the lines belonging to the stretching vibrations of the CH_3 group of toluene, which has two $C =$ bonds. If, with a change in the molecule, the vibrations of the main characteristic structural element are disturbed, then the lines of the other characteristic elements appear in the spectrum more clearly. The identification of characteristic structural elements with their inherent aggregate of characteristic lines represents the first step towards establishing a correlation between the Raman spectra and the molecule structure.

Suspending Thermal Degradation in Metalorganic Perovskite Solar Cells

R. Jasiunas^{1*}, R. Xia², Zh. Fei², N. Drigo², F.D. Bobbink², Zh. Huang², M. Franckevicius¹, V. Gulbinas¹, M. Mensi², X. Fang³, C. Roldán-Carmona², M.K. Nazeeruddin², P.J. Dyson²

¹ Center for Physical Sciences and Technology, Vilnius, Lithuania

² Institute of Chemical Sciences and Engineering, CH-1951 Sion, Switzerland

³ Anhui Institute of Optics and Fine Mechanics, Chinese Academy of Sciences, Hefei 230031, China

**Corresponding author: rokas.jasiunas@ftmc.lt*

Lead halide perovskite materials are one of the most promising candidates for new generation photovoltaic technologies, witnessing incredible development pace during last decade. However, it is still far beyond commercialization stage, mostly because of limitations caused by their intrinsic instability. In this work the easy way to reduce both thermal degradation and improve hydrophobicity of perovskite material was demonstrated by employing the salt 1-(4-ethenylbenzyl)-3-(3,3,4,4,5,5,6,6,7,7,8,8,8-tridecafluoro-octyl-imidazolium iodide (ETI) as an additive [1]. Methylammonium lead triiodide (MAPbI₃) pristine material is preserved by reducing out-diffusion of methylammonium cation (MA⁺) occurring due to intrinsic thermal degradation. ETI additive has markedly stabilized high efficiency solar cells based on MAPbI₃ perovskite, preserving ~83% of the initial efficiency after 700 hours of continuous light illumination and heating (60 °C). These results suggest a strategy to tackle the intrinsic thermal decomposition of most of state-of-the-art perovskite compositions.

[1]. Xia, R. et al. Retarding Thermal Degradation in Hybrid Perovskites by Ionic Liquid Additives. Adv. Funct. Mater. 1902021 (2019).

Aggregation of Molecules in Liquid Ethylene Glycol, its Formations in the Raman Spectra and Non-Empirical Calculations

H.A. Xushvaktov, A. Jumabaev^{*}, G. Murodov, A. Absanov, G. Sharifov

Faculty of Physics, Samarkand State University, Samarkand, Uzbekistan

^{*}*Corresponding author: jumabaev2@rambler.ru*

The ethylene glycol molecule consists of two groups of CH₂OH atoms, which are joined by a simple bond to each other through carbon atoms. Therefore, rotation of these groups with relative to each other— different spatial isomers are possible. In this regard, although the CH₂OH groups are the same, the mutual arrangement of OH bonds is such that these CH₂OH groups of the monomer should differ somewhat from each other by the atomic charges and the bond length between the atoms. Anyway, the hydrogen atoms of the OH groups can form a hydrogen bond. Of interest is the structure of an aggregate of molecules bonded through hydrogen bond. In the Raman spectra, a fragment of the spectrum has been studied, in which there are signs of the formation of a simple hydrogen bond. Non-empirical calculations for dimeric formation were carried out when one of the OH groups is involved.

The CH₂OH groups of ethylene glycol molecules in some cases differ in bond lengths and charge distributions of atoms in the molecule. The fact indicates that the CH₂OH groups are rotated relative to each other. Such a rotation is associated with a barrier caused by the interaction of OH bonds at the ends of the molecule. Calculations have evidenced that intermolecular hydrogen bonds can form between molecules of ethylene glycol through the formation of dimeric aggregates. A hydrogen atom of one OH group of one molecule and one of the oxygen atoms of another molecule participate in the formation of the bond. According to the calculations, the energy of dimer formation is 4.6 kcal/mol.

In principle, for ethylene glycol molecules, two hydrogen bonds are possible between CH₂OH group and appeared a chain form in are complex.

The formation of an H-bond in a dimer reveals to the appearance of a number of bands in the vibrational spectra, which are associated with mutual vibrations and the vibrations of molecules near the hydrogen bond. These bands are located in the region from 10 cm⁻¹ to 100 cm⁻¹. Raman activity in the Raman spectra is too small and can hardly be fixed against the background of the wing of the Rayleigh line, the length of which is up to 200 cm⁻¹.

Influence of Water Saturation with Hydrogen on its Properties as Solvent and Extractor

D. Khropost, Y. Myagchenko*, M. Oleksiienko

Faculty of Physics, Taras Shevchenko National University of Kyiv, Kyiv, Ukraine

Corresponding author: myagchy@ukr.net

Hydrogen-rich water has antioxidant properties, antiallergic, anti-inflammatory, anti-lipid effects, improves the metabolism that is actively used in modern medicine. In particular, in apitherapy associated with the manufacture of drugs with aqueous propolis solution. It is proved that in comparison with unsoluble medical products it has a high adsorption capacity. It is an important criterion for the degree of absorption of the active substance into the body's tissues. Also in the form of aqueous alcohol solution the medicine uses hypericin, that improves the properties of this substance for the human body.

The device for creating a neutral catholite consists of a cathode and an anode between which there is no partition. We add sodium hydrogen carbonate to the water to activate process.

We use an RGB spectrometer for experimental part of our research. In our investigation we also analyse the temperature effects of hydrogen-rich water.

The investigated property of hydrogen-rich water is very promising and is already used for preventive and healing properties in some countries of the world because the water is absolutely safe and simple to apply and in the same time so useful and beneficial.

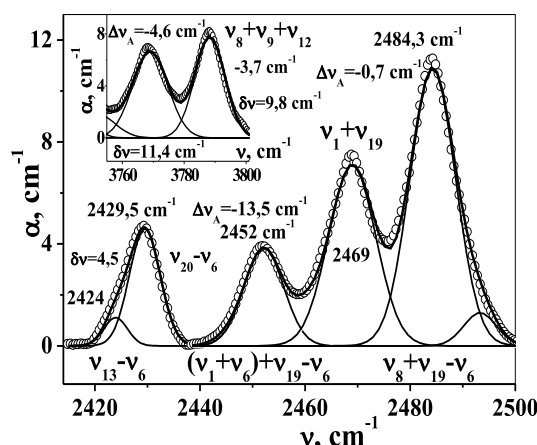
Multiple Fermi Resonances in Liquid Benzol

N.E. Kornienko*, O.L. Pavlenko

Taras Shevchenko National University of Kiev, Ukraine

*Corresponding author: nikkorn@univ.kiev.ua

The frequencies of inactive vibrations of C_6H_6 ν_3 , ν_4 , ν_{12} , ν_{13} , ν_{14} , ν_{15} , as well as vibrations of ν_8 and ν_{20} involved in the Fermi resonances (FR) $\nu_1+\nu_6\approx\nu_8$ (R_1) and $(\nu_1+\nu_6)+\nu_{19}\approx\nu_8+\nu_{19}\approx\nu_{20}$ (R_2 (ν_{20} , $R_1+\nu_{19}$))) are qualified by comparing the experimental spectral data with the results of quantum chemical calculations (QCC) (B3LYP functional, basis 6-311G(d,p), 6-311++G(d,p)) for $^{12}C_6H_6$, $^{13}C^{12}C_5H_6$, and C_6H_6 molecules in a liquid medium. It is significant that the vibrational modes in liquids have wave properties and, due to the spatial accumulation of nonlinear resonant wave processes, their intensity can vary in a complex way, which does not allow the use of the theory of the FR for individual molecules. By repeating the spectral fragments of the FR $R_{1,2}$ when they are summed up with other vibrations resolved by symmetry, all the more complex multi-wave FRs are formed. For example, in the IR spectrum of liquid benzene in the FR band $R_2-\nu_6$ (see Fig. 1), an additional frequency $\nu_1+\nu_{19}$ appears. In the interval of $2520-2680\text{ cm}^{-1}$, the FR $R_1+\nu_{17}$ (A_{2u}), $R_1+\nu_{12}$ (E_{1u}) and the additional line $\nu_9+\nu_{19}$ (E_{1u}) are superimposed. In the region of $4550-4700\text{ cm}^{-1}$, the FR bands $R_2+\nu_1+\nu_6$ and $R_2+\nu_8$ are superimposed. In the FR region of $R_2-\nu_6$, the 3rd order band $(\nu_8+\nu_{19})-\nu_6$ is more intense than the 2nd order band $\nu_{20}-\nu_6$, and the weakest component 2452 cm^{-1} refers to the composite tone $[(\nu_1+\nu_6)+\nu_{19}]-\nu_6$, Fig. 1. A similar situation is realized in the region of R_2 , as well as for the FR $R_2+\nu_6$ and $R_1+\nu_3$, $R_1+\nu_9+\nu_{12}$. It is significant that the components with the participation of the sum tones $\nu_1+\nu_6$ are characterized by large values of



anharmonic shifts $\Delta\nu_A < 0$. For example, for the component $[(\nu_1+\nu_6)+\nu_{19}]-\nu_6$ $\Delta\nu_A = -13.5\text{ cm}^{-1}$, and for $(\nu_8+\nu_{19})-\nu_6$ $\Delta\nu_A = -0.7\text{ cm}^{-1}$, Fig. 1. The results of the QCC confirmed that $\nu_8 > \nu_1+\nu_6$. However, in the Raman spectrum for the FR R_1 , the ν_8 band intensity is less than that of $\nu_1+\nu_6$, which led to a long erroneous assignment of oscillations. Many FRs form a kind of “ladder” between

oscillatory and electronic states, which leads to an increase in their interaction.

Manifestation of Cluster Excitations in Dielectric Properties of Liquid Water

V.N. Makhlaichuk*

Department of Theoretical Physics and Astronomy, Odessa I.I.Mechnikov National University, Odesa, Ukraine

*Corresponding author: interaktiv@ukr.net

The main attention in this work is focused on the physical nature of the effective polarizability of water molecules in liquid water. The last is defined in accordance with the standard formula (Clausius–Mossotti) for the static dielectric permittivity ε of molecular system:

$$\frac{\varepsilon - 1}{\varepsilon + 2} = \frac{4\pi}{3} n \alpha(t), \quad \alpha(t) = \alpha_{eff}(t) + \frac{d_{eff}^2(t)}{3k_B T_c t}, \quad (1)$$

where $\alpha_{eff}(t)$ is the effective polarizability of a water molecule and $d_{eff}(t)$ is its effective dipole moment, n and T are the numerical density and temperature correspondingly, k_B is the Boltzmann constant (it will be in the sequel included to temperature), $t = T / T_c$, T_c is the critical temperature. Considering water in its range of liquid states as a mixture of tetramers and dimers for its dielectric permittivity we can write:

$$\frac{\varepsilon - 1}{\varepsilon + 2} = \frac{4\pi}{3} \left[n_d \alpha_d + n_t \alpha_t + \frac{1}{3T} \left(n_d (\bar{d}_d^2 + \langle \delta \bar{d}_d^2 \rangle) + n_t \langle \delta \bar{d}_t^2 \rangle \right) + \dots \right]$$

where n_d and n_t are densities of components, α_d and α_t are their averaged electron polarizabilities, \bar{d}_d is unperturbed dipole moment of a dimer, $\delta \bar{d}_d$ and $\delta \bar{d}_t$ are increments of the dipole moments for a dimer and tetramer due to their thermal excitations. We consider the mean square values of dipole moment of tetramer caused by thermal violating of the anti-parallel disposition of dipole moments for dimers at opposite sides of tetramer. According to this assumption we suppose that the effective polarizability of tetramers is reduced to the sum of two effective polarizabilities for two dimers. This assumption is not quite correct for an isolated tetramer, however in liquid water the interaction of a tetramer with its non-regular surroundings changes the situation essentially. There is concentration of dimers, arising because of disintegration of tetramers, calculated.

Intermolecular Interactions in Gaseous Monohydric Alcohols

L. Meyliev¹, B. Kuiliev¹, I. Doroshenko^{2*}

¹ Faculty of Physics, Karshi State University, Karshi, Uzbekistan

² Experimental Physics Department, Taras Shevchenko National University of Kyiv, Ukraine

*Corresponding author: dori11@ukr.net

FTIR spectra of gaseous monohydric alcohols (methanol, ethanol, 1-propanol and 1-butanol) were registered at room temperature in the spectral range 750-4000 cm^{-1} using Bruker FTIR spectrometer Vertex 70 [1]. Due to the presence of hydroxyl group in alcohol molecules they can form hydrogen-bonded clusters. In the registered spectra of all investigated samples one can note a wide absorption band near 3200 cm^{-1} (see, for example, Fig. 1). It corresponds to the stretching OH vibrations of the molecules, which are involved in hydrogen-bonded clusters, and is an evidence of hydrogen bond existing in gaseous alcohols [2].

Experimental spectra are interpreted using the results of quantum-chemical simulation of structure and vibrational spectra of monohydric alcohols.

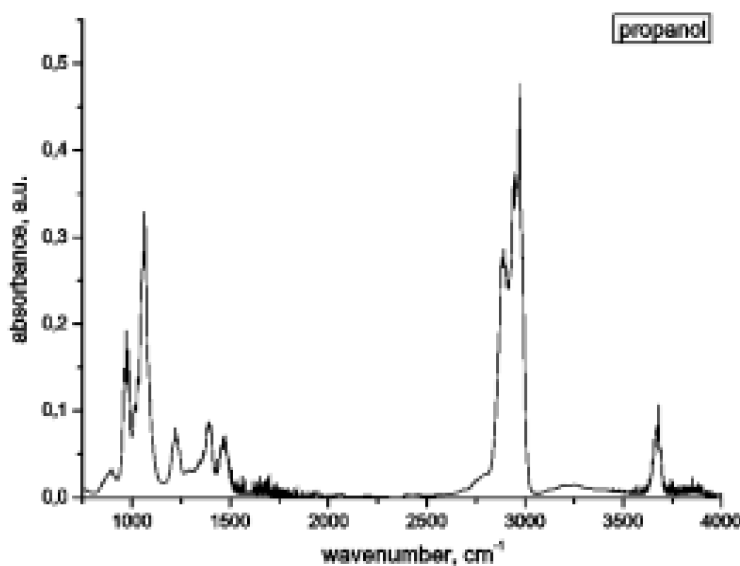


Fig. 1. FTIR spectrum of gaseous propanol.

- [1]. I. Doroshenko, V. Pogorelov, V. Sablinskas. Infrared absorption spectra of monohydric alcohols // Dataset Papers in Chemistry, vol. 2013, Article ID 329406, 2013.
- [2]. I. Doroshenko. Clustering processes in monohydric alcohols. – LAP LAMBERT Academic Publishing, Saarbrücken, Germany. - 2015. – 74 p.

Investigation of the Weak Hydrogen Bonded $\text{H}_2\text{CO}\cdots\text{HX}$ ($\text{X}=\text{F}, \text{Cl}$) Complexes by Means of Quantum Mechanical Methods

K.G Tokhadze¹, G. Murodov*², A. Amonov^{1,2}, G. Nurmurodova^{1,2}

¹ Department of Physics, St. Petersburg State University, Saint-Petersburg, 199034 Russia

² Department of Physics, Samarkand State University, Samarkand 140104, Uzbekistan

**Corresponding author: mgulamhon@rambler.ru*

The study of molecular complexes such as formaldehyde which is containing the carbonyl group is of considerable interest. The molecular complexes of $\text{H}_2\text{CO}\cdots\text{HX}$ ($\text{X}=\text{F}, \text{Cl}$) are simplest compounds of this type. Therefore, among of many complexes, the title complexes have been studied as a model system to clarify the nature of weak hydrogen bonded complexes and for the properties of carbonyl containing species. With the titled complexes many reliable computational reports have been performed the results with high-level quantum mechanical methods. In the recent reports emphasized, for a good agreement between the theoretical and experimental calculated frequencies, should be taken into account the strong bend-stretching couplings in gas phase data. The fact requires to solve multidimensional Schrodinger equations. In this study the equilibrium nuclear configurations for $\text{H}_2\text{CO}\cdots\text{HX}$ ($\text{X}=\text{F}, \text{Cl}$) complexes have been calculated in the MP2/6-311++G(3df,3pd), approximations with the basis set superposition error taken into account. The calculations of frequencies and intensities of vibrational absorption bands in harmonic and anharmonic approximations revealed a number of interesting effects in the changes of these spectral parameters upon formation of dimers. The binding energy of the complexes in the equilibrium configuration obtained in the above approximation with the basis set superposition error taking into account using the GAUSSIAN 16 and GAUSSIAN 09 suite of codes. The stabilization energies obtained for $\text{H}_2\text{CO}\cdots\text{HF}$ and $\text{H}_2\text{CO}\cdots\text{HCl}$ complexes 5.1 kcal/mol and 3.3 kcal/mol, respectively.

The basic aim is to offer reliable models for better understanding the nature of H-bonded molecular complexes with advanced quantum mechanical methods. This allows one to carry out comparative analysis of computational and experimental reports on the title complexes.

- [1]. V. P. Bulychiev, A.M. Kochevarnikov, and K.G. Tokhadze. // Optics and spectroscopy - 2017. -V.122.-N.6.-p.883-891.
- [2]. Alfred Karfen and Eugene S. Kryachko. // J.Phys. Chem. A, -2005.-V.109.-N.39.-p.8930-8937.

Polymethine Type of Electron Transitions in Merocyanine Derivatives of Aminocoumarine

A.O. Gerasov¹, A.P. Naumenko^{*2}, O.D. Kachkovsky³

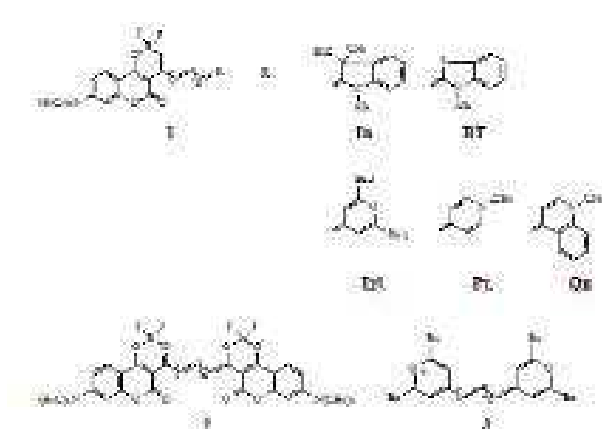
¹ Spectrum Info Ltd. Fine Chemicals, Contract Manufacturing, Organic Dyes, Kiev, Ukraine

² Taras Shevchenko National University of Kyiv, Faculty of Physics, Kyiv, Ukraine

³ Institute of Bioorganic Chemistry and Petrochemistry of the National Academy of Sciences of Ukraine, Kyiv, Ukraine

**Corresponding author: a_naumenko@univ.kiev.ua*

The well-known merocyanines are widely used in applied technology upon conversion of lighthare neutral unsymmetrical linear conjugated compounds containing both donor and acceptor terminal groups. It was proposed these dyes to consider as the intermediate derivatives between the corresponding cationic cyanines and anionic polymethine dyes containing the highly polarizable collective system of π -electrons.



Here we presents the results of spectral and quantum-chemical study of the features of the electron transitions into two lowest excited states in the merocyanines containing the invariable acceptor amino-coumarin group and variable donor group.

The careful study of electron structure of triad: vinylogous series of merocyanines and their parent cationic and anionic symmetrical polymethine dyes shows their similarity and distinction;

so, the distribution of electron densities in the chain of the merocyanine is similar to charge distribution in the chain of the parent ionic dyes, whereas the occupancies at bonds in merocyanine differ, in essence, and hence is similar to the polyenes with the considerable alternated bond lengths. Based on charge distribution at molecular fragments, it is found that the donor and acceptor strengths of the terminal groups decrease appreciably in merocyanines, in compare with their values in the cationic and anionic dyes, correspondingly. The fragmentary charge distribution is sensitive to the chemical constitution of the variable donor residue.

Spectral investigation shows that the shape of the longwavelength absorption band and shape of the minimum in the fluorescence excitation anisotropy spectra in all three types of the studied linear conjugated molecules are very similar: this indicates on “cyanine limit” in the merocyanines derivatives aminocoumarin, what confirmed not only by the narrow high intensive spectral band in the absorption spectra (similarity of the first electron transition), but also by the similarity of their fluorescence excitation anisotropy (similarity of the second electron transition).

Heat Transfer in Halogen-Substituted Ethanes: Freon HFC-152a

V.V. Sagan*, V.A. Konstantinov, A.V. Karachevtseva, V.P. Revyakin

Department of Thermal Properties and Structure of Solids and Nanosystems,
B. Verkin Institute for Low Temperature Physics and Engineering, Kharkov, Ukraine

**Corresponding author: sagan@ilt.kharkov.ua*

It is known [1] that all halogen-substituted ethanes form «plastic» phases, and in the series $C_2F_6 \rightarrow C_2Cl_6 \rightarrow C_2Br_6$ the entropy of the structural phase transition decreases ($\Delta S_f/R$ changes, respectively, as $4.32 \rightarrow 2.87 \rightarrow 1.45$) [2]. It was suggested that, in a disordered cubic phase of compounds of the type C_2X_6 , the molecules are orientationally disordered in such a way that the C–C axis can be parallel to any of the four spatial diagonals of the cube. This gives a contribution to ΔS_f equal to $R \ln 4 = 1.39R$. It is also assumed that during the structural phase transition, disordering is achieved as a result of the internal rotation of one CX_3 group relative to another, as well as due to the rotation of the molecule as a whole around the C–C axis. For C_2Br_6 , these two types of motion make only a small contribution to ΔS_f , but for C_2F_6 this contribution is significant.

In this work, the isochoric thermal conductivity of 1,1-difluoroethane (freon HFC-152a) was investigated on samples of different densities in the orientationally disordered phase. Below the melting point $T_m = 154.56^\circ K$ [3–4], 1,1-difluoroethane forms a body-centered cubic orientationally disordered phase with two molecules in the unit cell [5]. With further cooling below $108^\circ K$, it is transformed into a more ordered monoclinic structure, the space group Pc with $Z = 6$. The jump in density during the transition is about 4%. The packing of molecules in the low-temperature phase occurs under the influence of the formation of weak C–H \cdots F bonds. It was found that the thermal conductivity of all samples sharply decreases ($\approx 15\%$) during the $\alpha \rightarrow \beta$ transition, and then increases with increasing temperature in the orientationally disordered phase. Possible mechanisms for such behavior are discussed.

- [1]. N. Parsonage, L. Staveley, Disorder in Crystals, Clarendon Press, Oxford (1978).
- [2]. T. Koide, M. Tsujino, K. Savada, and T. Oda, Bull. Chem. Soc. Japan, 47, 2998 (1974).
- [3]. J. W. Magee, Int. J. Thermophys., 19, 1397 (1998).
- [4]. W. Blanke and R. Weiß, Fluid Phase Equil., 80, 179 (1992).
- [5]. M. Brunelli and A.N. Fitch, Z. Kristallogr., 217, 395 (2002).

The "Associate of Dyes + Surfactant" Systems: Spectroscopy and Computer Simulation

S.A. Shapovalov*, V.K. Ponomarov, N.O. Mchedlov-Petrosyan

Institute of Chemistry V.N. Karazin National University, Kharkiv, Ukraine

*Corresponding author: serghey.a.shapovalov@karazin.ua

This work discusses the association of cationic dye (pynacyanol, PC) with anionic dye (ethyleosin, EE), and also the interaction of these dyes with surfactants (as a cationic surfactant – cetylpyridinium bromide, as an anionic surfactant – sodium dodecyl sulfate, as a nonionic surfactant – triton X-100, TX). The purpose of the study was spectrophotometric determination of the evidence of interactions between polyatomic particles at low (10^{-6} – 10^{-4} M) concentrations in aqueous solutions and the estimation of energy (the standard enthalpy of formation) of associative particles. At first, the optimization of the geometry of structures was carried out, and then, the values of the standard enthalpy of the associates were determined by semiempirical methods AM1 and PM3 [1, 2].

It should be noted that the theoretically grounded interaction of "PC-EE" is actually realized in aqueous solutions. The absorption spectra of this system evidenced about it. On Fig. 1, spectrum 3 corresponds to the algebraic sum of the individual spectra of both dyes (there is an additivity of light absorption). Spectrum 4 is experimentally obtained. Its difference from the total spectrum shows the existence of the formation of associates according to the scheme: $PC^+ + EE^- \rightleftharpoons PC^+ \cdot EE^-$.

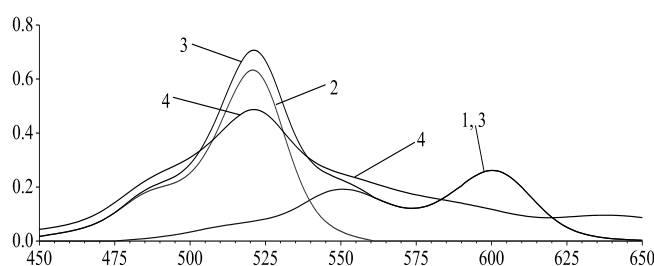


Fig. 1. Absorption spectra PC ($5,52 \cdot 10^{-6}$ M) with additions EE ($5,72 \cdot 10^{-6}$ M). Spectrum: 1 – PC; 2 – EE; 3 – algebraic sum of 1 and 2; 4 – experimental spectrum of the mixture PC and EE.

The energy utility of the interactions between the cation of the dye and the surfactant is confirmed by rather high values of the standard enthalpies of formation.

- [1]. S.A. Shapovalov. The Association Processes of Protolytic Forms of Dyes in Solutions. Dissimilar Association. Kharkiv, 2014. – 250 p. – ISBN 978-966-2445-78-7.
- [2]. Shapovalov Serghey A. Cation-anionic Association of Organic Dyes in Aqueous Solutions: Structure and Properties of Associates // Modern Organic Chemistry Research. – 2017. – Vol. 2, – № 4. – p. 195 – 203.

Dimerization of Cyanine Dyes: Results of Quantum-Chemical Simulation

S.A. Shapovalov*

Institute of Chemistry V.N. Karazin National University, Kharkiv, Ukraine

*Corresponding author: serghey.a.shapovalov@karazin.ua

Cyanines are known for their practical applications in the series of some dyes [1]. Previously, we studied the spectroscopy and energetics of dimerization of astraphloxin. This report discusses the possible dimerization and polymerization of structural analogues: 1,1'-diethyl-2,2'-carbocyanine chloride (CAS Number 2768-90-3), 1,1'-diethyl-2,2'-dicarbocyanine iodide (CAS Number 14187-31-6), 1,1'-diethyl-4,4'-cyanine iodide (CAS Number 4727-49-5), 1,1'-diethyl-4,4'-carbocyanine iodide (CAS Number 4727-50-8). These cyanines are poorly soluble in water, but are highly soluble in alcohols and are characterized by very high extinction coefficients (from 96000 and more). Thus, the high intensity of light absorption still makes it possible to study the interaction of these cationic dyes with organic anions even at very low concentrations in aqueous solutions. Polymerization is considered in accordance with schemes: $Ct^+ + Ct^+ \rightarrow (Ct^+)_2$, $(Ct^+)_2 + Ct^+ \rightarrow (Ct^+)_3$ and so on.

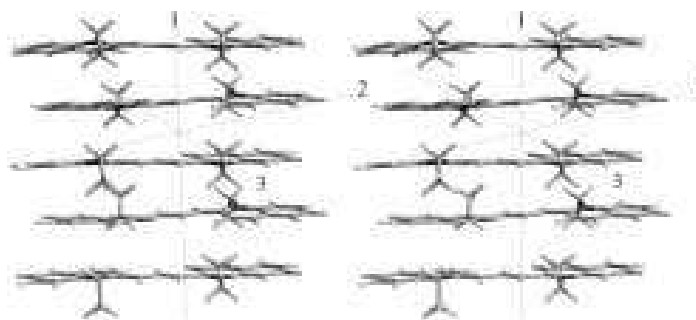


Fig. 1. The optimized construction of 1,1'-diethyl-2,2'-carbocyanine pentamer (stereo, distance between the planes of the structure is equal to 3.7...3.8 Å); the energy is 79.1 kcal/mol (MM+ method).

It turned out that the most energy-efficient of a number of possible options is coplanar arrangement of cations (as an example, see fig. 1). The obtained energy data are in agreement with the previously obtained data on spectrophotometric measurements and deconvolution analysis of the light absorption bands [2].

- [1]. S.A. Shapovalov. Processes of Self-Association of Dyes in Solutions. – Riga: Academic Publishing of European Union, 2018. – 122 p. – [ISBN 978-613-9-82294-2].
- [2]. S.A. Shapovalov, E.A. Samoilov. Regularities of Homo- and Heteroassociation of the Pinacyanol Cation in Aqueous Solution // Russian Chemical Bulletin. – 2008. – T. 57. – № 7. – p. 1405 – 1415.

Theoretical Evaluation of Two-Photon Absorption Properties of Benzoxazoles Undergoing Excited State Intramolecular Proton Transfer

Y. Syetov*

Oles Honchar Dnipro National University, Dnipro, Ukraine

*Corresponding author: e-mail: setov2003@yahoo.com

Two-photon absorption (TPA), a simultaneous absorption of two photons, — is a non-linear optical process with intensity depending on the square of the incoming light. The TPA process has been gaining greater interest from a number of areas, particularly in the fields of two-photon fluorescent microscopy and imaging, three-dimensional microstructure optical data storage, optical switching, optical power limiting, photodynamic therapy. 2-(2'-hydroxyphenyl)benzoxazole (HBO), 2,5-bis(2-benzoxazolyl)phenol (DBP) and 2,5-bis(2-benzoxazolyl)hydroquinone (BBHQ) (Fig. 1) are benzoxazole derivatives with single and double hydrogen bonds undergoing photoinduced excited state intramolecular proton transfer (ESIPT). The ESIPT converts enol structure of the molecules with OH...N hydrogen bonds into keto structure with O...HN hydrogen bonds and causes appearance of fluorescence with an anomalously large Stokes shift. Two-photon absorption spectra of HBO, DBP and BBHQ are modeled by time-dependent density functional theory calculations. In contrast to the linear absorption, where the transitions to the two lowest excited states are prominent, the two-photon absorption cross sections are significant for the transitions to higher states which are weak in one-photon absorption spectra. The 2,5-bis(2-benzoxazolyl)phenol and 2,5-bis(2-benzoxazolyl)hydroquinone demonstrate the maximum cross section of about ten times larger than that of 2-(2'-hydroxyphenyl)benzoxazole. The largest value of the cross section is calculated for 2,5-bis(2-benzoxazolyl)hydroquinone to be about 1500 units of Goeppert-Mayer for excitation at 600 nm.

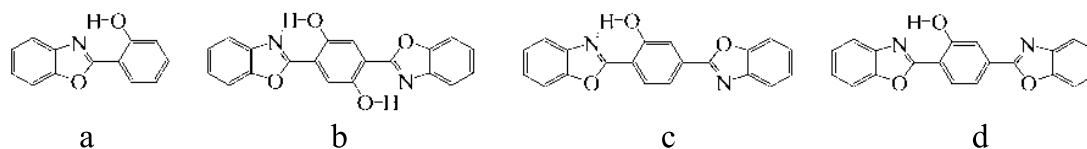


Fig. 1. Molecular structure of HBO (a), BBHQ (b) and two conformations of DBP (c,d).

Manifestations of Intermolecular Interactions in the IR Spectra of Adsorbed Species

A. Tsyganenko^{1*}, O. Pestsov¹, R. Belykh¹, R. Novikov¹,
M. Shelyapina¹, V. Petranovski²

¹ Faculty of Physics, St.Petersburg State University, St. Petersburg, Russia 198504.

² Centro de Nanociencias y Nanotecnologia de la Universidad Nacional Autonoma de Mexico, 22860 Ensenada, Baja California, Mexico

**Corresponding author: atsyg@yandex.ru*

Vibrational spectra of surface compounds provide unique information about the structure of adsorbed layers, properties of surface sites and the nature of intermolecular interactions. They are not complicated by the rotational structure and can be studied in a broad range of temperatures, not limited by points of condensation or crystallization as in solutions or matrices.

Spectra of adsorbed molecules are affected by lateral interactions, which can be repulsive or attractive [1]. Static interaction changes the energies of adsorption and shifts the bands of test molecules. The mechanism of repulsive interaction includes relaxation induced by adsorption. Co-adsorption of acid and basic molecules demonstrates the effect of induced acidity or basicity, when the strength of surface sites changes dramatically due to the presence of weakly adsorbed molecules. Dynamic (resonance dipole-dipole) interaction accounts for the changes in the position and contour of the bands. It manifests itself even in the spectra of symmetric weakly adsorbed molecules. The most intense bands of such molecules as SF₆, CF₄ or NF₃ become split into two components with the distance and intensity ratio depending on the geometry of adsorbed layer.

Using FTIR spectra of ¹²CO-¹³CO mixtures it was shown that CO forms with Cu⁺ or Ni⁺ ions in zeolites mono-, di- and tricarbonyl compounds. For Ni-USY zeolite a phenomenon of “isotopic isomerism” was established when two CO molecules in dicarbonyls are not equivalent, and those of mixed isotopic content are of two kinds with slightly different band positions. Spectra of microwave treated Cu-MOR samples pumped off at temperatures below 400°C exhibit two anomalies at 3593 and 3512 cm⁻¹, whose contour is typical of that of “Evans holes” arising as a result of Fermi resonance with other states. Experiments are in progress to establish the role of copper and microwave treatment in this phenomenon.

Acknowledgement: The work was supported by RFBR and CITMA, grant No. 18-53-34004

- [1]. A.N. Dobrotvorskaia, O.S. Pestsov, A.A. Tsyganenko. Lateral interaction between molecules adsorbed on the surfaces of non-metals // Topics in Catalysis. – 2017. – V. 60. – N. 19 – 20. – p. 1506 – 1521.

Effect of Argon Environment on Vibrational Spectra of Tert-Butanol

D. Vashchuk, I. Doroshenko*, A. Vasylieva

Taras Shevchenko National University of Kyiv, Ukraine

**Corresponding author: dori11@ukr.net*

Tert-butanol (tert-butyl alcohol, or 2-methyl-propan-2-ol) belongs to the class of tertial monohydric alcohols, molecules of which can form hydrogen-bonded clusters in condensed state [1, 2]. Tert-butanol molecule has no conformational isomers, so it is rather convenient object for spectroscopic investigation.

Quantum-chemical simulation of tert-butanol molecules in free state and in argon environment were carried out. Geometry parameters were optimized at DFT/B3LYP level of theory with 6-31G(d, p) basis set for both cases. Vibrational IR frequencies were calculated and compared for vacuum and for argon environment. It is shown that vibrational modes in the presence of argon are red-shifted in a few wavenumbers.

Calculated IR spectra of tert-butanol in argon environment were compared to the experimentally registered spectra of tert-butanol trapped in a low-temperature argon matrix [2, 3].

- [1]. I. Doroshenko, V. Pogorelov, G. Pitsevich, V. Sablinskas. Cluster structure of liquid alcohols: vibrational spectroscopy study. – LAP LAMBERT Academic Publishing, Saarbrücken, Germany. - 2012. – 288 p. (in Russian).
- [2]. I. Doroshenko, G. Pitsevich, V. Pogorelov. // Nanosystems, nanomaterials, nanotechnologies. – 2012. – V.10, №1. – P. 203-215.
- [3]. V. Pogorelov, I. Doroshenko, P. Uvdal, V. Balevicius, V. Sablinskas. // Molecular Physics. – 2010. – V. 108, is. 17. – P. 2165-2170.

Argon Matrix Effect on IR Spectra of Small Water Clusters from Quantum-Chemical Calculations

A. Vasylieva^{*1}, I. Doroshenko¹, V. Pogorelov¹

¹ Taras Shevchenko National University of Kyiv, Ukraine

^{*}Corresponding author: tonyavasileva1@gmail.com

Investigation of small water clusters is a natural starting point for an accurate description of water in its myriad forms. The method of matrix isolation [1,2] is now a well-known technique in chemical and physical research, the main idea of which is to isolate the molecules of investigated substance in the traps (vacancies) of inert solvent. Two types of interactions are observed in real molecular systems in matrix isolation. The first one is the interaction field created by guest molecules themselves in a matrix trap, and the second — by host matrix molecules [3].

The influence of argon matrix on small water clusters are investigated by quantum-chemical simulation of structure and IR vibrational spectra of water clusters isolated in fcc argon crystal fragment [4]. Comparison of calculation results are performed for water clusters in vacuum and in solid argon matrix. In addition, obtained IR frequencies and intensities for water clusters in argon are compared with experimentally registered FTIR spectra of water trapped in a low-temperature argon matrix at 15 and 25 K.

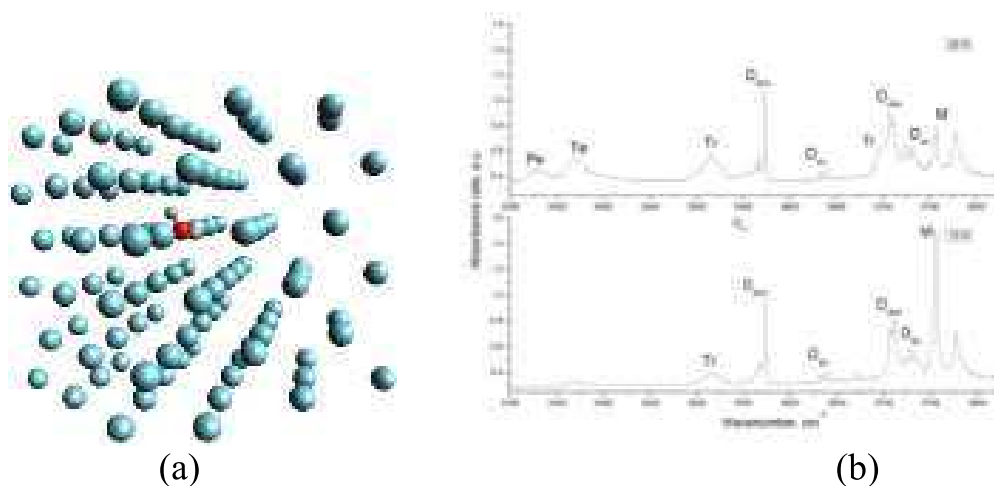


Fig. 1. (a) Water monomer in fcc argon crystal fragment composed of 107 Ar atoms; (b) FTIR spectra of water in an Ar matrix at 15 and 25 K

- [1]. G. Pitsevich, E. Shalamberidze, A. Malevich, V. Sablinskas, V. Balevicius, and L. Pettersson, *Mol. Phys.* 115, 2605 (2015).
- [2]. J. Ceponkus, P. Uvdal, and B. Nelander, *J. Chem. Phys.* 138, 244305 (2013).
- [3]. A. Vasylieva, I. Doroshenko, O. Doroshenko, and V. Pogorelov, *Fiz. Nizk. Temp.* 45, No. 6 (2019).
- [4]. S. Stepanian, A. Ivanov, and L. Adamowich, *J. Mol. Spectr.* 320, 13 (2016).

Performances of a New Iridium (III) Complex in Orange Phosphorescent and White Hybrid OLEDs

D. Volyniuk^{1*}, K. Leitonas¹, J. Simokaitiene¹, M.D. Thiyagarajan²,
U.M. Balijapalli², M. Pathak², K. Sathiyarayanan², J.V. Grazulevicius^{1*}

¹ Kaunas University of Technology, Department of Polymer Chemistry and Technology, Kaunas, Lithuania

² Chemistry Department, School of Advanced Sciences, VIT University, Vellore, 632014, Tamil Nadu, India

**Corresponding authors: dvolynyuk@gmail.com, juozas.grazulevicius@ktu.lt*

This work deals with investigations of new highly efficient phosphorescent iridium (III) complex based on benzoimidazophenanthridine as the main ligand. To demonstrate potential of this complex as phosphorescent emitter for optoelectronic applications, it was thoroughly characterized by different methods including luminescence spectrometry, cyclic voltammetry, thermogravimetric analysis, differential scanning calorimetry and photoelectron emission spectrometry. In addition, OLEDs exhibiting warm orange electrophosphorescence were developed using this complex, thus demonstrating its potential application in electroluminescent devices. Electroluminescence spectra of the devices were characterized by CIE1931 colour coordinates of (0.539, 0.459) and colour temperature of 2088 K. Their maximum external quantum efficiency reached 17.5 %. Such performance in OLEDs was achieved due to efficient orange phosphorescence with quantum yield of 60 % at room temperature. This work also deals with the development of white hybrid solution-processed OLEDs exploiting ultralow concentration of newly synthesized iridium (III) complex as phosphorescent dopant in combination with blue fluorescent emitter (host) and green emitter exhibiting thermally activated delayed fluorescence emitter. The designed and fabricated by spin coating white hybrid devices were characterized by high quality (human-eyes-friendly) electroluminescence with CIE1931 coordinates of (0.335, 0.392), colour temperature of 2910K and colour rendering index of 72 as well as high maximum external quantum efficiency of 8.7 %.

Acknowledgements

This work was supported by the project of scientific co-operation program between Latvia, Lithuania and Taiwan (grant No. S-LLT-19-4).

Photoactivity of Silver Ions in Solutions of Organic Compounds

T.V. Zashivailo^{1*}, V.I. Kushnirenko²

¹ National Technical University of Ukraine "Igor Sikorsky Kyiv Polytechnic Institute", Kyiv, Ukraine

² V. Lashkarev Institute of Semiconductor Physics, NASU, Kyiv, Ukraine

**Corresponding author: t_zash@ukr.net*

Study of photochemical transformations in solutions activated with silver promotes an elucidation of various physical processes that occur in such systems. In present work, the photochemical transformations in organic ($C_3H_8O_3$, C_2H_5OH , CH_3OH) aqueous solutions with an admixture of silver are studied taking into account the photoactivity of the Ag^+ ion.

While investigating the photochemical transformations in above-mentioned solutions activated by silver ions (10^{-5} – 10^{-1} mol/l), the absorption, photoluminescence (PL) and PL excitation spectra of the solutions were measured. The solutions involved do not luminesce at room temperature but at 150–180K they strongly emit under UV irradiation. The spectra under observation are conditioned by an electron transition between energy levels of the Ag^+ ion which are deformed due to the interaction with the environment.

At room temperature, in given solutions under irradiation by the light with the spectral distribution that meets the absorption region of the Ag^+ ion, the photochemical transformations occur, resulting in the transformations of Ag^+ ions in an insoluble Ag^0 association. The rate of photochemical transformations from the Ag^+ ions to the Ag^0 satisfactorily correlates with the energy values of electron detachment from organic solvent and with the maximum peak positions of absorption bands for given organic solvents in the aqueous solutions. Under irradiation with the visible light, the photochemical transformations in such systems ran rather slowly, during several months. Under storing in the dark over a long period of time, the solutions under observation did not lose their own luminescent properties. During measuring the absorption spectra of the solutions, the photochemical transformations ran very slowly and therefore those did not influence the experiment.

The investigation of photochemical processes that occur in the solutions with silver complexes allowed us to elucidate the influence of media on the impurity Ag^+ ion and to determine a number of medium parameters that describe their properties.

3

Crystals

X-Ray Crystallography and Vibrational Investigations of New Organic Complexes for Nonlinear Optics

M. Drozd^{1*}, I. Bryndal², T. Lis³, J. Zaręba⁴ and H. Ratajczak^{1,3}

¹ Institute of Low Temperature and Structure Research Polish Academy of Sciences, Wrocław, Poland

² Wrocław University of Economics, Wrocław, Poland

³ Faculty of Chemistry, Wrocław University, Wrocław, Poland

⁴ Technical University of Wrocław, Wrocław, Poland

**Corresponding author: m.drozd@intibs.pl*

Searching for new nonlinear materials is a main goal of many scientific center around the World. These compound are used in new lasers, optics, computers optical fiber technology and electronics. In these investigations the two main strategies are observed. Firstly new organic complexes with highest first order hyperpolarizability are discovered, but these compounds have usually wrong mechanical and physical properties. On the other hand the organic-inorganic hybrids are produced as very good candidates for practical using in industry, because the high hyperpolarizability is connected with good durability.

In this work we present new noncentrosymmetric complexes based on organic compounds, only. In this paper, four hydrogen bonded complexes 2-amino-pyridinium 2,5-dinitrophenolate, [(2APy)⁺·(2,5-DNP)⁻], 2-amino-pyridinium 4-nitrophenolate-4-nitrophenol [(2APy)⁺·(4-NP)⁻·(4-NP)], 2,3,6-trimethyl-pyridinium 2,3,5,6-tetrachlorophenolate [(2,3,6C)⁺·(TCP)⁻] and 3,5-dimethyl-pyridine-2,3,5,6-tetrachlorophenol [(3,5L)·(TCP)] were obtained and characterized by X-ray diffraction. The single crystal structure of (1)-(3) reveals that substituted phenol-pyridine complexes were found to crystallize as salts linked by N-H···O hydrogen bonds, whereas (4) crystallizes as formally molecular adduct (1:1) linked by O-H···N hydrogen bond.

Additionally, the detailed vibrational studies results are presented, also. According to presented spectra the analysis of hydrogen bonds network in investigated crystal was made. The spectroscopy data seems to be in good agreement with crystallographic X-ray results.

The nonlinear properties (first order hyperpolarizability) were examined according to Kurtz-Perry method on the powder samples. All investigated complexes are classified as good candidates for practical using in NLO field of knowledge.

Upconversion and Photodarkening Effects of Femtosecond Laser Filamentation in Er-doped Chalcohalide Glass

I. Blonskyi¹, V.M. Kadan*¹, O. Shpotyuk^{2,3}, L. Calvez⁴, I. Pavlov^{1,5},
S. Pavlova¹, A. Dmytruk¹, A. Rybak¹, P. Korenyuk¹,

¹ Institute of Physics of the NAS of Ukraine, Kyiv, Ukraine

² Vlokh Institute of Physical Optics, Lviv, Ukraine

³ Jan Dlugosz University in Czestochowa, Czestochowa, Poland

⁴ Univ. Rennes, CNRS, Rennes, France

⁵ Middle East Technical University, Ankara, Turkey

*Corresponding author: kadan@iop.kiev.ua

Upconversion fluorescence of Er³⁺ ions (1 at.%) excited with femtosecond laser pulses of different repetition frequencies (seed laser 76 MHz, and laser amplifier 1 kHz) is studied in Er-doped chalcohalide glass of 65GeS₂-25Ga₂S₃-10CsCl composition. Strong weakening of fluorescence efficiency at 530 nm and 560 nm and photoinduced darkening is observed under 1 kHz excitation, which is most probably caused by free carriers generated by two-photon absorption. On the other hand, neither weakening nor photodarkening is observed under 76 MHz excitation, this being presumably due to concomitant thermal annealing. Taking an advantage of upconversion fluorescence, the femtosecond filamentation associated with positive changes in refractive index is recorded in the Er-doped glass, whereas exceeding the threshold of thermal melting is accompanied by decrease in the refractive index.

Influence Optic-Acoustic Hybridization on Thermal Properties of Molecular Solids

A.I. Krivchikov^{*}, O.A. Korolyuk

B. Verkin Institute for Low Temperature Physics and Engineering of NAS of Ukraine, Kharkov, Ukraine

^{*}*Corresponding author: krivchikov@ilt.kharkov.ua*

One of the unsolved problems of solid state physics is the nature of boson peak and microscopic description of low temperature anomalies of thermal properties of disordered solids. The heat capacity of a 2-bromobenzophenone (2-BrBP) single crystal measured at temperatures from 0.4 K to 30 K demonstrates anomalies inherent in disordered solids: instead of the Debye law, the heat capacity shows a linear temperature dependence and a boson peak, i.e. the peculiarities typical of solids with disorder [1]. Within the framework of the phenomenon of hybridization of a low lying optical branch with an acoustic branch [2], a qualitative explanation is given of low temperature glassy anomalies of the thermal properties of molecular crystals. A comparative analysis of data on the heat capacity of various molecular crystals and glasses has been carried out, and a new correlation has been revealed between the boson peak energy and the Debye heat capacity.

The universal behavior of the thermal conductivity of amorphous solid is discussed within the framework of the soft potential model [3]. The universal temperature behavior of the low-temperature thermal conductivity $\kappa(T)$, namely, T^2 growth at low temperatures and a plateau with further increase in temperature is determined by the same process, resonant scattering of acoustic phonons by low-energy localized states.

- [1]. A. Jeżowski, M Strzemechny, A.I. Krivchikov and et al. Glassy anomalies in the heat capacity of an ordered 2-bromobenzophenone single crystal //Physical Review B. – 2018. – v. 97. – N. 20. – p. 201201. – v. 280. – N. 5-6. – p. 365-370.
- [2]. M.I. Klinger, A. M. Kosevich. Soft-mode-dynamics model of acoustic-like high-frequency excitations in boson-peak spectra of glasses //Physics Letters A. – 2001. – v. 280. – N. 5-6. – p. 365-370.
- [3]. M.A. Ramos, U. Buchenau. Low-temperature thermal conductivity of glasses within the soft-potential model //Physical Review B. – 1997. – v. 55. – N. 9. – p. 5749.

Phonon Spectrum and Heat Transport in Metal Thio- and Senenophosphates

V. Liubachko^{1,2*}, A. Oleaga¹, A. Salazar¹, K. Glukhov², Yu. Vysochanskii²,
A. Kohutych², A. Pogodin²

¹ Departamento de Física Aplicada I, Escuela de Ingeniería de Bilbao, Spain

² Institute for Solid State Physics and Chemistry, Uzhgorod University, 88000 Uzhgorod, Ukraine

*Corresponding author: correctus@live.com

We present a combined theoretical and experimental data in order to perform an essential discussion on peculiarities of thermophysical properties in metal thio- and senenophosphates. The thermal diffusivity D measurements of $[\text{Cu,Ag}]^{1+}[\text{In,Bi}]^{3+}\text{P}_2(\text{Se,S})_6$ compounds were carried out with a high resolution ac photopyroelectric calorimeter technique [1]. The heat capacities C of the considered crystals have been calculated through the evaluation of the phonon spectra using density-functional perturbation theory [2]. Thermal conductivity κ has been calculated by combining the experimental D and the calculated C following equation $\kappa=C*D$. The mean free path Λ can be extracted as $\Lambda=3D/v$, where v is the average phonon velocity which can be calculated by the slopes of three acoustic phonon branches near the Γ point of the Brillouin zone with taking into account the elastic modulus. For each compound the Debye temperature T_D was estimated taking the Debye frequency as a value of the long-wave lowest energy optic mode frequency. Fig.1a demonstrates an important thermal anisotropy in these crystals and in fig.1b Λ at $T=130\text{K}$ vs. T_D with a quite good linear dependence.

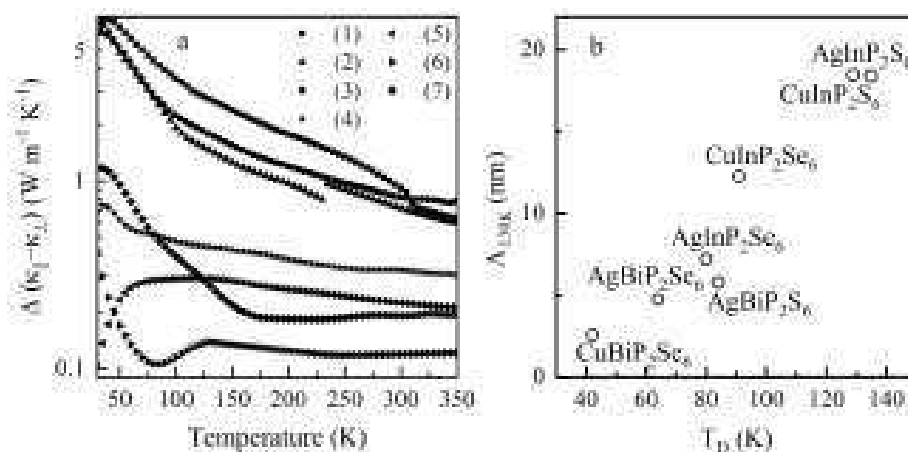


Fig. 1. (a) temperature dependence of anisotropy of thermal conductivity in (1) CuInP_2S_6 , (2) $\text{CuInP}_2\text{Se}_6$, (3) AgInP_2S_6 , (4) $\text{AgInP}_2\text{Se}_6$, (5) AgBiP_2S_6 , (6) $\text{AgBiP}_2\text{Se}_6$ and (7) $\text{CuBiP}_2\text{Se}_6$ layered crystals, (b) Λ of heat transferring phonons at 130K versus T_D along the layers.

[1]. A. Oleaga et al. // *Thermochimica Acta*. – 2007. – V. 459. p. 73-79.

[2]. S. Baroni et al. // *Rev. Mod. Phys.* – 2001. – V. 73. p. 515-562.

Effect of Impurities and Disordering on the Photoluminescence of Crystals and Glasses in the System $\text{Li}_2\text{O} - 7\text{GeO}_2$

O.V. Ohienko*, V.N. Moiseienko, M.D. Volnyanskij

Physics, Electronics and Computer Systems Department, Oles Honchar Dnipro National University, Dnipro, Ukraine

*Corresponding author: kombi21251@outlook.com

In this work, the photoluminescence spectra of weakly polar ferroelectric crystals $\text{Li}_2\text{Ge}_7\text{O}_{15}$ [1] and $\text{Li}_2\text{O}-7\text{GeO}_2$ glasses [2] were studied. The photoluminescence spectra for all samples were excited by a semiconductor laser with $\lambda_{\text{ex}}=405\text{nm}$ in 90-degree geometry. The spectra were recorded using a modified laser spectrometer based on the double monochromator DFS-12. For all initial samples was observed the wide intensive luminescence band with maximum in the region of 525–550nm. The spectral distribution of intensity and the position of the maximum of the band for a $\text{Li}_2\text{Ge}_7\text{O}_{15}$ crystal depended on the excitation wavelength ($\lambda_{\text{ex}}=405\text{nm}$ or 365nm were used). The spectral profile of the luminescence band was broadened in glass containing of 0.67% copper. The intensity of the luminescence band decreased 6 times for glass doped with Cr^{3+} ions (0.01%) as compared with glass containing Cu^{2+} ions. The intense luminescence band of Cr^{3+} ions with $\lambda_{\text{max}}=659\text{nm}$ was appeared starting from 600. In order to identify quantitative differences in the measured spectra, they were decomposed into spectral components. The parameters of the spectra are presented in the table.

Sample	Luminescence band		Spectral components		
	λ_{max} , nm	$\Delta\lambda_{1/2}$, nm	λ_1 , nm	λ_2 , nm	λ_3 , nm
$\text{Li}_2\text{Ge}_7\text{O}_{15}$	548	97	530	565	648
$\text{Li}_2\text{O}-7\text{GeO}_2:\text{Cu}^{2+}$	537	108	530	552	-
$\text{Li}_2\text{O}-7\text{GeO}_2:\text{Cr}^{3+}$	532	89	532	-	-

The assumption about the nature of the broad luminescence band observed in both nominally pure and doped glasses and crystals was made: the source of luminescence can be germanium - oxygen complexes $[\text{GeO}_4]$ and $[\text{GeO}_6]$ of the tetrahedral and octahedral configuration in the material structure.

[1]. Таганцев А. К. // Письма в ЖЭТФ – 1987 – Т. 45 – р. 352-355

[2]. Volnianskii M. D., Nesterov O. O., Trubitsyn M. P. // Ferroelectrics – 2014 – V. 466 – N. 1 – p. 126-130

Magnetic Resonance Properties of $\text{ErAl}_3(\text{BO}_3)_4$ Crystal

S.N. Poperezhai^{*1}, V.A. Bedarev¹, D.N. Merenkov¹, M.I. Kobets¹,
A.A. Zvyagin¹, T. Zajarniuk², A. Szewczyk², M.U. Gutowska², I.A. Gudim³

¹ B.Verkin Institute for Low Temperature Physics and Engineering of NAS
of Ukraine, Kharkiv, Ukraine

² Institute of Physics, Polish Academy of Sciences, Warsaw, Poland

³ Kirensky Institute of Physics, Krasnoyarsk, Russia

**Corresponding author: Sergey.Poperedjay1986@gmail.com*

The rare-earth alumoborates have become of considerable interest for detailed evaluation due to their valuable luminescent and non-linear properties. Erbium alumoborate $\text{ErAl}_3(\text{BO}_3)_4$ is interesting representative of this family. The multiplet $^4I_{15/2}$ is the ground state of the Er^{3+} ion ($S=3/2$, $L=6$, $J=15/2$) in this trigonal crystal. The multiplet $^4I_{15/2}$ is splitted by the crystal field and the ground doublet is separated by $\sim 46 \text{ cm}^{-1}$ from the first excited doublet [1]. Therefore, only one absorption line, associated with transitions between two levels of the main doublet, should be observed in the ESR spectrum. However, a low-intensity additional resonance line was previously detected in the ESR spectrum of $\text{ErAl}_3(\text{BO}_3)_4$ crystal at 4.2 K [2]. The goal of the present work is to clarify the cause of such peculiarities in the ESR spectrum of $\text{ErAl}_3(\text{BO}_3)_4$.

A triplet structure of the main line and a low-intensity additional line had been observed in the ESR spectra at 4.2 K an inclined magnetic field direction from the trigonal axis c of the crystal. In general, the measurements data indicate the observation of spin-cluster resonance [3] which is caused by the existence of magnetically ordered groups of rare-earth ions. In the framework of this model, the appearance of an additional low-intensity line is associated with the flipping of a couple of moments, and the triplet structure arises due to the flips of one magnetic moment in the cluster.

The calorimetric method was used for detect the magnetic clusters in $\text{ErAl}_3(\text{BO}_3)_4$. It was shown that the magnetic subsystem of the crystal inputs a significant contribution to the specific heat capacity at low temperatures. The clusters are due to the establishment of short-range magnetic order in the crystal. The additional absorption line and the triplet structure of the main line have been observed in the ESR spectra and both result from such clusters presence.

[1]. A.V. Malakhovskii, V.V. Sokolov, I.A. Gudim, J. Alloys and Comp., 698, 364 (2017).

[2]. V.A. Bedarev, D. N. Merenkov, M.I. Kobets, S.N. Poperezhai, S.L. Gnatchenko, and I.A. Gudim, Low Temp. Phys. 44, 863 (2018).

[3]. M. Date, M. Motokawa, Phys. Rev. Letters 16, 1111 (1966).

Raman Spectra of Novel Non-Linear Optical Material $\text{PbGa}_2\text{Ge}(\text{S,Se})_6$

N. Mazur¹, V. Dzhagan¹, V. Yukhymchuk¹, Ye. Havryliuk¹, A. Litvinchuk²,
L. Piskach³, M.Ya. Valakh^{1*}

¹ V. Lashkaryov Institute of Semiconductor Physics, NAS of Ukraine, Kyiv, Ukraine

² University of Houston, Houston, Texas, USA

³ Lesya Ukrainka Eastern European National University, Lutsk, Ukraine

**Corresponding author: mvalakh@gmail.com*

Non-linear optical materials are broadly used for frequency conversion of laser emission, including NIR and MIR ranges. It is needed for molecular spectroscopy, optical radars operating in atmosphere, innovative medical diagnostics, and various optoelectronic devices. There is a large number of non-linear materials for visible range, but in the IR the only common compound are $\text{AgGa}(\text{S,Se})_2$. Their low radiation damage threshold stimulates further search for alternative materials. New promising quaternary chalcogenides $\text{PbGa}_2\text{Ge}(\text{S,Se})_6$ were obtained recently[1-3]. Their non-linear optical constants and especially radiation damage threshold are much higher than those of traditional $\text{AgGa}(\text{S,Se})_2$.

Here, we report for the first time the phonon spectra of the $\text{PbGa}_2\text{Ge}(\text{S,Se})_6$, experimentally obtained by Raman spectroscopy and compared to the those calculated by DFT. The latter theoretical approach has proved by us to be very efficient in confirming the structure and phonon spectra of multinary chalcogenides [4,5]. The difficulty with calculating phonons in these complex crystals is a large number of atoms in the unit cell consisting of 16 formula units of $\text{PbGa}_2\text{Ge}(\text{S,Se})_6$. It is formed by chain-like structures of $\text{Ga}(\text{S,Se})_4$ and $\text{Ge}(\text{S,Se})_4$ tetraedra, with the connected with each other tetragonal pyramids $\text{Pb}(\text{S,Se})_4$ filling voids between them. Such unit cell structure featured for many multinary chalcogenides, facilitates qualitative understanding of their phonon spectra. The $\text{Ga}(\text{S,Se})_4$ and $\text{Ge}(\text{S,Se})_4$ tetraedra possess very characteristic patterns of vibrational frequencies, similar to molecular crystals. Therefore, the spectrum of vibrational frequencies of $\text{PbGa}_2\text{Ge}(\text{S,Se})_6$ is formally formed by only four "molecules". Comparison of our experimental and calculated frequencies shows very good agreement, with deviation not exceeding several percent in most cases. We further confirm applicability of the above "molecular" approach to the phonon spectrum of $\text{PbGa}_2\text{Ge}(\text{S,Se})_6$ by comparing its spectrum with spectra of other multinary chalcogenides containing same tetraedra.

[1]. Z.-Z. Luo, C.-S. Lin, H.H. Cui et al // Chem. Mater. 2015, 27, 914.

[2]. Y.-Z. Huang, H. Zhang, C.S. Lin et al // Crystal Growth & Design 2018, 182, 1162.

[3]. A. Fedorchuk, O. Parasyuk, O. Cherniushok et al // J. Alloys & Comp. 2018, 740, 294.

[4]. M.Y. Valakh, V. Dzhagan, Ye. Havryliuk et al // phys. stat. sol. (b) 2018, 255, 1700230.

[5]. M.Y. Valakh, A.P. Litvinchuk, V.M. Dzhagan, // RSC Advances 2016, 6, 67756.

Raman Spectroscopy of Potassium- and Sodium-Containing Argyrodites

Yu.M. Azhniuk^{1,2*}, A.I. Pogodin¹, O.P. Kokhan¹,
I.P. Studenyak¹, D.R.T. Zahn³

¹ Faculty of Physics, Uzhhorod National University, Uzhhorod, Ukraine

² Institute of Electron Physics, Ukr. Nat. Acad. Sci., Uzhhorod, Ukraine

³ Semiconductor Physics, Chemnitz University of Technology, Chemnitz, Germany

*Corresponding author: yu.azhniuk@gmail.com

Among the crystals of the argyrodite family, copper- and silver-containing compounds, in particular $\text{Cu}_6\text{PS}_5\text{I}$, $\text{Cu}_6\text{PS}_5\text{Br}$, and $\text{Cu}_6\text{PS}_5\text{Cl}$, are characterised by high electrical conductivity with a pronounced ionic component useful for potential applications as solid electrolytes, supercapacitors, ion-selective membranes, and other electrochemical devices. In the last decade, lithium-containing $\text{Li}_6\text{PS}_5\text{X}$ (with $\text{X} = \text{Cl}$, Br and I) argyrodite superionic conductors synthesised by a mechanochemical technique or a liquid-phase technique have been widely studied as promising materials for all-solid-state batteries.. To our knowledge, neither potassium-, nor sodium-containing halogenthiophosphates have been reported so far. Here we report on the synthesis of $\text{K}_6\text{PS}_5\text{Br}$, $\text{K}_6\text{PS}_5\text{Cl}$, $\text{Na}_6\text{PS}_5\text{Br}$, and $\text{Na}_6\text{PS}_5\text{Cl}$ compounds and their characterisation by Raman spectroscopy.

Potassium and sodium halogenthiophosphates were synthesised by a two-step technique from elemental substances and relevant alkali halides. Raman measurements were carried out at room temperature using a Horiba LabRAM 800 spectrometer with excitation by a Cobolt Fandango solid-state laser (514.7 nm).

Raman spectra of $\text{K}_6\text{PS}_5\text{Br}$, $\text{K}_6\text{PS}_5\text{Cl}$, $\text{Na}_6\text{PS}_5\text{Br}$, and $\text{Na}_6\text{PS}_5\text{Cl}$ reveal a noticeable similarity to those of chemically related copper and lithium halogenthiophosphates with the most intense peak near 420 cm^{-1} . This is most probably direct evidence for their argyrodite structure with pronounced PS_4 tetrahedral structural groups. The Raman spectra show that the structure of these argyrodite compounds depends on the cation species much stronger than on the halogen atoms. The features in the high-frequency part of the spectra imply that the structure of the sodium-containing argyrodites most likely differs from the cubic structure of $\text{Cu}_6\text{PS}_5\text{Br}$ and $\text{Cu}_6\text{PS}_5\text{Cl}$ argyrodites as well as from the lower-symmetry structure of $\text{K}_6\text{PS}_5\text{Br}$ and $\text{K}_6\text{PS}_5\text{Cl}$. Additionally, features at $446\text{--}449\text{ cm}^{-1}$ and $472\text{--}473\text{ cm}^{-1}$ in the Raman spectra of the synthesised $\text{Na}_6\text{PS}_5\text{Br}$ and $\text{Na}_6\text{PS}_5\text{Cl}$ compounds can be related to the presence of different crystalline polythiophosphate species.

Physical Properties of Crystalline $\text{TlIn}(\text{S}_{1-x}\text{Se}_x)_2$ Solid Solution: Theoretical and Experimental Study

T. Babuka^{*1,2}, O.O. Gomonnai^{3,4}, K.E. Glukhov¹, L.Yu. Kharkhalis¹,
M. Ludemann⁵, D.R.T. Zahn⁵

¹ Institute for Physics and Chemistry of Solid State, Uzhhorod National University, Uzhhorod, Ukraine

² Institute of Physics, Faculty of Mathematics and Natural Science, Jan Dlugosz University in Czestochowa, Czestochowa, Poland

³ Optics Department, Uzhhorod National University, Uzhhorod, Ukraine

⁴ Vlokh Institute of Physical Optics, Lviv, Ukraine

⁵ Semiconductor Physics, Chemnitz University of Technology, Chemnitz, Germany

**Corresponding author: tanya.babuka@gmail.com*

Recently, layered crystals have attracted research interest due to their promising structural and physical properties. A possibility to create new multifunctional artificial materials obtained through the arrangement of several layered crystals became a new subject of studies. One of the representatives of such a class of layered materials is TlInS_2 [1]. It is well known that there are three routes to influence the physical properties of semiconductor crystals: (1) doping with various elements; (2) formation of a homogeneous solid solution; and (3) the use of nanostructures. In our investigations, one of these methods, namely the formation of solid solutions, was applied. The electronic and vibrational properties of solid solutions of $\text{TlIn}(\text{S}_{1-x}\text{Se}_x)_2$ ($x = 0.10, 0.15, 0.25$) crystals were investigated using first-principle calculations and experimental measurements. For the investigation of the electronic properties, the methodology which was previously tested for another chalcogenide crystal was employed [2]. As a result of these calculations the energy band spectra, band gap values, the partial density of states and Mulliken charge population for $\text{TlIn}(\text{S}_{1-x}\text{Se}_x)_2$ solid solutions were obtained. Also, the vibrational properties of the considered solid solutions were investigated. The phonon dispersion curves and partial density of phonon states using density functional theory (DFT) were calculated. The phonon frequencies of $\text{TlIn}(\text{S}_{1-x}\text{Se}_x)_2$ crystals was studied experimentally by Raman spectroscopy. Unpolarised Raman spectra were measured using a Dilor XY 800 spectrometer equipped with a CCD camera. A Kr^+ (647.1 nm) laser was used for excitation. The measurements were performed in the frequency range of $16\text{--}340\text{ cm}^{-1}$ in the temperature range of $30\text{ K} \leq T \leq 293\text{ K}$. Experimentally obtained values were compared with the theoretically calculated data.

[1]. V. Grivickas, P. Scajev, V. Bikbajevs, O.V. Korolik, A.V. Mazanik. // Phys. Chem. Chem. Phys. – 2018. – V. 1. – p. 1 – 13.

[2]. L. Kharkhalis, K.E. Glukhov, T. Babuka, M.V. Liakh. // Phase Transitions. – 2019. – V. 92 – N. 5. – p. 1 – 10.

Manifestation of Intermolecular Interaction in IR Spectra of Behenic Acid Crystal

S.N. Firsunin¹, L.M. Babkov^{*1}, T.V. Bezrodna², T.A. Gavrilko², J. Baran³

¹ Saratov State University, Saratov, Russia

² Institute of Physics, NAS of Ukraine, Kyiv, Ukraine

³ Institute of Low Temperatures and Structure Research, PAN, Wroclaw, Poland

**Corresponding author: lmbabkov@gmail.com*

Fatty acids have been the focus of intense researches since the early 1900s because they are the major components of oils and fats. Lately, an interest on these compounds results from their utilization in the chemical, food and pharmaceutical industries for the production of coatings, plastics, cleaning products, phase change materials for energy storage, and biodiesel. These applications require a good knowledge of their properties and phase behavior as it influences the characteristics of the consumer products.

The aim of the study was to evaluate the effect of intermolecular interaction and hydrogen bonding on the structure and vibrational IR spectrum of crystalline behenic acid, $\text{CH}_3(\text{CH}_2)_{20}\text{COOH}$ (kC_{22}) based on molecular modeling.

For the first time, the density functional theory B3LYP/6-31G (d) method implemented in the GAUSSIAN-03 and GAUSSIAN-09W software package was used for modeling the structures and IR spectra of molecular systems: optimal geometries of kC_{22} molecule and its dimer, as well as kC_4 molecule, its dimer, and two dimer-dimer systems (Fig. 1). Using kC_4 in modeling the dimer-dimer system instead of kC_{22} was a necessary measure: a similar procedure for the kC_{22} is technically much more cumbersome, it would require a very large time resource. The approach did not significantly affect the final result, and the intensity distribution in the calculated IR spectra of the complex of dimers kC_4 is consistent with the experimental one for kC_{22} .

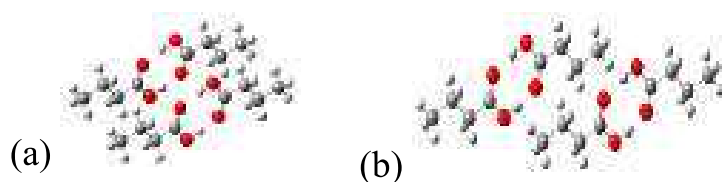


Fig.1. The structures of the kC_4 dimer complexes: (a) “ring-to-ring”, (b) “ring-to-tail”.

The IR spectra of polycrystalline kC_{22} samples sandwiched between two KBr windows were measured with a Bruker IFS 88 FTIR spectrometer in a spectral range $400\text{--}4000\text{ cm}^{-1}$ in a wide temperature range from 11 to 360 K using a 2 cm^{-1} resolution and 64 scans for every spectrum. The effect of intermolecular interaction on the IR spectrum of carboxylic acids, in particular, the behenic acid, is clearly manifested in the ranges of $1100\text{--}1500\text{ cm}^{-1}$ and $2700\text{--}3200\text{ cm}^{-1}$. The obtained results can be estimated as preliminary, requiring additional confirmation on the basis of calculations with account of changes in the orientation of the dimeric rings and the methyl groups in the dimer complexes relative to each other.

IR Spectra of Rubrene and Structural-Dynamic Model of its Molecule

M.M. Kinder^{1*}, L.M. Babkov¹, T.V. Bezrodna², L.V. Viduta²,
T.A. Gavrilko², J. Baran³

¹ Saratov State University, Saratov, Russia

² Institute of Physics, NAS of Ukraine, Kyiv, Ukraine

³ Institute of Low Temperatures and Structure Research, PAN, Wroclaw, Poland

Corresponding author: lmbabkov@gmail.com

In recent years, among other polycyclic aromatic hydrocarbons, orthorhombic rubrene ($C_{42}H_{28}$, 5,6,11,12-tetraphenyltetracene, Rub) single crystals were reported to have the highest charge carrier mobility among organic semiconductors, up to $\sim 40 \text{ cm}^2/\text{Vs}$, which is comparable to that of amorphous silicon. But despite the advances in applications, there are controversies as to the Rub conformational changes both in the bulk and thin layers which effect its liability to oxidation on the open air, so better understanding of the Rub molecular dynamics is crucial for improving the performance of organic devices.

Here we report on the structural-dynamic model of one of stable conformers of the rubrene molecule (Fig. 1) constructed by the density functional theory method B3LYP/6-31G(d). The program complex Gaussian-3 and -9 was used in the calculations of the parameters of the adiabatic potential and the IR spectrum of the rubrene molecule.

The room temperature IR absorption spectra of polycrystalline rubrene thin film vacuum deposited onto a freshly cleaved KBr(100) surface were measured with a Bruker IFS 88 FTIR spectrometer in a spectral range $400\text{--}4000 \text{ cm}^{-1}$ using a 2 cm^{-1} resolution and 64 scans for every spectrum. For the first time, the minimized energy values of the Rub molecule: -2808790 kJ/mol (total) and -8151199 kJ/mol (electron) and the geometric parameters of the molecule were calculated. The lengths of the C-H bonds are within $1.07\text{--}1.09 \text{ \AA}$, C-C bonds – $1.34\text{--}1.44 \text{ \AA}$, and the angles are within $118\text{--}122$ degrees.

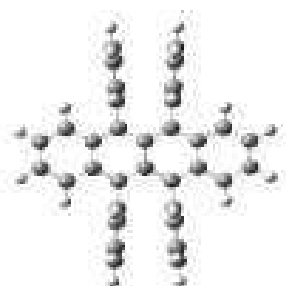


Fig.1. The optimal structure of rubrene molecule

The calculated vibrational spectrum of the Rub molecule and its experimental IR absorption and Raman spectra well agree with each other. It is shown that normal vibrations of the molecule are strongly delocalized in the region of $500\text{--}1650 \text{ cm}^{-1}$. In accordance with the selection rules for symmetry, about half of the normal vibrations have low intensity. Further research on Rub electronic spectra are in progress.

Gold Nanoprisms on a Modified Glass Substrate for Enhancing Raman Spectroscopy Signal

T.I. Borodinova^{1*}, V.I. Styopkin², S.V. Snegir³, V.G. Kravets⁴

¹ F.D. Ovcharenko Institute of Biocolloid Chemistry, National Academy of Science, Kyiv, Ukraine

² Institute of Physics, National Academy of Science, Kyiv, Ukraine

³ Department of Physics, University of Konstanz, Konstanz, Germany

⁴ School of Physics and Astronomy, the University of Manchester, United Kingdom

*Corresponding author: borodinova@ua.fm

Gold nanoparticles (Np) are widely used for enhancing of a molecular signals during Raman spectroscopic studies. The enhancement mainly depends on the size, shape of the particles, the dielectric environment around them and adsorption position of molecules. Therefore, Np surface should be free from any detergents (reducing agents, stabilizers, etc.) for achieving strong and free from artefacts signals.

Herein we present the results of micro Raman spectroscopy studies of rhodamine R6G using free from detergents gold nanoprisms (GNs). These GNs have being grown directly on a modified glass surface. Briefly, the glass was covered initially with (3-aminopropyl)triethoxysilane and then with polyvinylpyrrolidone. The thickness of layers is equal to 16÷20 nm and 12÷15 nm, respectively, and extracted from ellipsometric measurements (Woollam M-2000F). Modified glass it was immersed into a mixture of alcohols (ethanol/ethylene glycol/glycerin) containing 1 mM HAuCl₄ for 48 h under T=80° C to induce formation of the nanoprisms. Synthesized in this way Au nanoprisms have a surface free from stabilizer.

The solution of rhodamine R6G (4 µM) in anisole containing 3% of PMMA was deposited on the surface with gold nanoprisms and without (as the control). Raman spectra (Renishaw, RM 1000, objective ×50) revealed presence of separate bands of rhodamine R6G dye and PMMA. The monitored signals were enhanced up to 10⁴ times (fig.1, curve 2) when excited with laser beam ($\lambda_{exc} = 632,8$ nm) which was focused on a group of gold nanoprisms (Fig.1, inset, point 2).

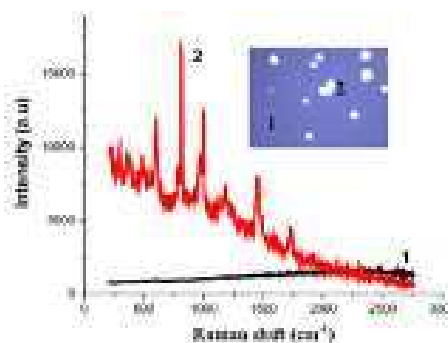


Fig. 1. Raman scattering spectra of rhodamine R6G adsorbed on a glass surface without (curve 1) and with gold nanoprisms (curve 2).

Structural and Optical Studies of Layered Heterogeneous Semiconductor Crystals $\text{Pb}_{1-x}\text{Mn}_x\text{I}_2$

A.P. Bukivskii^{1*}, Z.D. Kovaliuk³, R.V. Gamernyk², G.B. Stryganyuk⁴,
Yu.P. Gnatenko¹, P.M. Bukivskii¹

¹ Institute of Physics, NAS of Ukraine, Kyiv, Ukraine

² Lviv State University, Lviv, Ukraine

³ Chernivtsi Department of the Institute of Problems of Materials Science

⁴ Helmholtz-Zentrum für Umweltforschung, Leipzig, Germany

*Corresponding author: ap.bukivskii@gmail.com

The layered semiconductor PbI_2 crystals are promising materials for the development of highly sensitive scintillation detectors of X-rays and gamma radiation. In this paper, $\text{Pb}_{1-x}\text{Mn}_x\text{I}_2$ crystals grown by the Bridgman method with different concentrations of Mn^{2+} ions ($X = 0.03, 0.05$ and 0.10) were investigated.

The performed morphological studies of the surface using a scanning electron microscope showed that these solid solutions are a system with a rather heterogeneous distribution of manganese ions.

X-ray diffraction studies showed the presence of a 2H-polytype phase of PbI_2 for small concentrations of manganese. For large concentrations (10%) of manganese, both narrow reflexes and reflexes in the form of semi-amorphous halo are observed. The first correspond to PbI_2 4H-polytype, and the second to a non-uniform solid solution of $\text{Pb}_{1-x}\text{Mn}_x\text{I}_2$ of 2H-polytype. The formation of small MnI_2 clusters is also not excluded. These studies showed the absence of any metallic inclusions of Pb or Mn atoms.

Investigation of low-temperature ($T = 4.5\text{K}$) spectra of photoluminescence (PL) and exciton reflection spectra (ER) showed that in the spectra of PL at $T = 4.5\text{ K}$ for the given concentrations of Mn there are three groups of lines: exciton PL in the 2.4921 eV region, which is characteristic of pure PbI_2 crystals, and in the 2.4362 eV spectral region, recombination of donor-acceptor pairs with phonon repetitions on the longwave wing is observed. These two PL groups are characteristic of the regions of pure PbI_2 . In the short-wave part of the spectrum at energies 2.5453 eV for $X = 0.03$, 2.5457 eV for $X = 0.05$ and 2.5986 eV for $X = 0.10$ there is a radiation of the localized on the fluctuations of the potential of the crystal field of excitons, which manifests itself in the regions of $\text{Pb}_{1-x}\text{Mn}_x\text{I}_2$ solid solution. This is confirmed by the fact that the maximum of the PL band at 2.5457 eV coincides with the second maximum in the ER spectrum. In addition, this band is shifted linearly to the short-wave side with increasing concentrations of Mn.

Luminescence Properties of NaY(MoO₄)₂ Polycrystals Doped with Praseodymium (III) Ions

V.P. Chornii^{1,2}, V.V. Boyko¹, S.G. Nedilko², Yu.A. Hizhnyi²,
M.S. Slobodyanyk², K.V. Terebilenko², O.V. Gomenyuk³, V.I. Sheludko³

¹ National University of Life and Environmental Sciences of Ukraine, Kyiv, Ukraine

² Taras Shevchenko National University of Kyiv, Kyiv, Ukraine

³ Oleksandr Dovzhenko Hlukhiv National Pedagogical University, Hlukhiv, Ukraine

*Corresponding author: vchornii@gmail.com

Great attention toward complex oxides materials studies as hosts for rare-earth of (RE) ions has been paid mainly due to their wide absorption bands in a range from vacuum ultraviolet to visible range of light and possible excitation energy transfer from a host to dopants. Thus, the majority of papers have been devoted to luminescence properties of RE ions in various oxides, in particular, in molybdates of general formula A^IB^{III}(MoO₄)₂, where A^I – alkali metal, B^{III} – Y, Bi, La ions [1,2]. The presence of Y, Bi or La in oxide as cations simplifies introduction of RE ions into host lattice because of close ionic radii and the same charge states of these cations and RE - dopants. Pr³⁺- doped oxide compounds intensively studied as perspective red phosphors for application in light-emitting diodes, plasma display panels, field emission displays, etc [2]. At the same time no data on synthesis and luminescence of the Pr³⁺- doped NaY(MoO₄)₂ was reported so far.

A series of solid solutions of NaY_{1-x}Pr_x(MoO₄)₂ (x = 0.01 - 0.15) composition have been prepared by conventional solid state reactions. The phase composition of prepared samples was determined by powder X - Ray diffraction and IR spectroscopy. Photoluminescence (PL) properties were studied using diode-pumped laser ($\lambda_{\text{ex}} = 473 \text{ nm}$) and powerful Xenon lamp DXeL-1000 as PL excitation sources.

It was found that studied samples reveal intensive red luminescence when excited in the region of the $^3\text{H}_4 \rightarrow ^3\text{P}_J f - f$ transitions in the Pr³⁺ ions. The most intensive peaks in photoluminescence spectra are related with $^1\text{D}_2 \rightarrow ^3\text{H}_4$ (593 - 615 nm), $^3\text{P}_0 \rightarrow ^3\text{H}_6$ (615 - 635 nm) and $^3\text{P}_0 \rightarrow ^3\text{F}_2$ (645 - 660 nm) radiation transitions in the Pr³⁺ ions. PL properties have been analyzed on the base of own and literature data on intrinsic luminescence of host and electronic structure calculations.

- [1]. Y. Ding, J. Liu, M. Zeng et al. Tunable morphologies, multicolor properties and applications of RE³⁺ doped NaY(MoO₄)₂ nanocrystals via a facile ligand-assisted reprecipitation process // Dalton Transactions. – 2018. – V. 47. – p. 8697 – 8705.
- [2]. L. Hou, S. Cui, Z. Fu et al. Facile template free synthesis of KLa(MoO₄)₂:Eu³⁺, Tb³⁺ microspheres and their multicolor tunable luminescence // Dalton Transactions. – 2014. – V. 43. – p. 5382 – 5392.

Peculiarities of Resonant Interaction in Paired Impurity Centers of 2-Fluoronaphthalene in Naphthalene

T.V. Bezrodna, N.D. Curmei*, G.V. Klishevich, V.I. Melnik,
V.V. Nesprava, O.M. Roshchyn

Institute of Physics, National Academy of Sciences of Ukraine, Kyiv, Ukraine

**Corresponding author: Curmei_ND@ukr.net*

Low-temperature fluorescence spectrum of 2-fluoronaphthalene in naphthalene at $C < 0.1\%$ consists of two identical series of bands corresponding to two types of impurity centers formed from single molecules. With increasing admixture concentration, a new series of satellites is observed in the fluorescence spectra, consisting of narrow bands located on the long-wave side of the corresponding 0-0 bands of both series. Similar series of bands also appear in the absorption spectra of samples with an admixture concentration of more than 0.1%. So, on both sides of the band $\nu_{02} = 31226 \text{ cm}^{-1}$ doublets from narrow bands approximately of the same intensity are observed: from the long-wave side at a distance 17 and 25 cm^{-1} (long-wave doublet), and from the short-wave side (short-wave doublet) at distances 15 and 24 cm^{-1} . In the fluorescence spectra of such crystals, one series of doublet bands is observed, which position resonantly coincides with the corresponding bands in the absorption spectra of the long-wave doublet. Fluorescence corresponding to the shortwave doublet is absent. Symmetrical arrangement of a pair of doublet bands relative to a single impurity center in the absorption spectra of 2-fluoronaphthalene in naphthalene at high concentrations, the characteristic polarization and the absence of fluorescence associated with the shortwave doublet may indicate the formation of two types of pairwise impurity centers, each consisting of two translationally nonequivalent molecules in one crystal cell. Collective absorption of naphthalene molecules located in one cell of the crystal can be considered as one system with two equiprobable states: the first molecule of the cell is excited, and the second one is not excited and vice versa. With respect to excitation, both molecules of the unit cell are indistinguishable. Thus, molecules of the elementary cell in the crystal field and the electrons in the electric field of the atomic nucleus are related to a principle of the identity of identical particles.

Thus, the presence of the identity of particles leads to the existence of two types of wave functions (symmetric and antisymmetric) related to the split levels of the corresponding systems. Value of the splitting depends on the nature of the interacting particles: a) in the case of S-T-splitting, the operator of the interaction energy of identical particles (electrons) is proportional to $\sim 1/r$; b) for the case of Davydov splitting, the dipole-dipole interaction between the molecules of the unit cell of the crystal is $\sim 1/r^3$, where r is the distance between the identical particles.

Modeling of Vibrational Spectra of $\text{Re}_x\text{W}_{1-x}\text{O}_3$ Solid Solutions

J. Gabrusenoks^{*1}, R. Eglitis¹, J. Purans¹

¹ Institute of Solid State Physics University of Latvia, Riga, Latvia

^{*}*Corresponding author: gabrusen@latnet.lv*

The structure and vibrational spectra of $\text{Re}_x\text{W}_{1-x}\text{O}_3$ solid solutions were simulated at the *ab initio* level with the CRYSTAL14 program patch. An all-electron Gaussian type basis set and Hybrid functionals were used. Calculations were made for different ordered crystalline structures. The cubic lattice parameter show a simple linear behavior of the composition x . Calculations of composition values $x > 0.5$ give a stable crystal lattice of cubic symmetry. If $x < 0.5$ crystalline lattice has imaginary oscillation frequencies, which means instability of cubic crystalline lattice for this solid solution composition. The change in the density of the oscillation states for various values of the solid solution composition is discussed.

Boron Impurities Effect on Titanium Carbide: the Atomic, Electronic and Elastic Properties

T.V. Gorkavenko^{*1}, I.V. Plyushchay¹, O.I. Plyushchay²

¹ Taras Shevchenko National University of Kyiv, Kyiv, Ukraine

² G.V. Kurdyumov Institute for Metal Physics of NAS of Ukraine, Kyiv, Ukraine

**Corresponding author: tvgorka@gmail.com*

One of the most valuable ways to create the TiC–TiB₂ hetero ceramics is the reactive hot pressing of TiC–B₄C precursors. Hence, the actual problem is to uncover the atomic mechanisms of titanium diboride nucleation mechanisms of TiB₂, as well as the theoretical study of the peculiarities of the electronic and elastic properties of TiC with boron impurities.

The first-principle calculation of the atomic, electronic and elastic properties of TiC supercell composed of 24 atoms with boron impurities is presented. The density functional theory in the general gradient approximation using the software package ABINIT has been used for numerical calculation.

The total energy of 24 titanium carbide atoms supercell and boron impurity atoms with different numbers and locations of impurity atoms was calculated. As a result of this study, it was found that impurity boron atoms in titanium carbide do not exhibit a propensity to clustering. The atomic structure changing of titanium carbide in the presence of boron impurities is discussed. The equilibrium distances between adjacent planes of TiC supercell with boron impurities in the substitution and interstitial positions were calculated and analyzed. Our ab initio calculations confirm that the boron atoms being captured by carbon vacancies lead to an increase in the distance between (111) planes in TiC and increase the probability of further boron incorporation into TiC lattice.

The electronic structure of the Ti₁₂C₁₂ supercell, in which carbon atoms were replaced by the impurity boron atoms was calculated. The impurity subzone formed due to the presence of boron impurities is located between the local electron spectra of 2s and 2p carbon states by about 0.24 Hartree below the Fermi level [1]. There is also a slight increase in the density of electronic states directly below the Fermi level. Different coordinate locations of boron impurity atoms affect only on the shape and half-width of the impurity subzone.

The overall compression modulus of 24 titanium carbide atoms supercell and boron impurity atoms with different numbers and locations of impurity atoms was calculated, at the same time certain patterns are not revealed.

[1]. T.V. Gorkavenko, I.V. Plyushchay, A.I. Plyushchay. Ab initio Modeling of Boron Impurities Influence on Electronic Structure of Titanium Carbide // Journal of Nano- and Electronic Physics. – 2018. – V. 10. – N. 6. – p. 06018-1 – 06018-4.

Ab Initio Modelling of Interaction of Transition Metal Dopants with Edge Dislocation in Silicon

T.V. Gorkavenko*, I.V. Plyushchay

Taras Shevchenko National University of Kyiv, Kyiv, Ukraine

*Corresponding author: tvgorka@gmail.com

The calculation of interaction of the edge dislocation with impurity transition metals (Cr, Mn, Co, Ni, Cu) in Si is presented, using the density functional theory in the general gradient approximation. The supercell was composed of 180 Si atoms with the dipole of two edge dislocations and with one of impurity atom near each of the dislocation cores.

The interaction curves of the edge dislocations with impurity atoms in silicon are presented (Fig.1, *a*). The form of the interaction curves corresponds to the well-known Lennard-Jones potential [1, 2]. The equilibrium positions and the binding energies of impurity transition metals near the edge dislocation cores are calculated. The binding energies values are quite large, which indicates the possibility of the impurity atmosphere formation around the dislocation core that is experimentally observed.

The electronic structure of supercell with the dipole of two edge dislocations with impurity transition metals for different impurities positions was calculated and analyzed. In general, the spectra obtained correspond to the spectra of pure Si. The forbidden band is significantly reduced. For most of the positions of the investigated impurities, the sharp peak appears in the forbidden band near the Fermi level (Fig. 1, *b*). Analysis of local spectra allows us to associate this narrow peak near the Fermi level with the electronic states of impurity atoms. The intensity and the fine structure of the impurities peaks depends on the positions of the impurity atoms.

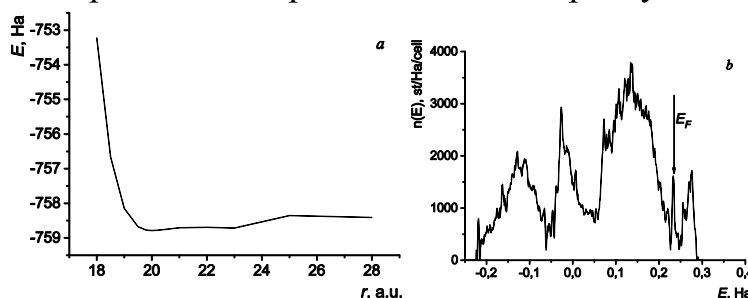


Fig.1. The interaction curve (*a*) and the electronic density of states (*b*) of Si supercell with the dipole of two edge dislocations and Ni.

[1]. T.V. Gorkavenko, I.V. Plyushchay, O.I. Plyushchay, V.A. Makara. Ab Initio Modelling of Interaction of the Edge Dislocation with Oxygen and Carbon Impurity Atoms in Silicon // Journal of Nano- and Electronic Physics. – 2017. – V. 9. – N. 4. – p. 04025-1 – 04025-4.

[2]. T.V. Gorkavenko, I.V. Plyushchay, O.I. Plyushchay, V.A. Makara. Ab initio Calculation of Impurity-Dislocation Interaction in Silicon // Journal of Nano- and Electronic Physics. – 2018. – V. 10. – N. 4. – p. 04030-1 – 04030-5.

FTIR Spectroscopy and DSC Studies of Equimolar Binary Mixtures of Saturated Fatty Acids: Stearic and Behenic Acids

T.A. Gavrilko^{1*}, I.I. Gnatyuk¹, N.A. Holovina², N.D. Shcherban³,
J. Baran⁴, M. Drozd⁴

¹ Institute of Physics, NAS of Ukraine, Kyiv, Ukraine

² L.V. Pisarzhevsky Institute of Physical Chemistry NAS of Ukraine, Kyiv, Ukraine

³ Lesya Ukrainka Eastern European National University, Lutsk, Ukraine

⁴ Institute of Low Temperature and Structure Research, PAS, Wroclaw, Poland

**Corresponding author: gavrilko@gmail.com*

In this work the polymorphism of equimolar binary mixture of saturated fatty acids (FA): stearic, $C_{18}H_{37}OOH$ (SA), and behenic, $C_{22}H_{43}OOH$ (BA), is explored, for the first time, on the micro-scale using DSC measurements complemented by FTIR spectroscopy and X-ray diffraction (XRD). Wide application for FA in the chemical and pharmaceutical industries requires a good knowledge of their properties and phase behavior, but the study of the crystal forms of pure FA, as well as their binary mixtures still is a challenging task. FA are known to exhibit very rich polymorphism with three crystal modifications, in all these modifications the FA molecules are arranged in a double layer structure of molecules hold together by hydrogen bonds between the carboxyl groups and by van-der-Waals forces between the methyl groups. It seemed interesting to study the influence of these kinds of interactions on the polymorphism of the SA-BA binary mixture.

By XRD (Bruker D8 Advance, $Cu_{K\alpha}$ radiation) and DSC (Perkin-Elmer Model 8000) measurements, the existence of a unique phase for the SA-BA equimolar mixture was detected, which indicates the formation of a new compound or a solid solution. Using the models of the temperature effect on vibrational spectra of molecular crystals developed by G.O. Puchkovska [1-3], temperature variable FTIR spectra (Bruker IFS-88, SPECAC Variable Temperature Cell P/N 21.500 with Eurotherm controller 847) were analysed, and it was shown that the structural changes revealed by DSC analysis are associated with an increase of conformational disorder and reorientational motions that contribute to lattice instabilities and the high-temperature phase transition of the SA-BA mixture.

- [1]. G.O. Puchkovska. Manifestation of Structure, Dynamics and Polymorphism in Vibrational Spectra of Molecular Crystals.- Thesis for the Degree of Doctor in Physical and Mathematical Sciences, Kyiv, 1988.
- [2]. G.O. Puchkovska, S.P. Makarenko, V.D. Danchuk, A.P. Kravchuk, J. Baran, E.N. Kotelnikova, S.K. Filatov. Dynamics of molecules and phase transitions in the crystals of pure and binary mixtures of n-paraffins. *Journal of Molecular Structure* 614 (2002) 159–166.
- [3]. G.O. Puchkovska, S.P. Makarenko, V.D. Danchuk, A.P. Kravchuk. Temperature study of resonance intermolecular interaction in normal long-chain carboxylic acid crystals using IR absorption spectra, *Journal of Molecular Structure* 744–747 (2005) 53–58.

Revealing the Role of Defects in the Luminescence Processes in Li_2MoO_4 Crystals by Complex Experimental and Computational Studies

Yu. Hizhnyi^{1*}, S. Nedilko¹, V. Chornii^{1,2}, I. Tupitsyna³, O. Dubovik³,
G. Yakubovskaya³

¹ Taras Shevchenko National University of Kyiv, Kyiv, Ukraine

² National University of Life and Environmental Sciences of Ukraine, Kyiv, Ukraine

³ Institute for Scintillation Materials NAS of Ukraine, Kharkiv, Ukraine

**Corresponding author: hizhnyi@univ.kiev.ua*

The crystals of lithium molybdate Li_2MoO_4 are considered as perspective scintillation materials for cryogenic scintillation bolometers. Understanding of peculiarities of the scintillation (or luminescence) processes in Li_2MoO_4 is a very important step for elaboration of crystals with optimal scintillation characteristics. This work presents the results of complex computational and experimental studies aimed to reveal the mechanisms of luminescence and excitation energy transfer in Li_2MoO_4 crystals. These studies include growth and characterization of samples with various concentrations of point defects, post-growth treatment of the samples, optical absorption and luminescence spectroscopy, TSL measurements as well as the electronic band structure calculations of perfect and defect-containing Li_2MoO_4 crystals.

Single crystals of Li_2MoO_4 were grown by the Czochralski technique in a Pt crucible in room atmosphere or dry air. The luminescence characteristics under photo- and X-ray excitations, the IR and optical transmission spectra, TSL characteristics of the Li_2MoO_4 crystals were measured and analyzed.

The geometry optimized calculations of the electronic band structures and optical constants of ideal and defect-containing Li_2MoO_4 crystals were performed in a super-cell approach using the FP-LAPW method [1]. Several kinds of point defects were considered in calculations. The partial densities of states, the linear optical properties (including absorption and reflectance spectra) and defect transition levels (ionization energies of the defects) were calculated and analyzed. The influence of point defects on the luminescence and energy transfer processes in Li_2MoO_4 crystals was discussed using the obtained results of experiments and calculations.

[1]. P. Blaha, et al, 2001. ISBN 3-9501031-1-2.

EPR and Far Infrared Study of Double Molybdate $\text{CsGd}(\text{MoO}_4)_2$

K. Kutko¹, V. Khrustalyov^{1*}, S. Poperezhai¹, D. Kamenskyi²

¹ B.Verkin Institute for Low Temperature Physics and Engineering of the National Academy of Sciences of Ukraine, Kharkiv, Ukraine

² High Field Magnet Laboratory (HFML – EMFL), Radboud University, Nijmegen, The Netherlands.

*Corresponding author: khrustalyov@ilt.kharkov.ua

$\text{CsGd}(\text{MoO}_4)_2$ belongs to a family of double molybdates compounds with layered crystal structure. They attract a significant attention due to rich phase diagrams and the giant rotational and conventional magnetocaloric effects. Here we report a multi-frequency electron paramagnetic resonance (EPR) and far-infrared (FIR) studies of the $\text{CsGd}(\text{MoO}_4)_2$ which directly probe transitions between electronic levels. Since the splitting of ground state in this compound is relatively small (tens of GHz) [1], the EPR spectroscopy is the most appropriate technique to study the crystal electric field splitting. Fig. 1a shows the EPR spectra of the Gd^{3+} ions in $\text{CsGd}(\text{MoO}_4)_2$ for different frequencies. In all spectra we observe wide absorption peak with g-factor slightly lower than 2. The frequency-field dependence of EPR peak shows on fig.1b (filled circles). The FIR spectra of this compound measured in magnetic fields up to 30T reveals the presence of two peaks. One of them is magnetic field dependent EPR peak (filled squares in Fig.1b). At 0.63 THz we observe the absorption peak (open triangles in Fig.1b) which is not sensitive to the magnetic field applied and have the lattice origin. We demonstrate that easy axis approximation with rhombic distortion of the Gd^{3+} environment is enough to describe the EPR spectra and other magnetic properties of $\text{CsGd}(\text{MoO}_4)_2$.

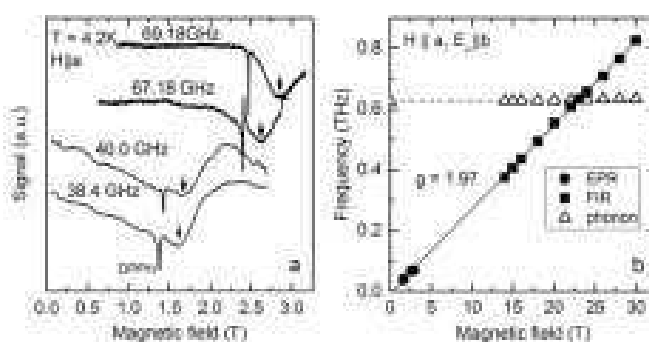


Fig. 1. (a) EPR spectra of the Gd^{3+} ions in $\text{CsGd}(\text{MoO}_4)_2$; (b) frequency-field dependence of electron and phonon excitations.

- [1]. A. Feher, P. Stefanyi, A. Orendacova, et. al. Low-temperature and magnetoresonance properties of a layered $\text{CsGd}(\text{MoO}_4)_2$ crystal // Sov. J. Low. Temp. Phys. – 1988. – V. 14. – p. 723 – 724.

Far-Infrared Spectroscopy Study of $\text{KDy}(\text{MoO}_4)_2$ in Magnetic Field

K.V. Kutko^{1*}, S.M. Poperezhai¹, N.M. Nesterenko¹, D.L. Kamenskyi²

¹ B.Verkin Institute for Low Temperature Physics and Engineering of the National Academy of Sciences of Ukraine, Kharkiv, Ukraine

² High Field Magnet Laboratory (HFML – EMFL), Radboud University, Nijmegen, The Netherlands

*Corresponding author: kkutko@ilt.kharkov.ua

$\text{KDy}(\text{MoO}_4)_2$ exhibits the pseudo Jahn-Teller type phase transition at the temperature $T_{PT} \sim 14$ K, which is accompanied with the renormalization of the electronic excitation spectrum [1]. The magnetic field about 4T, applied along the maximal value of g-factor (at 45° from the axis **a** or **b** in the *ab* plane) leads to the structural transformation of this crystal [2], as supposed, to the high temperature phase. In this work the low-energy spectra up to 70 cm^{-1} at 1.4 K have been studied by Far-Infrared (FIR) spectroscopy in external magnetic field. We have studied the magnetic field dependencies of the electronic and the phonon excitations obtained from experimental FIR Fourier-transmission spectra at $E_\omega || \mathbf{c}$, $\mathbf{H} || \mathbf{b}$, $\mathbf{k} || \mathbf{b}$ (see Fig.1). The behavior of electronic excitations in magnetic field corresponds to the transitions between Zeeman components of the ground and first excited levels. The important feature on frequency field dependence is the region of intersection of electronic branches and phonon excitation which has similar energy (circle in the Fig.1). We discuss the possible linkage of this feature with the phase transition, induced by magnetic field.

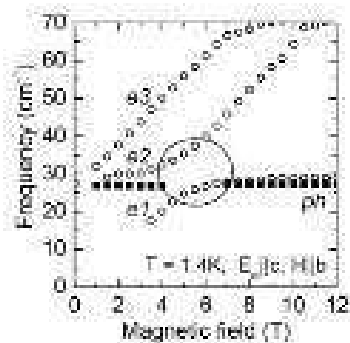


Fig. 1. The magnetic field dependencies of the low frequency excitations at $E_\omega || \mathbf{c}$, $\mathbf{H} || \mathbf{b}$, $T=1.4\text{K}$; *e1*, *e2*, *e3* – electronic and *ph* – phonon excitations.

- [1]. A.A. Zvyagin, K. Kutko, D. Kamenskyi et al. Observation of spontaneous ferriquadrupolar order in $\text{KDy}(\text{MoO}_4)_2$ // Phys. Rev. B. – 2018. – V. 98. – p. 064406 (5pp).
- [2]. M. J. M. Leask, O. S. Tropper, M. L. Wells. Antiferrodistortive Jahn-Teller ordering in $\text{KDy}(\text{MoO}_4)_2$ // J. Phys. C: Solid State Phys. – 1981. – V. 14. – p. 3481 - 3498.

Nonequivalent Ytterbium Centers in BaCaBO₃F:Yb

P. Loiseau¹, S.A. Klimin^{2*}

¹ Laboratoire de la Chimie de la Matière Condensée de Paris, France

² Institute of Spectroscopy RAS, Troitsk, Moscow, Russia

*Corresponding author: klimin@isan.troitsk.ru

BaCaBO₃F (BCBF) is nonlinear crystal perspective as media for self-doubling lasers [1]. It crystallizes in the $P6_2m$ space group [1], while possible structural phase transition to trigonal R3 group is discussed [2]. Yb-doped BCBF has been studied earlier and it was shown that the spectrum of Yb³⁺ ion is complex and can not be described in the frame of the single optical site [3]. In this study we compare the absorption spectra of two BCBF:Yb samples with sufficiently different concentration of ytterbium.

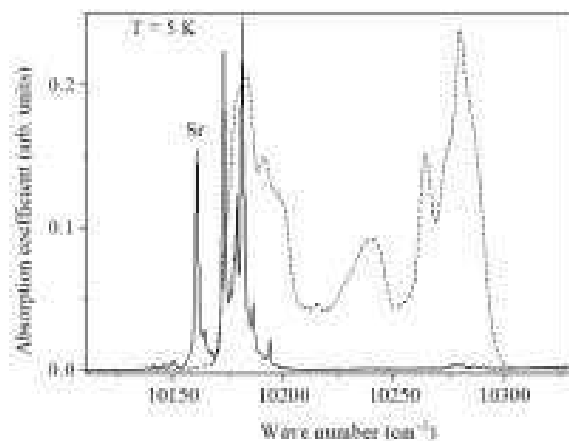


Fig.1 Absorption spectra of BCBF S1 (dashed line) and S2 (solid one) at 5 K in the region of the Yb³⁺ ⁴F_{5/2} multiplet.

The samples were grown by Czochralski technique. Two samples, S1 (Yb 3 at%) and S2 (Sr 10 at%, Yb < 0.1 at%) were studied. The absorption spectra for both samples are presented in Fig. 1. The comparison of the spectra allows to make the following conclusions. At higher concentrations the inhomogeneous broadening does not allow to resolve fine structure of the spectral line. Even at lower concentrations several different optical centers exist due to, possibly, different sorts of centers arising to solve the problem of charge compensation.

The support of the Presidium RAS (Program No. 5 “Photonic technologies in probing inhomogeneous media and biological objects”) is acknowledged.

- [1]. K. Xu, P.Loiseau, G.Aka. BaCaBO₃F: A nonlinear optical crystal investigated for UV light generation // J. Cryst. Growth. – 2009. – V. 311. – N. 8 – p. 2508 - 2512.
- [2]. R.K. Li, Q.D. Zeng. Crystal growth, structure and phase transition of the nonlinear optical crystal BaCaBO₃F // J. Cryst. Growth. – 2013. – V. 382. – N. 1 – p. 47 - 51.
- [3]. K.I. Schaffers, L.D.Deloach, S.A.Payne. Crystal growth, frequency doubling, and infrared laser performance of Yb³⁺:BaCaBO₃F // IEEE Journal of Quantum Electronics. – 1996. – V. 32. – N. 5 – p. 741 - 748.

Percolation Threshold in the Conductivity of $\text{Al}_x\text{Ga}_{1-x}\text{N}:\text{Si}$ Films as Studied by IR-Reflectivity

S.A. Klimin^{1*}, N.N. Novikova¹, V.A. Yakovlev¹, T.V. Malin²,
K.S. Zhuravlev², A.M. Gilinsky²

¹ Institute of Spectroscopy, RAS, Troitsk, Moscow, Russia

² Rzhzanov Institute of Semiconductor Physics, SB RAS, Novosibirsk, Russia

*Corresponding author: klimin@isan.troitsk.ru

Aluminum and gallium nitrides are widely used in a light-emitting devices, photodetectors, microwave transistors, and so on. New possibilities for the development of light sources are opened due to new effects discovered in these objects (e.g., superradiance [1], conductivity in doped samples [2]). In this work IR-reflectivity of the $\text{Al}_x\text{Ga}_{1-x}\text{N}:\text{Si}$ films was studied with the aim to obtain dependences of their properties on the concentration x .

Si-doped lLayers of solid solutions $\text{Al}_x\text{Ga}_{1-x}\text{N}$, 1.2 μm thick, were grown on the sapphire (0001) substrates with buffer layer of AlN ~ 300 nm. The reflectivity spectra were measured using Bruker IFS66 spectrometer. Optical parameters were extracted from modeling reflectivity spectra applying the following model for dielectric function:

$$\varepsilon(\nu) = \varepsilon - \frac{\varepsilon_\infty \nu_p^2}{\nu^2 + i\nu\nu_\tau} + \frac{S^2}{\nu_{T0}^2 - \nu^2 - i\nu\gamma}$$

Both conductivity measurements, and plasma frequencies ν_p demonstrate a threshold behavior.

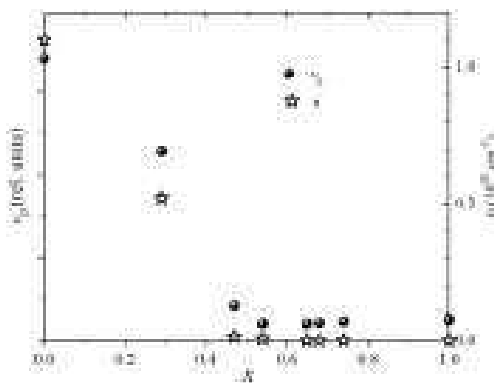


Fig. 1. Plasma frequency S_p and dependence on the concentration x .

Support by the Presidium RAS (Program No. 5 “Photonic technologies in probing inhomogeneous media and biological objects”) and by RFBR (grant No. 18-52-00008) is acknowledged.

[1]. P.A. Bokhan, et.al. Luminescence and superradiance in electron-beam-excited $\text{Al}_x\text{Ga}_{1-x}\text{N}$, // J. Appl. Phys. – 2014 – V. 116. – p. 113103 - 1 - 6.

[2]. H. Yamada, et.al. Deep-level traps in lightly Si-doped n -GaN on free-standing m -oriented GaN substrates // AIP Advances. . – 2018 – V. 8. – p. 045311 - 1 - 9.

Electronic Structure of RCoO₃ Compounds. Spin-Crossover Effects

A.A. Lyogenkaya^{*1}, G.E. Grechnev¹, A.S. Panfilov¹, I.P. Kobzar¹,
V.O. Pashchenko¹, L.O. Vasylechko², V.M. Hreb², A.V. Kovalevsky³

¹ B.Verkin Institute for Low Temperature Physics and Engineering of NAS of Ukraine, Kharkiv, Ukraine

² Lviv Polytechnic National University, Lviv, Ukraine

³ CICECO - Aveiro Institute of Materials, University of Aveiro, Aveiro, Portugal

**Corresponding author: lyogenkaya@ilt.kharkov.ua*

In RCoO₃ cobaltites the Co³⁺ ions can exist in three different spin states corresponding to the low (LS), intermediate (IS) and high (HS) spin values. The energy difference between these states is rather small and their relative positions appear to be very sensitive to external factors such as temperature, pressure and magnetic field.

We have performed DFT+U calculations of electronic structure of RCoO₃ compounds that indicate the possibility of the LS–IS spin states crossover when the unit cell volume increases due to thermal expansion (Fig. 1). This situation particularly manifested in magnetic, transport, and structural properties. Based on this we have studied the effects of temperature and hydrostatic pressure on magnetic susceptibility of RCoO₃ including chemical pressure effect in La_{1-x}Pr_xCoO₃ ($x=0, 0.1, 0.3$) compounds.

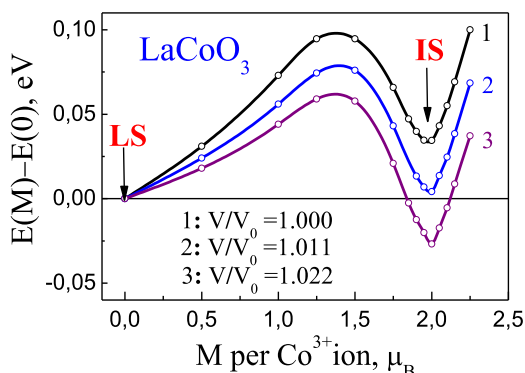


Fig. 1. Dependence of the total energy of LaCoO₃ on magnetic moment of Co³⁺ ion (calculated for volumes close to the theoretical volume V₀).

The obtained experimental results are analyzed with the use of the two-level model in terms of a change in population of the excited state of Co³⁺ ions under the action of temperature and pressure. One of the main results of the work is a quantitative estimation of the anomalously large volume dependence of the excited state energy which is a principal source of the temperature dependence of this parameter due to the effect of thermal expansion.

We acknowledge partial support of the Ukrainian MES under project DB/Feryt, N 0118U000264. This work was performed using computational facilities of grid-cluster LTPE of the NASU.

Linear Dielectric Response of Cobalt Iron Boron Alloys

V.O. Lysiuk¹, S.G. Rozouvan^{2*}, V.S. Stashchuk², V.V. Stukalenko²

¹ V. Lashkaryov Institute of Semiconductor Physics, NAS of Ukraine, Kyiv, Ukraine

² Department of Physics, Taras Shevchenko National University of Kyiv, Ukraine

**Corresponding author: sgr@univ.kiev.ua*

Dielectric permittivity dispersive curves of Co, Fe and B based alloys were numerically calculated by the all-electron full potential linearized augmented plane wave (LAPW) method. The momentum matrix elements were evaluated in detail for the LAPW basis, and the optical spectra were calculated taking into account the Brillouin zone symmetry and possible bands combinations. The frequency dependent three diagonal components of dielectric permittivity tensor were obtained. A case of nonzero ϵ_{O-2ns} off-diagonal element was discussed as indicating on difference in primitive vectors orientation in respect to optical anisotropy of the crystal. Optical properties of the alloy were studied experimentally by spectral ellipsometry. The alloy densities of states properties can be explained taking into account d- zones and p- zones localization. Theory conclusions were experimentally illustrated by applying scanning tunneling microscopy with atomic spatial resolution.

Manifestation of Crystal Size Effect in Polaritonic Luminescence from Rare-Gas Solids

A.N. Ogurtsov^{*}, O.N. Bliznjuk, N.Yu. Masalitina

National Technical University “KhPI”, Kharkov, Ukraine

^{*}*Corresponding author: anogurtsov@ukr.net*

The exciton-photon interaction leads to the formation of polaritonic states energetically positioned at both sides of the initial exciton. In a large ideal crystal of cubic symmetry, where the interval of the longitudinal-transverse splitting does not contain excitonic levels, the polaritonic dispersion branches lie beyond this interval at both sides of its boundaries. On the contrary, in a crystalline grain comparable or less in size than the wavelength in the substance, the interval of the longitudinal-transverse splitting is filled in continuously by excitonic states intercepting a significant part of the oscillator strength of the excitonic transition. Previously the formation of the lower polaritonic state was traced by the red shift of the luminescence from Rare-gas solids (solid Kr and Xe) relative to the bottom E of the lowest excitonic band. In the present paper we explore the new crystal growing technique, which allowed to obtain the samples with essentially improved crystallographic properties and to resolve the internal structure of the luminescence bands at the edge of exciton absorption. The experiments were carried out at the SUPERLUMI experimental station at HASYLAB, DESY, Hamburg. Unlike previous works, where the red polaritonic shift was small commensurably with a weak inelastic polariton-photon scattering, a large polaritonic shift of luminescence is not due to energy dissipation, the energy conservation law being met due to equal probabilities for opposite-sign energy shifts. Such effect is possible if the crystalline grains are comparable in size with light wavelength, which provides the filling in the interval of the longitudinal-transverse splitting by excitons with sufficient oscillator strength. And the sample structure must be perfect enough to lowering the exciton scattering rate with respect to the rate of the polariton formation through exciton-photon coupling. For the first time the excitation spectra of free-exciton luminescence band were recorded simultaneously below the bottom of excitonic band E and within the interval of the longitudinal-transverse splitting. The luminescence of non-equilibrium polaritons was observed both within the longitudinal-transverse splitting interval and at photoexcitation below E . The excitation spectrum below the bottom of excitonic band is determined by competition of two processes. The first one is the creation of excitons by photons with energy E at the Lorenz tail of excitonic absorption. The second process is a competing absorption related to the direct formation of two-site excitonic polarons (self-trapped excitons).

Phonon and Magnon Raman Scattering in MnPS₃ Single Crystal

A.V. Peschanskii^{*1}, T.Ya. Babuka^{2,3}, K.E. Glukhov², M. Makowska-Janusik³, S.L. Gnatchenko¹, Yu.M. Vysochanskii²

¹ B.Verkin Institute for Low Temperature Physics and Engineering of the National Academy of Sciences of Ukraine, Kharkov, Ukraine

² Institute for Solid State Physics and Chemistry, Uzhgorod National University, Uzhgorod, Ukraine

³ Institute of Physics, Jan Dlugosz University in Czestochowa, Czestochowa, Poland

**Corresponding author: peschansky@ilt.kharkov.ua*

The interest in the magnetic properties of the MnPS₃ crystals is caused by unusual placement of the manganese ions forming the honeycomb lattice. For the first time the evolution of polarized Raman spectra of MnPS₃ near the phase transition $T_N = 78$ K is presented in fig.1a. To extract the magnetic scattering we subtracted the phonon spectra from the spectra presented in fig.1a. It was found that the magnetic scattering spectrum has a complex shape which is associated with the presence of both a two-magnon (~ 177 cm⁻¹) and phonon-magnon (~ 156 cm⁻¹) bands (fig.1b). We have found a kink-stepped behavior of the 116.5 and 151.6 cm⁻¹ vibrational modes upon cooling at T_N (fig.1c). This indicates a strong interaction between the phonon and the magnetic subsystems. The vibrational properties of the MnPS₃ crystal were calculated taking into account the LDA approximation with DFT-D (OBS) dispersion correction implemented in the CASTEP package.

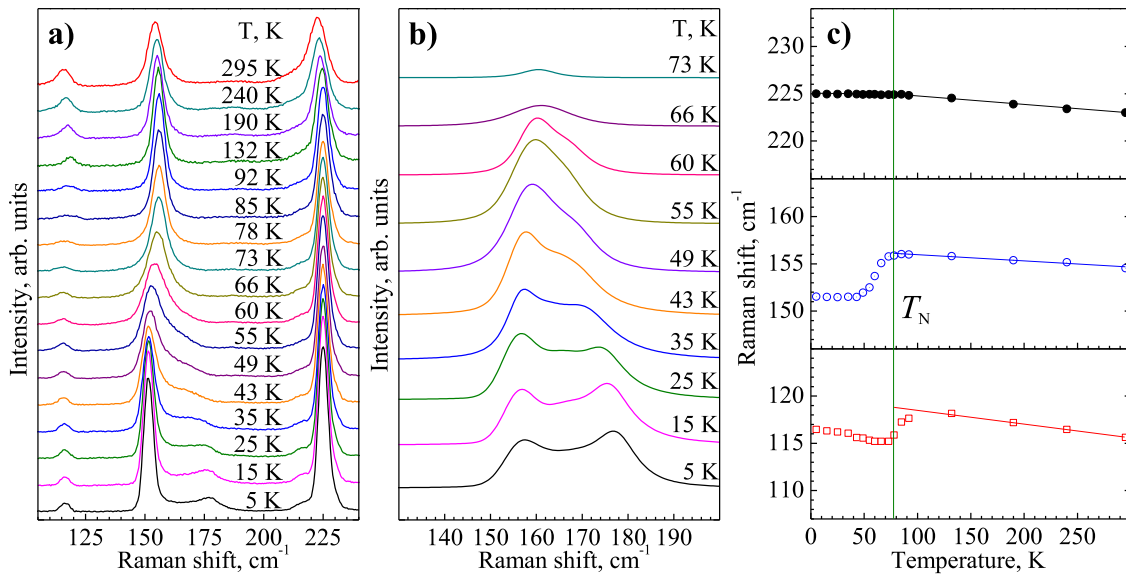


Fig. 1. Temperature dependence of: a) Raman spectra, b) magnetic scattering, c) frequency of B_g phonon modes: \square – 116.5, \circ – 151.6, \bullet – 225.0 cm⁻¹

The obtained results demonstrate the good accordance with experimental Raman spectra. According to performed calculations, the manganese ions are involved in the 116.5 and 151.6 cm⁻¹ vibrational modes.

Investigation of Magnetic Phase Transition in LiNiPO₄ Single Crystal by Raman Scattering

A.V. Peschanskii*

B. Verkin Institute for Low Temperature Physics and Engineering of the National Academy of Sciences of Ukraine, Kharkov, Ukraine

*Corresponding author: peschansky@ilt.kharkov.ua

The interest in the magnetic properties of the LiNiPO₄ crystals is caused by a strong linear magneto-electric effect in the antiferromagnetic state. In our earlier studies, there were presented Raman spectra below (5 K) and above (25 K) of the phase transition to a magnetically ordered state [1]. Here, we report for the first time the evolution of polarized Raman spectra of LiNiPO₄ near the phase transition at $T_N = 21.8$ K presented in fig. 1: a) – A_g , b) – B_{1g} , c) – B_{3g} modes. The observed low-frequency peaks are attributed to one-magnon and two-magnon scattering. The origin of these magnetic excitations is discussed in comparison with the neutron scattering data [2].

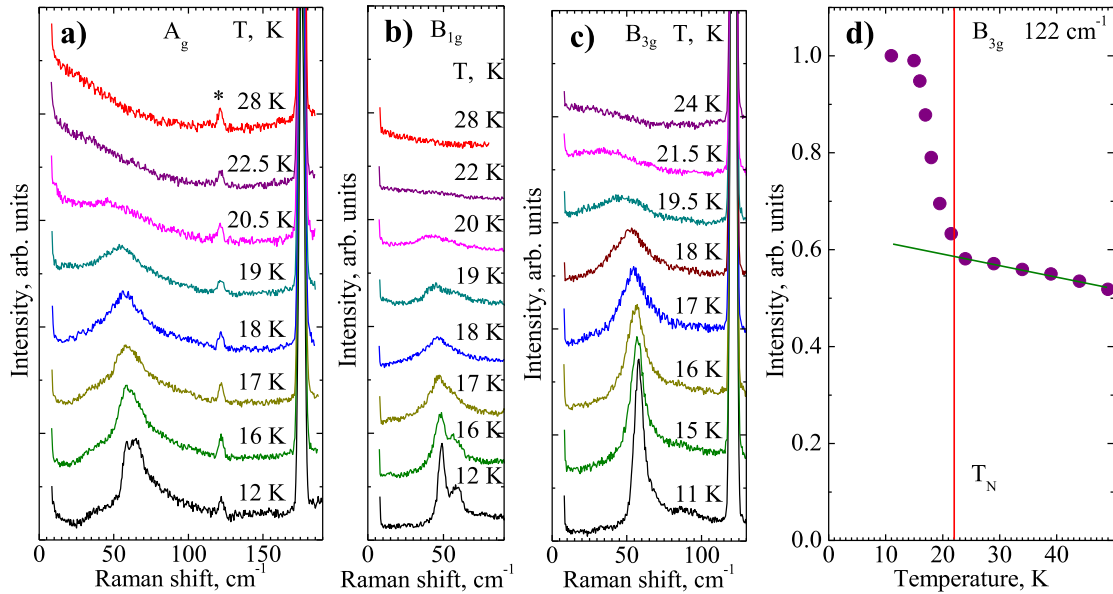


Fig. 1. Temperature dependence of polarized Raman spectra for: a) A_g , b) B_{1g} , c) B_{3g} modes and d) intensity of B_{3g} phonon modes 122 cm⁻¹

During the transition to the antiferromagnetic state, we revealed a change in the intensities of the Raman lines. This effect is the most pronounced for the B_{3g} modes. As an example, the temperature evolution of the integral intensity of the line corresponding to B_{3g} phonon modes 122 cm⁻¹ is shown in fig. 1d. At the same time the frequency position and the linewidth of this mode don't demonstrate the marked changes at T_N .

- [1]. V.I. Fomin, V.P. Gnezdilov, V.S. Kurnosov, A.V. Peschanskii et al. // Low. Temp. Phys. – 2002. – V. 28. – N. 3 – p. 203 – 209.
- [2]. T.B.S. Jensen, N.B. Christensen, M. Kenzelman, et al. // Phys. Rev. B – 2009. – V. 79. – 092413 (4).

Methods for Calculating Magneto-Optical Properties in Ferromagnetic Materials

V. Stashchuk¹, V. Stukalenko^{*1}, S. Rozouvan¹

¹Department of Physics, Taras Shevchenko National University of Kyiv

^{*}*Corresponding author: stu@univ.kiev.ua*

Various calculations techniques have been widely used for studying optical and magneto-optical characteristics in ferromagnetic materials,. Optical conductivity of the materials $\sigma(h\nu) = 4\pi\varepsilon_0 n(h\nu)\kappa(h\nu)$, where h - is the Planck constant, ν - is frequency of light, ε_0 - is the electric constant, $n(h\nu)$, $\kappa(h\nu)$ - are the refractive index and the extinction coefficient of the complex refractive index $\tilde{n}(h\nu) = n(h\nu) - i\kappa(h\nu)$, is in proportion to the density of states. Contributions to the optical conductivity $\sigma(h\nu)$ consist of additive sums of conductivities affected by interband transitions of electrons with different spins. The materials magneto-optical properties can be explored by measuring the values of the complex Kerr angle ($\tilde{\Theta}(h\nu) = \theta(h\nu) - i\eta(h\nu)$) of the reflected light, where the real part $\theta(h\nu)$ is the rotation of the plane polarization of the light, the complex part $\eta(h\nu)$ - is light ellipticity. We calculated optical and magneto-optical properties of ferromagnetics applying theoretical models which were reported earlier in the literature. It allowed us to find a connection between conductivity and measured numbers of the complex Kerr angle $\tilde{\Theta}$, in order to establish the most proper technique for the experimental data processing. The behavior of the dispersion curves of optical conductivity diagonal and non-diagonal components depends on options of the sign of imaginary part of the complex Kerr angle and refractive index, which should be taken into account at some point in data analysis. The differences between dispersion dependencies are insignificant in the energies region higher then 4.5 eV.

Ellipsometric Studies of $(\text{Cu}_{1-x}\text{Ag}_x)_7\text{SiS}_5\text{I}$ Mixed Crystals

I.P. Studenyak^{*1}, A.I. Pogodin¹, V.I. Studenyak¹, B. Grančič², P. Kúš²

¹ Applied Physics Department, Uzhhorod National University, Uzhhorod, Ukraine

² Department of Experimental Physics, Comenius University, Bratislava, Slovakia

**Corresponding author: studenyak@dr.com*

$(\text{Cu}_{1-x}\text{Ag}_x)_7\text{SiS}_5\text{I}$ mixed crystals belong to the family of compounds with argyrodite structure and are known as the superionic conductors. In the present paper we study the spectral dependences of the refractive index and extinction coefficient for $(\text{Cu}_{1-x}\text{Ag}_x)_7\text{SiS}_5\text{I}$ mixed crystals in the wide spectral range by the ellipsometry technique.

Synthesis of $\text{Cu}_7\text{SiS}_5\text{I}$, $\text{Ag}_7\text{SiS}_5\text{I}$ and $(\text{Cu}_{1-x}\text{Ag}_x)_7\text{SiS}_5\text{I}$ mixed crystals was performed in vacuumed (0.13 Pa) quartz ampoules. Synthesis of $\text{Cu}_7\text{SiS}_5\text{I}$ and $\text{Ag}_7\text{SiS}_5\text{I}$ compounds was carried out by the two-temperature method, the maximum temperature values of synthesis were 1465 K for $\text{Cu}_7\text{SiS}_5\text{I}$ and 1229 K for $\text{Ag}_7\text{SiS}_5\text{I}$ which were on 50 K above the melting point. Synthesis of $(\text{Cu}_{1-x}\text{Ag}_x)_7\text{SiS}_5\text{I}$ mixed crystals was carried out by the direct one-temperature method from the previously synthesized $\text{Cu}_7\text{SiS}_5\text{I}$ and $\text{Ag}_7\text{SiS}_5\text{I}$ at the maximum temperature value of 1465 K (during 24 hours), the temperature of annealing was 573 K (72 hours). Increase of Ag content leads to the increase of cubic lattice parameter in $(\text{Cu}_{1-x}\text{Ag}_x)_7\text{SiS}_5\text{I}$ mixed crystals, the variation of the lattice parameter with $\text{Cu} \rightarrow \text{Ag}$ cationic substitution is described by the Vegard's law.

Spectroscopic ellipsometer M-2000V was used for optical constant measurements. Refractive indices n and extinction coefficients k for $(\text{Cu}_{1-x}\text{Ag}_x)_7\text{SiS}_5\text{I}$ mixed crystals were obtained from the spectral ellipsometry measurements which were carried out in the spectral range of 0.3–1.0 μm . In the transparency region the refractive index dispersion is observed, besides, the refractive index increases when approaching to the absorption edge. The two anomaly dispersion regions of refractive index are revealed in the regions of the extinction coefficient increase. The long wavelength anomaly corresponds to the band-to-band optical transition and the spectral position of this anomaly relates to the energy pseudogap value. Another short wavelength anomaly possibly corresponds to the interband Van Hove-Phillips singularity.

The compositional dependences of the refractive index and energy pseudogap for $(\text{Cu}_{1-x}\text{Ag}_x)_7\text{SiS}_5\text{I}$ mixed crystals were obtained from the spectral ellipsometry measurements. It should be noted that the energy pseudogap values in this case were determined as the spectral position of the short wavelength knee which was observed on the spectral dependences of extinction coefficient k . The nonlinear decrease of energy pseudogap with Ag content increase as well as the nonlinear dependence with a maximum for refractive index are revealed.

Characterization of Solid Catanionic Mixtures of Alkyltrimethylammonium Bromides and Even Saturated Fatty Acids by XRD, Differential Scanning Calorimetry and FTIR Spectroscopy

T.A. Gavrilko^{*1}, I.I. Gnatyuk¹, V.I. Styopkin¹, N.D. Shcherban²,
J. Baran³, M. Drozd³

¹ Institute of Physics, NAS of Ukraine, 46, Nauky Ave., 03028 Kyiv, Ukraine

² L.V. Pisarzhevsky Institute of Physical Chemistry NAS of Ukraine, 31, Nauki Ave., 03028 Kyiv, Ukraine

³ Institute of Low Temperature and Structure Research, PAS, 2, Okolna Str., 50-950 Wroclaw, Poland

**Corresponding author: gavrilko@gmail.com*

Catanionic surfactants (CAS) are chemical species consisting of a pair of amphiphilic anionic and cationic molecules. They show a remarkable ability to self-assemble giving a variety of structures at the air/water interface and in solution that makes them attractive for applications in industry, medicine, cosmetics, and pharmacology. However, a relationship between the molecular structure and macroscopic properties of CAS is not fully understood so far.

Here we study the crystalline structure and phase transitions of equimolar catanionic mixtures of alkyltrimethylammonium bromides (n TAB) and fatty acids (n FA). The effect of a combination of the $N^+(CH_3)_3$ headgroup with different alkyl chain lengths, $(CH_2)_{18}$ and $(CH_2)_{16}$ of n TAB, as well as their different asymmetry with the n FA chain lengths $(CH_2)_{12}$ through $(CH_2)_{22}$ was elucidated. XRD (Bruker D8 Advance, $Cu_{K\alpha}$) showed a layered structure of the studied complexes, the lamella thickness being dependent on the symmetry of alkyl chains of the constituents. With DCS (Perkin-Elmer Model 8000) and temperature variable FTIR spectroscopy (Bruker IFS-88, SPECAC Variable Temperature Cell P/N 21.500), the phase transition temperatures were identified and molecular dynamics in various phases was elucidated based on theoretical model of the temperature dependence of Davydov splitting of vibrational excitons in molecular crystals. It is concluded that the balance between the electrostatic interactions between the FA and TAB heads, and the hydrophobic interactions between the aliphatic chains, results in their specific arrangement within the bilayers, and a corresponding crystal packing model is proposed.

Influence of Mn^{+2} Ions on Parameters of the NQR Spectrum I^{127} of a Mixed Layered Semiconductor $\text{Pb}_{1-x}\text{Mn}_x\text{I}_2$

I.G. Vertegel*, E.D. Chesnokov, O.I. Ovcharenko, A.V. Bondar,
A.P. Bukivskii, I.I. Vertegel, Yu.P. Gnatenko

Institute of Physics of NASU, 46, Prospect Nauky, Kyiv 03680

*Corresponding author: vertegel_igor@ukr.net

In this work, for the first time, the concentration dependence of the NQR spectrum I^{127} ($\pm 3/2 \leftrightarrow \pm 5/2$) parameters of $\text{Pb}_{1-x}\text{Mn}_x\text{I}_2$ layered semiconductor crystals for different Mn concentration ($x = 0.0, 0.03, 0.05, 0.1$) was investigated. The obtained results show that for $\text{Pb}_{1-x}\text{Mn}_x\text{I}_2$ crystals ($0 \leq x \leq 0.05$) Mn^{2+} ions preferably replace Pb^{2+} ions in the crystalline layers, which cause a change in the width of the I^{127} NQR line, but does not change the NQR frequency of I^{127} line ($\pm 3/2 \leftrightarrow \pm 5/2$).

It was found that for the I^{127} NQR spectrum of the $\text{Pb}_{1-x}\text{Mn}_x\text{I}_2$ crystals the total integral intensity of the lines with $x = 0.03$ and $x = 0.05$, converted per unit mass, more than an order of magnitude exceeds the intensity of the NQR line for pure PbI_2 crystals. This result shows that the intensity of the NQR line for the investigated crystals is determined by the ferromagnetic nature of the exchange interaction of manganese ions.

In order to determine the mechanism of the interaction of nuclear spins I^{127} with the $\text{Pb}_{1-x}\text{Mn}_x\text{I}_2$ crystal lattice, we studied the concentration dependence of the spin-lattice nuclear quadrupole relaxation time T_1 . The values of time T_1 are determined, for $x=0$, $T=77$ K, $T_1=7.2 \pm 1.4$ mc; at $x=0.05$; $T_1=6.6 \pm 1.2$ mc, with $x=0.1$; $T_1=6.05 \pm 1.2$ mc. It was also established that the decrease in the magnetization of the system of nuclear spins has a single-exponential type. It is known [1] that in PbI_2 crystals at $T=77$ K, the main mechanism of spin-lattice relaxation is the modulation of the intracrystalline field by flexural vibrations. The results obtained by us indicate that in the crystals under study for $x=0.05$ and $x=0.1$, the thermal modulation of the magnetic dipole interaction of Mn^{+2} ions with the nearest I^{127} nuclei also acts as a spin-lattice relaxation mechanism.

The study of the concentration dependence of the integral intensity of the NQR spectra parameters for different Mn concentrations ($0.00 \leq x \leq 0.10$) have been performed. This allowed us to assume the formation of nanocluster domains in the $\text{Pb}_{1-x}\text{Mn}_x\text{I}_2$ crystal.

- [1]. B.E.Vugmeister, M.D.Clinchuk, U.M.Zaritskii et al. Spin-lattice relaxation due to flexural vibrations in layered crystals. Sov.Phys.JETP, vol.42, No.5, 1975. P.892-895.

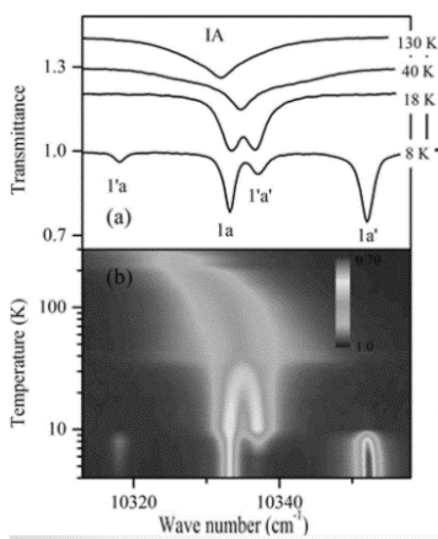
Optical spectroscopy of Kramers ions in studying rare-earth francisites $\text{Cu}_3\text{RE}(\text{SeO}_3)_2\text{O}_2\text{Cl}$

S. A. Klimin

Institute of Spectroscopy RAS, Troitsk, Moscow, Russia

e-mail: klimin@isan.troitsk.ru

Rare-earth (RE) francisites, $\text{Cu}_3\text{RE}(\text{SeO}_3)_2\text{O}_2\text{Cl}$ [1-5], are synthetic counterparts of the natural mineral francisite, $\text{Cu}_3\text{Bi}(\text{SeO}_3)_2\text{O}_2\text{Cl}$. They are 2D frustrated magnets, with possible Kosterlitz-Thouless transition from a paramagnetic state to a phase with quasi-long-range spin order [2]. RE francisites have a magnetic system composed of two subsystems, namely, RE and copper ones. The strongest d-d interactions in weakly interacting between each other copper planes lead to a magnetic ordering at low temperature, the Neel temperature being 24 K for bismuth ancestor of the family and in the range 32-39 K for the RE series of the compounds. RE magnetic subsystem can be highly anisotropic, which can results in spin-reorientational transitions. In



this study, optical low-temperature measurements of $f-f$ electronic transitions in compounds with Kramers RE ions, were performed, with the aim to investigate magnetic ordering and RE single-ion anisotropy in francisites family.

Transmission spectra in a wide spectral (1800 – 12000 cm^{-1}) and temperature (4 – 300 K) ranges were measured with the aid of a Fourier spectrometer Bruker IFS125HR for the compounds with RE = Sm, Yb, Er, Nd, Dy. The example of the spectra for the $\text{Cu}_3\text{Yb}(\text{SeO}_3)_2\text{O}_2\text{Cl}$ is shown in Fig. 1.

The author is grateful to P.S. Berdonosov and E.S Kuznetsova (Lomonosov Moscow State University), who kindly supplied him with the samples. The support of RFBR (grant № 19-02-00251) is acknowledged.

Fig. 1. Two phase transitions in $\text{Cu}_3\text{Yb}(\text{SeO}_3)_2\text{O}_2\text{Cl}$.

(a) Transmission spectra at various temperatures, (b) the intensity map.

- [1] A. Pring, B.M. Gatehouse, W.D. Birch, Amer. Mineral. 75 (1990) 1421.
- [2] M. Pregelj, O. Zaharko, A. Günther, et al., Phys. Rev. B 86 (2012) 144409.
- [3] K.V. Zakharov, E.A. Zvereva, P.S. Berdonosov, et al., Phys. Rev. B 90 (2014) 214417.
- [4] K.V. Zakharov, et al., Phys. Rev. B 94 (2016) 054401.
- [5] P.S. Berdonosov, V.A. Dolgikh, Rus. J. Inorg. Chem. 53 (2008) 1353.

4

Liquid Crystals

Visualization of the Topological Defects in Liquid Crystal Cells

P. Golub*, M. Vasnetsov

Department of Optical Quantum Electronic Institute of Physics of the NAS of Ukraine, Kyiv, Ukraine

**Corresponding author: pvgolub@live.com*

We report the series of the experiments which main aim was the visualization of a topological defect i.e. making it visible with naked eye. The several methods of the visualization are proposed and discussed. We observed that small spheres with size about 1 μm and same sized diamonds and cylinders are well visible in the liquid crystal (LC) cell, but they produce strong distortion of the order parameter around them and, as result, distortion of the disclination itself.

Other objects that were used to visualize the topological defect were bubbles and it was first observed that quite big bubble (up to 0.5 mm) could be moved by the disclination without strong distortion of the disclination and disordering. However the bubbles are easily aggregated to one big bubble which is hard to move by disclination in a cell.

To visualize the motion of the defect the jump of the selective reflectance wavelength on the defect could be used. It is well visible in thin cell and causes no distortion in LC order. It can be used for precise measurements of chirality variations and other measurements based on external influence.

Optical Transmittance and Luminescence Studies of Liquid Crystal Dispersions of CeO₂ Nanoparticles

A.N. Samoilov*, V.K. Klochkov, P.O. Maksimchuk, S.S. Minenko,
L.N. Lisetski

Institute for Scintillation Materials of NAS of Ukraine, Kharkov, Ukraine

**Corresponding author: samoilovisma@gmail.com*

Optical transmission spectra have been studied (Shimadzu UV-2450) for dispersions of CeO₂ nanoparticles in nematic (5CB) and cholesteric (mixture of cholesterol esters M5) liquid crystal (LC) matrices. LC+CeO₂ dispersions in the dopant concentration range of 0.01-0.1% (mass) were obtained by adding the appropriate amount of the ~10 nm size nanoparticles in the powder form to the LC matrix in the isotropic state, followed by ultrasonication (UZD 22/44). For all the systems studied, optical transmission slightly varied with temperature in the LC state range, with a transmission jump at the isotropic transition similar to that observed in other LC+nanoparticle systems [1]. Certain particular features were observed, with apparent transition from “disordering” to “ordering” effects on the nematic matrix at a certain CeO₂ concentration. In the cholesteric matrix, small temperature-dependent effects of the dispersed nanoparticles on the selective reflection band could be noted. Since CeO₂ is known as an inorganic “nanoluminophore”, we also studied the luminescence spectra, and traces of the CeO₂ luminescence band could be detected on the strong background of the LC matrix luminescence.

[1]. Lisetski, L.N., Minenko, S.S., Samoilov, A.N., Lebovka, N.I. Optical density and microstructure-related properties of photoactive nematic and cholesteric liquid crystal colloids with carbon nanotubes // Journal of Molecular Liquids. – 2017. – V. 235. – p. 90 – 97.

Optical Linear and Nonlinear Properties of Hybrid Liquid Crystal Cells Containing Gold Island Films

S. Bugaychuk^{*1}, L. Viduta¹, V. Styopkin¹, O. Boiko¹, L. Tarakhan¹

¹Institute of Physics of NAS Ukraine, Kyiv, Ukraine

**Corresponding author: bugaich@iop.kiev.ua*

Liquid crystal (LC) materials are very well known in practical applications due to their ability to change the optical transmission when an electric field is applied. Nonlinear optical properties are caused by changes in the birefringence of the LC cells under the action of laser radiation. Devices that exhibit nonlinear optical properties are of great interest for manipulating laser beams and for optical information processing. A typical simplest LC cell contains of two substrates coated with a transparent ITO electrode and an LC layer between them. As a rule, the interface between organic LC molecules and the inorganic surface of the substrate has a complicated physicochemical structure, which may include one or even several bi-layers.

Nonlinear optical properties in LC cells are associated with the reorientation of LC molecules in the cell volume under the action of light [1]. LCs possess the highest nonlinear response (third order nonlinear susceptibility is $\chi^{(3)} \sim 10^{-1} - 10^{-2}$ esu), but at the same time with a major drawback for applications, which is a slow response time (usually, $\tau > 100 \mu\text{s} - \text{up to } 100 \text{ s}$). The process of reorientation of LC molecules can be initiated from the surface of the substrate when a non-uniform charge distribution on this surface is induced. We have obtained that such a surface-induced photorefractive effect leads to an increase in the optical nonlinear susceptibility in hybrid LC cells containing a silicon substrate with a non-uniform surface [2]. The big challenge is to reduce the response time, which we explore in hybrid cells containing a film with gold islets. We have fabricated hybrid LC cells that include one of the substrates where a gold island film is deposited [3]. This paper reports on the first studies of linear and nonlinear optical properties, as well as their temporal kinetics in such cells, depending on the average size of the islands in the gold film, and on the thickness of the LC layer.

- [1]. I.C. Khoo. Nonlinear Optics in Liquid Crystalline Materials // Physics Reports. – 2009. – V. 471. – p. 221 – 267.
- [2]. S. Bugaychuk, A. Iljin, O. Lytvynenko, L. Tarakhan, L. Karachevtseva. Enhanced Nonlinear Optical Effect in Hybrid Liquid Crystal Cells Based on Photonic Crystal // Nanoscale Research Letters. – 2017. – V. 12 – N. 449. – p. 1 - 9.
- [3]. L. Viduta, T. Gavrilko, A. Marchenko, V. Nechytskyi, S. Senenko, R. Ferodovich, P. Shabatyn. Structure and Electroluminescent Properties of Thin Tetracene Layers on Gold Island Films // Ukr. J. Phys. – 2012. – V. 57. – N. 2. – p. 260 – 265.

**Nanoconfinement of Nematic Liquid Crystals to Mesoporous Silica
Particles: Surface Interactions and Adsorbed Species Density
Distribution by FTIR, Raman, and CARS Spectroscopies**

J. Baran¹, A. Dementjev³, M. Drozd¹, I. Gnatyuk^{2*}, T. Gavrilko²,
R. Karpicz³, N. Shcherban⁴

¹Institute of Low Temperature and Structure Research, PAS, Wrocław, Poland

²Department of Photoactivity, Institute of Physics, NAS of Ukraine, Kiev, Ukraine

³Department of Molecular Compound Physics, Center for Physical Sciences and Technology, Vilnius, Lithuania

⁴Institute of Physical Chemistry NAS of Ukraine, Kyiv, Ukraine

**Corresponding author: ivan.gnatyuk@gmail.com*

Mesoporous silica molecular sieves of MCM-41 type loaded with nematic liquid crystal are suitable model systems for investigation of mechanisms of the liquid crystal molecules alignment and their interaction with the surface. These systems were earlier characterized by FTIR and dielectric spectroscopies, and DSC analysis. However, it was not possible to analyse properly the amount of loaded probe molecules and to evaluate the filling degree and the density of surface species of partially filled silica composites. Here we report an application of CARS spectroscopy for visualization of probe molecules nanoconfined to mesoporous silica particles. As far as we know, such studies have not previously been reported in the literature.

In this work, samples of different composite systems formed by mesoporous silica particles (Al-MCM-41, KIT-6, and SBA-15) loaded with nematic liquid crystals (4-cyano-4'-pentylbiphenyl (5CB), or two commercial hydrogen-bonded liquid crystalline mixtures composed of different homologues of alkylbenzoic $C_nH_{2n+1}-C_6H_4-COOH$ and alkylcyclohexane carboxylic acids $C_nH_{2n+1}-C_6H_{10}-COOH$ ($n=2-4$) with different terminal groups and alkyl chain lengths) as probe molecules were prepared in order to study their interaction with the pore surface. DSC analysis (Perkin-Elmer Model 8000) and FTIR spectroscopy (Bruker IFS-88) were applied to analyse the amount of loaded probe molecules. A home-built CARS microscope with a simple and compact laser (EKSPLA Ltd.) was used to visualize the studied systems. The images were registered in the forward mode at the 1600 and 2800 cm^{-1} region. Strong CARS resonance was detected for 5CB and alkylbenzoic acid at 1605 cm^{-1} corresponding to C=C stretching vibrations which allows direct mapping of the loaded probe molecules in the pores.

It was found that Al-MCM-41 molecular sieves showed the maximum density of the surface species and filling uniformity, while in the other studied matrices the amount of absorbed molecules was less and their density distribution not uniform. Possible reasons for the observed differences are discussed assuming different interaction of the probe molecules with the host.

Whence Has Laser Physics Led Optics to the World of Photonic Crystals?

I.P. Ilchyshyn^{*1}, E.A. Tikhonov²

¹ Departments of Photoactivity, and ²Coherent and Quantum Optics, Institute of Physics, NASU, Kyiv, Ukraine

**Corresponding author: ilchyshynigor@gmail.com*

With the perception of the physics of photonic crystals (PC), a new fields of science and practice emerged and the most vivid one among embodiments was fiber communication lines. Despite of existing PC in the world of wildlife [1] and the notorious zone theory of solid state physics, the first impetus to the development of PC representation became the with problem of lasing in liquid crystal lasers [2], and then - of laser generation in light scattering media [3] .

In the first case, the understanding came with the into account the confinement of the lasing modes outside (or inside) the band gap, in the second case –into account localization of stimulated radiation on closed trajectories of chaotic scattering in the active medium. The use of the concept of "forbidden zone" was the result of theoretical justification of PC physics applied to media on chiral liquid crystals (CLC) [2].

The report presents the results of the discovery of a dip in the fluorescence spectrum within the selective reflection band (~band gap) of a homogeneously oriented helical structure of CLC [2]. We noted that two other outside this band parts of the fluorescence spectrum remained unaffected. In our CLC matrix lasing modes were localized in the center of the selective reflection band. This is a reason that did not allow us to accept the interpretation of the phenomenon on the concepts of PC, which contradicted to the description in the framework of the common lasing model of the distributed feedback (DFB) [4]. After several years, when lasing was realized on the CLC with a more wider selective reflection band, the lasing spectra were typically outside this band, that allowed to link and justify such a result with the forbidden zone of the PC. Thus a new era in optics has began that is, so rich for new ideas and concepts, a direction called the photonic crystals. The report provides a qualitative interpretation of the reasons for the different spectral behavior of the lasing line spacing relative to the selective reflection band (in fact to forbidden bandgap) for different CLC using conclusions of the energy structure of photonic crystals.

[1]. E. Yablonovich. Photonic bandgap structures // JOSA -1993- V. B10 - p. 283 - 290.

[2]. I.P. Ilchishin, E.A. Tikhonov, V.G. Tishchenko M.T. Shpak, Generation of tunable radiation by impurity cholesteric liquid crystals // JETP Lett.- 1980- V. 32 - p. 24-27.

[3]. E.A Tikhonov, V.P. Yashchuk. Lasing stipulated by multiple random light scattering // Xplore IEEE.- 2005-DOI: 10.1109 // CAOL.2005.1553816.

[4]. H. Kogelnik, and S.V. Shank, Coupled-wave theory of distributed feedback lasers // J. Appl. Phys. -1972- V. 43 – p. 2327- 2335.

Electrooptical Effects in Liquid Crystal Cells with Photosensitive Chalcogenide Glasses Surfaces

Yu. Kurioz^{1*}, P. Korniychuk²

¹ Institute of Physics, NAS of Ukraine, Kyiv, Ukraine

² Zhytomyr State University, Zytomyr, Ukraine

**Corresponding author: kurioz@iop.kiev.ua*

We present investigations of electro- and light- effects in liquid crystal cells with micron photosensitive chalcogenide glassy As_2S_3 films as command surface. Reorientation of easy axis in a cell with nematic liquid crystal 5CB under the low intensity illumination with non-polarized beam and decreasing of the Fredericks transition in dc field was observed. We believe that those effects are due to polarity increasing of the surface by light irradiation causes a reorientation of the director of liquid crystal near the photosensitive surface of chalcogenide film. As a consequence, the energy of interaction between the molecules of liquid crystals and the external electric field near the surface overcomes the anchoring energy and as a result of the LC director reorientation in polar plane take place in this case. Light-induced microlenses in a LC cells with chalcogenide surfaces As_2S_3 were formed. The results obtained clearly show a great potential of chalcogenide glassy materials for their applications in advanced optical and nonlinear optical devices on liquid crystals based.

Temperature Dependence of the Reflection Indicator of Wall Layers of Epitropic Liquid Crystals

A.A. Goryuk, V.I. Mikhailenko, A.Yu. Popovskii*

National University "Odessa Maritime Academy", Odessa, Ukraine

**Corresponding author: alexejpopovskij57@gmail.com*

In order to study the temperature dependence of the refractive index ultrathin nitrobenzene wall-adjacent layers we used two models – the two-component model [1-2] and the Mayer-Saupe-Neugebauer model [3-4].

Two component model. Some isotropic liquids near the surface of a solid substrate form orientationally ordered wall-adjacent layers, which were named as epitropic liquid crystals (ELC). This model postulates the existence of monomers and dimers in the wall-adjacent layer which are in a dynamic equilibrium with each other. The structure of such layers is as follows: dimers predominate directly near a solid substrate, further there exists a thin transition layer, in which the monomer percentage increases with the distance to the solid substrate, and further the ELC turns to an isotropic liquid.

Mayer – Zaupe - Neugebauer model. This model is based on the following assumptions:

1. A model of a crystal with one molecule in a unit cell can be applied in a case of an uniaxial liquid crystal (LC).
2. The average value of polarizability does not depend on the phase state of the LC and on the value of its order degree.

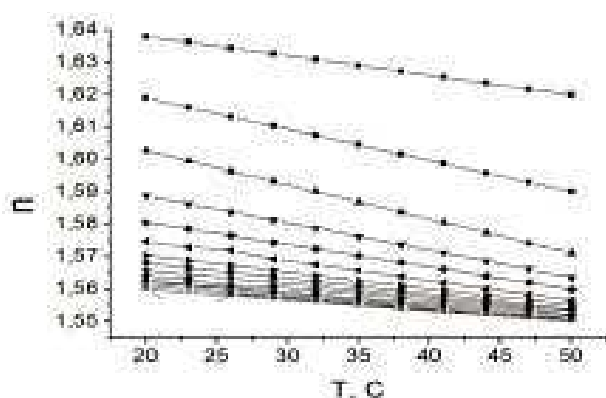


Fig. 1. Theoretically calculated dependences $n_h(T)$ for different thicknesses of nitrobenzene interlayer. Upper curve corresponds to the thickness 20 nm and the lower curve to the thickness – 90 nm.

The dependences of the nitrobenzene refractive index vs temperature for various thicknesses of the wall-adjacent layer were theoretically calculated (Fig. 1). These dependences are in good agreement with experiment. For an ELC layer, it is necessary to take into account the temperature dependence of the density and of order parameter also. For the isotropic phase, the temperature behavior of these dependences is determined primarily by the decreasing of the liquid density while its heating.

- [1]. Popovskii A.Yu., Mikhailenko V.I. //Ukr. J. Phys., 2014, V.59, #3, P.299-302.
- [2]. Popovskii A.Yu., Kuznetsova A.A., Mikhailenko V.I. Journal of Applied Spectroscopy 73(4):499-503, 2006.
- [3]. Neugebauer H.E.J. Clausius-Mossotti equation of certain types of anisotropic crystals // Can. J. Phys. – 1954. – V. 32, N1. – P. 1–8.
- [4]. Saupe A., Maier W. Methoden zur bestimmung des ordungsgrades nematischer kristallinflüssiger schichten // Z. Naturforsch. – 1961. – B. 16a, H.4. – S. 816–824.

5

**Biomolecules and
Polymers**

Application of Model Lipid Membranes to the Problem of Drug-Membrane Interactions

O.V. Vashchenko, N.A. Kasian, L.V. Budjanska*, L.N. Lisetski

Institute for Scintillation Materials of NASU, Kharkov, Ukraine

**Corresponding author: l.budjanskaja92@gmail.com*

Lipid membranes work as barriers, which leads to inevitable drug-membrane interactions *in vivo*. These interactions affect the pharmacokinetic properties of drugs, such as their diffusion, transport, distribution, and accumulation inside the membrane [1]. Model lipid membranes are extensively used to address the challenge of drug-membrane interactions.

In the present work, multilayer structures of fully hydrated L- α -dipalmitoylphosphatidylcholine (DPPC) were used as monolipid membrane model. Individual and joint effects of drugs in mono- and multi-compound model lipid membranes have been studied by means of differential scanning calorimetry, Fourier IR spectroscopy, thermogravimetry analysis and optical microscopy.

It has been shown that addition of anti-tubercular antibiotic cycloserine together with drug excipients calcium stearate or magnesium stearate to DPPC membranes resulted in a previously unknown synergic membranotropic effect, as distinct from another excipient, stearic acid. Dependence of the joint effects on chemical structure of the excipients was traced.

Using multi-compound membranes, two different mechanisms underlying lipid re-arrangement were established, as well as independence of the effects of lipid composition on the type of drug-membrane interaction.

A new technique was proposed to study joint membranotropic effects of water-soluble drugs in DPPC membranes. By means of the technique, facilitation of passive transmembrane diffusion of antiviral drug tilorone in the presence of anti-inflammatory drug dimethylsulfoxide was shown, as well as importance of the order of drug administration.

[1]. D. Lopes, et al. Shedding light on the puzzle of drug-membrane interactions: experimental techniques and molecular dynamics simulations // *Progr. Lipid Res.* - 2017.- V. 65.- p. 24-44.

Light Scattering in a Dilute Solution of Hydroxypropylmethylcellulose

L.Yu. Babiy, L.Yu. Vergun*, Yu.F. Zabashta

Taras Shevchenko National University of Kyiv, Ukraine

**Corresponding author: verlen73@ukr.net*

The light scattering in a dilute solution of hydroxypropylmethylcellulose is studied. Hydroxypropylmethylcellulose is used as a binder for solid dosage forms. The experimental time dependences of light scattering coefficient ξ (the ratio of light scattering at an random moment to the light scattering at the initial time) are obtained in the temperature range from 303K to 353K. It was found that the experimental dependences obtained in the temperature interval 333K-343K have the character of intense fluctuations that exceed the experimental errors. This behavior indicates that the investigated temperature interval is an interval of some first-order phase transition. The hypothesis about the formation of clusters of hydroxypropylmethylcellulose molecules in rod-shaped form [1] is proposed. Additionally, experiments of density of water solution of hydroxypropylmethylcellulose and distilled water in the temperature range 303K-353K were performed. Based on experimental data of temperature dependence of density, it was shown that the hydrated shells of hydroxypropylmethylcellulose molecules and their clusters are disordered. Their density is less than that of free water.

[1]. M.M.Lazarenko, O.M.Alekseev, Yu.F.Zabashta. The structure of polymer clusters in aques solution of hydroxypropylcellulose//Ukr.J.Phys.-2019.-V.64,N.3.-pp.238-244.

Solid-State NMR Study of Local Disorder Nearby Proton Motion Path in Low-Dimensional H-Bonded Proton-Conducting Materials

L. Dagys¹, V. Klimavicius², V. Balevicius^{3*}

¹ Department of Chemistry, University of Southampton, Southampton, UK

² Eduard-Zintl Institute for Inorganic and Physical Chemistry, University of Technology Darmstadt, Darmstadt, Germany

³ Institute of Chemical Physics, Vilnius University, Vilnius, Lithuania

*Corresponding author: vytautas.balevicius@ff.vu.lt

The solid-state NMR spectra and ^1H – ^{13}C cross-polarization magic angle spinning (CP MAS) kinetics was studied in poly(vinylphosphonic acid) (pVPA), i.e. material with high degrees of freedom of motion of protons along the H-bonded chains. It was shown that the CP kinetic data for CH_2 group, i.e. for the system containing adjacent ^1H – ^{13}C spin pairs with a definite dominant dipolar coupling can be described using the isotropic spin-diffusion approach [1]. The local order parameter $\langle S \rangle \approx 0.61$, determined as the ratio of the measured dipolar ^1H – ^{13}C coupling constant and the calculated static dipolar coupling constant, is significantly lower the values deduced for related sites in other polymers and in series of amino acids. The observed phenomenon reflects the effect of remote mobile protons on the dipolar coupling in the pairs of adjacent spins and the local disorder.

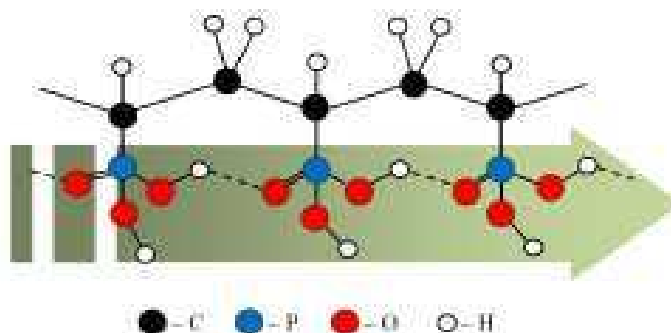


Fig. 1. Proton motion path in pVPA.

- [1]. L. Dagys, V. Klimavicius, T. Gutmann, G. Buntkowsky, V. Balevicius. Quasi-Equilibria and Polarization Transfer between Adjacent and Remote Spins: ^1H – ^{13}C CP MAS Kinetics in Glycine // J. Phys. Chem. A – 2018. – V. 122. –p. 8938 – 8947.

Influence of the Value of the External Load on the Mechanism of Ice Melting

S.R. Bobrovnik*, L.Yu. Vergun, O.S. Svechnikova

Taras Shevchenko National University of Kyiv, Kyiv, Ukraine

**Corresponding author: sergeybobrovnik97@gmail.com*

The question about mechanism of melting ice was considered in [1]. In this work, using the torsion pendulum method, the real and imaginary parts of the complex shear modulus were determined. Determination of these values was carried out by measuring the frequency and amplitude of free damped oscillations of an empty polyethylene cuvette and cuvette with ice. For this purpose in the system using external load created some stress state described in [2]. It is known that in different conditions ice exhibits elasticity, nonlinear viscosity, fragile destruction, etc. [3]. It is also known that in the polymer systems, including in polyethylene, there are specific defects-supervacancies [4]. The number of these defects and the mechanism of their formation are determined by the influence of external factors. Thus, the application of the torsion pendulum method in the study of melting of ice requires the perfect determination of mechanisms occurring in the system "polyethylene cuvette-ice" at different values of external load.

The frequency and decrement of free damped oscillations of an empty polyethylene cell and cuvette with ice in the temperature range 223-283 K at different values of external loading is experimentally determined. It is established that during melting the nature of disordering in structure of polymer system and in structure of ice is changed at different values of external load. A hypothesis about the existence of some limit value of load is determined, which determines the mechanism of bulk or surface melting in the cuvette. This fact can significantly affect the analysis of the obtained results using the torsion pendulum method.

- [1]. N.L. Sheiko, O.Yu. Aktan, Yu.F. Zabashta, T.Yu. Nikolayenko. // Ukrainian Physical Journal .- 2010.- V. 55.-N.3.-p.300-306.
- [2]. L.A. Bulavin, O.Yu. Aktan. // Industrial Laboratory.Diagnostics of materials.-2009.-V.75.-N5.-pp.50-54
- [3]. T. Brox, M. Skidmore, J .Brown. // Journal of Glaciology.-2015.-V.61.-N.225.-pp.55-64.
- [4]. L.A .Bulavin, E.Yu. Aktan. Yu.F. Zabashta. // Polymer Science.Ser.A.-2003.-V.45.-N.10.-pp.1007-1010.

Influence of Weak Magnetic Fields on the Optical Properties of Water and its Catholytes

K.I. Bublikova*, I.M. Klimenko, O.S. Sereda, Y.O. Myagchenko

Faculty of Physics, Taras Shevchenko National University of Kyiv, Kyiv, Ukraine

**Corresponding author: bublikovakaterina24@gmail.com*

All processes in living organisms (bacteria, mushrooms, plants, animals, people) on Earth occur with the participation of water. Water is extremely sensitive to external influences. Changing its characteristics certainly influences the course of biochemical processes in a living organism. Recently, much attention has been paid to such characteristics of water as its oxidation-reduction potential (ORP or Redox), methods and devices that can be used to influence the ORP of water. Water with a changed ORP in the negative sense acquires the properties of electron donor substance and behaves like a powerful antioxidant. In addition, in such a water, we dissolve such hydrophobic substances, for example, as propolis, which contains a lot of flavonoids - antioxidants. The processes of extracting substances from plants in our catholytes are effective even at room temperature. In our experiments, we extracted hypericin from grasses of St. John's wort. Hypericin is a dye-sensitizer to excite oxygen in a singlet state and used in photo-dynamic therapy for the treatment of cancer.

- [1]. L.Y. Vergun, O.A. Zagorodnia, K.O. Teliman. Molecular Mechanism of Disordering the Epidermis Structure under Effect of Static Magnetic. Field // Journal of Physical Science and Application.- 2013.- V. 3(5).- p.- 311-314
- [2]. L.A. Bulavin, L.Yu. Vergun, Yu.F. Zabashta, Ye.O. Teliman. // Kolloid. Zhurnal, 2015.- V. 77.- No.3.- p.1-6 (In Russian).

2D-Boron Nitride Nanoparticles and Doxorubicin Interaction with Cancer Cells: CARS Imaging and FTIR Spectroscopy

O. Gnatyuk^{1*}, G. Dovbeshko¹, I. Polovyi¹, D. Kolesnik², O. Pyaskovskaya²,
G. Solyanik², A. Dementjev³, R. Karpicz³, O. Posudievsky⁴

¹Department of Physics of Biological Systems, Institute of Physics, NAS of Ukraine, Kiev, Ukraine

²R.E. Kavetsky Institute of Experimental Pathology, Oncology and Radiobiology, NAS of Ukraine, Kyiv, Ukraine

³Department of Molecular Compound Physics, Center for Physical Sciences and Technology, Vilnius, Lithuania

⁴L.V. Pisarzhevsky Institute of Physical Chemistry, NAS of Ukraine, Kyiv, Ukraine

**Corresponding author: hrysantemka@ukr.net*

Nowadays, new types of nanoparticles, drugs and drug delivery systems are developed constantly; therefore, a question of interaction between these systems and cell cultures stands constantly. Optical microscopy with staining agents is considered to be conventional method for cell visualization. However, such method is not always suitable for a task.

In our work, the CARS spectroscopy and microscopy techniques was used, which allow us to obtain stain-free cell images at infrared frequencies. In the experiment, the Lewis lung carcinoma cells treated in vitro with doxorubicin and boron nitride at various concentrations were used.

A home-built CARS microscope with a simple and compact laser (EKSPLA Ltd.) was used. The cell images are registered in the forward and EPI mode at the 1600, 1360 and 2800 cm⁻¹ region.

During the experiment, it was shown that in most cases, more contrast and intense cell images we obtained in EPI mode. It is interesting to note, that bright points of luminescent nature in the image of cells appeared after repeated scans. It is may be due to the release of cytochrome C during apoptosis. Previously, we observed the appearance of a band at 1555 cm⁻¹ in Raman spectra of cells during apoptosis.

The differences in the morphology of the reference cells and cell after treatment were registered. The features of the cell cultures FTIR spectra, after exposure to doxorubicin and boron nitride, are discussed.

Acknowledgement

This work has been supported by the HORIZON 2020 project 690853-assymcurv, NATO 985291, Development of 2D materials and "smart" sensors for medical and biological purposes 11/1 2019, joint Ukrainian - Lithuanian R&D projects 2018 – 2019 № M/19-2019.

Physicochemical Investigation of the Complexation between Melatonin and Randomly Methylated β -Cyclodextrin in Solution and in Solid State

G.V. Grygorova*, V.K. Klochkov, S.L. Yefimova, Yu.V. Malyukin

Department of Nanostructured Materials, Institute for Scintillation Materials NAS of Ukraine, Kharkiv, Ukraine

**Corresponding author: grigorova@isma.kharkov.ua*

Melatonin (MT) is a natural product, and is produced in the pineal gland and excreted as a hormone in humans. Melatonin has important effects on circadian and seasonal rhythms, sleep–wake cycle, immune functions, bone growth, antioxidant protection and tumor inhibition. It is proved that melatonin has showed not only directly anticancer effect that means reducing promotion and progression of the tumor. Although melatonin has significant properties as specified, its usage is limited due to low water solubility and sensitivity to light. However, the amphiphilic structure of melatonin makes it suitable for the formation of inclusion complexes by insertion into the rigid hydrophobic cavity of cyclodextrins (CDs). In recent years, inclusion complexes with CDs have been widely used to improve the solubility of water-insoluble drugs, enhance the physical and chemical stability of drugs, eliminate undesired properties of drugs, and improve the bioavailability.

In this study, the formation of inclusion complex of MT with randomly methylated β CD (RM β CD) in solutions and solid states was investigated. MT complex with RM β CD was characterized by phase solubility studies, which demonstrated Higuchi's A_L-type phase solubility profiles, indicating the 1:1 stoichiometric inclusion complexes. The stoichiometry and stability constants of the formed complexes were examined by means of the continuous variation method (the Job plot). The effect of pH on the calculated formation constants for the MT- RM β CD complexes has also been investigated. Studies of MT- RM β CD complexes photostability reveal that MT in the packed form is a more stable than pure MT. The solid MT-RM β CD complex was prepared by the co-evaporation method. The evidence for the host-guest solid complex formation was quantitatively estimated by differential scanning calorimetry (DSC) and Fourier transform infrared spectroscopy (FT-IR) analysis. Obtained results confirm energetically favorable interactions between MT and RM β CD molecules in solid state. This study presents new data, which could help in the development of pharmaceutical formulations with optimal drug release profile.

Allosteric Effects of Ligands Binding to Human Serum Albumin as Studied by Chemical Relaxation Spectroscopy Methods

T.O. Hushcha

V.P. Kukhar Institute of Bioorganic Chemistry and Petrochemistry of the NAS of Ukraine, Kyiv, Ukraine

**Corresponding author: hushcha@bpci.kiev.ua*

Allostery is an efficient means for regulation of protein function that is expected to play an increasing role in drug discovery. The binding of a ligand at an allosteric site results in a conformational change involving protein dynamics. Allostery was the subject of extensive studies mainly aimed at the assessment of thermodynamics and kinetics of protein-ligand interactions. However, the development of corresponding models at a molecular level gives rise to need of a complementary information. One question is which components of the internal protein dynamics relate to binding affinity of the ligands with receptor.

Here we investigated the thermodynamic and kinetic parameters of chemical relaxation in aqueous human serum albumin (HSA) solutions in presence and absence of two ligands. We used myristic acid as one ligand, which belongs endogenous compounds. Another ligand was anticoagulant drug warfarin. We applied the broadband acoustic spectroscopy and molecular dynamics simulation methods to obtain thermodynamic binding parameters and time constants of internal dynamics in the binary and ternary complexes of HSA with ligands.

We found that entropy contributions to the free energy of binding predominate in the formation of binary and ternary complexes of HSA with myristic acid and warfarin. Favorable entropy contributions were found to result from the lower rate of the protein conformational transitions and higher rate of the hydration water mobility in HSA bound with ligands as compared to unbound protein. We also found that the changes of the characteristic times of the internal protein dynamics that arise upon formation of the ternary HSA-ligands complex correspond to allosteric interaction. We showed that dynamics of the global conformational changes of HSA domains in binary and ternary complexes with ligands correlate with the internal mobility of HSA in the unbound state. This finding gives an evidence for the concept of "conformational selection" as the mechanism of HSA interaction with ligands. The concept asserts that ligand in the course of recognition process selects the most suitable conformation among available ensemble of equilibrium protein structures.

A.O. Kostetskiy^{1*}, Yu.P. Piryatinski¹, A.B. Verbitsky¹, P.M. Lutsyk²

² Aston University, Aston Triangle, B47ET Birmingham, UK

*Corresponding author: tohakostet@gmail.com

Aqueous solution of nanostructured melanin forms intermolecular complexes and this leads to the quenching of excimer emission and an increase of the intensity of the emission of free excitons.

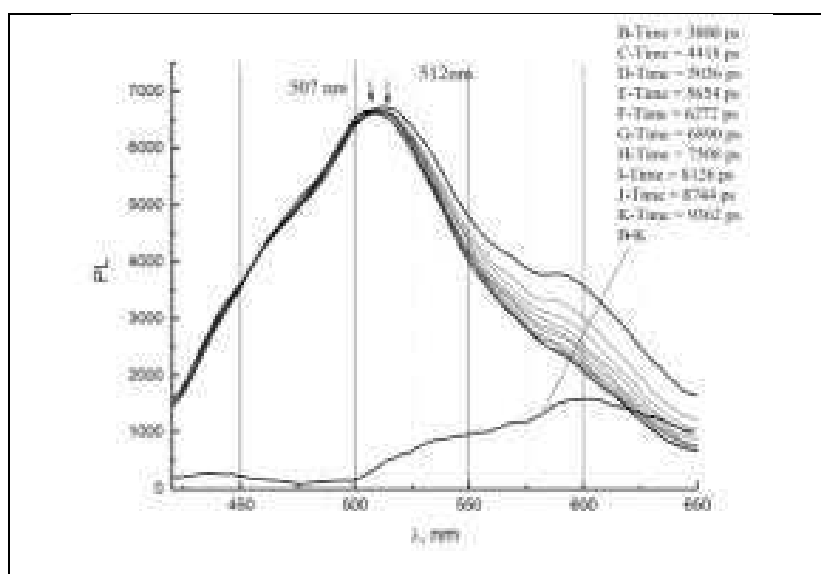


Fig. 1. Time-resolved emission spectra of melanin ($\lambda_e=405\text{nm}$).

These changes were explained by the presence of pre-dimer states in melanin nanoclusters, which are acting as the traps of free excitons and being followed by relaxation to excimer emission ($\lambda(\text{PL}) > 512 \text{ nm}$). However, in TRES spectra at low temperatures (5K and 77K) the corresponding bands disappear that indicating about excimer nature of melanin emission.

Photoluminescence (PL) decays and time-resolved emission spectra (TRES) of nanostructured melanin were studied. The results of these studies will be analyzed and discussed.

- [1]. A.O. Kostetskyi, Yu.P. Piryatinski, A.B. Verbitsky, P.M. Lutsyk. Effect of the charge state on the photoluminescence spectra of melanin // MCLC, DOI: . 10.1080/15421406.2018.1542084 (to be published).

Spectroscopic Studies of Infectious Pancreatic Necrosis Virus, its Major Capsid Protein and RNA

V.M. Kravchenko^{*1}, Yu.P. Rud², L.P. Buchatski^{2,3},
Ye.Yu. Stepanenko¹, V.M. Yashchuk¹

¹ Faculty of Physics, Taras Shevchenko National University of Kyiv, Kyiv, Ukraine

² Institute of Fisheries of the National Academy of Agrarian Sciences of Ukraine,
Kyiv, Ukraine

³ Laboratory of Physico-Chemical Biology, ESC Institute of Biology, Taras
Shevchenko National University of Kyiv, Kyiv, Ukraine

**Corresponding author: vladyslaff@gmail.com*

Infectious pancreatic necrosis virus (IPNV) causes severe disease of salmonid fishes (trout, salmon, *etc.*). The IPNV virion consists of a double-stranded viral RNA, surrounded by a protein capsid. The aim of the work was to determine the role of IPNV virion constituents (capsid proteins and viral RNA) in the formation of spectral properties of the whole IPNV virions.

Measured are UV-Vis absorption, fluorescence, fluorescence excitation, phosphorescence and phosphorescence excitation spectra of IPNV virions, major capsid protein (MCP) and viral RNA dissolved in different buffers.

It is shown that UV absorption of IPNV virions is caused by absorption of both capsid proteins and viral RNA. Fluorescence of IPNV MCP and virions may be attributed to tyrosine and tyrosine + tryptophan, respectively. Low temperature phosphorescence of virions can be attributed to that of capsid proteins rather than viral RNA. IPNV RNA phosphorescence spectrum exhibits electronic-vibrational structure and may be due to emission of adenine links.

Spectral-Luminescent Manifestation of Guanine Complexes in Telomere Fragment at Low Temperatures

V.Yu. Kudrya^{*1}, A.P. Naumenko¹, I.Ya. Dubey², V.V. Negrutsk²,
Yu.S. Kreminska¹, V.M. Kravchenko¹

¹ Department of Physics, Kyiv National Taras Shevchenko University, Kyiv, Ukraine

² Institute of Molecular Biology and Genetics of NASU, Kyiv, Ukraine

**Corresponding author: vladkudrya@ukr.net*

Telomere is the end part of chromosomal DNA protecting the chromosome and participating in the lengthening and replication of DNA macromolecule. Telomeres contain a large number of repeated sequences of 6 nucleotides TTAGGG. Their shortening can lead to apoptosis. Telomere, as well as poly- and oligonucleotides, contains pi-electron systems and, thus, its structural changes can be studied using optics spectroscopy (as it was shown by us [1]). In current literature, the main attention is paid to the spectral manifestation in optical absorption of guanine (G) complexes formed in telomere, and there is a gap in the knowledge about their luminescent properties. In the present study the spectral properties of samples of the telomere DNA fragment – d(AGGGTTAGGGTTAGGGTTAGGG) (Tel22) oligonucleotide held at different temperature regiments were investigated at low temperatures.

The optical absorption, fluorescence and phosphorescence of several types of Tel22 samples (sample 1 – Tel22 folded into the G-quadruplex structure and immediately frozen, other samples – sample 1 heated to 363K, 353K, 343K, 333K, 323K and then shock frozen) were investigated at 78K. The band at 295 nm associated with G-quadruplexes was observed in optical absorption for all types of investigated Tel22 samples. Only the band associated by us with G-quadruplexes was observed in the fluorescence for the non-heated sample and the sample heated to 323K. Two bands (associated with: (1) G-complexes, (2) "free" guanine pi-electron systems) were observed in the fluorescence spectra for other four Tel22 samples. The phosphorescence of all samples was the emission of the complex formed by adenine (A) and thymine (T) chromophores [1]. Besides, the additional structured band in phosphorescence (in excitation wavelength range 310-320 nm) associated with "free" guanines was observed for the sample heated to 363K. In our opinion, these facts are the spectral manifestation of thermal defolding of G-quadruplex structure in Tel22 and formation of G-intermediates started above T=323K.

- [1]. V.M.Yashchuk, V.Yu.Kudrya, I.Ya.Dubey, K.I.Kovalyuk, O.I.Batsmanova, V.I.Mel'nik, G.V.Klishevich. Luminescence of telomeric fragments of DNA macromolecule // Mol. Cryst. Liq. Cryst. – 2016. – V. 639. –p. 1 – 9.

Low Temperature Luminescent Studies of Emissive Guanine Substitute for Biopolymers Detection

V.Yu. Kudrya^{*1}, A.P. Naumenko¹, V.M. Yashchuk¹, Y. Mely²,
Ya.O. Gumenyuk³

¹ Department of Physics, Kyiv National Taras Shevchenko University, Kyiv, Ukraine

² Laboratoire de Biophotonique et Pharmacologie, Faculte de Pharmacie, UMR 7213 CNRS, Universite de Strasbourg, France

³ National University of Life and Environmental Sciences of Ukraine, Kyiv, Ukraine

**Corresponding author: vladkudrya@ukr.net*

Biopolymers of nucleic acids and nucleotides manifest autoluminescence with high quantum yield only at low temperatures that is well below the physiological range. At room temperature the quantum yield of nucleotides is reported to be low, about 10^{-5} – 10^{-4} [1]. The detection of nucleic acids becomes possible using luminescent probes with a respectable quantum yield of luminescence at room temperature which could be incorporated in the biopolymer macromolecule chain [2-3]. Herein, the luminescent properties of such type probe – deoxythienoguanosine (dthG), an emissive substitute of guanine – were studied at low temperatures.

The fluorescence and phosphorescence of dthG were investigated at 78K in aqueous and TRIS-HCl-buffer solutions. It was previously described [3] two optical absorption and fluorescence centers at room temperature that were attributed to two keto-enol tautomers of dthG. In contrast to room temperature, at 78K only one emission band was observed in fluorescence spectra that was close to longwave fluorescence band at room temperature and could be associated with the tautomer possessed longwave absorption. This phenomenon can be explained by the excitations energy transfer in frozen solution between two types of optical centers mentioned above. The similar conclusion was for phosphorescence: only one tautomer phosphorescence band was observed. The spectral position of this band maximum essential differed for aqueous and buffer solutions (~50nm).

[1]. D.Onidas, D.Markovitsi, S.Marguet, A.Sharonov, T.Gustavsson. Fluorescence properties of DNA nucleosides and nucleotides: A refined steady-state and femtosecond investigation // J. Phys. Chem. B.- 2002.- N.106.- P.11367-11374.

[2]. M.Sholokh, R.Sharma, D.Shin, R.Das, O.A.Zaporozhets, Y.Tor, Y.Mely. Conquering 2-Aminopurine's Deficiencies: Highly Emissive Isomorphic Guanosine Surrogate Faithfully Monitors Guanosine Conformation and Dynamics in DNA // J. Am. Chem. Soc. – 2015. – V. 137. – N. 9. – p. 3185 – 3188.

[3]. M.Sholokh, R.Improta, M.Mori, R.Sharma, C.Kenfack, D.Shin, K.Voltz, R.H.Stote, O.A.Zaporozhets, M.Botta, Y.Tor, Y.Mely. Tautomers of a Fluorescent G Surrogate and Their Distinct Photophysics Provide Sensitive Information Channels // Angew. Chem. Int. Ed. – 2016. – V. 55. –p. 7974 – 7978.

**Optical Properties of New Core-Fluorinated Azo-Containing
Poly(azomethine)s with Ether Linkages and Aliphatic Moieties
in the Main Chain**

A. Kovalchuk¹, Ya. Kobzar¹, I. Tkachenko¹, Yu. Kurioz^{*2},
V. Nazarenko², O. Shekera¹, V. Shevchenko¹

¹ Institute of Macromolecular Chemistry, NASU, Kyiv, Ukraine

² Institute of Physics, NASU, Kyiv, Ukraine

**Corresponding author: kurioz@hotmail.com*

The aim of this work was to study the optical properties of the core-fluorinated azo-containing polyazomethines (Azo-Pam`s) with 1,4-tetrafluorobenzene or 4,4'-octafluorobiphenylene dioxyphenylene units and aliphatic fragments in the main chain. Azo-containing polymers (APs) have attracted much attention as materials for biology, optoelectronics, nanomanipulation field, etc. Moreover, the introduction of azomethine group into these polymers enhances not only their optical properties and, therefore expands their practical application. APs polymers and particularly Azo-Pam`s have the useful combination of chemical and physical properties such as liquid crystalline states, high nonlinearity and an ability to form metal complexes [1]. It was shown that the optical properties of such polymers can be improved by the inclusion of fluorine fragments. Fluorinated polymers demonstrate high thermal stability and have low dielectric constant and dielectric losses. It should be noted that the presence of flexible moieties in a polymer backbone allows regulating the different properties (solubility, thermostability, optical and liquid crystalline properties) of the resulting materials [2].

- [1]. S.C Suh., S.C. Shim, Synthesis and properties of a novel polyazomethine, the polymer with high photoconductivity and second-order optical nonlinearity // *Synthetic Metals*. – 2000.- V. 114. – N.1. - p. 91–95.
- [2]. Ya.L. Kobzar, I.M. Tkachenko, V.N. Bliznyuk, O.V. Shekera, T.M. Turiv, P.V. Soroka, V.G. Nazarenko, V.V. Shevchenko. Synthesis and characterization of fluorinated poly(azomethine ether)s from new core-fluorinated azomethine-containing monomers // *Designed Monomers Polymers*. – 2016 – V.19. – N.1.- p. 1–11.

Study of the Interaction of Bovine Serum Albumin with Gemcitabine

A.I. Lesiuk^{*1}, O.P. Dmytrenko¹, T.O. Busko¹, O.L. Pavlenko¹
I.P. Pundyk¹, T.M. Pinchuk-Rugal¹, M.P. Kulish¹, V.I. Chegel²,
A.M. Lopatynskyi², M.I. Kanyuk³

¹ Department of Physics of Functional Materials, Physics Faculty, National Taras Shevchenko University of Kyiv, Kyiv, Ukraine

² V.Ye. Lashkaryov Institute of Semiconductor Physics of the National Academy of Sciences of Ukraine

³ Palladin Institute of Biochemistry of the National Academy of Sciences of Ukraine

**Corresponding author: lesiuk.andrey@gmail.com*

The interaction of bovine serum albumin (BSA) with gemcitabine was investigated by analyzing the spectrum of fluorescence, which occurs due to presence of two tryptophan aminoacid residues in the structure of BSA molecule.

The quenching of fluorescence intensity with increase of gemcitabine concentration in the solution was shown (Fig. 1). From experimental data the Stern-Volmer quenching constant and binding constant were found. Decrease of the last one with temperature growth lets us conclude the prevailing static mechanism of the quenching. The binding energy of BSA and gemcitabine was obtained $\Delta G \approx -3.1 \cdot 10^4$ J/mol, which coincides with the value obtained from molecular docking study in package AutoDock Vina (version 1.1.2) [1].

The calculated changes of entropy and enthalpy are attributed to both hydrogen bonds and hydrophobic interactions of BSA and the drug. Using the Forster's nonradiation energy transfer theory, the average distance from gemcitabine to the tryptophan residues was found, which is in a good agreement with the docking results (Fig. 2).

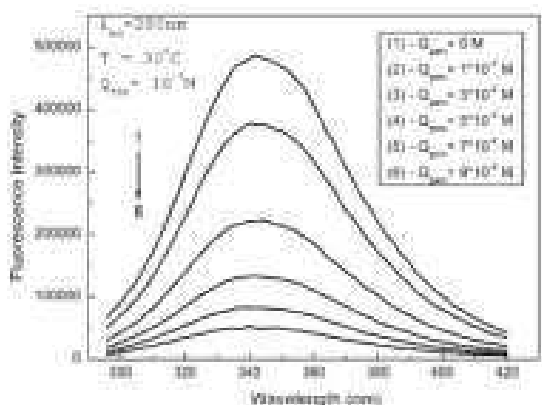


Fig. 1. Fluorescence intensity quenching

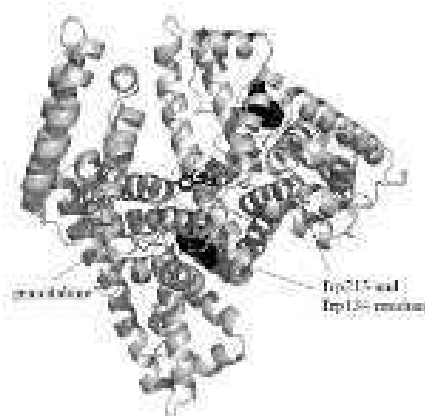


Fig. 2. Molecular docking study

[1]. O. Trott and A.J. Olson. // J. Compute Chem. – 2010. – V. 31. – N. 2. – p. 455 – 461.

Molecular Mobility in a Concentrated Glucose Solution under the Influence of a Weak Magnetic Field

A.A. Vialtseva*, L.Yu. Vergun, Yu.F. Zabashta

Taras Shevchenko National University of Kyiv, Ukraine

**Corresponding author: a.vialtseva@gmail.com*

It is known that the formation of clusters occurs in aqueous solutions of glucose, which may be the result of a change in the structure of the solution, including under the action of a magnetic field [1]. The structure of concentrated solutions of sugars was considered in [2]. The purpose of the work is to determine how the magnetic field affects molecular mobility in a concentrated glucose solution. The temperature dependences of density for solutions of glucose with a concentration of 40%, which were treated and untreated by a magnetic field, were obtained. It was established that magnetic field processing leads to an increase in the density of the solution. The time dependencies of the relative intensity of light scattering for solutions of glucose 40% were obtained at different action regimes of the magnetic field. It is established that the application of a magnetic field causes the appearance of significant fluctuations in the intensity of light scattering, which essentially prevails the error of the experiment. It is shown that the change in the duration of the magnetic field does not change the magnitude of the specific intensity of light scattering. It was found that after removal of the magnetic field, the intensity of fluctuations for almost 60 minutes practically does not decrease. On the basis of experimental data, a hypothesis is made that observable intensity fluctuations are the result of the occurrence in the system of self-oscillations under the action of a magnetic field. An increase in the density of solutions, as were exposed to the magnetic field caused by the hydrodynamic interaction between clusters.

- [1]. L.A. Bulavin, L.Yu. Vergun, Yu.F.Zabashta, K.O. Ogorodnik. Saccharide solutions under the magnetic field action// Ukr.J.Phys. -2016.-V.61.-N.7.-pp.583-587.
- [2]. V.Molinero, T.Cagin, W.Goddard. Sugar, water and free volume networks in concentrated sucrose solution// Chemical Physical Letters. -2003.-№377.- p.469-474.

About Mechanism of Charge Carriers Release from Traps Stimulated by Molecular Vibrations in Silicon Organic Polymers

V. Sugakov¹, N. Ostapenko^{*2}, Yu. Ostapenko², O. Kerita²

¹ Institute for Nuclear Research, NASU, Kyiv, Ukraine

² Institute of Physics, NASU, Kyiv, Ukraine

**Corresponding author: nina.ostapenko@gmail.com*

Transport and localization of charge carriers in organic semiconductors belong to the main processes making basis for the operation of optoelectronic devices. The dependence of the energy spectrum of charge carriers generated from traps in organic polymers has a quasi-continuous character. However, in the work [1], for the first time the discrete character of the activation energy (the energy necessary for a charge carrier release from trap) has been found in the investigation of poly (di-n-hexylsilane) by the fractional TSL method. In order to explain such a discrete character, the model of charge carriers release from traps due to the absorption of optical vibration quanta by the carrier has been proposed [2]. The effect depends on the ordering of polymers. In the present paper, the dependence of the process of charge carriers release in silicon organic polymers poly (di-n-hexylsilane), poly (di-n-heptylsilane), poly (methylphenylsilane), poly (di-n-pentylsilane and poly (di-n-phenylsilane) on their ordering is investigated using the fractional TSL method in the temperature range 5-50 K. It is proved that the role of optical vibrations in the processes of charge carriers release is manifested as appearance of discrete activation energies, coincidence of their values with the quanta of optical vibrations obtained from the Raman spectra, and appearance of additional maxima on the TSL curves. The manifestation of these characteristics essentially depends on the ordering of the polymers. The observed effects give the instrument for obtaining information about the interaction of the carries trapped in polymer with molecular vibrations. Comparing experimental and theoretical data about manifestation of the vibrations in the structure of TSL curve we obtain numerical information about the probabilities of charge transition from the trapped state to the conductive region stimulated by separate vibration.

[1]. A. Gumenyuk, N. Ostapenko, Yu. Ostapenko, O. Kerita, S. Suto. // Chem. Phys. – 2012. – V. 394. – p. 36 – 39.

[2]. V.I. Sugakov, N.I. Ostapenko. // Chem. Phys. – 2015. – V. 456. – p. 22 – 27.

The Effect of 2D WS₂ Nanoparticles on Protein Secondary Structure and Amyloid Formation

I.O. Polovyi*, G.I. Dovbeshko, O.P. Gnatyuk, T.O. Hanulia

Department of Physics of Biological Systems, Institute of Physics NASU, Kyiv, Ukraine

**Corresponding author: ipoliov@gmail.com*

Amyloid fibrils are known as aggregations of conformationally modified protein molecules that appear during a course of Alzheimer's, Parkinson's diseases, neuropathic amyloidosis etc. The structure of amyloid fibrils is usually described as non-covalent aggregations of predominantly antiparallel β -sheets [1]. Previously, it was shown that WS₂ nanoparticles can inhibit formation of amyloid fibrils, while MoS₂ nanoparticles were shown as a fibril formation accelerator. Therefore, since chemical properties of WS₂ and MoS₂ are similar, we suppose that WS₂ nanoparticles can both inhibit or accelerate formation of amyloid fibrils.

In this study we described the dual effect of 2D WS₂ on amyloidogenesis of Hen Egg White Lysozyme (HEWL) at different pH (2.5, 3.5, 5.5, 11.5). We used Fourier-transform infrared spectroscopy (FTIR) and Fluorescent analysis with dye Thioflavin T (ThT) that is highly specific to amyloid structures. The results of FTIR spectroscopy showed that when 2D WS₂ nanoparticles were present while incubation, the amount of antiparallel β -sheets were lower by 7% at pH=11.5. At lower pH the difference was not higher than 4% (at pH=5.5) but the effect was opposite.

ThT is a fluorescent dye that has high specificity to amyloid structures. As a ratiometric fluorophore ThT has the excitation (from 340 nm to 440 nm) and fluorescence (from 440 nm to 490 nm) peaks shifted upon binding with amyloid fibrils. Although quantitative analysis remains challenging for such method, we used ratio of fluorescence intensity at 440 nm (excitation 340nm) to fluorescence intensity at 490 nm (excitation 440 nm). As a result, when 2D WS₂ nanoparticles were present during incubation, the ratio was higher approximately by 20%. Thus, 2D WS₂ nanoparticles affect the protein-protein interaction of amyloidogenesis; moreover, such nanoparticles may be used to inhibit the process.

Acknowledgements. The work was supported by projects: 690853-assymcurv-H2020-MSCA-RISE-2015/ H2020-MSCA-RISE-2015); NATO 98 5291, STCU 6175, "Development of 2D materials and "smart" sensors for medical and biological purposes" 11/1 2018; Joint Polish-Ukrainian Projects (20122014, 20152017, 20182020)

[1]. Rambaran, R. N., & Serpell, L. C. (2008). Amyloid fibrils. *Prion*, 2(3), 112-117.
doi:10.4161/pri.2.3.7488./mnlg

Comparison of Absorption Spectra in Conformers of NAD(P)

A.M. Rashevskaya^{*1}, J.G. Terentieva¹

¹ Faculty of Physics, Taras Shevchenko National University of Kyiv, Ukraine

^{*}Corresponding author: anr0202@gmail.com

The spectrophotometry of NAD and NAD(P) dehydrogenase coenzymes has been a target of research over the last few decades due to the stark difference in the behavior of their absorption peaks in oxidized vs. reduced forms. The adenine residue in oxidized $\text{NAD}^+/\text{NAD(P)}^+$ ensures consistent UV absorption in near-visible range, with a prominent peak at about 260 nm. The reduced form $\text{NADH}/\text{NAD(P)H}$ has an additional absorption peak at about 340 nm, absent in the other form due to the stabilization of occupied orbitals in the presence of positive charge, which provides a larger electronic gap. [1]

A series of optimization calculations using GAUSSIAN 03 software employing the TD-PM6 method revealed two major general conformer configurations of NAD(P)^+ : one with non-parallel nucleobase residues, and another one with their almost parallel layout (Fig. 1A). UV-Vis spectra of both of these conformers (Fig. 1B, lines 2, 3) are in decent agreement with known experimental data, correctly displaying the characteristic peaks of NAD(P). The semi-empirical approach falls short in describing the disappearance of the 340 nm peak in NAD(P)^+ , observed experimentally (Fig 1B, line 1).

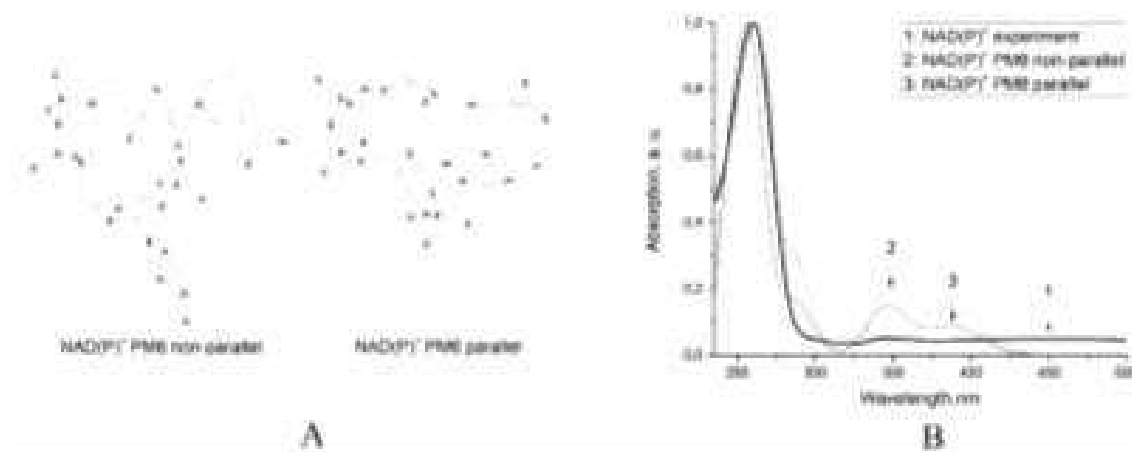


Fig. 1. (A) Optimized geometries of two major conformer configurations of NAD(P)^+ ; (B) experimental (1) and calculated (2, 3) UV-Vis spectra of NAD(P)^+ . [QC methods: PM6, TD-PM6]

[1]. J. De Ruyck, M Famerée et al. Towards the understanding of the absorption spectra of $\text{NAD(P)H}/\text{NAD(P)}^+$ as a common indicator of dehydrogenase enzymatic activity // Chem. Phys. Lett. – 2007 – V. 450. – N. 1–3. – p. 119–122.

Modification of Polyvinyl Alcohol Properties by Embedded ZnO Nanoparticles

G.Yu. Rudko^{*1}, O.F. Isaieva¹, E.G. Gule¹, V.I. Fediv²,
A.O. Kovalchuk¹, A.M. Yaremko¹

¹ V. Lashkaryov Institute of Semiconductor Physics, National Academy of Sciences of Ukraine, Kyiv, Ukraine

² Bukovinian State Medical University, Chernivtsi, Ukraine

**Corresponding author: g.yu.rudko@gmail.com*

Polymers are a highly diverse class of materials which are available in all fields of human activities. Consumption of polymers grows rapidly due to their below average cost and ease of manufacture. The variety of polymers applications is steadily increasing. With the development of nanophysics, polymers acquired a new important field of high-tech applications. Firstly, polymers are known for their amenability for synthesis of quantum dots. They provide robust colloidal stability over a wide scope of solvents and nanoparticles, thus they are extensively used in various wet chemistry growing procedures. Secondly, polymers are the sought-after materials for stabilizing nanoparticles properties vs. ambient conditions, thus they are used for producing polymer-based nanocomposites with embedded quantum dots. When considering a nanocomposite, a key issue is an understanding of the variation of inner polymeric structure by the nanoparticles embedded and important challenge is to reveal the bonds between a particle surface and the surrounding polymer.

We report on the studies of nanocomposite consisting of polyvinyl alcohol embedded with inorganic ZnO nanoparticles. Raman spectroscopy was used as an experimental tool for rigorous testing of the bonds between nanoparticles and polymeric macromolecules. To analyze the processes of the energy exchange between the polymeric matrix and nanoparticles the photoluminescence spectroscopy was used. The experimental results demonstrate that, besides the appearance of the bands of ZnO nanoparticles vibrations, the vibrational spectrum inherent for polyvinyl alcohol is rearranged. Namely, vibration bands corresponding to carbonyl groups in acetate residuals as well as the features related to secondary alcohols and monosubstituted acetylenes disappear. Incorporation of nanoparticles also leads to the changes in the ensemble of hydrogen bonds in the polymer thus indicating the formation of interfacial bonds between macromolecules and particles surfaces. Cross-interfacial energy exchange between the polymeric matrix and inorganic inclusions was revealed by the comparison of the luminescence excitation and emission spectra.

Spectroscopic Study on Binding of a Tricationic *meso*-Porphyrin to Double-Stranded Synthetic Polynucleotides

O.A. Ryazanova^{*1}, I.M. Voloshin¹, A.Yu. Glamazda¹, L.V. Dubey²,
I.Ya. Dubey², V.A. Karachevtsev¹

¹ Department of Molecular Biophysics, B. Verkin Institute for Low Temperature Physics and Engineering, NAS of Ukraine, Kharkiv, Ukraine

² Department of Synthetic Bioregulators, Institute of Molecular Biology and Genetics, NAS of Ukraine, Kyiv, Ukraine

^{*}Corresponding author: ryazanova@ilt.kharkov.ua

Binding of a tricationic water soluble *meso*-porphyrin, TMPyP³⁺ (Fig. 1) to double-stranded poly(A)·poly(U) and poly(G)·poly(C) has been studied in 5 mM phosphate buffer, pH6.9, of low and near-physiological ionic strengths in a wide range of molar phosphate-to-dye ratios (*P/D*). The techniques of absorption, polarized fluorescence and Raman spectroscopy as well as resonance light scattering were used. Two competitive binding modes were revealed. At *P/D* < 3.5 outside binding of the porphyrin to polynucleotide backbone is prevailed with self-stacking of the porphyrin chromophores for poly(G)·poly(C) and without him for poly(A)·poly(U). In the first case substantial quenching of porphyrin fluorescence was observed (up to 43% from initial) [1], whereas for the second one the emission intensity increases monotonically (Fig. 2). Light scattering data evidences the formation of large scale porphyrin aggregates near the stoichiometric binding ratio for both systems. At *P/D* > 30 the embedding of the partially stacked porphyrin *J*-dimers into the polymer groove is supposed, it is accompanied by emission enhancement.

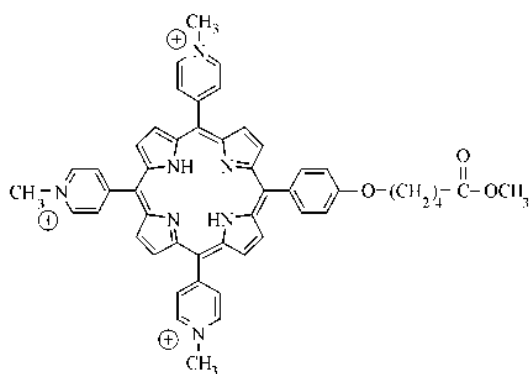


Fig. 1. Molecular structure of tricationic *meso*-porphyrin TMPyP³⁺.

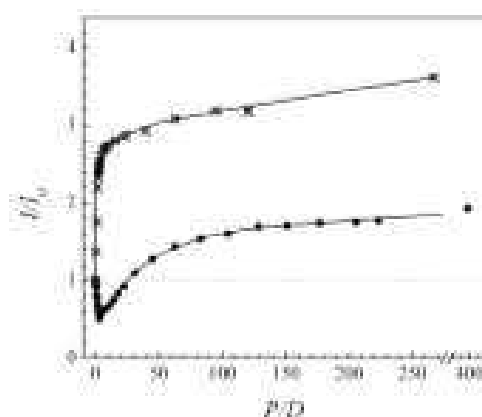


Fig. 2. Dependence of the TMPyP³⁺ relative fluorescence intensity on *P/D* upon titration by poly(A)·poly(U) (×) and poly(G)·poly(C) (●) [1].

- [1]. O. Ryazanova, V. Zozulya, I. Voloshin, A. Glamazda, I. Dubey, L. Dubey, V. Karachevtsev. Interaction of a tricationic *meso*-substituted porphyrin with guanine-containing polyribonucleotides of various structures // *Methods and Applications in Fluorescence*. – 2016. – V. 4. – N. 3. – 034005.

Spectroscopic Study on Binding of TMPyP⁴⁺ Porphyrin to Single-Stranded poly(rA)

O.A. Ryazanova*, I.M. Voloshin, V.N. Zozulya

Department of Molecular Biophysics, B. Verkin Institute for Low Temperature Physics and Engineering, NAS of Ukraine, Kharkiv, Ukraine

*Corresponding author: ryazanova@ilt.kharkov.ua

Binding of *meso*-tetrakis(4-N-methyl-pyridyl)porphine, TMPyP⁴⁺ (Fig. 1), to single-stranded poly(rA) has been studied in 2 mM phosphate buffered solution, pH 6.9, of low ionic strength in a wide range of molar phosphate-to-dye ratios (*P/D*) by absorption and polarized fluorescence spectroscopy.

It was found that binding to poly(rA) results in 16 nm red shift and 28% hypochromism of the porphyrin absorption spectra as well as in splitting of the fluorescence band, enhancement of the emission intensity and rise of the fluorescence polarization degree up to 0.075 (Fig. 2). However, comparison of the fluorescence titration curves (Fig. 2) with those obtained earlier for single-stranded inorganic polyphosphate, poly(P) [1], shows that binding of TMPyP⁴⁺ to poly(rA) is substantially different. So for TMPyP⁴⁺ + poly(P) titration curve is biphasic, substantial quenching of porphyrin fluorescence (82 %) is observed at low *P/D* values, since conformation of poly(P) chain was shown to promote formation of continuous self-stacked TMPyP⁴⁺ aggregates electrostatically bound to poly(P) exterior. While monotonically increasing titration curve observed in the case of poly(rA) evidences that outside electrostatic binding of the porphyrin does not accompanied by self-stacking of the TMPyP⁴⁺ chromophores.

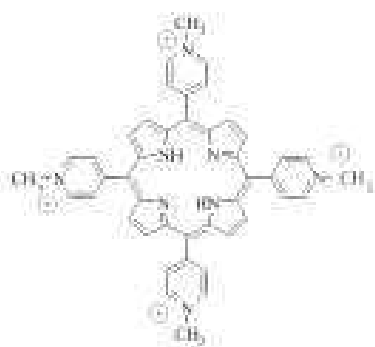


Fig. 1. Molecular structure of tetracationic *meso*-porphyrin TMPyP⁴⁺.

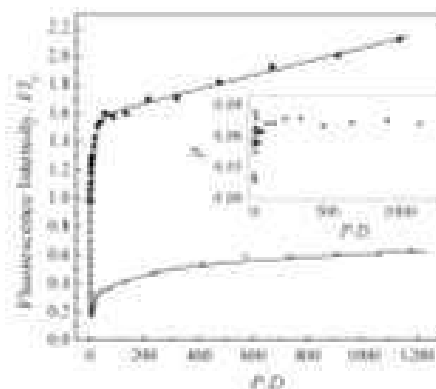


Fig. 2. Dependence of the TMPyP⁴⁺ relative fluorescence intensity and polarization degree (inset) on *P/D* upon titration by poly(A) (●) and poly(P) (▽) [1].

- [1]. V. Zozulya, O. Ryazanova, I. Voloshin, A. Glamazda, V. Karachevtsev. Spectroscopic detection of tetracationic porphyrin H-aggregation on polyanionic matrix of inorganic polyphosphate // Journal of Fluorescence. – 2010. – V. 20. – N. 3. – p. 695–702.

Formation of Noncovalent Complexes of Antimalarial Artemisinin-type Agents with Ascorbic Acid and Membrane Phospholipids: Joint Mass Spectrometry and Quantum Chemical Study

V.A. Pashynska¹, S.G. Stepanian^{*1}, A. Gomory²

¹ Molecular Biophysics Department, B. Verkin Institute for Low Temperature Physics and Engineering of the National Academy of Sciences of Ukraine, Kharkiv, Ukraine

² Institute of Organic Chemistry of Research Centre for Natural Sciences of the Hungarian Academy of Sciences, Budapest, Hungary

**Corresponding author: stepanianl@ilt.kharkov.ua*

The current joint study by electrospray ionization mass spectrometry (ESI MS) and quantum chemical DFT/B3LYP/aug-cc-pVDZ methods covers the examining of biologically significant interactions of the artemisinin-type antimalarial agents with molecules of ascorbic acid (ACA) and membrane phospholipid dipalmitoylphosphatidylcholine (DPPC). The urgency of such a study is determined by the necessity to evaluate if the joint usage of the artemisinin-type drugs with ascorbic acid (widely used supporting vitamin preparation or element of the patient's food) can modulate the drugs biological activity, because of their complexation. Formation of stable noncovalent complexes of the artemisinin-type agents (artemisinin, dihydroartemisinin, α -arthemether and arthesunate) with ascorbic acid molecules in the polar solvent methanol has been revealed by ESI MS probing of the double model systems of the antimalarial drug and ACA with 1:1 molar ratio. In the spectrum of the model system of ACA and DPPC (1:10 molar ratio), the peak of cationized complexes $[\text{ACA}\cdot\text{DPPC}\cdot\text{Na}]^+$ with m/z 933.2, is identified. Then, the triple systems containing the artemisinin-type agent, ACA and DPPC in the molar ratio 1:1:10 have been examined. The results reveal a competition between ACA and DPPC for binding with the antimalarial agents, because of the peaks of the clusters artemisinin-type drug \cdot ACA, artemisinin-type drug \cdot DPPC and ACA \cdot DPPC observation in the mass spectra. To elucidate structure and energetic characteristics of the noncovalent complexes observed in the ESI MS experiments the model *ab initio* calculations of dihydroartemisinin and ACA complexes and clusters of the drugs molecules with the polar phosphatidylcholine head of DPPC have been performed by DFT/B3LYP/aug-cc-pVDZ method. The calculation results confirm the stability of the complexes studied in vacuum as well as in methanol/water surrounding (PCM calculation results) and allow us to identify the most energetically profitable structures of the noncovalent complexes. The results obtained testify to the possibility of modulation of the biological activity of arthemisin-type agents and ascorbic acid under their combined usage in therapeutic practice.

Peculiarities of Zn^{2+} Ion Interactions with Single-Stranded PolyC in Neutral Solution

E.L. Usenko^{*}, V.A. Valeev, V.A. Sorokin

Department of Molecular Biophysics, B. Verkin Institute for Low Temperature Physics and Engineering of NAS of Ukraine, Kharkov, Ukraine

^{*}*Corresponding author: usenko@ilt.kharkov.ua*

Single-stranded regions in double-stranded biological molecules induced by polymerase activity are involved in replication, transcription and translation processes in living cells [1]. Ions of heavy and transition metals (TM) can violate these processes inducing mutagenesis and carcinogenesis [2]. On the other hand, an optimal concentration of TM is a required condition for normal functioning of living cells. One of the possible mechanisms by which TM ions affect cellular processes is their ability to form specific coordination bonds with heteroatoms of nucleic acid nitrogen bases.

Zn^{2+} ions effect on the conformation of poly(C) in cacodylic buffered solution pH 7.0 was studied using differential UV spectroscopy and absorption melting techniques.

A three-dimensional phase diagram and its two-dimensional components were constructed for poly(C) – Zn^{2+} system. The phase diagram revealed a region, in which ordered single-stranded structures are formed being stabilized by Zn^{2+} -mediated crosslinks involving N3(C). The phase diagram also demonstrated that behavior of poly(C) – Zn^{2+} system is similar to the effect of retrograde condensation observed earlier in some binary solutions of simple liquids.

The atoms coordinating Zn^{2+} ions in polyC were determined. A dependence of Zn^{2+} to polyC binding constant on the metal ion concentration was obtained. It was shown that Gibbs free energy of Zn^{2+} binding to N3 of poly(C) is a linear function of the binding degree. It is characterized with positive cooperativity conditioned mainly by dehydration of ions and bases upon the formation of metal complexes.

- [1]. C.H. Ke, A. Lokszejn, Y. Jiang, M. Kim, M. Humeniuk, M. Rabbi, P.E. Marszalek. Detecting solvent-driven transitions of poly(A) to double-stranded conformations by Atomic Force Microscopy // Biophysical Journal. – 2009. – V. 96. – p. 2918-2925.
- [2]. A. Hartwig. Recent advances in metal carcinogenicity // Pure and Applied Chemistry. – 2000. – V. 72. – p. 1007-1014.

6

Nanoobjects

Fabrication of Photonic Crystals and Nanocomposites on the Base of Synthetic Opals: Is it Really Promising?

M.P. Derhachov

Department of Physics, Electronics and Computer Systems, Oles Honchar Dnipro National University, Dnipro, Ukraine

Corresponding author: derhachov_mp@dnu.dp.ua

Synthetic opals consisted of amorphous, regularly arranged SiO_2 spheres with a mean diameter of several hundreds of nanometers have been considered as prospective matrix for creating photonic crystals for last several tens of years. Owing to a periodic modulation of dielectric constant at the scale of light wavelength, there are spectral regions where the density of optical states is seeking a value as low as possible in the real opal structure. An existence of such regions allows to manage spatial and spectral parameters of spontaneous emission emerged inside opal. On the other hand, porous structure of bare synthetic opals can be used to create nanocomposites by infiltrating the opal pores with variable materials. The multifunctional units may be fabricated in such a way.

The work is devoted to analysis of optical phenomena in real synthetic opals infiltrated with light emitters, active dielectrics and metals. The influence of multiplied scattering and structure disordering on the emission efficiency is discussed [1, 2]. Besides, the main peculiarities of infiltration techniques caused by possible chemical interaction between opal matrix and embedding substances are also considered [3, 4]. The limitation in choice of infiltrator with prominent properties is shown. An appearance of size effects and the intensity enhancement in the Raman spectra of the nanocomposites is discussed.

- [1]. Moiseyenko, V.N. The Effects of Disorder on the Optical Spectra of Synthetic Opals / V.N. Moiseyenko, M.P. Dergachov, A.V. Yevchik, O.O. Spichak, V.S. Gorelik // Springer Proceedings in Physics, Nanoplasmonics, Nano-Optics, Nanocomposites, and Surface Studies, Ed. by O. Fesenko, L. Yatsenko. - 2015. - V.167. - P. 315-327.
- [2]. Moiseyenko, V. Modification of Optical Properties of 2,5-bis(2-benzoxazolyl) hydroquinone in Opal Photonic Crystals / V. Moiseyenko, M. Dergachov, B. Abu Sal, A. Yevchik // Ukrainian Journal of Physical Optics. - 2013. - V.14, No. 4. - P.225-232.
- [3]. Derhachov, M. Structure, Optical and Electric Properties of Opal–Bismuth Silicate Nanocomposites /M. Derhachov, V. Moiseienko, N. Kutseva, B. Abu Sal, R. Holze, S. Pliaka, A. Yevchyk// Acta Physica Polonica A - 2018. - V.133, No. 4. - P. 847-850.
- [4]. Moiseyenko, V.N. Formation and Raman Characterization of Nanocrystalline Phase of Active Dielectrics in Synthetic Opal Pores / V.N. Moiseienko, M.P. Derhachov, N.O. Kutseva, B. Abu Sal, R. Holze, N. Brynza // Springer book “Nanophysics, Nanomaterials, Nanotechnology, Surface Studies and Applications”, Ed. by O. Fesenko, L. Yatsenko. – 2016, P. 215-227

Correlation Mechanism of Cold Electrons Filtration in Resonant Tunneling Devices

V.N. Ermakov^{*}, E.A. Ponezha

Bogolyubov Institute for Theoretical Physics, NAS of Ukraine, Kiev, Ukraine

^{*}Corresponding author: vterm@bitp.kiev.ua

The thermal distribution of charge carries is the essential limitation for the use of nanoelectronic devices. In such systems with a small number of charge carries (low current) subjected to scattering, the information component may be lost. In Ref. [1] it was reported about the energy-filtered cold electron transport at room temperature in the tunneling device where a nanoparticle embedded in a dielectric matrix served as a quantum dot (QD). The cold electron transport was detected from extremely narrow differential conductance peaks with the width at half maximum of 15 mV at room

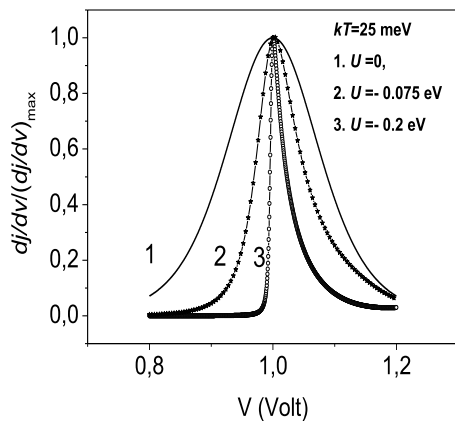


Fig. 1. Normalized differential conductance peaks for different values of the splitting energy U .

temperature. We proposed the explanation of the effect of suppressing the temperature distribution of the current carriers in the QD where levels are four-fold degenerated. We argued that the attractive electron correlations could be caused by an interaction of electrons with low energy phonons. The attractive energy $|U|$ exceeds in value the Coulomb repulsion. With negative values of U , the splitting levels in the QD can have lower energies than the Fermi energy of the source electrode. The tunneling current through these levels will not be affected by the temperature. The analogous mechanism of nonlinearity with the

strong electron-phonon interaction has been considered in Ref. [2] and was developed in Ref. [3]. We have shown that the widths of differential conductance peaks decrease with increasing the splitting energy $|U|$ and become close to the observed ones [1] when $|U| = 0.5$ eV at temperature $kT = 25$ meV (see Fig. 1).

[1]. Pradeep Bhadrachalam, et al. Nature communications /DOI:10.1038/ncomms 5745 (2014)

[2]. V.N. Ermakov // Physica E, 8, 99-105 (2000).

[3]. A.S. Alexandrov and A.M. Bratkovsky // Phys. Rev. B, 67, 235312-8 (2003).

Adsorption of Double-Stranded Polynucleotide on Graphene/Graphene Oxide: UV-Absorption Spectroscopy and Molecular Dynamics Simulation Study

V.A. Karachevtsev^{*}, M.V. Karachevtsev, V.A. Valeev,
A.M. Plokhotnichenko

B. Verkin Institute for Low Temperature Physics and Engineering, National Academy of Sciences of Ukraine, Kharkiv, Ukraine

**Corresponding author: karachevtsev@ilt.kharkov.ua*

Hybridization of nucleic acids with graphene nanomaterials is of great interest due to its potential application in nanomedicine. Graphene oxide (GO) is a water soluble derivative of graphene (Gr), which has unique characteristics such as good water dispersibility, facile surface functionalization, and high mechanical strength. Existence of flat sp^2 -hybridized sections surrounded with different oxygen-containing groups facilitates efficient interaction of GO with biomolecules of different structures. Among them adsorption of DNA/RNA on GO has received special attention because of promising applications in genosensing and gene delivery.

In this contribution the adsorption of double-stranded polynucleotide poly(rA)·poly(rU) on graphene oxide in the aqueous suspension was studied by UV-absorption spectroscopy. Comparison of the total light absorption of poly(AU) aqueous solution and GO aqueous suspension with their mixture showed that after mixing the optical density increases. This indicates the interaction of the polymer with GO, as a result of which the absorption of light by the polymer increases due to stacking interaction between π - π systems of two components. Poly(AU) binding with GO is also confirmed by the comparison of melting curves of the samples poly(AU):GO and free poly(AU), which demonstrates the decrease of the hyperchromic coefficient of polymer on GO at high temperatures.

Adsorption process of the short oligonucleotide duplex r(AU)₁₅ on Gr by employing molecular dynamics is considered too. We discuss the process duplex disordering on Gr, binding energy and influence of the oligomer start arrangements (parallel and perpendicular) relative to Gr surface on the adsorption.

The obtained spectral information about the adsorption of poly(AU) on graphene oxide and the results of the MD simulations can be useful in potential applications of graphene nanomaterial such as the development of novel genosensors and nanosized scaffolds for drug delivery.

This work was supported by the National Academy of Sciences of Ukraine (NASU) (Grant N 15/19-H, Grant N 07-01-18/19). N.V.K. acknowledges support from the NASU: Grant N 4/H-2019.

Characterization of Graphene Oxide and Single-walled Carbon Nanotubes Composites: Raman Spectroscopy and Conductivity Temperature Dependence

N.V. Kurnosov^{*}, V.A. Karachevtsev

B. Verkin Institute for Low Temperature Physics and Engineering, National Academy of Sciences of Ukraine, Kharkiv, Ukraine

^{}Corresponding author: n.kurnosov@ilt.kharkov.ua*

Graphene oxide (GO) and single-walled carbon nanotubes (SWNTs) are carbon nanomaterials that have unique physical properties and are promising for various applications in such technological areas as nanoelectronics, photonics and sensing. GO sheets have domains containing both sp^2 hybridized electrons of carbon atoms and sp^3 -electron structures of carbon bound with oxygen-containing groups. GO can be freely dispersed in water bringing up an important advantage which SWNTs lack. SWNTs instead have pronounced structure-dependent electronic and optical properties as well as high electrical and thermal conductivity. Therefore, 3D hybrid composite structures containing both 2D GO and 1D SWNTs are currently among the main research topics due to possible synergistic effect and improved characteristics when compared to those of individual components. In this work we have studied the composite films of strongly oxidized GO and SWNTs (CoMoCAT synthesis method) as well as GO and SWNT films. The preparation of films was based on vacuum filtration from aqueous suspensions obtained, in turn, through ultrasound treatment and centrifugation. Raman spectra were registered in the range of $1200\text{--}1800\text{ cm}^{-1}$ where D-bands and G-bands of both GO and SWNTs are located. Comparison of composite film spectrum with those of GO and SWNTs revealed changes in bands spectral position and width attributed to interaction between GO and SWNTs in composite. D/G ratio was evaluated which allowed us to estimate the mean size of GO sp^2 hybridized domains. We have also performed electrical conductivity measurements in the temperature range of $5\text{--}291\text{ K}$ for composite and SWNT films, while GO film has shown no conductivity. Temperature dependencies of conductivity were analyzed in the framework of 3D Mott and Arrhenius models. It was shown that SWNT and composite films obtained can be classified as disordered semiconductors. The revealed differences between such parameters as mean length and energy of electron hopping were attributed to energy barriers at contacts of SWNTs and GO in the composite film.

This work was supported by the National Academy of Sciences of Ukraine (NASU) (Grant N 15/19-H within the program “Fundamental Problems of the Creation of New Nanomaterials and Nanotechnology”, Grant N 07-01-18/19). N.V.K. acknowledges support from the NASU: Grant N 4/H-2019.

Micro and Nanocrystalline Cellulose - Oxide Composites: Comparative Analysis of Spectroscopic Properties

S.G. Nedilko^{*1}, P.O. Teselko¹, S.L. Revo¹, V.P. Scherbatskii¹,
V.A. Barbash², O.V. Yashchenko², M. Androulidaki³,
A. Papadopoulos³, S. Hamamda⁴

¹ Physics Faculty, Taras Shevchenko National University of Kyiv, Kyiv, Ukraine

² National Technical University of Ukraine "Igor Sikorsky Kyiv Polytechnic Institute", Prospect Peremogy, 37, Kyiv, Ukraine

³ Institute of Electronic Structure & Laser (IESL) of Foundation for Research & Technology Hellas (FORTH), Heraklion 711 10 Crete, Greece

⁴ Laboratory of Thermodynamics and Surface Treatment of Materials, University Frères Mentouri, B.P. 325 Route Ain El Bey, Constantine 25017, Algeria

**Corresponding author: SNedilko@univ.kiev.ua*

It is common knowledge that cellulose molecules are formed by residues of beta-glucose molecules and are characterized only by a linear structure. As a result, cellulose easily forms fibers. Cellulose is the main component of the cells shells of higher plants. Its mass fraction in the wood is about 50%, in cotton fibers - up to 98, in the jute crust - up to 75%. Microcrystalline/nanocellulose (MCC/NC) can be used to prepare flexible, suitable for electric charge accumulation or optically transparent paper. Such paper is an attractive substrate for electronic devices because it is recyclable, compatible with biological objects, and it easily degrades [1]. That is why, composites on the base of cellulose matrix, especially micro/nano composites, now are under intensive studies.

In this work we talk about fabrication of the sets of "cellulose-oxide" micro/nanocomposite materials and study of their morphology, structure and some physical properties. For this purpose the sets "ceramics" and gel - like composite materials that consist of micro/nanocellulose and luminescent oxide dielectric micro/nanoparticles of vanadates, phosphates etc. compounds were prepared.

Experimental results about structure, morphology and some other properties were obtained. Non-destructive solid-state control methods were used for research: XRD; TGA; SE, TE and optical microscopy; luminescent, FTIR, reflection and absorption light spectroscopy as well.

The measurements revealed mutual influence of composite components. Their electronic and vibronic spectra consist of features related with separated constituents, but details caused by their interaction were found too. Obtained results confirmed perceptiveness of similar cellulose based composites for application.

Optical Centers in $\text{Re}_2\text{SiO}_5\text{:Ce}^{3+}$ Crystals and Nanocrystals

V. Seminko^{*}, P. Maksimchuk, I. Bessalova, Yu. Malyukin

Institute for Scintillation Materials, National Academy of Sciences of Ukraine, 61072, 60 Nauky Ave., Kharkiv, Ukraine.

^{*}*Corresponding author: seminko@ukr.net*

Cerium-doped oxyorthosilicates (Re_2SiO_5) are well-known as highly-efficient scintillation materials with high scintillation yield (~ 25000 photons/MeV) and short decay time (less than 40 ns). However, their usage in scintillation techniques is limited by high afterglow level.

$\text{Lu}_2\text{SiO}_5\text{:Ce}^{3+}$ and $\text{Y}_2\text{SiO}_5\text{:Ce}^{3+}$ (C=1 at.%) nanocrystals were synthesized by the sol-gel technique. The crystal structure of Re_2SiO_5 nanocrystals ($P2_1/c$ space group) differs from the crystal structure of Re_2SiO_5 bulk crystals ($C2/c$ space group) with 9- and 7-oxygen-coordinated cation positions (Gd_2SiO_5 -type structure) instead of 6- and 7- coordinated ones observed for Re_2SiO_5 bulk crystals. Interestingly, photoluminescence spectra of $\text{Lu}_2\text{SiO}_5\text{:Ce}^{3+}$ and $\text{Y}_2\text{SiO}_5\text{:Ce}^{3+}$ (C=1 at.%) nanocrystals consisted of the bands related to both centers, while X-ray luminescence spectra are formed by emission of Ce2 centers only. Also, the treatment in oxidative atmosphere led to redistribution of intensities of Ce1 and Ce2 optical centers at X-ray excitation indicating involvement of oxygen vacancies as trap centers in the processes of electron-hole pair relaxation.

Formation of oxygen vacancies occurs mainly on the sites of non-silicon-bonded oxygen which has sufficiently less binding energy as compared to other oxygen ions. While for bulk Lu_2SiO_5 and Y_2SiO_5 the distance between cation site and non-silicon-bonded oxygen ions is almost the same for Re1 and Re2 sites (2.16 Å and 2.166 Å, respectively), for bulk Gd_2SiO_5 (and so, for Lu_2SiO_5 and Y_2SiO_5 nanocrystals) the surrounding of Re1 site includes only one non-silicon-bonded oxygen, and the surrounding of Re2 site includes three non-silicon-bonded oxygen ions. So, the oxygen vacancies in cerium-doped crystals and nanocrystals with Gd_2SiO_5 -type structure are located preferentially near Ce2 ions. Electrons formed at X-ray excitation can move far away from their point of origin, but finally they are trapped on the oxygen vacancies near Ce2 centers and recombine with holes trapped on the same Ce2 centers. In this way Ce2 become dominant in X-ray, but not photoluminescence spectra of $\text{Lu}_2\text{SiO}_5\text{:Ce}^{3+}$ and $\text{Y}_2\text{SiO}_5\text{:Ce}^{3+}$ nanocrystals.

[1]. V.Seminko et al. Different Roles of Ce^{3+} Optical Centers in Oxyorthosilicate Nanocrystals at X-ray and UV Excitation // Crystals. – 2019. – V. 9. – N. 2. – p. 114.

Exciton Self-Trapping in TDBC J-Aggregates in Thin Polymer Films

A.V. Sorokin^{*1}, I.Yu. Ropakova¹, S. Wolter², S.L. Yefimova¹,
S. Lochbrunner², Yu.V. Malyukin¹

¹ Institute for Scintillation Materials of NAS of Ukraine, Kharkiv, Ukraine

² Institute of Physics and Department of Life, Light and Matter, University of Rostock, 18051 Rostock, Germany

**Corresponding author: sorokin@isma.kharkov.ua*

We studied the exciton dynamics of TDBC J-aggregates formed in two types of polymer films, namely uncharged spin-coated PVA films and charged layer-by-layer PDDA films. It was found that despite the similarity of the main steady-state spectral characteristics of the J-aggregates in the polymer films their fluorescence quantum yields are strongly different ($\eta^{\text{spin}} \sim 4\%$ and $\eta^{\text{LbL}} \sim 0.5\%$) and both are much smaller than in solution ($\eta^{\text{sol}} \sim 31\%$).

Using optical microscopy and AFM images the different morphologies of the TDBC aggregates in the two types of polymer films were characterized. For spin-coated films a quasi-one-dimensional, rod-like morphology of the J-aggregates was found similar to that in solution. However, for LbL films the morphology of the aggregates transforms to two-dimensional, island-like structures.

Due to the more rigid environment in the polymer films the exciton-phonon coupling constant of the J-aggregates becomes quite large resulting in efficient exciton self-trapping. The latter is supposed to be responsible for the lower quantum yields in the films compared to solution. Exciton self-trapping manifests itself at low temperatures (~ 80 K) in a red-shifted fluorescent band with a long decay time.

Using time-resolved emission spectra it was shown that the features of the self-trapping processes are different for both types of the studied polymer films. For the quasi 1D TDBC aggregates in the spin-coated films barrierless exciton self-trapping dominates. For the 2D TDBC aggregates in the LbL films exciton self-trapping occurs via a barrier with a height of 220 cm^{-1} . As a result fluorescence quenching is for TDBC J-aggregates in LbL films at room temperature much stronger than at low temperatures.

Nanospectroscopy and Proton Transport Phenomena of TiO₂/Nafion Nanocomposites

G. Telbiz^{*1}, E. Leonenko¹, V. Juhymchyk²

¹L.V. Pisarzhevsky Institute of Physical Chemistry, NAS. of Ukraine, Kyiv, Ukraine

²V.Ye. Lashkaryov Institute of Semiconductor Physics NAS of Ukraine, Kyiv, Ukraine

**Corresponding author gtelbiz@yahoo.com*

Fuel cell using hydrogen as fuel represents a promising alternative since it can be integrated into an energy conversion using renewable sources and reducing polluting emissions. The application of the most advanced materials research methods to one of the most pressing needs of our times, the production and storage of sustainable energy, is at the core of the research nanoparticles on the performance of the Nafion/TiO₂ composite membranes in high temperature. In the framework of the research on the nature and mechanism of action by Raman and infrared spectroscopy, AFM, XPS, SEM, XRD, TPD MS, the properties of active titanium oxide additive polymer membranes are investigated. Effect of concentration of proton generation additions to the total and specific proton conductivity of composite polymer membranes depending on the concentration of proton-generating additives and relative humidity had been estimated. Preliminary tests of proton conductivity (the direct injection of protons) that was performed on the composite membrane, has highlighted the benefit of doped titania nanocomposites addition to the conductivity in the temperature range up to 240 °C, that maintained at 10⁻³-10⁻⁵S, as compared to the commercial Nafion membrane. The above may be a prerequisite for efficient behavior of composite polymer membrane in conditions close to the operating conditions of fuel cells.

Mechanisms of $\text{LnVO}_4\text{:Eu}^{3+}$ Nanoparticle Catalytic Activity

S.L. Yefimova*, P.O. Maksimchuk, K. Hubenko, Yu.V. Malyukin

Department of Nanostructured Materials, Institute for Scintillation Materials NAS of Ukraine, Kharkiv, Ukraine

*Corresponding author: efimova@isc.kharkov.ua

Redox-active nanomaterials, which are able to generate or scavenge free radicals and reactive oxygen species (ROS), are of growing interest in modern technologies ranging from catalysis, photovoltaic cells, UV protective screens to nanomedicine including cancer diagnosis and treatment. In our previous papers, we reported on biological activity of rare-earth orthovanadate nanoparticles $\text{LnVO}_4\text{:Eu}^{3+}$ (pro-/ antioxidant properties, effects on bioenergy processes in cell mitochondria, selective accumulation in cell nuclei, *etc.*) that makes such redox nanomaterials very prospective for biomedical applications and requires deep understanding the mechanisms of their redox activity [1-3].

In this work, we report on abnormal dynamics of hydroxyl radicals generation under UV irradiation of water solution containing small ($d=2$ nm) $\text{GdYVO}_4\text{:Eu}^{3+}$ nanoparticles. An analysis of the increase in $\cdot\text{OH}$ concentration in time allows two parts in the $\cdot\text{OH}$ generation curve to be revealed. The first slower part is shown to be associated with a predominate radical scavenging mechanism and explained by the presence of ions with a changeable valence state ($\text{V}^{4+}/\text{V}^{5+}$) and oxygen vacancies in the structure of $\text{GdYVO}_4\text{:Eu}^{3+}$ NPs. The second faster part is associated with photo-induced holes interaction with water molecules adsorbed at the surface of NPs followed by the hydroxyl radical production. The mutual contributions of the two mechanisms are changed in time and the depletion of the scavenging mechanism is observed in about 90 min after UV irradiation start. Our finding is a next step to understand the mechanism of NPs redox-activity for taking greater advantage of such nanomaterials in biomedical application.

- [1]. G. Grygorova, V.K. Klochkov, Ye. Mamotyuk, Yu.V. Malyukin, Cerium Dioxide CeO_{2-x} and Orthovanadate ($\text{Gd}_{0.9}\text{Eu}_{0.1}\text{VO}_4$) Nanoparticles for Protection of Living Body from X-Ray Induced Damage // in: Nanomaterials for Security, Springer. - 2016. – p. 289–296.
- [2]. K. Hubenko, S. Yefimova, T. Tkacheva, P. Maksimchuk, I. Borovoy, V. Klochkov, N. Kavok, O. Opolonin, Yu. Malyukin, Reactive oxygen species generation in aqueous solutions containing $\text{GdVO}_4\text{:Eu}^{3+}$ nanoparticles and their complexes with methylene blue // Nanoscale Res. Lett. – 2018. – V.13. – p. 100.
- [3] Klochkov, V.K.; Grigorova, A.V.; Sedyh, O.O.; Malyukin, Yu.V. The Influence of Agglomeration of Nanoparticles on Their Superoxide Dismutase-Mimetic Activity // Colloids Surf. A: Physicochem. Eng. Aspects. – 2012. – v.409. – P. 176–182.

Laser-Driven Structural Transformations in Dextran-Graft-PNIPAM Copolymer / Au Nanoparticles Hybrid Nanosystem: The Role of Plasmon Heating and Attractive Optical Forces

O.A. Yeshchenko^{*1}, A.P. Naumenko¹, N.V. Kutsevol², I.I. Harahuts²

¹ Physics Department, Taras Shevchenko National University of Kyiv, Kyiv, Ukraine

² Chemistry Department, Taras Shevchenko National University of Kyiv, Kyiv, Ukraine

**Corresponding author: yes@univ.kiev.ua*

A laser induced structural transformations in dextran grafted-poly(N-isopropylacrylamide) copolymer/Au nanoparticles (D-g-PNIPAM/AuNPs) hybrid nanosystem in water have been observed. The laser induced local plasmonic heating of Au NPs leads to Lower Critical Solution Temperature (LCST) phase transition in D-g-PNIPAM/AuNPs macromolecules accompanied by their shrinking and aggregation. The hysteresis non-reversible character of the structural transformation in D-g-PNIPAM/AuNPs system has been observed at the decrease of laser intensity, i.e. the aggregates remains in solution after the turn-off the laser illumination. This is an essential difference comparing to the case of usual heating-cooling cycles when there is no formation of aggregates and structural transformations are reversible. Such fundamental difference has been rationalized as the result of action of attractive optical forces arising due to the excitation of surface plasmons in Au NPs. The attractive plasmonic forces facilitate the formation of the aggregates and counteract their destruction. The laser induced structural transformations have been found to be very sensitive to matching condition of the resonance of the laser light with surface plasmon resonance proving the plasmonic nature of observed phenomena (Fig. 1).

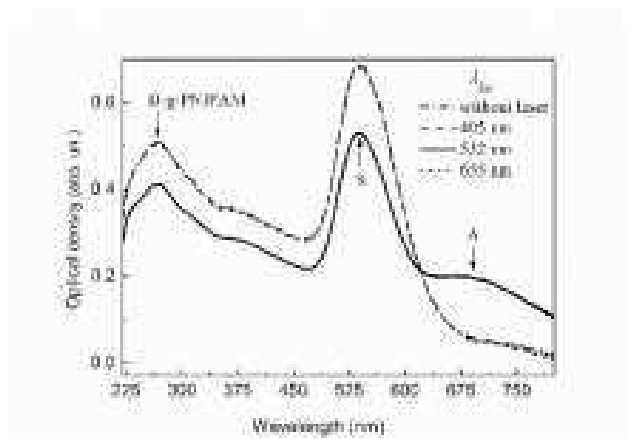


Fig. 1. Extinction spectra of Au NPs in D-g-PNIPAM/AuNPs nanosystem after laser illumination with various wavelengths (laser intensity 425 W/cm²) and without illumination.

Effect of Temperature on Dielectric Relaxation Processes in Nanoparticle Suspensions

L.V. Batyuk*¹, V.P. Berest²

¹ Department of Medical and Biological Physics and Medical Information Science/ Kharkiv National Medical University, Kharkiv, Ukraine

² Department of Molecular and Medical Biophysics / V.N. Karazin Kharkiv National University, Kharkiv, Ukraine

*Corresponding author: liliya-batyuk@ukr.net

As is known, polarization and dielectric losses are determined by the structure of the polymer and the features of the thermal motion of macromolecules. About the type of conductivity of polymer dielectrics is judged, as a rule, by indirect data due to small values of their concentration. This significantly limits information about the mechanism of conductivity of polymers. The properties of a dielectric in a sinusoidal electric field are described by the complex dielectric constant, which takes into account the loss factor, and the circular frequency [1, 2]. In this work a model for calculating the temperature dependence ($T=0\div 50^\circ\text{C}$) of the dielectric relaxation of water molecules in the centimeter wavelength range ($f=9\text{ HHZ}$; $\lambda=3.0\pm 0.2\text{ cm}$) for the ultra-dispersed diamonds (UDD). This material has a cluster structure, includes an inert core, represented by sp^3 -hybridized carbon atoms, and a functionalized surface layer, characterized by the presence of certain functional groups on the cluster surface: $-\text{OH}$, $-\text{NH}_2$, $-\text{CH}_2\text{OH}$, $-\text{CO}(\text{NH}_2)$. These groups provide a high antioxidant activity of this material, which was estimated by the method of microwave dielectrometry of the resonator type [3]. From our theoretical calculations, it follows that UDDs have a great potential for polarization in electric fields. The behavior of the temperature dependence of dielectric permittivity (ϵ') and the tangent of the dielectric loss angle ($\text{tg}\delta$), obtained experimentally, indicate the presence of relaxation processes in the structures. It was revealed that during hydration, UDD intensively adsorb moisture, which is accompanied by a significant increase in the dielectric polarization of the samples. Desorption of water molecules under room conditions occurs rather slowly. UDD particles form near-surface water layers at the grain boundaries and the water phase. The presence of such layers can lead to a low-frequency dispersion of the interlayer Maxwell–Wagner polarization, which can be an additional source of information about the nature of the distribution and relaxation of charges in the samples under study. The electric field of the UDD active surface forms a new phase of the structure formation of water between the free water layer and the active surface of the UDD grains. The structured layer is a potential barrier for free water molecules and for molecules oriented by the UDD active surface electric field. It can be concluded that the interfacial region is the most durable impermeable layer capable of increasing the electrical and mechanical characteristics of the structures under consideration. Our agreement with the results of other methods indicates the legitimacy of using the Debye theory to describe the dielectric relaxation of water molecules in UDD suspensions. The proposed computational model for the temperature dependences of the dielectric relaxation of water molecules ensures the accuracy of agreement with experimental data up to 76%.

[1]. Dielectrics in Electric Fields / G.R. Gorur. – New York Basel. – 2003. – p. 569.

[2]. I.V. Gofman, E.M. Ivan'kova, I.V. Abalov, V.E. Smirnova, E.N. Popova, O. Orell, J. Vuorinen, V.E. Yudin. // Polymer Science, Series A. – 2016. – V. 58. – N. 1. – p. 87 – 94.

[3]. L. Batyuk, N. Kizilova. Book of Abstracts Sixth International Conference on Radiation and Applications in Various Fields of Research, RAD 2018, 18.06 -22.06. - Ohrid, Macedonia. – 2018. – p. 267.

Efficient Organo-Inorganic Nanocomposites Based on Xanthene Dyes and Silicon Dioxide Doped Polymer

T.V. Bezrodna^{1*}, O.I. Antonenko², L.F. Kosyanchuk², O.M. Roshchin¹,
V.I. Bezrodnyi¹, V.V. Nesprava¹, A.M. Negriyko¹, A.O. Yaskovets¹

¹ Institute of Physics NASU, Kyiv, Ukraine

² Institute of Macromolecular Chemistry NASU, Kyiv, Ukraine

**Corresponding author: tomaalone@yahoo.com*

The key property for the different applications in the case of dye lasers, especially the ones operating in the pulse-periodic regime is a working lifetime, which depends on dye stability in the solid matrix, during both storage and running.

In recent years, the scientists show much interest to the organo-inorganic materials, since their applications improve considerably the properties of laser elements. This work deals with organo-inorganic nanocomposites, produced by direct mixing of organic compounds (initial components of the polymer matrix, polyurethane acrylate, and diluted dyes) with silicon dioxide nanoparticles. Effects of inorganic fillers on spectral, photophysical and generation characteristics of widely used xanthene dyes, Rhodamine 6G and Rhodamine B, in the polymer medium have been investigated.

Spectral properties of pure organic and aerosil-doped samples, obtained by frontal photopolymerization method of oligomer mixture, have been studied. The analysis of absorption and luminescence spectra has showed that SiO₂ nanoparticles affect self-aggregation processes of xanthene dyes. In low-polar polyurethane acrylate, dye ion pairs are formed due to electrostatic attraction between counterions, which results in the appearance of an additional short-wave absorption peak. Nanoparticle doping of the polymer matrix causes strong adsorption of the dye molecules due to electrostatic interactions of xanthene positively charged cations with negatively charged SiO₂ surface. This process hinders sterically H-dimer formation, access of oxygen and free radicals. Compared to pure polyurethane acrylate, dye luminescence intensity and photostability growth has been observed in organo-inorganic SiO₂-doped polymer nanocomposites. The mechanism of aerosil nanoparticle effects on xanthene spectral and photophysical properties is adsorption of the dye molecules in the SiO₂ porous structure. In this work, considerable increase in efficiency of laser generation has been shown for the organic dyes, inserted to the nanoparticle-doped polymer.

The developed new organo-inorganic nanocomposites allow to improve significantly operating characteristics of laser materials, based on organic dyes in polymer media.

IR and X-ray Investigation of Mixed Oxides Fe–Co–O Nanoparticles as Ammonia Oxidation Catalyst Prepared by Sol-Gel Method: Effect of Calcination Temperatures

O.N. Bliznjuk^{*}, N.Yu. Masalitina, A.N. Ogurtsov

National Technical University “KhPI”, Kharkov, Ukraine

^{*}*Corresponding author: onbliznjuk@ukr.net*

In this research work we report a modified sol-gel method to synthesis pure cobalt oxide and mixed oxides Fe–Co–O as the alternative catalyst for ammonia selective catalytic oxidation [1]. Pure $\text{Co}(\text{NO}_3)_2 \cdot 6\text{H}_2\text{O}$ and mixture of $\text{Co}(\text{NO}_3)_2 \cdot 6\text{H}_2\text{O}$ and $\text{Fe}(\text{NO}_3)_3 \cdot 9\text{H}_2\text{O}$ at the molar ratio $\text{Fe}/\text{Co} = 1,5; 2; 3$ were dissolved in distilled water. Aqueous solution of 1M NH_4OH was used as the precipitating agent. A suitable amount of citric acid solution was dropped into the obtained solution with the molar ratio of citric to metals of 2. The obtained solution was stabled within 30 minutes and evaporated at 70–80°C until the gel was obtained. The gel was then dried at 110°C for 3 hours. We have investigated the effect of changing the obtained solid calcinations temperature 250–850°C for 3 hours with the heating rate is 3°C/min. The IR spectra and XRD indicated the formation of Co_3O_4 at 300–700°C for pure cobalt oxide. IR spectra of cobalt oxide sample demonstrated two strong bands due to $\nu(\text{Co-O})$ modes at $\sim 663\text{cm}^{-1}$ and $\sim 577\text{cm}^{-1}$, which is clear evidence for presence of crystalline Co_3O_4 . The XRD results of the composite samples calcined at different temperatures for 2 h show, that the diffraction peaks can be indexed to the Co_3O_4 with spinel structure. As the temperature increases from 250°C to 550°C, the intensity of the diffraction peaks increases slightly, this suggests that the crystallinity of the Co_3O_4 compound rises. XRD of $\text{Co}_3\text{O}_4\text{--Fe}_2\text{O}_3$ being calcined at 250–850°C was determined. The XRD of the composite, which was calcined at 450°C, demonstrated all diffraction peaks of CoFe_2O_4 as a major phase together with all diffraction peaks of unreacted $\alpha\text{-Fe}_2\text{O}_3$ phase and Co_3O_4 phase. The different diffraction data including relative intensity of the main diffraction lines of crystalline phases present and their crystallite size (determined from the Scherrer's equation) indicated that mixed solids calcined at 450–850°C consisted of CoFe_2O_4 together with $\alpha\text{-Fe}_2\text{O}_3$ and Co_3O_4 phases. Study showed that solid-solid interaction between Fe_2O_3 and Co_3O_4 took place at temperature starting from 450°C yielding nanosized cobalt ferrite; increasing the calcination temperature within 650–850°C led to complete conversion of the reacting ferric and cobaltic oxides producing cobalt ferrite having a crystallite size in the nano range (15–40 nm). The study of ammonia selective catalytic oxidation to N_2O over Fe–Co–O composite catalyst showed that calcination at 450°C results to the highest activity.

- [1]. A.S. Savenkov, O.N. Bliznyuk, P.V. Kuznetsov, et al. Modeling of ammonia oxidation on a platinoid catalyst, taking into account the N_2O formation // Russian Journal of Applied Chemistry. – 2015. – V. 88. – N. 10. – p. 1563–1569.

Structure, Energy Spectrum and Luminescent Properties of 0D Perovskites in Zeolite Matrix

I.M. Dmitruk¹, Y.A. Vikhrova¹, A.M. Dmytruk², N.I. Berezovska¹

¹Physics Faculty, Taras Shevchenko National University of Kyiv, Kyiv, Ukraine

²Photon Processes Department, Institute of Physics, NAS of Ukraine, Kyiv, Ukraine

*Corresponding author: igor_dmitruk@univ.kiev.ua

Perovskite materials of different dimensionality are promising due to insensitivity of their electronic energy spectrum to structure defects [1]. But they require protection from the environment. That can be accomplished by surfactant coverage or by incorporation into porous matrix, for instance, mesoporous silica matrix [2]. We attempt impregnation of zeolite single crystal with cesium lead iodide perovskite. Small size of zeolite pores supposes incorporation of 0D perovskite clusters like Cs_4PbI_6 .

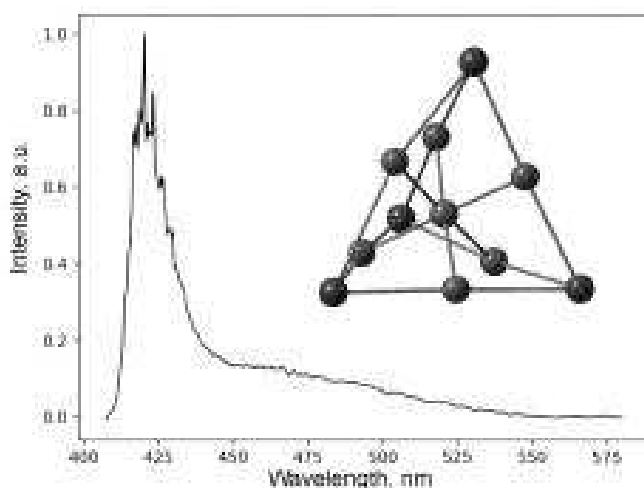


Fig. 1. Luminescence of zeolite crystal impregnated with cesium lead iodide perovskite. Inset – optimized structure of Cs_4PbI_6 0D perovskite cluster.

Narrow band at 425 nm may be interpreted as luminescence of perovskite clusters in the pores, while longer-wavelength shoulder can be attributed to perovskite film and larger nanocrystals at the surface of zeolite. We have performed DFT calculations of Cs_4PbI_6 0D perovskite cluster to compare its predicted energy spectrum with the experimental results presented above.

- [1]. M.V.Kovalenko, L.Protesescu, M.I.Bodnarchuk. Properties and potential optoelectronic applications of lead halide perovskite nanocrystals // Science 358, 745-750 (2017).
- [2]. D.N.Dirin, L.Protesescu, D.Trummer, et al. Harnessing Defect-Tolerance at the Nanoscale: Highly Luminescent Lead Halide Perovskite Nanocrystals in Mesoporous Silica Matrixes // Nano Lett. 16, 5866-5874 (2016).

Luminescent Spectroscopy of Lanthanum Vanadate Nanoparticles Doped with Europium and Erbium Ions

O. Chukova^{1*}, S.A. Nedilko¹, S.G. Nedilko¹, A. Slepets¹, T. Voitenko¹,
M. Androulidaki, A. Papadopoulos², E. Stratakis²

¹ Taras Shevchenko National University of Kyiv, Ukraine

² Institute of Electronic Structure & Laser, Foundation for Research & Technology Hellas, Heraklion, Crete, Greece

**Corresponding author: chukova@univ.kiev.ua*

Rare earth vanadates are applied in many areas due to their excellent luminescence properties. They are used to detect the structures of biological macromolecules, to determine the chemical composition of living cells, to distinguish malignant tumors and living tissue. The orthovanadates are applied in fields of laser hosts, catalysts, phosphors, sensors and polarizers.

Lanthanum vanadate nanoparticles doped with europium and erbium ions and co-doped with calcium ions were prepared by aqueous nitrate-citrate sol-gel synthesis route taking citric acid as a complexing agent. Phase composition, crystal lattice parameters and microstructure of the synthesized samples were studied by various methods.

The XRD analysis has revealed dependence of crystal structure on dopants concentration: monoclinic monazite-type structure for low dopant concentration and tetragonal zircon-type structure for high dopant concentration.

The photoluminescence spectra showed narrow lines caused by f-f transitions in the rare earth dopants. Distributions of these lines intensity differ for the samples with different concentrations for both Er^{3+} and Eu^{3+} ions. This effect can be related with different symmetry of the rare earth ions sites in the monoclinic and tetragonal crystal phases. It was shown that crystal structures of the samples also effects on intensity and distribution of the lines intensity in emission spectra.

This work has received funding from Ministry of Education and Science of Ukraine and from the EU-H2020 research and innovation program under grant agreement No 654360 having benefited from the access provided by Institute of Electronic Structure & Laser of Foundation for Research & Technology Hellas, Heraklion, Crete, Greece and Servei de Microscopia Division of Universitat Autònoma de Barcelona, Spain within the framework of the NFFA-Europe Transnational Access Activity.

Spectroscopy of Bacteria Synthesized Nanoparticles

V.N. Ermakov^{*1}, V.I. Podolska², Z.R. Ulberg²

¹Bogolyubov Institute for Theoretical Physics, NASU, Kyiv, Ukraine

²Ovcharenko Institute for Biocolloidal Chemistry, NASU, Kyiv, Ukraine

^{*}Corresponding author: vterm@bitp.kiev.ua

The mechanism of electromagnetic waves absorption by the bacteria capable to synthesize the silver nanoparticles (AgNPs) was proposed. Such charged NPs were located in a cell wall and had a weak connection to the matrix. They can shift under the electromagnetic field influence and lose their energy due to viscous friction. In this way the electromagnetic wave absorption is carried out. Absorption rate depends on a particles size. Taking in account this effect, the dependence of absorption coefficient on AgNPs size was

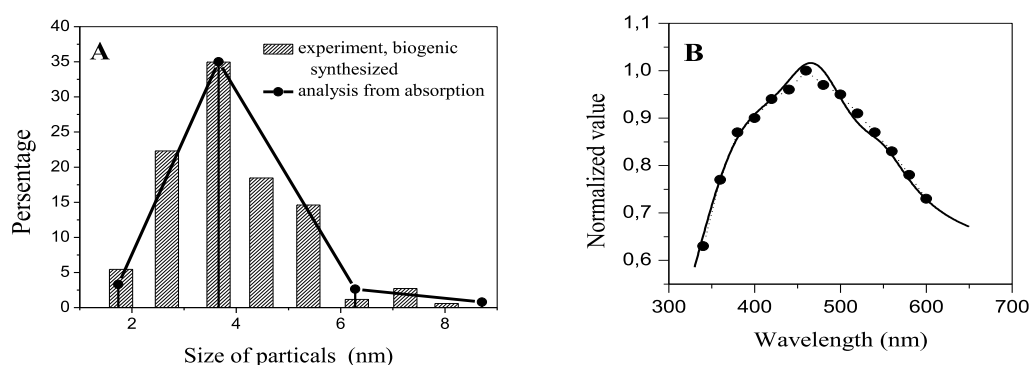


Fig.1. Biogenic AgNPs size distribution (A) and light absorption (B)

calculated. The NPs size distribution is determined by the cultivation conditions and cell wall composition. The method of a size distribution determination was developed. It based on the using of an experimentally obtained dependency of absorption coefficient on absorbed light wave length in suspension with NPs filled bacteria. An experimentally obtained from TEM data size distribution of biogenic AgNPs synthesized by bacteria is shown in Fig.1A [1]. Appropriate to such a distribution experimental dependence of absorption coefficient on wave length is presented in Fig.1B (points). The distribution is obtained by matching of calculated absorption (Fig.1B, solid line) with experimentally obtained data is presented in Fig.1A (solid line). Similar calculations the AgNPs size distribution in the cases of biochemical synthesis and pulse electric field stimulation were fulfilled.

[1]. V. I. Podolska et al. Material Science and Nanostructures – 2011. – N. 4. - p.66.

Low-Dimensional Carbon Nanohybrids

A.Yu. Glamazda^{*1,3}, S.G. Stepanian¹, M.V. Karachevtsev¹,
A.M. Plohotnichenko¹, L. Adamowicz², V.A. Karachevtsev¹

¹ Department of Molecular Biophysics, B. Verkin Institute for Low Temperature Physics and Engineering of NAS of Ukraine, Kharkiv, Ukraine

² Department of Chemistry and Biochemistry, University of Arizona, Tucson, USA

³ Faculty of Radio Physics, Biomedical Electronics and Computer Systems, V.N. Karazin Kharkiv National University, Kharkiv, Ukraine

**Corresponding author: alex.glamazda@gmail.com*

The nanohybrids of single-walled carbon nanotube (SWNT) and graphene oxide (GO) have the promising potential for the development of new intelligent devices with wide range of applications. The combination of properties of carbon low-dimensional materials consolidated into nanohybrids gives the promising way to get the more prominent synergistic effect demonstrating that the properties of whole nanohybrid are more effective and more prospective than the sum of its separate components. It requires the detailed understanding of building of such nanohybrids. We present the study of SWNT-GO nanohybrids by the optical spectroscopic methods (UV-visible optical absorption, Raman spectroscopy) and theoretical calculations. We found the suppression of the bands assigned with electronic transitions between first pair of van Hove singularities in semiconducting SWNTs in the absorption spectra of SWNT-GO aqueous solution. It's explained by the charge transfer from GO to SWNTs and the induced upshift of the Fermi level (E_F) in SWNTs. We obtained the films from of SWNT-GO aqueous solution that is more perspective for practical objectives. The neighboring GO layers create pressure on SWNTs which are arranged between them in the film. That induces a shifting of Raman bands related to SWNTs to high-frequency region. In turn the GO layers are undergone a distortion reflected in an increase of Raman D-band related to GO that was supported by performed theoretical calculations. The D and G-bands assigned with GO demonstrate the blue shift in Raman spectrum of nanohybrid that can be explained by charge transfer from GO to SWNTs. That is in good agreement with performed ab-initio calculations.

This work was partially supported by funding from the National Academy of Sciences of Ukraine (NASU) (Grant N 15/19-H, Grant N 07-01-18/19). A.Yu. Glamazda and M.V. Karachevtsev acknowledge support from the NASU 1/H-2019.

Switchable Redox Activity of $\text{LnVO}_4\text{:Eu}^{3+}$ ($\text{Ln}=\text{Gd}, \text{Y}, \text{La}$) Nanoparticles

K.A. Hubenko*, S.L. Yefimova, P.O. Maksimchuk, N.S. Kavok,
V.K. Klochkov, Yu.V. Malyukin

Department of Nanostuctured Materials, Institute for Scintillation Materials National Academy of Sciences of Ukraine, Kharkiv, Ukraine

**Corresponding author: k.hubenko@gmail.com*

Reactive oxygen species (ROS) mainly including superoxide inions ($\text{O}_2^{\bullet-}$), hydroxyl radicals ($\bullet\text{OH}$), hydrogen peroxide (H_2O_2) and singlet oxygen ($^1\text{O}_2$) are known to have edged sword properties in the determination on cell fate. ROS are continuously generated in small amounts in normal cells. Intracellular ROS levels is regulated via a cell antioxidant defense system (superoxide dismutase, catalase, glutathione peroxidases, peroxiredoxins and other enzymes and antioxidants) converting excess of ROS into less reactive species (O_2 or H_2O , for instance) [1]. When the action of cell antioxidants become depleted, the level of ROS increases causing oxidative stress through the oxidation of lipids (lipid peroxidation), protein and DNA damage, etc. It is now generally accepted that the oxidative stress caused by imbalance on ROS production and scavenging is closely related to a broad spectrum of diseases including cancer as well as aging. So, control of the intracellular ROS level is critical for both normal and cancer cells.

Recently, nanoparticles (NPs) have been proposed to fulfill this function. It has been shown that metal oxide nanoparticle possess pro- and antioxidant activities depending on their surface properties, size, concentration and redox potential [1]. The brilliant example of antioxidant NPs (ROS scavenging agent) is cerium oxide NPs (nanoceria), which unique self-regenerative properties are the subject of numerous studies [2].

In this present study, we report switching the redox activity of orthovanade NPs doped with europium ions $\text{LnVO}_4\text{:Eu}^{3+}$ ($\text{Ln} = \text{Gd}, \text{Y}, \text{La}$). Evaluation of the redox activity of $\text{LnVO}_4\text{:Eu}^{3+}$ ($\text{Ln} = \text{Gd}, \text{Y}, \text{La}$) NPs was carried out using lipid oxidation measurement (conjugated dienes formation test), NPs redox-activity at UV- and X-ray irradiation. We can conclude that due to the features of $\text{LnVO}_4\text{:Eu}^{3+}$ NPs structure, both ROS generation and scavenging mechanisms are possible, their efficiency depends strongly on environmental conditions (irradiation type or its absence), so could be switched.

- [1]. C.A. Ferreira, D. Ni, Z.T. Rosenkrans, and W. Cai. Scavenging of reactive oxygen and nitrogen species with nanomaterials // Nano Research. – 2018. – N. 11. – p. 4955.
- [2]. Yu. Malyukin, V. Klochkov, P. Maksimchuk, V. Seminko, N. Spivak. Oscillations of cerium oxidation state driven by oxygen diffusion in colloidal nanoceria (CeO_{2-x}) // Nanosc. Res. Lett. – 2017. – N.12. – p. 566.

Excitation Dependent Photoluminescence of Nanostructured TiO₂ Powder Modified with Phenothiazine

O.F. Isaieva^{*1,3}, V.V. Naumov¹, V.V. Shymanovska², E.G. Gule¹,
G.Yu. Rudko^{1,3}

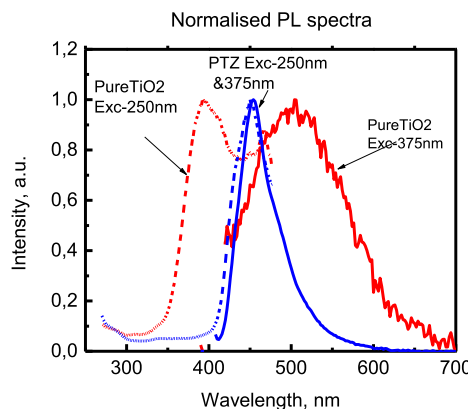
¹ Lashkaryov Institute of Semiconductor Physics, NAS of Ukraine, Kyiv, Ukraine

² Institute of Physics, NAS of Ukraine, Kyiv, Ukraine

³ National University "Kyiv-Mohyla Academy", Kyiv, Ukraine

**Corresponding author: oksanka.isayeva@gmail.com*

Titanium dioxide (TiO₂) is an efficient wide-gap metal-oxide semiconductor material with excellent electronic and optical properties utilized for photo-electric energy conversion in the UV range of the solar spectrum. To improve the TiO₂ photoactivity in the visible range, it requires doping or surface modification. In this work we studied room temperature photoluminescence of nanostructured TiO₂ powder modified with organic dye phenothiazine (PTZ). PL spectra of TiO₂/PTZ samples were measured using Shimadzu RF-1501 and MDR-23 grating spectrometers in the range 400-700 nm with two excitation wavelengths: at 250 nm (4.6 eV) and 375 nm (3.3 eV), both are above the TiO₂ band-gap. For pure TiO₂, two PL bands are observed: at 394 nm and 508 nm. The band at 394 nm is observed at excitation with 250 nm. This band refers to near-band-edge luminescence. The band at 508 nm is observed at excitation with 375 nm. This band can be either emission of self-trapped excitons localized on TiO₆ octahedral or defect-related emission. For TiO₂/PTZ, the PL intensity at 394 nm strongly depends on the concentration of PTZ. The concentration dependence of the PL intensity at $\lambda=508$ nm is questionable. In general, PL spectra depend on the excitation wavelength and/or intensity of the exciting light. 508-nm-emission does not depend on surface doping of TiO₂ with PTZ. The intensity of the near-band-edge luminescence of TiO₂ decreases with surface doping that probably indicates an increased rate of non-radiative transitions involving surface states. Research is in progress.



[1]. L. Kernazhitsky et al. // E-MRS 2018 Fall Meeting, Warsaw, 2018. – P. D.P24.

Interaction of Single Walled Carbon Nanotube with Graphene: Molecular Dynamics Study

M.V. Karachevtsev^{*1}, V.A. Karachevtsev¹

¹ Department of Molecular Biophysics, B. Verkin Institute for Low Temperature Physics and Engineering of NAS of Ukraine, Kharkiv, Ukraine

^{}Corresponding author: mkarachevtsev@ilt.kharkov.ua*

The hybridization of 1D carbon nanotubes and 2D graphene family is able to form 3D nanostructures with significantly improved physical and chemical properties, first of all, spectroscopic and electronic ones. These properties make such 3D nanostructures very attractive in many applications including nanoelectronics, nanophotonics, sensors, and nanocomposites.

We simulated the process of forming the hybrid of single walled carbon nanotubes (SWNT) with graphene by molecular dynamics method (MD) to obtain the energy favorable hybrid structures and to evaluate the interaction between components. In our calculations, we have used different SWNTs (diameters/chirality) and graphene sheet of different geometrical forms.

MD simulation showed that a small narrow sheet of rectangular graphene has two stable forms on the SWNT surface. These conformations depend on the diameter of the nanotube. For SWNT (20,0) (diameter - 1.5 nm), a graphene sheet is wrapped around the nanotube, and for the thinner SWNT (16,0) (diameter - 1.2 nm) the graphene sheet is aligned along the nanotube axis. In case of another graphene sheet (square shape and 5600 carbon atoms) our MD modelling showed a slight curvature of the graphene plane, and SWNT shifts from the center to the edge of the graphene sheet. The interaction energy of graphene hexagons stacked with the SWNT surface estimated by MD modelling has value about -5.3 kcal/mol.

This work has been supported by National Academy of Sciences of Ukraine (NASU) (Grant N 15/19-H within the program “Fundamental Problems of the creation of new Nanomaterials and Nanotechnology”, Grant N 07-01-19), Grant N 1/H-2019.

Peculiarity of the Electronic Structure of Calcium Apatite

L.I. Karbivska¹, V.L. Karbivskyy^{*1}, S.S. Smolyak¹

¹ Department of Nanostructures Physics, G.V. Kurdyumov Institute for Metal Physics, NAS of Ukraine, Kyiv, Ukraine,

**Corresponding author: karb@imp.kiev.ua*

The relevance of a comprehensive study of calcium hydroxyapatite $\text{Ca}_{10}(\text{PO}_4)_6(\text{OH})_2$ is due to a wide range of its practical application in nanomedicine, power engineering, in the field of communications and bioelectronic devices, electronics [1].

The uniqueness of the electronic structure of calcium hydroxyapatite is largely determined by the anomalous behavior of the d -shell of calcium and the characteristics of the formation of a chemical bond with its participation. The appearance of electron density on the initially empty calcium d -orbitals (Ca: $[\text{Ar}] 4s^2$) as a result of the formation of a chemical bond may be accompanied by the collapse of the orbit of its excited d -electrons — an effect arising due to the presence of a two-valley effective potential on calcium atoms. The presence of the inner well of an effective potential, separated by a positive potential barrier from the outer valley, leads to the formation of quasi-stationary levels in it. At some energies of an electron participating in a chemical bond, equal to the energy of this quasistationary level, the radial wave function of the electron penetrates abruptly into the atom, which leads to the formation of a stronger chemical bond and ensures the stability of the compounds. This effect takes place, for example, with partial replacement of calcium atoms by atoms of a radioactive element, for example, uranium or strontium, thanks to which apatites can be used as matrices for the disposal of radioactive waste.

Apatites also demonstrate the lability of the structure relative to the c axis. Carried quantum-mechanical calculations in the approximation of the density functional theory for apatite-like compounds indicate small changes in the shape of the curve of the total density of electronic states. Practically all the main features of the curves are saved, which indicates that the electronic structure is almost insensitive to the type of anion on the c axis up to their removal.

Comparison of theoretically calculated X-ray emission bands of apatite elements and spectral data showed their good agreement. The dominant role of the d -shell of calcium in explaining the anomalous stability of the apatite lattice in a wide range of non-stoichiometry coefficient is indicated.

[1]. V.L. Karbivskyy, A.P. Shpak. Apatite and apatite-like compounds. Electronic structure and properties. “Naukova Dumka” – Kyiv. –2010. – 483 p. (in Russian).

Quantum Control of Ground State Exciton Qubits in Single Quantum Dots

R.S. Kolodka^{*1}, A.J. Ramsay², I. Dmitruk¹

¹ Department of Physics, Taras Shevchenko National University of Kyiv, Ukraine

² Department of Physics and Astronomy, University of Sheffield, Sheffield, UK

**Corresponding author: roman.kolodka@gmail.com*

We study the coherent properties of a single ground state quantum dot exciton driven by optical pulses using a photocurrent technique [1]. Exciton state control is demonstrated via observation of Rabi flopping and Ramsey fringes. The studied single InGaAs quantum dot is embedded in an ni-Schottky diode. The sample temperature is approximately 20 K.

Two time-separated pulses with the pulse area of $\pi/2$ were used to manipulate the exciton state and a series of IV curves were measured for different time-delays. As the detuning is varied via the quantum confined Stark-effect the photocurrent oscillates as the exciton is tuned in and out of resonance with the time-delay between the two-pulses. The number of fringes within a defined energy interval is directly proportional to the temporal pulse separation. The resulting Ramsey interference provides a useful probe of the exciton coherence.

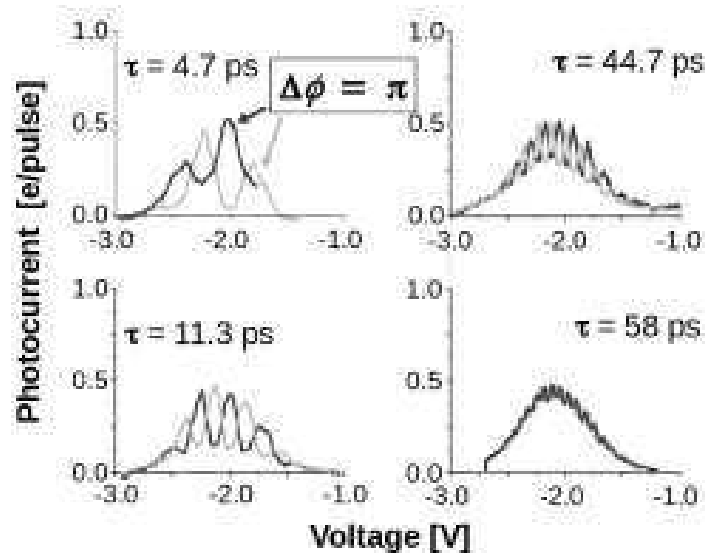


Fig. 1. Two laser pulses arrive to the sample separated in time by τ . The difference between the two measured IV-s (black and grey) is the additional phase difference $\Delta\phi = \pi$ between those two pulses.

[1]. Zrenner A., Beham E., Stufler S., Findeis F., Bichler M., Abstreiter G. Coherent properties of a two-level system based on a quantum-dot photodiode // Nature. - 2002. - V. 418 – p. 612.

Hydrogel-Silver Nanoparticle Composites for Biomedical Applications

O.M. Nadтока, P.A. Virych, A.P. Naumenko, N.V. Kutsevol*

Taras Shevchenko National University of Kyiv, Kyiv, Ukraine

**Corresponding author: kutsevol@ukr.net*

Polymeric hydrogels are used for biomedical applications as wound of various genesis dressing, artificial burn dressings, tissue technology, and water purification etc. The efficiency of such materials can be improved by incorporation of silver nanoparticles (AgNPs) which have high antibacterial activity. Size, size distribution (polydispersity), morphology, and surface charge of silver nanoparticles determine its biological activity and are strongly dependent on the method of nanoparticles synthesis. The reduction of silver ions in solution is one of the general methods for silver nanoparticles preparation. Use of UV-irradiation method for reducing of Ag^+ into polymer matrix seems is more appropriate way for preparation nanosystems for biomedical application.

This work was focused on the study of formation and structure of hydrogel–silver nanocomposites based on Dextran-graft-Polyacrylamide copolymers in non-ionic and anionic form. Nanocomposites were analyzed by DSC, TEM and UV-vis spectroscopy. It was registered that absorption peaks at 420 nm in UV–visible spectrum corresponding to Surface Plasmon resonance of AgNPs. But the character of the absorption bands were dependent on the condition of nanoparticles synthesis and chemical nature of polymer hydrogel.

The developed nanocomposites were evaluated for antibacterial application on *E. coli* and *St. aureus* and demonstrated high efficiency.

Formation of Cerium Fluoride Nanoparticle - Melanin Nanosystem Evidenced by Luminescent Studies

M.Yu. Losytskyy^{*1}, L.P. Buchatsky², T.V. Beregova², O.B. Shcherbakov³,
V.M. Kravchenko¹, V.M. Yashchuk¹

¹ Faculty of Physics, Taras Shevchenko National University of Kyiv, Kyiv, Ukraine

² Institute of Biology and Medicine, Taras Shevchenko National University of Kyiv, Kyiv, Ukraine

³ Zabolotny Institute of Microbiology and Virology, NAS of Ukraine, Kyiv, Ukraine

^{*}*Corresponding author: mlosytskyy@gmail.com*

Cerium fluoride (CeF₃) is a known scintillation material that could be used in a variety of applications. Particularly, CeF₃ nanoparticles (NP) were studied as scintillating part of sensitizer nanosystems for X-ray photodynamic therapy (XPDT) [1,2]. At the same time, to be introduced into the biological environment (e.g. blood), CeF₃ NP should be covered with a layer of biocompatible material. Here, we have studied the possibility of coating CeF₃ NP with the molecules of water-soluble melanin. For this, effect of melanin on the luminescence spectrum of CeF₃ NP in 50 mM TRIS-HCl buffer (pH 7.2) was studied.

Luminescence spectrum of Ce³⁺ ions in CeF₃ NP is known to consist of the bands near 286 and 304 nm corresponding to regular transitions in Ce³⁺ ions $^2D_{3/2} \rightarrow ^2F_{5/2}$ and $^2D_{3/2} \rightarrow ^2F_{7/2}$ respectively, as well as of the long-wavelength bands corresponding to perturbed states of Ce³⁺ that are attributed to defects of crystal lattice and surface ions [2]. Addition of water soluble melanin results in the decrease of CeF₃ NP luminescence intensity. Analysis of the spectra shows that this decrease is mostly due to disappearing of the broad long-wavelength band with the maximum near 335 nm. Such effect points to the binding of melanin molecules to the surface of CeF₃ NP. This result also proves that the long-wavelength bands of Ce³⁺ emission are connected with the NP surface that is consistent with [1]. The mechanism of luminescence quenching could be electronic excitation energy transfer from the perturbed states of Ce³⁺ to weakly fluorescent melanin molecules. If so, the obtained nanosystem CeF₃ NP - melanin could be further studied for X-ray acoustic or X-ray photothermal applications. Besides, it could be also used as a basic component for further development of XPDT sensitizer nanosystem.

- [1]. M.Yu. Losytskyy, L.V. Kuzmenko, O.B. Shcherbakov, N.F. Gamaleia, A.I. Marynin, V.M. Yashchuk. Energy Transfer in Ce_{0.85}Tb_{0.15}F₃ Nanoparticles-CTAB Shell-Chlorin e₆ System // Nanoscale Research Letters. – 2017. – V.12. – 294.
- [2]. D.R. Cooper, K. Kudinov, P. Tyagi, C.K. Hill, S.E. Bradforth, J.L. Nadeau. Photoluminescence of cerium fluoride and cerium-doped lanthanum fluoride nanoparticles and investigation of energy transfer to photosensitizer molecules // Phys. Chem. Chem. Phys. – 2014. – V.16. – P.12441-12453.

Analytical Calculation of the Acoustic Phonons Spectra and Group Velocities in the Quasi-2D-nanostructures

Yu.V. Lutsiuk, V.M. Kramar*

Yuriy Fedkovych Chernivtsi National University, Chernivtsi, Ukraine

**Corresponding author: v.kramar@chnu.edu.ua*

During the few last decades GaN/AlN and GaN/AlGaIn heterostructures are actively explored as promising materials for the manufacture of active elements of optoelectronics. Electronic, optical and transport properties of such heterostructures over a wide range of low temperatures are determined solely by the charge carriers scattering on acoustic phonons [1]. Quantization of acoustic phonons in nanostructures significantly affects these properties. These properties in ultra-thin structures are different from that's in bulk crystals because of significant quantization the acoustic phonons spectra. Based on the analogy with acoustics and classical mechanics many theoretical results for study the quantized states of acoustic phonons in quantum wells, nanowires and spherical quantum dots there were obtained. In particular, dispersion of dilatational, flexural and shear vibrational modes in thin films has been described in [2, 3]. However, all calculations in the above-mentioned works were performed numerically, which is uncomfortable for the theoretical study of electron-phonon interaction in such nanostructures.

Here we present the method of analytical solution of the problem of finding the spectrum of acoustic phonons in quasi-two-dimensional nanostructures of hexagonal symmetry within the framework of the continuum approach that is described in [3].

Our method is based on the application of Fourier series to the solution of systems of differential equations. His application made it possible to find analytical expressions for the dispersion dependences of the energies and group velocities for acoustic phonons of all polarizations in the such nanostructures - shear, dilatation-like and flexural. Specific calculations are made for the GaN- and AlN-type nanofilms of different thicknesses.

It is shown that the energies of quantized phonon states in ultra-thin films exceed the corresponding values of their energies in bulk crystals. The dispersion of the group velocities of phonons of various polarizations in such nanosystems is also substantially different.

- [1]. W. Knap, E. Borovitskaya, M.S. Shur, et. al. Acoustic phonon scattering of two-dimensional electrons in GaN/AlGaIn heterostructures // Appl. Phys. Lett. – 2002. – V. 80. – N. 7. – P. 1228-1230.
- [2]. N. Bannov, V. Aristov, V. Mitin, M.A. Stroscio. Electron relaxation time due to the deformation-potential interaction of electrons with confined acoustic phonons in a free-standing quantum well // Phys. Rev. B. – 1999. – V. 51. – N. 15. – P. 9930-9938.
- [3]. E.P. Pokatilov, D.L. Nika, A.A. Balandin. Phonon Spectrum and Group Velocities in AlN/GaN/AlN and related Heterostructures // Superlattices and Nanostructures. – 2003. – V. 33. – P. 155–171.

Effect of Cerium Ions on the Photocatalytic Properties of Mesoporous BaTiO₃/TiO₂ Nanocomposites

E.V. Manuilov^{1*}, T.A. Khalyavka², N.D. Shcherban³, V.V. Shymanovska¹,
V.V. Permyakov⁴, S.N. Shcherbakov⁵

¹Institute of Physics NAS of Ukraine, Kyiv, Ukraine

²Institute for Sorption and Problems of Endoecology NAS of Ukraine, Kyiv, Ukraine

³L.V. Pisarzhevskii Institute of Physical Chemistry NAS of Ukraine, Kyiv, Ukraine

⁴Institute of Geological Sciences NAS of Ukraine, Kyiv, Ukraine

⁵M.G. Kholodny Institute of Botany NAS of Ukraine, Kyiv, Ukraine

**Corresponding author: evm.sem18@gmail.com*

Composite materials seem to be one of the most promising nanomaterials today. Recently, great attention has been focused on the development of efficient catalysts based on titanium dioxide, titanates and mixed systems based on them for the degradation of organic pollutants in an aqueous medium. Nanoscale composite materials based on cerium, barium titanate and titanium dioxide were synthesized by thermal hydrolysis method. The obtained individual semiconductors TiO₂ and BaTiO₃ and as-synthesized Ce/xBaTiO₃/TiO₂ nanocomposites were characterized by X-ray diffraction, scanning electron microscopy, energy-dispersive spectrometry, transmission electron microscopy, nitrogen adsorption-desorption, UV-vis diffuse reflectance spectroscopy, Fourier transform infrared spectroscopy. The photocatalytic destruction of the model pollutants (Safranin T and Rhodamine B) was carried out under UV irradiation.

The synthesized porous CBTTO composites exhibited good photocatalytic activity compared to pure TiO₂ and BaTiO₃ due to their highest specific surface area and developed porous structure. It provides higher-efficiency transport for the reactant molecules, appearance of lattice defects and heterojunctions between the phases. It promotes the charge separation and increases their lifetime, thereby complicating the charge recombination

Obviously, the doping of BaTiO₃/TiO₂ samples with cerium increased their photoactivity. The Ce⁴⁺ cations existing on the photocatalyst surface can act as an acceptor or traps for TiO₂ conduction band electrons and inhibits electron-hole recombination. The electrons trapped in Ce⁴⁺ sites can be transferred to the adsorbed O₂, thus decreasing the electron-hole recombination rate. Such adsorbed O_{2ads}⁻ molecules are transformed into high reactive superoxide anions (O₂^{• -}). Moreover, the hydroxyl radical (OH[•]) can be also generated by surface hydroxyl groups while trapping photoinduced holes. The investigations showed that the introduction of cerium into xBaTiO₃/TiO₂ increases photoactivity of the composite by 20% or more.

XRD Investigation of Cerium-Containing Mn-Cu Mixed Oxide Catalyst for Ammonia Oxidation to N₂O

N.Yu. Masalitina*, O.N. Bliznjuk, A.N. Ogurtsov

National Technical University “KhPI”, Kharkov, Ukraine

**Corresponding author: nat_masalitina@ukr.net*

The process of low-temperature oxidation of ammonia on oxidizing catalysts has been investigated for production of N₂O to be used for medical purposes and organic synthesis. Cerium-containing catalysts under various technological parameters were investigated [1]. The presence of the cerium oxide component in the catalyst is necessary because it prevents catalyst particles from aggregation and improves their stability. The impact of ceria in these transformations originates from its high oxygen storage capacity (OSC) and the ability to switch between the Ce⁴⁺ and Ce³⁺ valence states, storing and releasing oxygen ions. The introduction of a metal into the ceria lattice disturbs the fluorite structure of CeO₂ and alters the local defect configuration. This increases the mobility of the oxygen species at high reaction temperature. It has been shown that Mn-Cu mixed oxide catalysts modified with ceria exhibit a lower energy for the creation of oxygen vacancies, which boosts the oxidation activity.

In this work, the promoted Mn-Cu-O catalysts by CeO₂ were primarily synthesized by co-precipitation. This method has been successfully applied for preparing ammonia oxidation catalysts. The catalysts were characterized by XRD technique. The XRD patterns exhibit relatively broad reflections that can be indexed to the fluorite structure of ceria; no phase separation is detected, even at the highest concentration of Mn and Cu in the samples. The average crystallite size of Mn-Cu-O, calculated by the Scherrer equation, is 25 nm. Smaller crystallites are obtained in the cerium -containing samples (10 nm for 15 % Ce and 8 nm for 10 % Ce in the catalyst), in line with the increased total surface area of the promoted oxides, which reaches values around 115 m²/g. A shift to higher angles of the characteristic ceria reflections is noticed over the Ce-containing materials, pointing to the formation of the corresponding solid solutions. The lattice parameters of catalysts with 15 % Ce ($a_{\text{cell}} = 0.5395$ nm) and with 10 % Ce as promoter in the Mn-Cu-O catalyst ($a_{\text{cell}} = 0.5382$ nm) are smaller than that of pure CeO₂ ($a_{\text{cell}} = 0.5463$ nm). The crystals exhibit a truncated octahedron-like morphology and form small agglomerates. The micrographs further confirm the decreased particle size in the cerium-containing samples.

- [1]. N.Yu. Masalitina, A.N. Ogurtsov The investigation of the influence of Mn-Bi-Cu-Ce-O catalyst on the environment-friendly green process of low-temperature ammonia oxidation to nitrous oxide / In: Book of Abstracts of the 4th International Conference on Radiation and Applications in Various Fields of Research, RAD 4 [Editor Goran Ristić]. –Niš : University, Faculty of Electronic Engineering, 2016. – P. 86

Spectroscopic Characterization of Hybrid Nanosystems “D-g-PAA/AuNanoparticle/Chlorin e6/Dox”

A. Naumenko*, N. Kutsevol, V. Chumachenko, Iu. Harahuts

Taras Shevchenko National University of Kyiv, Kyiv, Ukraine

**Corresponding author: a_naumenko@univ.kiev.ua*

In modern medicine, the development of systems for the selective delivery of drugs directly into the affected cells is relevant, without affecting the healthy cells. In recent years, the possibility of using nanocomposites based on polymers as targeted delivery of photosensitizers (PS) for photodynamic antitumor therapy (PDT) is actively explored. Nanocomposites containing PS have a number of advantages over the initial photosensitizing drugs, since they prevent the aggregation of PS molecules, which leads to a decrease in its activity. In addition, nanocomposites based on polymers can be additionally loaded with various drugs, which in turn enhance the effect of treatment.

Polymer matrices on the base of Dextran core Polyacrylamide (neutral and anion forms) as well as systems consisting of incorporated in a polymer matrix of gold nanoparticles and photosensitizer molecules or doxorubicin (2), triple systems “D-g-PAA/AuNPs/PS or Dox”(3), and, finally, the systems “D-g-PAA /AuNPs/PS/Dox” (4) have been sequentially investigated by methods of optical spectroscopy (spectrophotometry, photoluminescence, luminescence excitation spectra) . The measurements of spectra at various concentrations were carried out to determine the optimal composition of nanosystems.

It was found that in the presence of a photosensitizer or doxorubicin, an insignificant aggregation process in the system occurs as a result of the aggregation of the polymeric component due to the change in the hydrophilic-hydrophobic balance of the polymer matrix. This confirms the fact that Chlorine e6 and Doxorubicin interact with Polymer matrices. Aggregation processes are significantly enhanced in the four-component nanosystem D-g-PAA /AuNPs/Chlorine e6 /Doxorubicin, but the size of the gold nanoparticles does not change.

Nanocomposite synthesized in anionic branched polymer matrix D-g-PAA /AuNPs/Chlorine e6 is recommended for in vitro testing on cell cultures using photodynamic therapy, while the composite D-g-PAA /AuNPs/Dox - for testing for chemotherapy.

Acknowledgment. This publication is supported in part by the Ministry of the Education and Science of Ukraine under joint Ukrainian-Belarusian Research and Development Project “Design and Physico-Chemical Properties of Novel Multicomponent Nanosystems for the Treatment and Diagnostics of Solid Tumors” (2019-2020).

Effects of Surface-Extended Inorganic Particles on Phase Transitions and Spectral Luminescence Properties of 5CB Liquid Crystal

T.V. Bezrodna¹, G.V. Klishevich¹, V.I. Melnyk¹, V.V. Nesprava^{*1},
O.M. Roshchin¹, J. Baran², M. Drozd²

¹ Institute of Physics NASU, Kyiv, Ukraine

² Institute of Low Temperature and Structure Research PAN, Wroclaw, Poland

**Corresponding author: nesprava@iop.kiev.ua*

Colloidal suspensions based on liquid crystal media and inorganic fillers attract significant interest over the recent decades, since they can show unique optical, switching and mechanical properties, and also have good prospects for the applications in the optoelectronic devices, information display and storage technology. Observed new phenomena in such systems are caused by the intermolecular interactions on the phase separation boundary and the most pronounced in the case of anisometric particles, such as, carbon nanotubes (NT), clay platelets (organomodified montmorillonite OMMT) etc.

It is shown that small concentrations of NT do not practically change DSC thermograms of the 5CB liquid crystal possessing crystal-nematic and nematic-isotropic (N-I) phase transitions at $T=24$ and 37 C, correspondingly. Cooling of the sample results in the appearance of the nematic supercooled state (SCS), which transforms into a glasslike state (GLS) at $T \sim -18^\circ\text{C}$. The NT presence encourages GLS transformation into a stable crystal phase C_2 earlier, at $T=-27^\circ\text{C}$, compared to the bulk 5CB ($T=-22^\circ\text{C}$). 5CB doping with OMMT platelets decreases the C_2 melting temperature ($T=20^\circ\text{C}$) and results in two endothermic peaks at $T=35$ and 37°C at the N-I transition. The transition of SCS to a metastable crystal phase C_1 occurs even at $T=-9^\circ\text{C}$, while in the composite with OMMT-NT hybrid particles this process is delayed to $T=-18^\circ\text{C}$.

The obtained DSC results can be explained by the results obtained by polarizing microscopy and photoluminescence (PL) spectroscopy. Microphotographs show formation of large isolated NT clusters, not affecting structural alignment of the bulk 5CB medium and PL spectral characteristics as the 5CB excimer emission. 5CB+OMMT PL spectra contain an additional peak at 426 nm, which corresponds to emission from 5CB dimers in OMMT near-surface layers. The OMMT-NT particles form a homogeneous coagulation network and distort considerably the 5CB nematic alignment. This disordering results in the appearance of twisted conformations, typical of the 5CB monomer molecules, seen as a new short-wavelength PL band at 367 nm.

The presented analysis of the composite structure can explain the differences in the 5CB phase transition sequences depending on the type of doping inorganic fillers.

Synthesis and Properties of DNA Based Photonic Crystals

M. Olenchuk^{1*}, T. Hanulia¹, O. Perederii¹, A. Nikolenko^{1,2}, G. Dovbeshko¹

¹ Institute of Physics of NASU, Kyiv, Ukraine

² Institute of Semiconductor Physics of NASU, Kyiv, Ukraine

**Corresponding author: m.olenchuk@yahoo.com*

Creation of photonic crystals with new properties and their research is one of the most urgent problems in world science. Achievements in the creation of photonic crystals stimulate the development of photonics and opto-informatics. The obtaining of perfect three-dimensional globular structures by the method of colloidal self-assembly and the wide possibilities of modifying their optical properties by infiltration of substances of different chemical nature allows us to create new regular and stochastic nanocomposite materials with unique optical properties on their basis.

Opal type photonic crystals were made by colloidal self-assembly method. We found the conditions for the synthesis of spherical particles SiO₂ and the relative standard deviation of $\sim 5\%$ using a modified Stoeber method for hydrolysis of TEOS in the presence of ammonia as a catalyst. The average diameter of the globules of SiO₂ particles is 190 nm and it was measured by the method of photon correlation spectroscopy. We also made DNA based photonic crystals composites. In the spectra of Raman scattering, the bands 436, 485, 532, 798, 975, 1075 and 1212 cm⁻¹ that are characteristic of synthetic opal [1] are recorded and relate to fluctuations SiO₂, and the band 485 cm⁻¹ refers to defects in the structure of opal. The bands 326 cm⁻¹ and 532 cm⁻¹ are probably related to the fluctuations of the DNA components (up to adenine), the band 395 cm⁻¹ - to the deoxyribose in the DNA, and after annealing of the photonic crystals based on DNA are not observed. A band of 256 cm⁻¹ refers to hydrogen bonds in a DNA molecule. A wide range of hydrogen bonds in these samples, located in the area 4000-1800 cm⁻¹, was also recorded by the purpose of infrared spectroscopy. After the annealing of photonic crystals based on DNA, this area is significantly narrowing - almost 2 times, the bands belonging to the DNA disappear and new bands are not fixed. The crystals show an ordered structure with a globule size of approximately 200 nm, calculated from the position of the Bragg peak in scattering spectra and the appearance of macroscopic ordering. The photoinduced luminescence from crystals based on DNA differs from crystals obtained without DNA and after annealing of the photonic crystals based on DNA. The features of the properties of these new structures, their reception and possible use are discussed.

This work is supported by Ukrainian-Polish project M40 and Ukrainian-Polish mobility project between NASU and PAN

[1]. G Dovbeshko et al 2012 IOP Conf. Ser.: Mater. Sci. Eng. 38 012008

Peculiarity of Elastic Characteristics of Nanocomposites of Multiwalled Carbon Nanotubes, Colouring Agents and Polyethylene, Polyvinyl Chloride, Porous Polystyrene

A.P. Onanko*, M.P. Kulish, O.P. Dmitrenko, T.M. Pinchuk-Rugal,
M.A. Aleksandrov, D.V. Charny, Y.A. Onanko

Taras Shevchenko National University of Kyiv, Kyiv, Ukraine

**Corresponding author: onanko@univ.kiev.ua*

3D polymeric net is the sponge with the pores size $d \leq 10^4$ nm, due to it contains distillate water, assumes the diffusion of solutions, but does not pass through bacteria.

The quasitransversal ultrasonic (US) velocity $V_{\perp} = 768$ m/sec, shear module $G = \rho V_{\perp}^2 = 578$ Mpa, the quasilongitudinal US velocity $V_{\parallel} = 2485$ m/sec, dynamical elastic module $E = \rho V_{\parallel}^2 = 6.057$ GPa, Puasson coefficient $\mu = 0.442$, specific density polyethylene with low density high pressure $(C_2H_4)_n + 3\%$ multiwalled carbon nanotubes (MCNT) $\rho = 980.8$ kg/m³ were determined from the oscillogramm [1] on fig. 1.

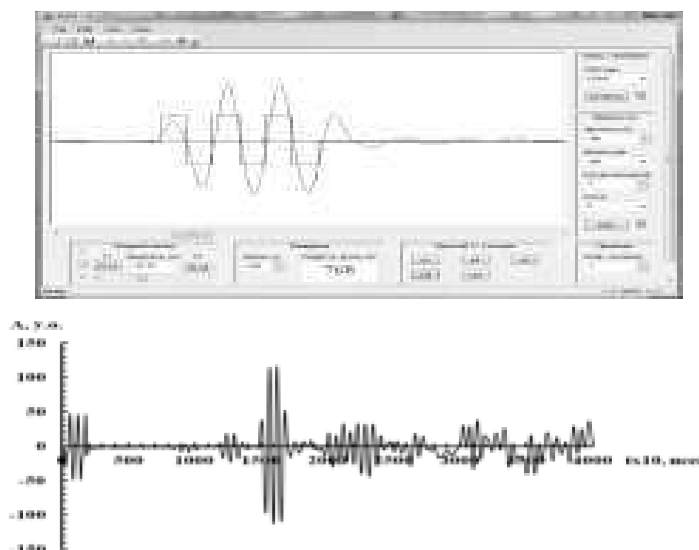


Fig. 1. The window illustration of data treatment of quasitransversal elastic waves velocity measuring $V_{\perp} = 768 \pm 10$ m/sec in nanocomposite polyethylene with low density high pressure $(C_2H_4)_n + 3\%$ multiwalled carbon nanotubes by impulse-phase method at frequency $f_{\perp} = 0,7$ MGz

The optimum concentration $C=5\%$ of polyvinyl alcohol $(C_2H_4O)_n$ radiation sutured hydrogel with the maximal absolute values of the static module E at compression, at extension; elastic limit σ_E ; effective fluidity limit σ_{fl} ; strength limit at compression σ_{st} in consequence of the formation of the polyvinyl spirit molecules nanoclusters.

[1]. Y.A. Onanko, S.A. Vyzhva, A.P. Onanko. Analysis of anisotropy measuring data in minerals // Mineralogical digest. – 2012. - № 62(2). - p. 284 - 287.

Photochemical Synthesis of Silver Nanoparticles and Their Impact on the Environment

D. Babusca¹, L. Sacarescu², L. Popescu^{*1}, D.O. Dorohoi¹, D. Creanga¹

¹ Alexandru Ioan Cuza University, Physics Faculty, Iasi, Romania

² Petru Poni Institute of Macromolecular Chemistry, Iasi, Romania

**Corresponding author: mdor@uaic.ro*

Nobel metal nanoparticles were intensively studied due to their peculiar properties and various applications. Every year the amount of silver nanoparticles intended for textile industry, cosmetics and pharmaceuticals exceeds tens of tones. Besides the benefits offered by silver antiseptic features, there is always the concern on their fate in the environment since silver nanoparticles are finally delivered in the water, air and soil where they can interact with biosphere components. We have designed an experimental study dedicated to silver nanotoxicity, based on citrate-silver nanoparticles produced by photochemical method. The colloidal suspension was obtained by silver ion reduction with citrate followed by controlled exposure to ultraviolet radiation of high energy photons. Physical characterization was carried out by electron microscopy and UV-Vis spectrophotometry. Fine granularity of generally symmetrical shape nanoparticles was evidenced by Transmission Electron Microscopy, the largest nanoparticle diameter not exceeding 40 nm. The Surface Plasmon Resonance spectral band was recorded for both suspensions, either before or after ultraviolet ray exposure, revealing the intensification of silver nanoparticle formation and UV photon impact. The nanotoxicity of silver nanoparticle suspension was tested on cereal culture plantlets during very early ontogenetic stages. Some biological and biochemical parameters were followed for about two weeks in the cereal plantlets grown in the presence of citrate-silver nanoparticle suspension. The discussion was done on the plantlet metabolic behavior by measuring the concentrations of chlorophylls and carotenes synthesized in the green tissue. The differences between control samples, supplied with only distilled water and test samples, supplied with different amounts of silver nanoparticles were analyzed statistically, to search for a threshold of nanotoxicity as well as for comparison with literature reports.

[1]. D. Dewez, V. Goltsev, H.M. Kalaji, A. Oukarroum, Inhibitory effects of silver nanoparticles on photosystem II performance in *Lemna gibba* probed by chlorophyll fluorescence// *Current Plant Biology*. – 2018. –vol. 16. – p. 15–21.

**Study of Some Interface Phenomena Related to
Magnetic Nanograins Stabilization in Fluid Suspensions
by Using Organic Coating Molecules**

C. Morosanu¹, L. Popescu^{*1}, D. Dorohoi¹, D. Creanga¹

¹Alexandru Ioan Cuza University, Physics Faculty, Iasi, Romania

**Corresponding author: mdor@uaic.ro*

The main part of biomedical applications of magnetic nanoparticles requires magnetic nanograin stabilization in the form of colloidal suspensions in water. To achieve this purpose the surface of magnetic nanocores needs to be modified with organic, hydrophilic molecules, able to interact with surface metal ions and to ensure either steric or electrostatic stabilization of the resulted colloidal suspensions. We present some preliminary data of our study focused on the quantum mechanical approach of several molecular substances able to develop stable interfaces with magnetic nanoparticles and, this way, to balance, the magnetic attraction forces among them through electric repulsions. Sodium oleate, ensuring steric stabilization and citric acid, ensuring electrostatic stabilization, are analyzed in detail in this paper, their energetic and microstructural parameters being presented comparatively. The roles of dipole moment and partition coefficient were emphasized aiming to better understand the effects of some interface phenomena in the optimization of magnetic nanoparticle suspension preparation for various applications in molecular biology and medicine. Further, practical yielding of magnetic metal oxides in the form of colloidal nanoparticles by coating with sodium oleate and respectively with citric acid is discussed.

- [1]. D.K. Kim, M. Mikhaylova, Y. Zhang, M. Muhammed, Protective Coating of Superparamagnetic Iron Oxide Nanoparticles // Chemical Materials -2003.-V. 15.-N. 8.- p. 1617–1627.

Diffuse Reflectance UV–Visible Absorption Spectra of Hybrid TiO₂/PTZ Composites

V. Shymanovska*¹, L. Kernazhitsky¹, T. Gavrilko¹, N. Shcherban²,
T. Khalyavka³, V. Naumov⁴.

¹ Institute of Physics NAS Ukraine, Kiev, Ukraine

² L.V. Pisarzhevskii Institute of Physical Chemistry NAS of Ukraine, Kyiv, Ukraine

³ Institute for Sorption and Problems of Endoecology NAS of Ukraine, Kyiv, Ukraine

⁴ Lashkaryov Institute of Semiconductor Physics NAS Ukraine, Kiev, Ukraine

*Corresponding author: vshymanovska@iop.kiev.ua

Here we report on TiO₂ doping with phenothiazine (PTZ) as an alternative approach to engineering a nonstoichiometric TiO₂ material. There is a great interest in hybrid TiO₂ structures activated with organic dyes.

We studied the effect of PTZ on diffuse reflectance UV–visible absorption spectra (DRUVv) of the nanocrystalline TiO₂ powders with anatase (*A*) structure. PTZ showing strong electron-donating ability could act as electron donor for TiO₂ known as good electron-acceptor material. The admixture of PTZ in *A*/TiO₂ causes a noticeable red shift in the edge of TiO₂ absorption and a significant narrowing of the band gap for direct and indirect electronic transitions. The narrowing of the band gap can occur due to an increase in the number of defects associated with Ti³⁺ and oxygen vacancies.

DRUVv spectra of powders were measured using Perkin-Elmer Lambda Bio 35 spectrophotometer in the range 200–1000 nm, which allowed converting data of corresponding spectra using the Kubelka–Munk equation. The value of E_g was estimated using the method proposed by Wood and Tauc by the extrapolation of the linear part of the plot $(hv \cdot \alpha(hv))^{1/n}$ versus $h\nu$ toward energy axis at $\alpha(h\nu)=0$.

The experiments have shown that mixing of TiO₂ (white powder) and PTZ (yellow powder) results in dark-blue colored powder TiO₂/PTZ. The admixture of PTZ in *A*/TiO₂ causes a noticeable red shift in the edge of TiO₂ absorption and a narrowing of the band gap for direct and indirect electronic transitions. The narrowing of the band gap can occur due to an increase in the number of defects associated with Ti³⁺ and oxygen vacancies of the (*V_O*)–Ti³⁺ type. The free electrons produced during the interaction between PTZ and *A*/TiO₂ are either captured by Ti⁴⁺ to form Ti³⁺ species on the lattice or got trapped in the oxygen vacancies (*V_O*). The electrons captured by Ti⁴⁺, on the either sides of the oxygen vacancy are involved in formation of Ti³⁺–*V_O*–Ti³⁺ defect complexes, and the electrons trapped by the oxygen vacancies contribute to the formation of the color centers (*F*, *F*⁺ or *F*²⁺).

IR-Spectroscopy of Partially Substituted (La,Ca)VO₄: Eu³⁺, Er³⁺ Nanoparticles

O. Chukova¹, S.A. Nedilko², S.G. Nedilko¹, A. Slepets^{2*}, T. Voitenko²

¹ Physics Faculty, Taras Shevchenko National University of Kyiv, Kyiv, Ukraine

² Chemistry Faculty, Taras Shevchenko National University of Kyiv, Kyiv, Ukraine

*Corresponding author: giva@online.ua

Today, among different types of modern materials, orthovanadates are an important family of rare earth compounds and have potential applications in the various fields of science, technologies and medicine, such as sensors, laser hosts, catalysts, phosphors etc. The aim of this work was to investigate the IR spectroscopy of La_{1-x-y}Er_{x/2}Eu_{x/2}Ca_yVO₄ (0 ≤ x, y ≤ 0.3) compounds.

The La_{1-x-y}Er_{x/2}Eu_{x/2}Ca_yVO₄ (0 ≤ x, y ≤ 0.3) samples were prepared by gel-sol synthesis. Infrared spectra (IR) of the samples were recorded on PerkinElmer IR spectrometer using the KBr pellet method in the range 1400–400 cm⁻¹.

IR spectroscopy study of the La_{1-x-y}Er_{x/2}Eu_{x/2}Ca_yVO₄ (0 ≤ x, y ≤ 0.3) system samples was performed to confirm their structure and composition (Fig. 1).

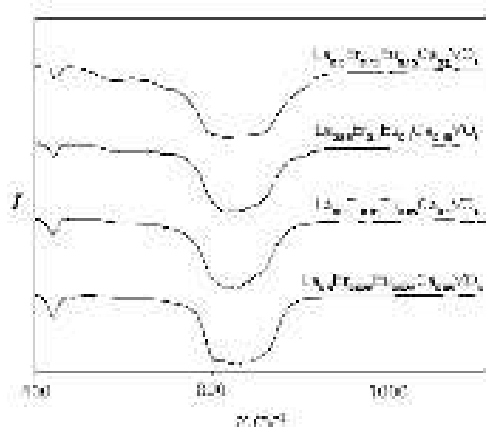


Fig. 1. IR absorption spectra of the La_{1-x-y}Er_{x/2}Eu_{x/2}Ca_yVO₄ (0 ≤ x, y ≤ 0.3)

Thus, spectrum of the undoped LaVO₄ contains separated peaks located near 440 cm⁻¹, those should be assigned to ν₄ vibration mode of the VO₄³⁻ anion. The stronger wide band in the range 700–1000 cm⁻¹ contain peaks around 820 and 875 cm⁻¹ those should be assigned to ν₃ and ν₁ vibration modes, respectively. It possible to see from curves that ν₃ mode is split on three weakly separated components for the La_{0.9}Er_{0.025}Eu_{0.025}Ca_{0.5}VO₄ and La_{0.8}Er_{0.05}Eu_{0.05}Ca_{0.1}VO₄ samples. These observation described above confirms results of the XRD study of the samples about monoclinic and tetragonal structures of the La_{1-x-y}Er_{x/2}Eu_{x/2}Ca_yVO₄ (0 ≤ x, y ≤ 0.3) samples.

Synthesis, Morphological Features and Electronic Structure of Composites Based on Hydroxyapatite and Ultradispersed Graphite

L.I. Karbivska¹, S.S. Smolyak¹, V.L. Karbivskyy^{*1}, D.A. Savchenko¹

¹ Department of Nanostructures Physics, G. V. Kurdyumov Institute for Metal Physics of the NAS of Ukraine, Kyiv, Ukraine

**Corresponding author: karb@imp.kiev.ua*

The composites were synthesized on the basis of nano-dispersed calcium hydroxyapatite, ultradispersed graphite, cellulose fibers and epoxy oligomer which has conductive properties due to modification with graphite. Composites have a high thermal stability inherent to hydroxyapatite, and may be promising for use in a wide range of industries, science and technology [1]. Such materials may be important for medicine, since conductive composites can transmit electrical impulses [2].

Table. 1. The binding energy (eV) and the full width at half maximum (eV) of the atomic core-levels lines of the investigated compounds.

Composite	O 1s	P 2p	Ca 2p _{3/2}	C 1s
(Ca ₁₀ (PO ₄) ₆ (OH) ₂ + graphite+cellulose)	531.6 (1.95)	134 (1.84)	348 (0.9)	284.0 (0.85), 285.1 (1.55), 290.2 (1.6)
(Ca ₁₀ (PO ₄) ₆ (OH) ₂ + graphite+cellulose+ epoxy oligomer)	532.2 (1.33)	-	347.4 (0.82)	284.0 (0.8), 285.2 (1.65) 289.5 (1.87), 290.4 (0.75)

Scanning electron microscopy (SEM), X-ray photoelectron spectroscopy (XPS), and the energy dispersive spectroscopy (EDS) were used to study these composites. Analysis of XPS data for both composites showed (Table 1) that the presence of the oligomer in the composite structure leads to a redistribution of atomic charges, namely, a decrease in the negative charge on oxygen atoms and an increase on calcium, which indicates a decrease in the ionic component of the chemical bond in the overall balance of the chemical bond. Consequently, the admixtures of graphite and epoxy oligomer affect the charge state of atoms and the nature of the chemical bond in the structure of apatite. By means of scanning electron microscopy and X-ray photoelectron spectroscopy, it was found that the Ca₁₀(PO₄)₆(OH)₂ + graphite + cellulose compound is a composite that contains both conductive and non-conductive components. This is confirmed by the data obtained by the energy dispersion spectroscopy, which indicate that the graphite in this sample is distributed unevenly. Modification of the composite with an epoxy oligomer with a hardener leads to the appearance of conductivity in the material.

- [1]. F.-F. Chen, Y.-J. Zhu, Z.-C. Xiong, L.-Y. Dong, F. Chen, B.-Q. Lu. and R.-L. Yang. // ACS Applied Materials & Interfaces. – 2017. – V. 9, N. 45. – p. 39534.
 [2]. A. Shahini, M. Yazdimamaghani, K.J. Walker, M.A. Eastman, H. Hatami-Marbini, B. J. Smith, J. L. Ricci, S.V. Madhally, D. Vashae, L. Tayebi.// International Journal of Nanomedicine. – 2014. – V. 9. – p. 167.

Structure and Vibrational Spectra of the MoS₂ – Nucleic Acid Bases Complexes: a Computational Study

S.G. Stepanian^{*1}, V.A. Karachevtsev¹, L. Adamowicz²

¹ B. Verkin Institute for Low Temperature Physics and Engineering, National Academy of Sciences of Ukraine, Kharkiv, Ukraine

² Department of Chemistry and Biochemistry, University of Arizona, 85721 Tucson AZ, USA

**Corresponding author: stepanian@ilt.kharkov.ua*

A feature of transition metal dichalcogenides (TMDs) dpm is the low vibration frequencies of these materials. For example, all vibrations of MoS₂ are observed in the region below 450 cm⁻¹. At the same time, most vibrations of biological molecules, whose complexes with TMDs are being actively studied at the present time, are located in the region of higher frequencies. This circumstance makes the methods of IR and Raman spectroscopy particularly effective in the study of the interaction of TMDs with biomolecules, since this allows direct monitoring of changes in the vibrational spectra of biomolecules when interacting with TDMs. In this study the interactions between nucleic acid bases (NABs) and MoS₂ monolayer were studied using quantum chemical methods DFT/M06-2X and MP2. The main aim was to determine changes in the IR and Raman spectra of NABs during the formation of their complexes with MoS₂. At the first stage, the structure and interaction energies between the NABs and a fragment of the surface of the MoS₂ were determined. The fragment consisted of 28 Mo atoms and 56 S atoms. We found the possibility of the formation of two types of NABs complexes with the fragment of MoS₂. These are non-covalent stacking complexes, as well as covalent complexes in which there is a coordination chemical bond between the edge Mo atoms and the NAB atoms having an electron lone pair. In stacking complexes, the interaction energy is in the range 15-30 kcal/mol, while in covalent complexes it is significantly higher (in absolute values) and is in the range 40-80 kcal/mol. The calculations also predicted significantly stronger spectral changes during the formation of covalent complexes. Additionally, we compared the interaction energies and vibrational spectra of NABs in complexes with MoS₂, graphene and graphene oxide.

This work was supported by the National Academy of Sciences of Ukraine (NASU) (Grant Np. 15/19-H within the program “Fundamental Problems of the Creation of New Nanomaterials and Nanotechnology”, Grant No. 07-01-18/19).

Infrared Spectroscopy of Functionalized Nanocarbon Particles with Different Structure

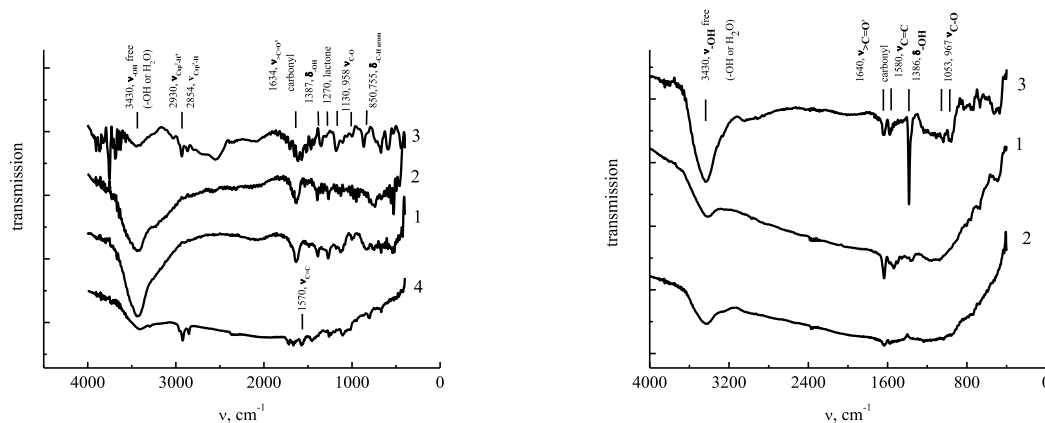
I. Ovsienko¹, L. Matzui¹, T. Len¹, D. Naumova², O. Syvolozhskyi^{*1}

¹Physical and ²Chemical Departments, Taras Shevchenko National University of Kyiv, Ukraine,

**Corresponding author: mail.olexiy@gmail.com*

The presented work is devoted to questions of covalent functionalization of different nanocarbon structures and possibilities of studying the degree of their functionalization by the method of infrared spectroscopy.

For functionalization the different nanocarbon structures have been choose. These are single wall and multiwall carbon nanotubes with different degree of structural perfection, carbon nanoplatelets and graphenelike structures. The functionalization of nanocarbon structures have been carried out by treat of them with strong oxidizers, such as solution of potassium permanganate in sulfur acid, mixture of concentrated sulfuric and nitric acids, some organic compounds. Also nanocarbon structures have been exposed to ultraviolet irradiation. Figure 1 presents the IR spectra for functionalized with different reagents nanocarbon structures.



a)

b)

Fig. 1. IR spectra for functionalized with solution of potassium permanganate in sulfur acid (a) CNT (1), TEG (2, 3), source TEG (4) and for dispersed in water TEG (b) during 3 hrs (1), 6 hrs (2) and 26 hrs (3).

As can be seen from the Figure, the form of the spectra is significantly different for different types of nanocarbon structures, different functionalized reagents and different functionalization time.

In the work the qualitative composition of functional groups on the surface of carbon, depending on the degree of its structural perfection and the type of functionalizing substance is analyzes in detail. A method for estimating the relative change of the quantitative composition of functional groups on the surface of a nanocarbon structures under functionalization is proposed.

Enhancement of Photoluminescence and Extinction of Light in Gold Nanoparticles/Shellac-Dye/Gold Film Planar Plasmonic Cavity

A.V. Tomchuk^{*1}, O.A. Yeshchenko¹, V.V. Kozachenko¹, A.P. Naumenko¹,
Yu.L. Slominskii², R.J. Knize³, M. Haftel^{4,5}, A.O. Pinchuk^{4,5}

¹ Physics Department, Taras Shevchenko National University of Kyiv, 64/13
Volodymyrska str., 01601 Kyiv, Ukraine

² Institute of Organic Chemistry, National Academy of Sciences of Ukraine, 5
Murmanska str., Kyiv 02660, Ukraine

³ Laser Optics Research Center, Physics Department, US Air Force Academy,
Colorado Springs, Colorado, 80840, USA

⁴ Department of Physics, University of Colorado at Colorado Springs, USA

⁵ Center for Plasmonics, Nanophotonics, and Metamaterials, Colorado Springs,
Colorado, 80918, USA

**Corresponding author: nastiona30@gmail.com*

Effects of plasmonic gap mode formation due to coupling between metal nanoparticles and thin metal film separated by thin dielectric luminescent film-spacer (gap) have been studied by means of light extinction and photoluminescence in three-layer planar *Au NPs monolayer / shellac-dye film / Au film* nanostructure with spacer thickness varied in the range of 8–47 nm. The 3-fold enhancement of light extinction and 90 nm red shift of the plasmon mode have been observed in extinction spectra. The 37-fold enhancement of dye photoluminescence and the significant (48 nm) red shift of dye photoluminescence band have been observed for *Au NPs monolayer / shellac-dye film / Au film* nanostructure in comparison with bare shellac-dye film for the spacer thickness of 8 nm. The decrease of the spacer thickness causes the increase of the enhancement factor of dye photoluminescence indicating the strengthening of the gap mode field. FDTD calculations of the dependence of the intensity of the field of gap mode on the gap thickness have demonstrated good quantitative agreement with experimental data that proves the key role of gap mode in the enhancement of the electromagnetic field in planar *metal NPs monolayer / dielectric film / metal film* plasmonic cavity nanostructures. The variation of the gap thickness provides the possibility to tune controllably the spectral position and enhancement factor of the light emission from the emitters located in the gap.

DNA Nucleotides-Assisted Exfoliation and Dispersion of Few-Layer MoS₂: Spectroscopy Control

N.V. Kurnosov¹, I.M. Voloshin^{1*}, V.A. Karachevtsev¹

¹ B. Verkin Institute for Low Temperature Physics and Engineering, National Academy of Sciences of Ukraine, Kharkiv, Ukraine

**Corresponding author: voloshin@ilt.kharkov.ua*

Two-dimensional (2D) transition metal dichalcogenides (TMDs), such as MoS₂, are currently in focus of extensive research efforts in materials and nano science due to their unique physical characteristics and potential application in many relevant technological areas including electronics, photonics, energy conversion and storage, catalysis, sensing, biology and nanomedicine. While the bulk TMDs have been studied for decades, a new burst of interest in this material appears when its dimension is downscaled to the monolayer level and quantum confinement effects begin to be observed. Colloidal suspensions of the 2D flakes can be prepared by ultrasound-induced exfoliation of TMDs in the liquid phase. This approach is widespread due to its simplicity and versatility. At that some stabilizers are usually exploited to produce large amounts of few-layer flakes using the exfoliation method.

In this work we have used DNA nucleotides deoxyadenosine monophosphate (dAMP) for the exfoliation of MoS₂ layers and their colloidal stabilization in aqueous medium. The preparation method of aqueous suspensions of MoS₂ layers is based on the ultrasound treatment of the aqueous suspension of MoS₂ microcrystals with dAMP added to this suspension (weight ratio 3:1) with following centrifugation. Each step of preparation of dispersed MoS₂ layers was controlled by the absorption spectroscopy and photoluminescence. Experimental observation of exciton emission bands in the spectral range of 1.8-2.2 eV indicates the production of few-layered MoS₂ including monolayers. We discuss different modes of MoS₂ aqueous suspension preparation with spectroscopy control to select optimal conditions for producing MoS₂ monolayers with high yield.

This work was supported by the National Academy of Sciences of Ukraine (NASU) (Grant No. 15/19-H within the program “Fundamental Problems of the Creation of New Nanomaterials and Nanotechnology”, Grant No. 07-01-18/19). N.V.K. acknowledges support from the NASU: Grant No. 4/H-2019.

7

Surfaces and Films

Glass–Ceramics Luminescent Transformers for WLEDs Application

S.G. Nedilko

Physics Faculty, Taras Shevchenko National University of Kyiv, Kyiv, Ukraine

**Corresponding author: SNedilko@univ.kiev.ua*

White light-emitting diodes (WLED), as a new type of luminescent devices, due to their excellent properties have played an important crucial role in applications of indicator, backlight, automobile headlight, such as long lifetime, energy saving, environment-friendliness, small volume etc. It is common knowledge that major commercial diode is the phosphor converted LED made of blue-emitting chip and $\text{Y}_3\text{Al}_5\text{O}_{12}:\text{Ce}^{3+}$ dispersed in organic silicone binder. However, this binder in high-power device ages easily and become yellow colored due to accumulated heat emitted from chip, which strongly affects the device properties, and therefore reduces its long-term reliability and lifetime [1].

Recently, new type of luminescent materials was proposed for high-power WLED: that is inorganic high thermal-stable transparent glass–ceramics light converter. This type of composite has to possess the host property of glass and reveal the optical performance of microcrystal phosphors.

We present here some literature data and the results of own study in this area. Three types of glass-ceramics nanostructured composites are described. These are composites based on alkali-borate, phosphate - molybdates and vanadate – borate glasses. In accordance, suitable crystalline compounds of various types were used as micro/nanocrystalline component of glass-ceramics materials. There were some orthoborate doped with RE ions, molybdates like to $\text{A}^{\text{I}}\text{B}^{\text{III}}(\text{MoO}_4)_2$ doped with RE ions (A^{I} – alkali metal, B^{III} – Y, Bi, La, RE = Eu, Pr), and vanadates nanocrystals.

Several experimental procedures were used to study structure, morphology and especially luminescent properties of noted composite systems: XRD, SEM, optical reflection, absorption, FTIR, and surely luminescent spectroscopy among them. Luminescent study was made in the wide range of luminescent light registration (300 – 1200 nm), wavelength of luminescence excitation (225 - 600 nm) and luminescence decay time 10 μs – 1 s.

Advantages and disadvantages of glass-ceramic luminescent coatings for LEDs were discussed on the basis of literary and own experimental data.

- [1]. Daqin Chen, Weidong Xiang, Xiaojuan Liang, Jiasong Zhong, Hua Yu, Mingye Ding, Hongwei Lu, Zhenguo Ji. Advances in transparent glass–ceramic phosphors for white light-emitting diodes - A review // Journal of the European Ceramic Society. – 2015. – V. 35. – p. 859 – 869.

Sensitivity of Physical Properties and Local Biological Reactions of Metals and Alloys Surfaces to Ultrafast Laser Treatment

N.I. Berezovska^{1*}, I.M. Dmitruk¹, O.P. Stanovyi¹, A.M. Dmytruk²,
I.V. Blonskiy², O.M. Mishchenko³, M.V. Pogorielov⁴

¹Physics Faculty, Taras Shevchenko National University of Kyiv, Kyiv, Ukraine

²Photon Processes Department, Institute of Physic, NAS of Ukraine, Kyiv, Ukraine

³Medical Faculty No. 3, Zaporizhzhia State Medical University, Zaporizhzhia, Ukraine

⁴ Department of Public Health, Medical Institute of Sumy State University, Sumy, Ukraine

**Corresponding author: n_berezovska@univ.kiev.ua*

The presented report deals with the study of the influence of parameters of pulsed laser radiation of femtosecond duration on the morphology, structure, physical and biological properties of the surfaces of metals (Ti) and Ti-based alloys applicable for dental and orthopaedic implants. The laser processing of the implant surfaces provides less surface contamination during such treatment in comparison with other methods, which improves the biological response of implants [1, 2].

Micro- and nanostructuring of Ti and Ti-based alloys surfaces have been achieved by the irradiation of the samples initial surfaces with Ti:sapphire femtosecond laser. Surface analysis by means of scanning electron microscopy and measurements of the light-scattering indicatrices of laser modified surfaces demonstrates an existence of several types of the samples morphology, in particular, the quasi-gratings with several different periods, micro- and nanogranular fine structure, nonperiodic structures with different surface roughness. Possible mechanisms of formation of such structures have been considered taking into account different types of the preliminary treatment of initial samples. The average wettability has been characterized by the measurements of the contact angles of the distilled water drops on the sample surfaces. There is a correlation between femtosecond laser treatment, surface hydrophobicity and cell growth: the higher hydrophobicity, the less proliferation of fibroblasts, in particular.

[1]. A.Y. Vorobyev, C. Guo. Direct Femtosecond Laser Surface Nano/Micro-structuring and its Applications // Laser & Photonics Rev. – 2013. – V. 7. – N. 3. – p. 385 – 407.

[2]. C. Mas-Moruno, B. Su, M.J. Dalby. Multifunctional Coatings and Nanotopographies: Toward Cell Instructive and Antibacterial Implants // Adv. Health. Mater. – 2019. – V. 8. – N. 1. – p. 1801103.

Mechanisms of CrO_4^{2-} Anions Adsorption on the Surface of Carbon Nanostructures : a DFT Approach

V. Borysiuk^{1*}, S. Nedilko¹, Yu. Hizhnyi¹

¹Taras Shevchenko National University of Kyiv, Faculty of Physics, Kyiv, Ukraine

**Corresponding author: borysyukviktor@gmail.com*

Detection and removal of heavy metals from waste water is a topical technological and industrial problem. One of the most promising methods of water purification from heavy metals is their adsorption by artificial adsorbents. At present, carbon nanostructured materials are intensively studied as adsorbents for efficient removal and storage of various toxic pollutants. The aim of this work is to clarify the mechanisms of the chromate compounds interaction with the surface of carbon nanotubes by theoretical modelling of the processes of molecular adsorption together with experimental studies of these processes by various, particularly, spectroscopic methods.

In this work we considered adsorption characteristics of CrO_4^{2-} anions on the surface of several types of carbon nanotubes (CNTs). Geometry-optimized calculations of the electronic structures were carried out at the Density Functional Theory (DFT) level within molecular cluster approach using Gaussian 09 software package [1]. The binding energies, relaxed geometries, electronic charges, and vibrational spectra of studied chromate compounds in the adsorbed and in the “free” states were calculated and compared each other. The energies and oscillator strengths of the electronic transitions between the ground and excited states, as well as the optical absorption spectra of the “free” and adsorbed anions are calculated using time-dependent DFT (TD-DFT) approximation. Effects of water solvent on studied adsorption behavior were considered in a polarizable continuum model (PCM).

The optical spectra (Raman, IR absorption and photoluminescence) of the systems containing carbon nanostructures were experimentally measured before and after adsorption of chromate compounds. The spectra revealed substantial difference that confirms the principal possibility of optical monitoring of the adsorption processes. The observed behaviour of experimental spectra were discussed on the base of the obtained calculation results.

[1]. Frisch M.J., Trucks G.W., Schlegel H.B., et al. // Gaussian 09 (Gaussian, Inc., Wallingford, CT, 2009).

Kinetics and Lifetime Distributions of PbCdI₂ Films Photoluminescence

A.P. Bukivskii^{1*}, Yu.P. Gnatenko¹, P.M. Bukivskii¹, Yu.P. Piryatinski¹,
I.V. Fesych², V.V. Lendel²

¹Institute of Physics NAS of Ukraine, Kyiv, Ukraine

²Taras Shevchenko National University of Kyiv, Kyiv, Ukraine

*Corresponding author: ap.bukivskii@gmail.com

As mentioned earlier [1], PbCdI₂ layered semiconductors are promising materials for the development of radiation detectors (for X- and γ-rays), since they exhibit intense photoluminescence (PL) and luminescence excited by X-rays (XRL) at room temperature. Intense PL and XRL of these materials is associated with the natural formation of PbI₂ nanoparticles (NP) embedded in CdI₂ matrix during the growth of the solid solution. Earlier we studied the nature of the luminescence caused by these NP [2] and discovered the way of obtaining PbCdI₂ films with a large concentration of PbI₂ NP of controlled sizes with optical properties similar to those of bulk crystals [1].

The PL measurements of the investigated films at room and liquid helium temperatures have shown PL bands of free excitons ($\lambda = 495$ nm $T=4.5$ K), donor-acceptor pairs ($\lambda = 508$ nm $T=4.5$ K), localized on stretched Pb-I bonds on the nanoparticles surface excitons ($\lambda = 550$ nm $T=4.5$ K and $T=300$ K), and donor-acceptor pairs including deep acceptor levels ($\lambda = 594$ nm $T=4.5$ K and $T=300$ K) [1] similar to those which are observed for Pb_{0.3}Cd_{0.7}I₂ bulk crystals.

The time-resolved PL studies which we are reporting gave us information about the response time of the materials and the dynamics of electronic processes occurring in these materials, which cause their intense luminescence.

The PL kinetics of Pb_{0.3}Cd_{0.7}I₂ films was measured using a lifetime spectrometer LifeSpec2 at room temperature and 4.5 K at different wavelengths. The analysis of the obtained PL kinetic data was carried out by approximation of the decay curve by a large number (N=200) of exponentials. This method allowed us to establish the lifetime distribution function and its peaks for each separate PL band.

The PL kinetics of mentioned above bands namely the band of exciton localized on stretched bonds, the bands of donor-acceptor pairs and the line of free exciton were analyzed and the lifetime distributions for these bands were obtained. It should be noted that the PL lifetime of major PL bands of Pb_{0.3}Cd_{0.7}I₂ films are quite similar to those of Pb_{0.3}Cd_{0.7}I₂ bulk crystals. Such films have fast optical response at room temperature.

[1]. Bukivskii A.P., Gnatenko Yu.P., Piryatinski Yu.P., et. al. // Book of Abstracts of XXIII ISSSMC, 20 - 25 September, 2017, Kyiv, Ukraine, p. 134.

[2]. A.P. Bukivskii, Yu.P. Gnatenko, Yu.P. Piryatinski, R.V. Gamernyk // Journal of Luminescence. – 2017. – v. 185. – p. 83 – 91.

InAs/InGaAs Structures with InAs Quantum Dot Array Confined by InAlAs Nano-Barriers: Deep Levels and Photoelectric Properties

O.I. Datsenko^{*1}, S. Golovynskyi^{2,3}, L. Seravalli⁴, G. Trevisi⁴, P. Frigeri⁴,
I. Golovynska², Baikui Li², Junle Qu²

¹ Department of Physics, Taras Shevchenko National University of Kyiv, Ukraine

² Key Laboratory of Optoelectronic Devices and Systems, College of Physics and Optoelectronic Engineering, Shenzhen University, Shenzhen, China

³ Institute of Semiconductor Physics, National Academy of Sciences, Kyiv, Ukraine

⁴ Institute of Materials for Electronics and Magnetism, CNR-IMEM, Parma, Italy

**Corresponding author: lesoto8g@gmail.com*

Metamorphic InAs/In_{0.15}Ga_{0.85}As structures with InAs quantum dot (QD) layers confined by InAlAs barriers have been studied by in-plane photocurrent (PC), thermally stimulated conductivity (TSC) and photoluminescence spectroscopies. Their properties have been compared with the barrier-free structures and those with only upper or lower barrier.

The PC and TSC spectra of all the structures reveal point defects such as EL2, EL6, EL7, EL8, EL9 and EL10 as well as three extended defects with activation energies of 0.43, 0.48 and 0.52-0.54 eV inherent in GaAs material. In addition, a hole trap at ($E_v + 0.55$ eV) has been detected in the TSC spectra and identified as HL3 defect. This defect was observed earlier in GaAs and InAs/GaAs nanostructures [1], but it was not found yet in metamorphic ones.

The TSC amplitude analysis shows that the introduction of barriers does not noticeably change the defect composition, though it should be noted that the defect response decreases for excitation energies corresponding to the edge absorption in InGaAs layers. The barrier structures reveal a lower dark current and PC at room temperature. All this can be understood considering that the InAs wetting layer is the effective in-plane conductivity channel in metamorphic structures [2].

The PC signal reveals a monotonous degradation under a stable excitation. This effect is related to the traps located just near the QDs. Being filled by electrons, they cause Coulomb screening of the wetting layer as a conductivity channel against the incoming excited electrons incoming [3].

[1]. M.M. Sobolev, A.R. Kovsh, V.M. Ustinov, A.Yu. Egorov, and A.E. Zhukov. Metastable Population of Self-Organized InAs/GaAs Quantum Dots // J. Electron. Mater. – 1999. – V. 28. – N. 5. – P. 491-495.

[2]. S. Golovynskyi, O.I. Datsenko, L. Seravalli, G. Trevisi, P. Frigeri, I. Babichuk, I. Golovynska, and J. Qu. Interband Photoconductivity of Metamorphic InAs/InGaAs Quantum Dots in the 1.3–1.55- μ m Window // Nanoscale Res. Lett. – 2018. – V. 13. – P.103.

[3]. S. Golovynskyi, O.I. Datsenko, L. Seravalli, G. Trevisi, P. Frigeri, I.S. Babichuk, I. Golovynska, Baikui Li and Junle Qu, Defect influence on in-plane photocurrent of InAs/InGaAs quantum dot array: long-term electron trapping and Coulomb screening // Nanotechnology. – 2019. – V. 30. – N. 30. – 305701.

Photocurrent Gain Enhancement in Planar Perovskite Photodetectors Based on Interdigitated Combs of Electrodes

R. Gegevičius*, M. Franckevičius, M. Treideris, V. Gulbinas

Center for Physical Sciences and Technology, Vilnius, Lithuania

**Corresponding author: rokas.gegevicius@ftmc.lt*

Perovskite solar cells have developed rapidly in recent years due to several factors, including their high light absorption capability, long carrier lifetime, high defect tolerance, and adjustable band gap. Since they were first reported in 2009, solar cells based on organic–inorganic hybrid halide lead perovskites have achieved a power conversion efficiency of over 24% [1]. Despite tremendous interest in solar cell research perovskite photodetectors still lack a basic understanding of their operating principles. Here, we study the performance of planar MAPbI₃ perovskite photodetectors produced on interdigitated comb of electrodes made from various metals. We demonstrate that hole blocking oxide layer between Cr metal electrode and perovskite enabled to reach responsivity of 152 A/W and external gain of more than 350. We suggest that the gain enhancement originates from the hindered extraction of photogenerated holes and the migration of ions, which creates additional hole traps at interfaces. These effects reduce the barrier for electron injection and enable the passage of a larger number of electrons during the prolonged lifetime of photogenerated holes. The achieved photodetector sensitivity, suggested gain enhancement approach and obtained better understanding of the photocurrent gain mechanism in hybrid metal halide perovskites open a way towards the further development of a cheap and easily producible planar perovskite photodetectors based on interdigitated electrode arrays.

[1]. National Renewable Energy Laboratory. Best Research-Cell Efficiencies. Available at <https://www.nrel.gov/pv/assets/images/efficiency-chart.png>. Accessed on 03 May 2019.

Defect Levels in Metamorphic InAs/InGaAs Quantum Dot Structures

S. Golovynskyi^{1,2,*}, O.I. Datsenko³, L. Seravalli⁴, G. Trevisi⁴, P. Frigeri⁴,
I. Golovynska¹, Baikui Li¹, Junle Qu¹

¹ Key Laboratory of Optoelectronic Devices and Systems, College of Physics and Optoelectronic Engineering, Shenzhen University, Shenzhen, P.R. China

² Institute of Semiconductor Physics, National Academy of Sciences, Kyiv, Ukraine

³ Department of Physics, Taras Shevchenko National University of Kyiv, Ukraine

⁴ Institute of Materials for Electronics and Magnetism, CNR-IMEM, Parma, Italy

*Corresponding author: serge@szu.edu.cn

We present the study of the influence of electron traps related to defects on photocurrent (PC) in plane of InAs/In_xGa_{1-x}As quantum dot(QD) arrays with different Indium content, grown by molecular beam epitaxy on GaAs substrates. Dynamics of near-IR-excited PC was found to be complex. A fast increase in PC at the beginning of illumination is followed by a monotonous degradation of PC under stable band-to-band excitation for only QDs and for transitions in the confining layers. The degradation dynamics in the structure with $x = 0.15$ was well fitted by allometric exponent $\sim \exp[-(t/\tau)^\beta]$ with different fitting parameters depending on the excitation energy.

The PC degradation was attributed to electron traps found near QDs by thermally stimulated current (TSC) spectroscopy. In particular, GaAs-inherent point defects EL6-EL10 and M0 were detected near the QD layer, while deeper levels related to extended defects were found in the buffer layer. We believe that the former traps, when filled by electrons due to the sample illumination, cause Coulomb screening of the wetting layer (WL) conductivity channel against the electrons coming from both the QDs and embedding InGaAs layers [1].

The PC degradation effect in the structure with $x = 0.31$ is found to be less pronounced, showing a long-term increase kinetics. This might be due to a higher density of the traps as revealed by TSC study. A significant fraction of these traps is suggested to be present not only around QDs; therefore, these traps can lead to the observed reduction of increase kinetics. With such a distribution of defects, it seems that the WL Coulomb screening is not effective.

These conclusions were supported by a theoretical simulation of the energy band profile of the system, including QD, WL and confining layers. Such model calculations were based on reliable experimental data coming from AFM and high-resolved TEM images.

[1]. S. Golovynskyi, et al., Defect influence on in-plane photocurrent of InAs/InGaAs quantum dot array: long-term electron trapping and Coulomb screening // Nanotechnology. – 2019. – V. 30. – N. 30. – 305701.

Wavelength Dependence of the Period of Surface Structures Induced by Harmonics of Ti:Sapphire Femtosecond Laser

E.S. Hrabovsky¹, I.M. Dmitruk¹, N.I. Berezovska¹,
A.M. Dmytruk², I.V. Blonskiy²

¹Physics Faculty, Taras Shevchenko National University of Kyiv, Kyiv, Ukraine

²Photon Processes Department, Institute of Physic, NAS of Ukraine, Kyiv, Ukraine

**Corresponding author: hrabovskye@gmail.com*

Laser induced periodic surface structures (LIPSS) attract attention due to the unique physical properties and simplicity, variability and precision of the surface treatment method. The ultrashort pulse laser processing of the surfaces of different materials provides various applications of modified surfaces in many fields. The laser processing parameters are crucial for certain characteristics of surface morphology, namely the periods of obtained quasi-gratings, the uniformity of structuring of large areas etc.

In present report we study the action of the fundamental frequency of a femtosecond laser and its higher harmonics (the second, the third) on the morphology, structure and physical properties of the surfaces of metals (tungsten, copper).

The morphology of surface structures formed under different harmonics of a Ti:Sapphire femtosecond laser (about 800 nm, 150 fs) on the surface of metals are studied with a SEM and laser light scattering.

The dependence of surface characteristics on the wavelength of laser processing could have practical usage for the formation of periodic structures of the desired repetition period – it is enough to use laser radiation with appropriate parameters. But special attention is required to distinguish the main LIPSS with period slightly smaller than laser wavelength from the other periodic structures with typically smaller periods. These additional structures are formed due to another mechanisms like capillary waves on the molten metal.

It was also noticed the formation of a smaller period structures as a result of splitting of the main bands at higher intensities of laser irradiation. It can be explained as a second harmonic generation on the surface or a nonlinearity of interaction of laser beam with the surface.

If we accept the interpretation of LIPSS as a result of interference of the incident wave and the surface plasmon-polariton wave the dependence of the LIPSS period on the wavelength of the laser radiation should reflect the dispersion curve of the surface plasmon polaritons. It can be compared with theoretically calculated one. Possible difference can be attributed to the change of electron density under band renormalization in the intense laser field.

The Use of Spectroscopy to Study Surfaces Modified by Ionic Implantation

D.Y. Nikolaieva¹, V.V. Honcharov^{*2}, V.O. Zazhigalov³

¹ Junior Academy of Sciences of Ukraine, Rubizhne, Ukraine

² Department of Medical and Biological Physics, Medical Informatics and Biostatistics, SE “Lugansk State Medical University”, Rubizhne, Ukraine

³ Department of Oxidative Heterogeneous-Catalytic Processes, Institute for Sorption and Problems of Endoecology of National Academy of Sciences of Ukraine, Kyiv, Ukraine

**Corresponding author: milostiprosim@i.ua*

Experimental spectroscopy is a remarkable method for studying thin films and modified layers.

Recently, applied systems and materials with modified surfaces have become topical. Ionic and plasma technologies are promising methods for producing such materials. One of these technologies is ionic implantation. This method allows to introduce target ions to a depth of 1 micron by imparting high energy to them. After bombardment, the surface significantly improves its physical, chemical and mechanical characteristics. At the same time, the material retains its shape, size, composition, etc.

However, when high-energy fluxes act on the surface, several processes occur, such as sputtering, terrain formation, structure compaction, etc. Therefore, by changing the parameters of implantation, it is possible to get different results on the surface of the material. In this case, qualitative and quantitative changes can be determined only by surface methods, in particular spectroscopic.

Thus, the combination of ionic implantation (as a method of influencing properties) and spectroscopy (as a research method) will allow to obtain nanoscale surfaces with specified characteristics. The use of computer modeling in this case will also make it possible to predict the properties or set the implantation mode.

XPS and XRD studies of implants obtained by varying the dose, processing geometry and other conditions were carried out. The structure and composition of the modified layers were studied. It is shown that the mechanical properties of the surface layer depend on the mode of implantation and the material of the target. The obtained results indicate the accuracy of this approach and the prospects of using these methods.

Investigation of the Characteristics of Nanoscale Steel Implant Layers

S.O. Kryvoruchko¹, A.O. Kryvoruchko¹, V.V. Honcharov^{*2},
V.O. Zazhigalov³

¹ Junior Academy of Sciences of Ukraine, Rubizhne, Ukraine

² Department of Medical and Biological Physics, Medical Informatics and Biostatistics, SE “Lugansk state medical university”, Rubizhne, Ukraine

³ Department of Oxidative Heterogeneous-Catalytic Processes, Institute for Sorption and Problems of Endoecology of National Academy of Sciences of Ukraine, Kyiv, Ukraine

**Corresponding author: milostiprosim@i.ua*

Research of materials with improved physical and chemical properties is a promising direction of modern science. Ion-beam surface treatment, in particular ionic implantation technology, has significant prospects for many methods (heat treatment, curing, metal treatment, plasma treatment) for improving the physical, chemical and mechanical properties of metals.

Ionic implantation is a method of introducing ions of high energy (10-2000 keV) into the surface layer of a material by bombarding its surface, thereby changing the physical, chemical, thermal, and others material characteristics. However, due to the small depth of penetration of ions they are difficult to explore. Therefore, some of the most effective ways to study implants are X-ray photoelectron spectroscopy, XRD of thin films, SEM and AFM. Since during the implantation a redistribution of charges in the surface layer occurs, there is an obvious expectation of a change in the electrical and thermal properties of the material.

In this work, we studied the synthesized implants on a steel foil support. It has been established that due to the implantation of nitrogen ions and metals, the roughness, microhardness, wettability, etc. change. Computer simulation has shown that the depth of the maximum concentration of implanted ions (the thickness of the modified layer) does not exceed 1 micron. This is evidenced by the results of the SEM. In this case, using X-ray spectroscopy, it was found that new compounds based on the embedded elements are formed in the modified material layer.

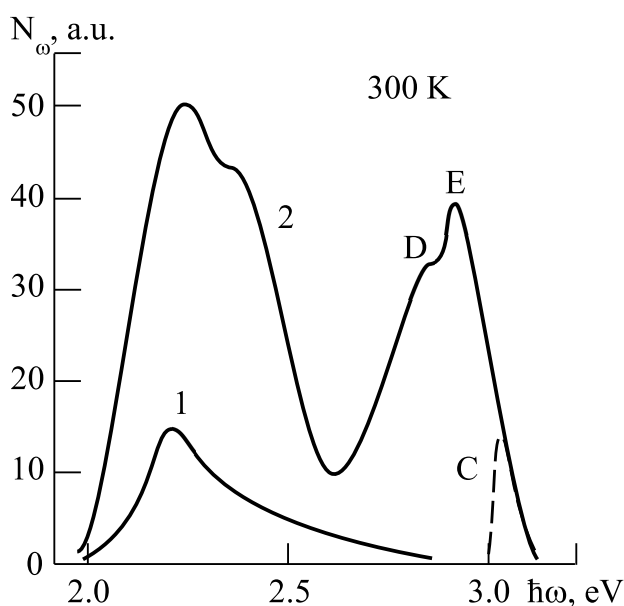
Luminescence of 6H-SiC:Te Diffusion Layers

V.P. Makhniy*, M.M. Berezovskiy, V.V. Melnyk,
V.M. Sklyarchuk, M.M. Slyotov

Yuriy Fedkovych Chernivtsi National University, Chernivtsi, Ukraine

e-mail: vpmakhniy@gmail.com

The polytypes 6H- and 4H-SiC were the semiconductors on the basis of which the first blue and violet injection LEDs were created in the 90s of the piston century and their serial production was adjusted. The low radiation efficiency characteristic of them, due to the indirect gap structure of hexagonal silicon carbide, in some cases can be compensated for by the high temporal stability of their parameters, especially when operating at elevated temperatures and ionizing radiation of various types. On the other hand, the considerable thermal and chemical resistance of all SiC polytypes cause certain technological difficulties in obtaining a material with the desired type and conductivity with a dominant edge radiation. In this work, the



luminescent properties of layers obtained by diffusion of titanium into single-crystal 6H-SiC substrates, manufactured by the Lely method with an electron concentration of $\sim 3 \cdot 10^{18} \text{ cm}^{-3}$, are analyzed. Their photoluminescence spectrum at 300 K is a wide asymmetric band with a maximum of about 2.2 eV, curve 1. In contrast to base substrates, 6H-SiC:Ti layers have weak hole conductivity, as evidenced by a change in the sign of the thermoelectric power. In the spectrum of their luminescence, an edge E-band also appears with a maximum

near 2.93 eV, curve 2. The dependence of the intensity I of this band on the level of excitation L obeys the law $I \sim L^{1.5}$, which is characteristic of the exciton recombination mechanism. Meanwhile, a sufficiently large half width indicates that it also includes the D-band (recombination on donor–acceptor pairs) and the C-band (interband transitions).

FTIR and Raman Investigations of the Si-C-N Films Deposited by Magnetron Sputtering

A.O. Kozak^{1*}, V.I. Ivashchenko¹, O.K. Porada¹, P.L. Scrynsky¹,
L.A. Ivashchenko¹, T.V. Tomila¹, V.S. Manzhara², O.M. Fesenko²

¹Institute for Problems of Materials Sciences, NAS of Ukraine, Kyiv, Ukraine

²Institute of Physics, NAS of Ukraine, Kyiv, Ukraine

*Corresponding author: andri.kozak@ipms.kiev.ua

Si-C-N films were deposited by DC magnetron sputtering the SiC target at different nitrogen flow rates (F_{N_2}) in the range of 0-20 sccm. The deposited films were studied by FTIR spectroscopy, Raman spectroscopy, X-ray diffraction and X-ray photoelectron spectroscopy. It was shown that all the deposited films were X-ray amorphous, whereas the Raman spectra indicate an existence of the crystalline nano-sized inclusions. The size of the inclusions strongly depends on F_{N_2} .

The Raman bands at 937 cm^{-1} and 1410 cm^{-1} that corresponds to LO Si-C and D (C-C) bands, respectively, were observed for the films deposited without nitrogen addition (Fig. 1 b). An addition of nitrogen ($F_{N_2} = 4\text{ sccm}$) promotes an increase of nitrogen in the films (up to 20 at. %) that is mostly bonded to silicon and less to carbon (Fig. 1a). These changes in chemical bonding promote an appearance of the additional Raman bands related to Si-N bonds at 425 cm^{-1} , 730 cm^{-1} and a reduction of the Si-C band. Any Raman bands were not revealed in the highly nitrogenated film in which the nitrogen content is equal to 22 at % due to large luminescence background, which is inherent to disordered carbon polymers containing a large amount of nitrogen [1]. The latter is confirmed by the results of FTIR measurements that clearly indicate the presence of the intensive $\text{C}\equiv\text{N}$ bonds at 2150 cm^{-1} only in the highly nitrogenated film (Fig. 1a). It follows that nitrogenation of the SiC films leads to their randomization due to the presence of a large number of different main bonds: Si-C, C-C, Si-N and $\text{C}\equiv\text{N}$.

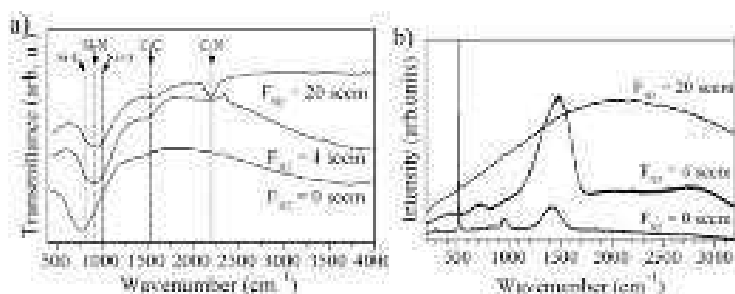


Fig. 1. FTIR (a) and Raman (b) spectra of deposited Si-C-N films

[1]. A.O. Kozak et.al. Structural, optoelectronic and mechanical properties of PECVD Si-C-N films: An effect of substrate bias // Mater. Sci. Semicond. Process. –2018.–V. 88.– p. 65–72.

Advances in Applications of Nanostructured Silicon as a New Multifunctional Material

M.M. Melnichenko^{*1}, K.V. Svezhentsova²

¹ Department of Physics, Taras Shevchenko National University of Kyiv, Kyiv, Ukraine

² Department of Physics and Technology of low-dimensional systems V.E. Lashkarev Institute of Semiconductor Physics NAS of Ukraine, Kyiv, Ukraine

**Corresponding author: realcrystallab@univ.kiev.ua*

For today silicon (monocrystalline, polycrystalline, amorphous, porous) is the main material of microelectronics and it presents a great interest for a new developing direction which is using a quantum size effects. The application of different modifications of silicon for creation of nano-electronics and nano-photonics devices put forward a number of innovative requirements for most processes and control methods during production of instruments and devices. Among the methods of obtaining nano-porous silicon layers the most common are: anodic electrolytic etching of single crystal silicon in the solutions based on the hydrofluoric acid application and chemical etching. The first allows a wide range of properties change of nanoporous silicon layers, but has some significant drawbacks, among them are: the complexity of communication with standard silicon technology, partial using of the area of the plate, the inability of mass processing. Chemical etching method makes it possible to grow thin films of nanostructured silicon and requires no special equipment; it is simple and high technological, which allows easy adaptation to the conditions of industrial production. The presented method of surface modification of single-crystal silicon by chemical etching makes it possible to obtain homogeneous nanostructured silicon layers with a thickness from 3 to 60 nm for application in micro- and nano-electronics as a new multifunctional material. These results could be applied to the creation of sensitive photodetectors for visible and ultraviolet diapasons. The method of scanning tunneling spectroscopy showed, that the changes of thickness of nanostructured silicon layers affects the type of conductivity, and it opens new perspectives for a practical application of nanostructured silicon in nano-electronics. The obtained current-voltage characteristics of nanostructured silicon layers showed different degree of filling of the valence band, the conduction band and the appearance on the curve of the tunneling conductance of the new peaks in the gas environment. The latter gives the possibility to use the method of scanning tunneling spectroscopy for generation of gas and bio sensors. The biosensor based on nanostructured silicon is very promising for use in so-called systems of lab-on-chip because it can be used for a rapid analysis of various immune responses and is fully compatible with silicon planar technology used in the manufacturing of the semiconductor devices.

Structure of Natural Film on Porous Silicon Surface by Ellipsometry

V.A. Odarych^{*}, L.V. Poperenko, I.V. Yurgelevych

Department of Physics, Taras Shevchenko National University of Kyiv, Kyiv, Ukraine

**Corresponding author: wladodarych@ukr.net*

Porous silicon (PC) is formed as a result of electrochemical etching of a monocrystalline silicon surface in an electrolyte based on an aqueous solution of HF with addition of acetone. The investigated sample is obtained by transmitting current with a surface density of $10 \text{ mA} \cdot \text{cm}^{-2}$ during 3 minutes. After the cessation of the current flow and getting of the sample from the electrolyte in the near-surface area of the PC the attenuation of electrochemical reactions involving atmospheric oxygen and possibly water vapor is observed. As a result of this aging process on the surface of the PC a film containing the remains of hollow pores, silicon oxides of various composition and unoxidized silicon is formed. Such films can be interesting as carriers of active impurities in biology and medicine, in gas and liquid sensors, etc.

In this paper the structure of such film is investigated and its optical characteristics are determined. The method of decorating of hollow pores was used for details of the film structure. The sample of the PC was maintained in isopropyl alcohol for 18 hours and then periodically with a certain interval ellipsometric parameters (EP) (a phase difference Δ and a ratio of the reflection coefficients $\text{tg}\psi$ in the p - and s -planes of the sample) were measured by laser ellipsometer LEF-3M-1 with a wavelength of 632.8 nm. The measurements were obtained in a wide area of the angles of incidence from 46 to 80°. The observations were carried out within 3 months.

It was found that as a result of the decoration, a strong maximum ($\text{tg}\psi \cong 18$) appears on the angular dependence of $\text{tg}\psi$ parameter. During the observation time the detected maximum has undergone some minor changes. Several models of the film were used to interpret the detected features of angular dependencies of EP. The film model best describes the experimental data according to that model in which the film has in its composition two layers. The outer layer that borders on the air has a refractive index of about 1.51, and the internal one that borders on the PC is 1.62. It was found that in the process of relaxation the ratio between the thicknesses and refractive indexes of the layers changes but the total thickness of the film remaining unchanged and equal to about 137 nm. The obtained values of the refractive index indicate that the film contains silicon dioxide, unoxidized silicon (protected by dioxide from oxidation) and empty pores which can be filled with extraneous agents, in particular, isopropyl alcohol.

Study of the Growth of Crystalline Oxide Structures on the Surface of Tungsten in the Air

S.G. Orlovskaya*, O.N. Zuy

I.I. Mechnikov's Odessa National University, Odessa, Ukraine

**Corresponding author: svetor25@gmail.com*

Tungsten oxides possess unique physicochemical properties and have great prospects for practical use as catalysts, gas sensors, energy coatings. Researchers are actively seeking effective methods for producing structured tungsten oxides that allow them to regulate their properties.

In this paper, studies of the laws governing the formation and growth of tungsten oxide crystals on the surface of a tungsten conductor heated by electric current in air are carried out. The studies were carried out using the "hot filament" method [1], which allows measuring the temperature of the sample and setting the required oxidation temperature. The study of the surface of the heated conductor showed that, at certain temperatures, threadlike crystals begin to appear on the surface of the main oxide, which thicken and later grow into branchy oxide structures (Fig. 1). With increasing temperature, the size of the crystals and their density on the metal surface increase. It is established that at first crystals grow more actively in the longitudinal direction, and then growth in the transverse direction prevails. In the future, the crystals overlap with each other side branches, their specific surface increases significantly. The study of the spectra showed that the oxide structures formed are mainly tungsten oxide WO_3 .

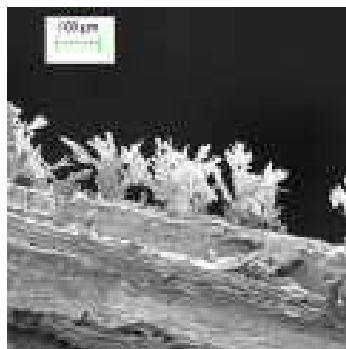


Fig. 1. The crystals on the surface of tungsten.

The effect of sample temperature on the size, shape, and density of crystals on the surface of tungsten was studied. It is shown that by setting a certain temperature regime, it is possible to regulate the properties of crystals. The growth rates of crystals in the process of their development are found. It is established that the average crystal growth rate is $0.5 \mu\text{m/s}$. A mechanism for the formation and growth of crystals on the surface of tungsten is proposed. It is shown that the shape of a tungsten conductor affects the density and growth rate of tungsten trioxide crystals.

- [1]. S.G. Orlovskaya, M.S. Shkoropado, F.F. Karimova. High-temperature oxidation and destruction of metal filaments in air// Ukr. J. Phys.- 2011.-V. 56, No. 12.- P. 1312-1315.

Interference of Ultrashort Radio Waves in a Two-layer Thin-film SystemI.A. Shaykevych¹, V.V. Lendel¹, L.Yu. Melnichenko^{*1}¹ Department of Physics, Taras Shevchenko National University of Kyiv, Kyiv, Ukraine**Corresponding author: lmeln@ukr.net*

Physical properties of electromagnetic waves of different ranges are subject to the same laws. Therefore, for the short-wave radio frequency range, it is possible to use well-known in optics of thin films the Airy formulas. In this paper, with the help of these formulas were considered the photometric properties of a massive aluminum mirror covered with a thin layer of polyethylene, onto which a thin film of aluminum was sputtered, for a wavelength of 1 cm radiowave. Thickness of a thin film of polyethylene and a thin aluminum film were subjected to variation. Formulas for optical conductivity and dielectric constant in the theory of free electrons were used to obtain the optical constant of aluminum, namely the refractive index n and the absorption index k for a wavelength of 1 cm. Electronic microcharacteristics for these formulas for aluminum were taken from the same source. On the basis of the obtained data, the refractive index of aluminum n for the length of the radio waves in 1 cm and the absorption coefficient k for the same wavelength were calculated mathematically. They were: $n = 2107$ and $k = 2211$. The fact that they are so great should not be a surprise, because in the far infrared region of the spectrum, they are also two orders of magnitude larger than in the visible spectrum. The refractive index for polyethylene was obtained from wellknown data on its transmission in the far infrared region of the spectrum. For the polyethylene, the refractive index for the wavelength of 0,06 cm in terms of data for transmission was $n=1,586$. Usually for a wavelength of 1 cm it is different, but, as calculations have shown, even a significant change in the refractive index of the polyethylene affects only the change in the thickness of its layer to save all other calculated system parameters, that is, the energy coefficient of reflection and the thickness of the aluminum film. Calculated on the basis of the data n and k , the energy coefficient of the reflection of a clean aluminum mirror at normal incidence of the radio waves on the mirror $R = 0,999$. Calculations for the aluminum mirror, covered by the two thin layers mentioned above, with the normal wave incidence, yielded the following results. For thickness of a thin layer of polyethylene 0,158 cm and thickness of a thin layer of aluminum 2×10^{-8} cm, the energy coefficient of reflection is minimal and is $R = 0,01$, that is 1%. This is several times smaller than in glass. When increasing the thickness of the aluminum film, it grows and at a thickness of this film in 10^{-5} cm actually coincides with the energy coefficient of the reflection of a clean aluminum mirror. Consequently, the considered system can be used for the invisibility of a massive aluminum object for a 1 cm radio wavelength.

8

Theory

Kinetic Energy of Electrons and Potential Energy of Atoms With an Open Electron Shell in the Basis of Slater Functions

A.I. Ahmadov*, F.G. Pashayev, D.B. Bairamova

Baku State University, Baku, Azerbaijan

Corresponding author: ahmadovazar@yahoo.com

In this work considers the calculation of the kinetic energy of electrons and the potential energy of atoms with an open electron shell. Calculations are carried out for the nitrogen N atom. Disregarding closed shells, the determinant wave functions, as in [1], can be represented as follows:

$$U = \frac{1}{\sqrt{7!}} \det \{ \dots (21m_l m_s) (21m'_l m'_s) (21m''_l m''_s) \} \quad (1)$$

When taking into account the "residual Coulomb interaction" between electrons, the degeneracy in the configuration is partially lifted and it splits into terms. The U_i atomic orbitals are represented as a linear combination of Slater functions

$$U_i = \sum_{q=1}^m C_{qi} \chi_q \quad (2)$$

The numerical values of the unknown coefficients C_{qi} are determined by solving the Hartree-Fock-Roothaan equations. Using the known determinant wave function, one can calculate the kinetic energy of electrons (\bar{T}) and the potential energy of an atom \bar{V}

$$\bar{T} = 2 \sum_{ipq} C_{pi}^* C_{qi}^* \int \chi_p^*(\vec{r}_1) \left[-\frac{1}{2} \nabla_1^2 \right] \chi_q(\vec{r}_1) dV_1 \quad (3)$$

$$\bar{V} = 2 \sum_{ipq} C_{pi}^* C_{qi}^* \int \chi_p^*(\vec{r}_1) \left[-\frac{Z}{r_1} \right] \chi_q(\vec{r}_1) dV_1 + \sum_{ijkl} \sum_{pqrs} C_{pi}^* C_{rk}^* C_{qi} C_{ql} (2A_{ij,kl} J_{pqrs} - B_{ij,kl} J_{pqrs}) \quad (4)$$

When obtaining formulas (3) and (4), we used the theorem on the calculation of matrix elements between determinant wave functions. Ways to calculate the coefficients, and are given in [1]. The atomic integrals appearing in (3) and (4) are easily calculated in the basis of the Slater functions. Based on formulas (3) - (4), computer programs were compiled and numerical values of the quantities (\bar{T}) and \bar{V} were calculated.

$$\bar{T} = 52,198602 \text{ a.u. and } \bar{V} = -106,440776 \text{ a.u.}$$

Calculations were carried out for the term. The reliability of the results obtained is verified by the virial theorem ($\bar{V} / \bar{T} = -2$) ($\bar{V} / \bar{T} = -2.03915$).

[1]. A.I. Ahmadov, F.G. Pashaev, D.B. Bairamova, A.G. Gasanov. Russian Physics Journal, vol.61, No. 10, p. 1848-1854 (2019).

Spectral Vibration-Electronic Concept of Structural Changes, Phase Transitions and Critical Phenomena

N.E. Kornienko, O.N. Korniiienko

Taras Shevchenko National University of Kiev, Kiev, Ukraine

Corresponding author: nikkorn@univ.kiev.ua

The crisis of science is manifested not only in the division of natural science into physics, chemistry, biology, medicine, etc. but also in the existence of only phenomenological theories of phase transitions (PT), as well as the insufficient use of a huge array of condensed matter (CM) spectroscopy data. We have created a nonlinear quantum concept (PT). It is established that the nature of the phase transition is associated with a number of new phenomena:

- 1) energy concentration (EC) at a special vibrational level as a result of nonlinear wave interactions (NWI) of vibrational modes,
- 2) strong vibrational-electron interaction (VEI), which leads to changes in electronic states (ES).

Spatial-temporal accumulation is characteristic of NWI; therefore, wave nonlinearity cannot be weak and plays an important role in nature. In the developed concept, the phonon discreteness of heats PT is of key importance. In H_2S and HBr , melting occurs when the librational modes $\nu_{\text{lib}} \approx 200 \text{ cm}^{-1}$ are excited, and in CO_2 , the deformation mode $\nu_8 = 660 \text{ cm}^{-1}$. The boiling of CO_2 and water occurs at the excitation of $2\nu_8$ and the stretching vibration ν_{OH} . When metals Mo and Ta are melted, the PT heat per \mathbf{Q}_1 atom corresponds to EC at high vibrational overtones $n h c \nu_{\text{max}}$, where $n = 10$ and 17 , and $h c \nu_{\text{max}} = k T_D$, T_D is Debye temperature. When the Si crystal melts, $Q_1 = 8 h c \nu_1$ ($\nu_1 = 520 \text{ cm}^{-1}$). In this case, Q_1 is much less than the work function A of an electron from metal or the width of the forbidden zone. Thus, high overtones with energy much lower than the binding energy control the change in the ES (strong VEI). It is proved that EC $\eta = n h c \nu_{\text{max}} / k T$ compared to $k T$ corresponds to changes in entropy ΔS ($\Delta S = \eta R$, $R = 8.31 \text{ J/(molK)}$). It is shown that for the set PT, it is actually $\eta = 2 \div 30$. The heats of structural transformations of solids are usually less than the melting heats and correspond to the frequencies of subharmonics and difference tones. The multiple ratios of the heat of boiling and melting for CO_2 , Cl_2 , CH_3COOH , and others, the correlation of the Q_1 values with the frequencies of the strong dipole modes in the IR spectra, as well as the discrete stages of the PT detected by us are significant confirmation of the spectral concept of the PT. When a substance is strongly excited in the critical region, instability of the uniform density distribution is manifested even at high pressures.

The Virtual Screening and Quantum Chemical Modeling for the Spectral Properties of π -Conjugation Systems

D.S. Stepaniuk^{1*}, M.A. Lanova¹, P.V. Trostyanko¹,
S.N. Kovalenko¹, O.N. Kalugin¹, V.V. Ivanov¹

¹ V. N. Karazin Kharkiv National University, School of Chemistry, Kharkiv, Ukraine

**Corresponding author: d.s.stepaniuk@gmail.com*

Screening of the libraries of molecules in order to identify the structures that would have given properties is extensively used in modern chemistry. Typically, this procedure is used to find "hits" - compounds that correspond to pharmacophores in the problem of finding structures with a certain bioactivity. In the present work, an attempt has been made to construct a systematic procedure for the selection of organic conjugated molecules which have necessary electronic structure parameters. Finding such compounds is a key element in a number of molecular electronics problems, for instance, in the development of dye-sensitized solar cells (DSSC). In such a case, the most important parameters are the wavelength of absorption band (λ , nm), the oscillator strength (f), the energies of high occupied and lowest unoccupied orbitals.

The present talk is devoted to finding of suitable for DSSC dyes. The library at our disposal contains about four thousand molecules, which are composed by different structural fragments, in various combinations. Among those fragments are oxazole, oxadiazole, coumarine, thiophene, furane, carbazole and other structures.

To identify the most suitable compounds, the preliminary semiempirical calculations have been performed. Among the semiempirical approaches the Pople-Pariser-Parr approach in combination with single-excited configuration interaction method (PPP/CIS) and full-valence AM1/ZINDO/S method. Such a preliminary analysis made it possible to identify the most promising systems. The subsequent (and more exact) calculations were performed by using TDDFT theory (B3LYP, CAM-B3LYP, M06-2X functionals). It is shown that, despite the significant differences in the theoretical foundations of approximate theories, even simplest models (PPP/CIS, ZINDO/S) provide an adequate result and guarantee effective screening of molecules. Comparison of the results obtained by B3LYP and other DFT functionals testifies a significant overestimation of λ in the B3LYP calculations for charge-transfer excitations. At the same time, the modified CAM-B3LYP as well as M06-2X functionals provide close to experimental data results.

Reconstruction of the Distribution Function of Implanted Ions on its Parameters

Ya.V. Choliy¹, M.V. Makarets^{1*}

¹Faculty of Physics, Taras Shevchenko National University of Kyiv, Kyiv, Ukraine

^{*}*Corresponding author: mmv@univ.kiev.ua*

Ion beams are an accurate tool for locally changing the properties of a solid after its irradiation. The distribution of stopped ions can be measured experimentally, or calculated as a solution of the kinetic equation, or modeled by the Monte Carlo method. Each of these methods has its advantages and disadvantages.

This paper proposes a method for reconstructing the distribution of ions on the depth of target, which uses its moments which are found from the kinetic equation. The exact implanted ions distribution according to [1] is:

$$\Pi(z) = \frac{1}{\pi \Delta \rho_p} \int_0^\infty \exp \left[-\frac{s^2}{2} + \frac{1}{4!} s^4 Ex - \frac{1}{6!} s^6 Ex_2 + \dots \right] \cos \left[s \frac{z - \rho_p}{\Delta \rho_p} - \frac{1}{3!} s^3 Sk + \frac{1}{5!} s^5 Sk_2 - \dots \right] ds, \quad (1)$$

where z – is depth, the parameters $\rho_p, \Delta \rho_p, Sk, Ex, Sk_2, Ex_2$ are connected with the moments of distribution [1]. The problem is that the series in (1) must be summed up in the form of such functions that, after integration, will give a positive bell-shape distribution. We have obtained the following distribution

$$\Pi_a(z) = \frac{1}{\pi \Delta \rho_p} \int_0^\infty \exp \left[-\frac{s^2}{2} \left(1 - \frac{16 Sk^2}{9 Ex} \right) - s \frac{64 Sk^3}{27 Ex^2} \arctan \left(s \frac{3 Ex}{8 Sk} \right) \right] \cos \left[s \frac{z - \rho_p}{\Delta \rho_p} + s \frac{32 Sk^3}{27 Ex^2} \ln \left(1 + s^2 \frac{9 Ex^2}{64 Sk^2} \right) \right] ds. \quad (2)$$

Its advantage is that it correctly describes the ion concentration measured in [2] in the range of 5 orders for strongly asymmetric distributions and are not known in the literature early.

- [1]. M.V. Makarets, Ya.V. Choliy. Equation for cumulants of fast ions spatial distribution // Visn. Kyiv Univ Tarasa Shevchenka. Ser. Fiz. – 2013 – N. 4. . – p. 815 – 820.
 [2]. Francois-Saint-Cyr H.G., Stevie F.A., McKinley J.M., et all. Diffusion of 18 elements implanted into thermally grown SiO₂ // J. Appl. Phys. – 2003. – V. 94. – N. 12. – p. 7433 – 7439.

Conductivity Effects of π -Conjugated System in External Electrostatic Field

V.V. Ivanov^{1*}, A.B. Zakharov¹

¹ School of Chemistry, V. N. Karazin Kharkiv National University, Kharkiv, Ukraine

*Corresponding author: vivanov@karazin.ua

Employment of π -conjugated systems for the molecular electronics purposes recently became the focus of multiple investigations. High technological attractiveness of electronic devices based on organic semiconductors is defined by the wide range of molecular properties that stems from the latter structure diversity. For the last decade special attention is paid to the conductivity effects in alternant and non-alternant hydrocarbons. Among them π -conjugated bicyclic compounds that attracts investigators are naphthalene and azulene molecules that is usually treated as the base for molecular field transistors.

In the present research we propose to use Coulson-Longuet-Higgins atom-atomic polarizabilities (AAP) as the parameter that describes electron conductivity effects:

$$\pi_{rs} = \frac{\partial \rho_r}{\partial h_s} = \frac{\partial^2 E}{\partial h_r \partial h_s}, \quad (1)$$

where ρ_r – electron density at r atomic orbital, $h_s = \langle s | H | s \rangle$ – coulomb integral for s orbital, E – energy of the system.

As the example the dependence of the π_{rs} on the value of external field intensity for azulene molecule with 2,6 junction computed within Huckel, and π -electron variants of Hartree-Fock (HF), coupled-cluster (CCSD), full configuration interaction (FCI) methods is given in Figure 1.

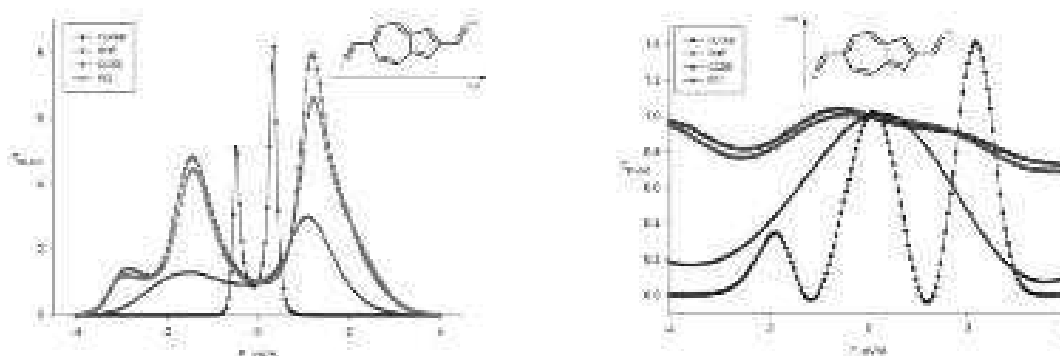


Fig. 1. Dependence of AAP on the strength of the external field.
(left - longitudinal, right - transverse)

As one can see the conductivity effects strongly depend on the external field. The importance of electron correlation effects was also demonstrated.

Influence of the Difference of the Scattering Potential of Impurity Atom and Carbon on the Energy Spectrum of Graphene

S.P. Repetsky¹, I.G. Vyshyvana¹, S.P. Kruchinin², R.M. Melnyk^{3*}

¹ Institute of High Technologies, Taras Shevchenko National University of Kiev, Ukraine

² Bogolyubov Institute for Theoretical Physics, NASU, Kiev, Ukraine

³ Physics and Mathematics Department, National University of “Kyiv-Mohyla Academy”, Kyiv, Ukraine

**Corresponding author: rmelnyk@ukr.net*

Graphene with introduced impurities became the basis of the latest functional materials. Quasirelativistic energy spectrum, which causes extremely high electron mobility, opens wide prospects for the use of graphene as a material for field transistors. However, the obstacle on this path is the absence of a gap in the energy spectrum of electrons. As recent studies have shown, the gap in the energy spectrum of graphene may occur under the influence of well-ordered impurities [1,2].

Within the single-band model, we performed numerical studies of the localization of impurity energy states, their influence on the width of the gap. For the small scattering potential, the slit parameters were obtained, depending on the values of the impurity density and the ordering parameter in the crystalline structure of graphene, identical with the theoretical calculations [2]. The complex dependence for large values of the difference between the scattering potentials of impurity atom and carbon atom is revealed. This is in the range of values not available for theoretical calculations, for types of impurities with high scattering potential. In the hypothetical case that only on one sublattice is the substitution of an atom of carbon by an impurity atom and the ordering parameter is equal to unit, width and position of the gap is proportional to the concentration of the impurity and the scattering potential. Such results coincide with the results in the case of small potentials. The disorder of the substitution atoms on the crystalline structure of graphene leads to the localization of the energy states inside the gap, decreases the width of the gap. At low concentrations of impurities, asymmetries of the localization of impurity states and of the density of energy states are manifested.

- [1]. S.P. Repetsky, I.G. Vyshyvana, S.P. Kruchinin, and S. Bellucci. Influence of the ordering of impurities on the appearance of an energy gap and on the electrical conductance of graphene // Scientific Reports, V. 8, 9123 (2018).
- [2]. S.P. Repetsky, I.G. Vyshyvana, S.P. Kruchinin, O.Y. Kuznetsova, R.M. Melnyk. Influence of the ordering of impurities on the energy spectrum and electrical conductance of graphene // Metallofiz. Noveishie Tekhnol., V.41, No. 4 (2019) (In Ukrainian).

Kramers – Kronig Relations in Femtosecond Optical Materials Research

V.S. Ovechko

Faculty of Radio Physics, Electronics and Computer Systems, Taras Shevchenko
National University of Kyiv, Kyiv, Ukraine

Corresponding author: ovs@univ.kiev.ua

Ninety two years have already been passed since prof. Kramers made a report, in which he formulated the dispersion relations for the real and imaginary parts of the dielectric susceptibility ($\chi(\omega)$). One year before Kramers Kronig (KK) obtained a relation for the refractive index $n(\omega)$ and $\alpha(\omega)$ – absorption coefficient. “On the one hand, the application of KK relations makes it possible to verify the values of optical characteristics for well – studied media. On the other hand it is necessary to develop the KK method itself in the theoretical sense” [1]. KK relations were proposed in order to ensure the implementation of the principle of causality for monochromatic optical fields. The latter is a consequence of the infinity of such fields in time.

We propose to investigate the propagation of femtosecond (fs) pulse in a medium with dispersion [2], in particular, the propagation of the so-called “forerunner” with the light velocity in a vacuum. The latter situation essentially reproduces the principle of causality. The implementation of the proposed method allows us to obtain the integral relations between Sin – and Cos –Fourier components of the fs – pulse and $n(\omega)$, $\alpha(\omega)$. Thus, the spectral characteristics of probe optical pulses are taken into account in the KK–relations.

- [1]. M.I. Kozak, V.N. Zhikharev, P.P. Puga, V.Yu. Loya. The Kramers – Kronig Relations: Validation via Calculation Technique // IJSET – 2017.–V4.–Issue12.–p.152–159.
- [2]. V.S. Ovechko, V.P. Myhashko. Spectral particularities of fs -pulses propagating in dispersive medium. // Ukr. J. Phys.- 2018.- Vol.63,- No. 6, - p.479–487.

Testing Anharmonicity of the H-F Vibrations in the Hydrogen Fluoride Dimer Using DFT Methods Including Dispersion Interaction

G.A. Pitsevich^{*1}, A.E. Malevich¹, I.Yu. Doroshenko², V.E. Pogorelov²

¹ Department of Physical Optics, Belarusian State University, Minsk, Belarus

² Experimental Physics Department, Taras Shevchenko National University of Kyiv, Ukraine

**Corresponding author: pitsevich@bsu.by*

The H-bonded systems were in focus of our interest for a long time [1-5]. This work allows us to make some general conclusions about the shape of the potential energy surfaces of clusters and complexes with hydrogen bonds of various strengths [6]. In this study the H---F hydrogen bond in the hydrogen fluoride dimer was analyzed using various DFT methods with and without including dispersion interaction. The hydrogen fluoride dimer geometry optimization was performed at the B3LYP/acc-pVQZ level of theory. Then the IR spectrum was calculated in harmonic and anharmonic approximations. To calculate 3D PES the center of the Cartesian coordinates system was moved on the H-bonded hydrogen atom. The X-axis was directed along donor hydrogen fluoride molecule. Y-axis was placed in dimer plane and Z-axis was directed perpendicular to the dimer plane. We use the Cartesian coordinates of the H-bonded hydrogen atom as a vibrational coordinates leaving all other atoms fixed in its equilibrium positions. These coordinates were varying in following intervals $-0.4 \leq X \leq 0.6$; $-0.8 \leq Y \leq 0.8$; $-0.8 \leq Z \leq 0$. In doing so the potential energy was calculated in $11 \cdot 17 \cdot 9 = 1683$ points. Using symmetry property $U(X, Y, Z) = U(X, Y, -Z)$ due to symmetry plane the number of the points where the potential energy was calculated was increased up to 3179. The 3D vibrational Schrödinger equation was solved using DVR method. The frequencies of the H-bonded H-F molecule were found. The comparison with data obtained in paper [6] was made.

- [1]. I. Doroshenko, V. Pogorelov, G. Pitsevich, V. Sablinskas. Cluster structure of liquid alcohols: vibrational spectroscopy study. – LAP LAMBERT Academic Publishing, Saarbrücken, Germany. - 2012. – 288 p. (in Russian).
- [2]. G. Pitsevich, A. Malevich, I. Doroshenko, E. Kozlovskaya, V. Pogorelov, V. Sablinskas, V. Balevicius. // Spectrochim. Acta Part A. – 2014. – V. 120. – p. 585–594.
- [3]. G. Pitsevich, A. Malevich, E. Kozlovskaya, I. Doroshenko, V. Pogorelov, V. Sablinskas, V. Balevicius. // Spectrochim. Acta Part A. – 2015. – V. 145. – p. 384–393.
- [4]. G. Pitsevich, A. Malevich, E. Kozlovskaya, I. Doroshenko, V. Sablinskas, V. Pogorelov, D. Dovgal, V. Balevicius. // Vib.Spectr. – 2015. – V. 79. – p. 67–75.
- [5]. G. Pitsevich, A. Malevich, E. Kozlovskaya, E. Mahnach, I. Doroshenko, V. Pogorelov, L.G.M. Pettersson, V. Sablinskas, V. Balevicius. // J. Phys. Chem. – 2017. – V. 121. – p. 2151–2165.
- [6]. E. Kozlovskaya, I. Doroshenko, V. Pogorelov, Ye. Vaskivskyi, G. Pitsevich. // J. Appl. Spectr. – 2018. – V. 84. – p. 929–938.

The Wannier-Mott Exciton's Dynamic Properties without Limitations on the Magnitudes of the Wave Vectors of Carriers

L.V. Shmeleva^{*1}, A.D. Suprun¹

¹ Department of Theoretical Physics, Faculty of Physics, Taras Shevchenko National University of Kyiv, Ukraine

Corresponding author: lshmel@univ.kiev.ua

Excitons are one of the means of energy, signal or charge transfer. The Wannier-Mott excitons deserve special attention. They have the internal structure of the hydrogen-like type and have additional capabilities for controlling the transfer processes. In addition, in the case of the soliton response of the crystal lattice to excitation, the transfer of information (internal degrees of freedom) can be realized.

The principal mechanism of exciton transport is acceleration in external fields. In the deformation stress fields, in particular. And the possibility of such acceleration is due to the long lifetime of the exciton. In Germany, for example, under conditions of an ideal crystal, the lifetime of an exciton is 10 μ s, and when ideality is violated (due to a stress field, for example) it rises. During acceleration, the wave vector \mathbf{k} of the dynamics of an exciton changes.

The question of the influence of the magnitude of this vector's components on the analogous characteristics κ of the dynamics of the internal relative motion of an electron and hole has not been studied practically. Here this question is considered: the dependence of κ on \mathbf{k} . Wherein, there were no restrictions on the magnitude of the wave vector \mathbf{k} in the domain of unambiguous ($0 \leq |\mathbf{k}| \leq \pi/2$) (dimensionless representations are used). It is shown that as the components of the wave vector \mathbf{k} change in this region, the components of the wave vector κ vary within $0 \leq |\kappa| \leq \pi/20$. This affects the magnitude of the components of the effective mass, since they are determined by the factors $1/\cos(\chi_\alpha k_\alpha \pm \kappa_\alpha)$. Here, the signs correspond to each of the carriers (plus to the electron, minus to the hole), and the factors χ_α are determined by the ratio of the band width. Obviously, during acceleration of an exciton (for example, in a stress field) the effective masses change. Such changes lead to a significant shift of the exciton spectrum, which depends on the reduced mass of the carriers. An estimate of the maximum possible magnitude of such an offset was made. It is suggested that the insignificant differences which it is observed in the position of these spectra may be due to the fields of dislocations and indirectly indicate their concentration.

9

Methods and Applications

Thin Spin-Dependent Splitting of Electronic Excitations and Their Dispersion in Single-Layered Graphene and Graphite

V.O. Gubanov^{*}, A.P. Naumenko, I.S. Dotsenko, M.M. Biliy, M.M. Sabov

Faculty of Physics, Taras Shevchenko University of Kyiv, Kyiv, Ukraine

^{*}*Corresponding author: vagubanov46@gmail.com*

The projective two-valued representations of spinor states for different points of Brollouin zones of single-layered graphene and crystalline graphite have been constructed for the first time.

For the first time, projective classes, which transform spin-dependent electronic wave functions at the points of high symmetry of the Brillouin zone have been determined for the above-mentioned structures. For the establishment of projective classes, for the first time, we found the method of constructing of factor systems, in particular, the correct factor system for spinor representations; the form of standard factor systems and the coefficients of their summing up to the standard for each projective class have been found.

The dispersion of the electronic states of these structures has been investigated by using the symmetric theoretical group methods. Taking into account the symmetry to inversion of time, compulsory spin-dependent finite splitting of electron energy spectra of graphene and crystalline graphite at different points of their Brillouin zones have been found.

It is shown that the results of the developed methods of theoretical-group analysis are consistent with the data of experimental and computational studies of energy spectra and multiplicities of degeneration of quantum states of π -electron graphene zones and crystalline graphite.

The results of the work can also be used to study the energy spectra of elementary excitations in magnetic structures, the spatial symmetry of which is described by Shubnikov groups of magnetic symmetry.

Wide-Field Second Harmonic Generation Microscopy Using a High Power Medium Pulse Repetition Rate Laser

D. Rutkauskas

Molecular Compounds Physics, Center for Physical Sciences and Technology,
Vilnius, Lithuania

**Corresponding author: danielis@ar.fi.lt*

A wide-field second harmonic generation (SHG) microscope was realized for fast imaging of large areas of histological samples using a high power medium pulse repetition rate femtosecond laser. Compared to a conventional scanning laser microscope our implementation circumvents the complexities of the scanning process and also offers a potential of faster image acquisition with sub-wavelength resolution due to parallelized data collection with a two-dimensional rather than point detection device. The function of Z-sectioning that is intrinsic to confocal but is lacking in the wide-field configuration was realized by utilizing the principle of the temporal focusing [1] resulting in the 5 μm fwhm of the excitation profile along the optical axis. The demonstrated speed of acquisition and ease of operation are thought to be important assets for intended applications of express *ex-vivo* cancer diagnosis and other modes of histological analysis.

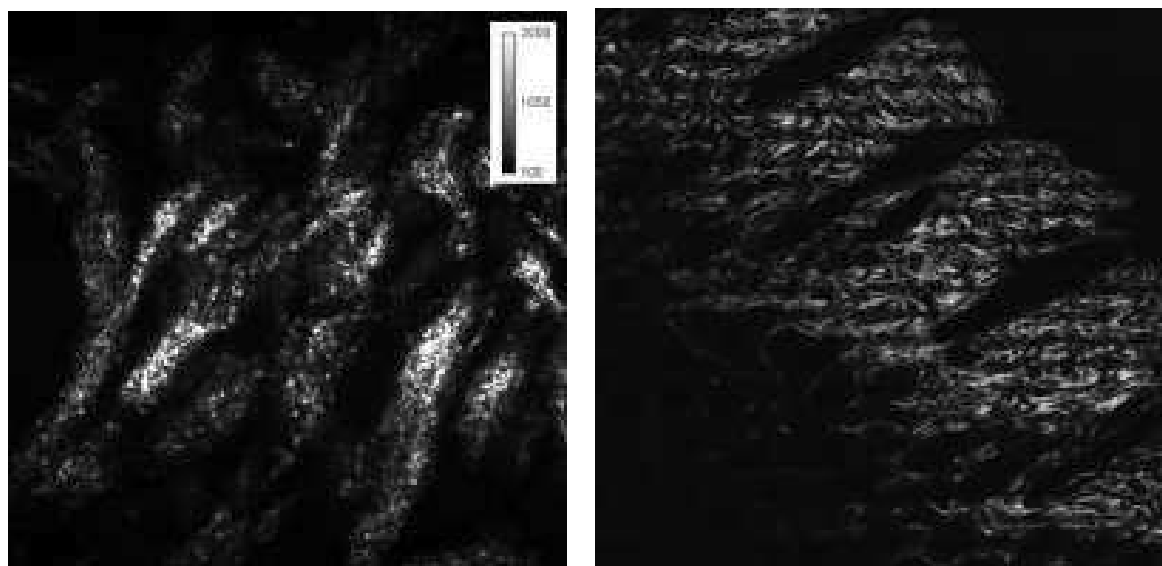


Fig. 1. SHG images of a mouse skin sample. A single field of view of $\sim 75 \times 75 \mu\text{m}^2$ sample area on the left. A tiled image of $\sim 1 \text{ mm}^2$ sample area on the right.

[1]. Dan Oron, Eran Tal and Yaron Silberberg. Scanningless depth-resolved microscopy // Optics Express. – 2005. – V. 13 – p. 1468-1476.

Steady State and Time-Resolved Fluorescence Studies of a Series of Modified 3-(2-Pyridyl)-1,2,4-Triazoles

S.S. Smola^{*1}, N.V. Rusakova¹, B.V. Zakharchenko²,
D.M. Khomenko², R.D. Lampeka²

¹ Department of Chemistry of Lanthanides, A.V. Bogatsky Physico-Chemical Institute of the NAS of Ukraine, Odessa, Ukraine

² Department of Chemistry, Kyiv National Taras Shevchenko University, Kyiv, Ukraine

**Corresponding author: sssmola@gmail.com*

The studies of the 1,2,4-triazole derivatives are intensified recently due to the possible application in the luminescent marking of biomolecules (primarily DNA structures) and chemosensors for the determination of metal ions, pH and polarity of the microenvironment, which allows to detect biochemical changes. These studies are based on their structural features and unique spectral characteristics. The absorption, internal and intermolecular energy transfer and emission processes in these systems are determined by their structural factors, in particular the introduction of functional groups whose influence is explained by several factors. First, the electron-donating or acceptor properties of the substituents that affect the π -conjugated ligand system as a whole. Second, the steric factors affecting the conformation of the ligand and its complexing properties.

The spectral-luminescent properties of a series of 3-(2-pyridyl)-1,2,4-triazole derivatives (Fig. 1), which may be promising "building blocks" for photometric and fluorescent chemosensors on metal cations, anions, or biologically active molecules, are investigated in this work. The compounds contain a pyridine protector in 5-position, which greatly enhances the emission properties of the compounds, and conducting substituents in the triazole ring is a suitable model for establishing the relationship between electronic substitution effects and absorption and radiation properties. The presence and quantity of tautomeric forms of substituted triazoles in chloroform and DMSO solutions at different concentrations was estimated using the TCSPC technique.

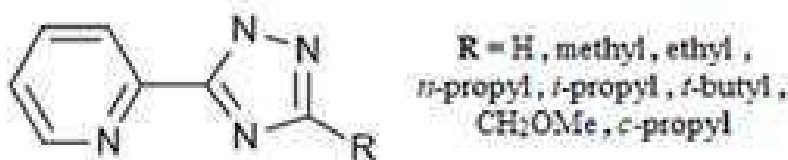


Fig. 1. Structure of 3-(2-pyridyl)-1,2,4-triazoles and excitation and emission spectra of ethyl-substituted compound in CHCl₃

Light Scattering in Glycerol under the Action of a Constant Magnetic Field and UV radiation

L.Yu. Vergun

Taras Shevchenko National University of Kyiv, Ukraine

Corresponding author: verlen73@ukr.net

Research on molecular mechanisms in glycerol under the influence of external factors can be used for development and improvement liquid fillers for liquid lenses [1]. It was shown that the presence of a constant magnetic field and UV-waves stabilizes the formation of a wall layer and the vibrational and rotary motions of molecules and its clusters. To continue studying this question the coefficients of light scattering of glycerol that was in the UV-irradiation zone, in the zone of the action of a constant magnetic field and in the zone of the action of a constant magnetic field and UV radiation were determined. The value of constant magnetic field is 22.4mT. Fig. 1 shows the results of the experiments. For comparison, the coefficient of light scattering ξ of raw glycerol is also given.

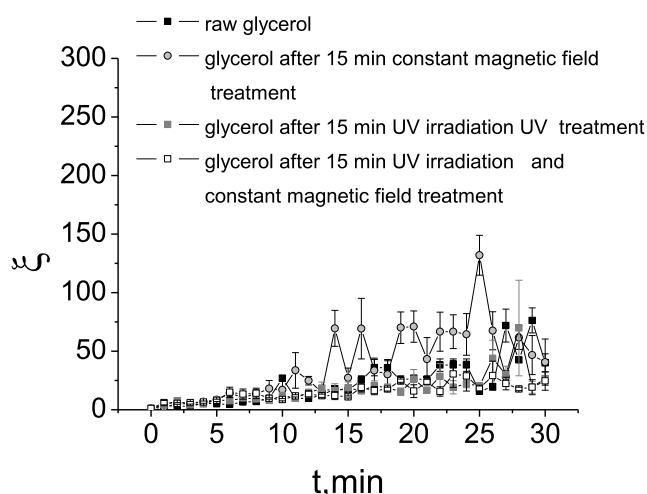


Fig. 1. Time-dependence of ξ

As can be seen from Fig. 1, the minimum fluctuations of concentrations are observed in the system after the treatment of glycerol with a constant magnetic field and UV radiation. The established fact confirms the studies performed in [1] on the stabilization of the wall layer between the liquid filler and the solid wall and ensuring a uniform location of the molecules and clusters in the system.

[1]. Liena Yu. Vergun. The Influence of the Magnetic Field and Ultraviolet Waves to the Liquid Fillers for Liquid Lense. Journal of Electrical Engineering 5 (2017) 349-351.

Possibilities of SRS-RL effect usage in Raman spectroscopy

V.P. Yashchuk

Department of Physics, Taras Shevchenko National University of Kyiv, Ukraine

Corresponding author: yavasil@ukr.net

Stimulated Raman scattering (SRS) and random lasing (RL) of lasing dyes interact closely in strongly scattering media (SSM) and occur as coupled phenomenon SRS-RL. This coupling introduces specific features into SRS phenomena. The main one of them is appearance of all molecule vibrations whose Stokes lines of Raman scattering find itself in the RL spectrum range. RL radiation promotes SRS occurring what contrasts to spontaneous Raman scattering which radiation is masked by their own luminescent radiation. SRS-RL phenomenon may be considered as specific CARS, where RL radiation is one component of bicomponent pump with continuous spectrum. Second one is laser monochromatic pump. Together their forms driving force which resonates with molecule vibration of all Raman frequencies within spectral range of RL. This phenomenon may be described with the system of two coupled equations for RL and SRS emission yielding expression for the SRS-RL spectrum, which may be used for vibration spectrum (VS) determination [1]. The procedure includes separation of continuous component of the SRS-RL spectrum (conditioned by RL) and linear one conditioned by SRS and mathematical manipulation with them. The resulting contour is proportional to the SRS nonlinear susceptibility $\chi^{(3)}$.

We developed iterative algorithm of SRS-RL spectrum decomposition which uses averaging of $\chi^{(3)}$. The algorithm processes the batch of initial $\{I_{SRS-RL}^n(\omega)\}$ spectra regardless of pumping intensity and other experimental factors. Vibration spectrum from each spectrum $I_{SRS-RL}^n(\omega)$ was determined as cubic nonlinear susceptibility $\chi_{SRS}^{(3)}(\omega) \sim \ln\left(\frac{I_{SRS-RL}^n(\omega)}{\widetilde{I}_{RL}(\omega)_i^n}\right)$ where $\widetilde{I}_{RL}(\omega)_i^n$ is RL spectrum calculated from initial SRS-RL spectrum and averaged susceptibility $\langle\chi_{SRS}^{(3)}(\omega)\rangle_i$ on i-th iteration to be continued until convergence. The algorithm was successfully tested with a set of SRS-RL spectra of dyes rodamine 6G and pyrromethene Pm597 in vesicular polymeric film.

Shape of the contour of the SRS lines is similar to CARS signal having a sharp dip on the wing of a Raman line, which «tones» it off on one side and increases the spectral resolution. This feature originated from interference between SRS and RL emission. Spectral range of Stokes lines detections may be controlled by the parameters influencing spectral position and width of RL spectrum. Such parameters are dye concentration and temperature. Last experiments have shown that these parameters may be managed effectively also by usage of additional dye whose RL radiation may initiates SRS of investigated dye.

[1]. Vasil P.Yashchuk, E.A Tikhonov, A.O.Bukatar et al., Quant. electronics, 41, No10, pp.875-880 (2011).

Influence of Bulk Multiple Scattering and Diffuse Reflection at Sample Boundaries on Random Lasing

V.P. Yashchuk^{1*}, M.V. Zuravskiy¹, O.A. Pryhodiuk¹

¹ Physics Department, Taras Shevchenko National University of Kyiv, Kyiv, Ukraine

**Corresponding author: yavasil@ukr.net*

The multiply scattered luminescent media where the specific type of positive feedback can be formed are of great interest for investigation due to their possible practical use. The positive feedback results in specific stimulated emission regime which results in random lasing (RL). The wide variety of the theoretical investigation was carried out for unbounded media and the influence of the light reflection at the medium boundaries is out of consideration. Nevertheless, the boundary reflection in those media is influential phenomenon that significantly effects photon lifetime within the active medium [1].

The work is devoted to the theoretical calculation of random lasing simulation by Monte-Carlo method and computing RL characteristics depending on the parameters of multiply scattering active medium. The influence of boundary reflection both on the pump and emission propagation was explored.

It was founded that within active medium the region of high photon density concentration is formed. Boundary reflection participates in photon distribution, RL formation and RL emergent energy equally with multiple scattering itself. The influence is significantly dependent on the sample thickness: the radiation energy increases under the thickness lowering. Influencing the RL efficiency via the medium thickness is increased by boundary reflection.

The result of this Monte-Carlo simulation is proved by experimental study of RL of rhodamine 6G in concentrated suspension silica microparticles in polyvinyl acetate matrix. It was testified that RL radiation energy increases under sample thinning to defined specific value.

The obtained results allow concluding the RL efficiency can be increased by manipulation of the sample thickness and diffusive reflection at the sample's borders. Practically the boundary reflection efficiency can be varied by the sample covering with diffusively scattering shell of dielectric particles.

[1]. V.P. Yashchuk, O.A. Prygodjuk, E.O. Tikhonov. Nonresonant feedback formation in the random laser// DOI: 10.1364/ASSP.2005.WB19 – 2005.

[2]. V.P. Yashchuk, M.V. Zhuravsky, O.A. Prygodjuk, Modelling and computing of random lasing dynamics// DOI:10.1109/LFNM.2011.6145037 – 2011 – p. 169 – 171.

Practical Problems in the Design of a Luminescent Converter for Si Solar Cells

V. Azovskyi*, V. Yashchuk

Department of Physics, Taras Shevchenko National University of Kyiv, Ukraine

*Corresponding author: vladimirazovskij@gmail.com

Remaining 67% of incident solar energy at the Earth surface (under AM1.5) not undergo photovoltaic conversion in Si Solar cells (SC). Si SC have both rapid shortwave and longwave decrease in sensitive characteristics. Spectral response of mono-Si solar cell increases with wavelength in the range of 400-890 nm with maximum at 890 nm, beyond this maximum decreased rapidly and found minimum at the wavelengths less than 400 nm and more than 1100 nm.[1] That is why the realization of efficient UV-to-Vis and NIR-to-Vis conversion has a huge potential in photovoltaics. In order to fix losses, it proposed to use luminescent converter, based on dyes sensitized polymers. For down conversion it is possible to make optically passive luminescent layer on the solar cell front surface. For the up-conversion the triplet-triplet annihilation process is possible at the back surface. Frenkel excitons, which are generated by the absorbed Solar light, transport excitation energy to molecular traps emitting light in the maximum spectral sensitivity of the solar cell in proposed luminescent converters or transformers. Applying of the luminescent converter does not change the design of the solar cell, but it increases its spectral sensitivity, which makes this technology a promising direction for commercial application.

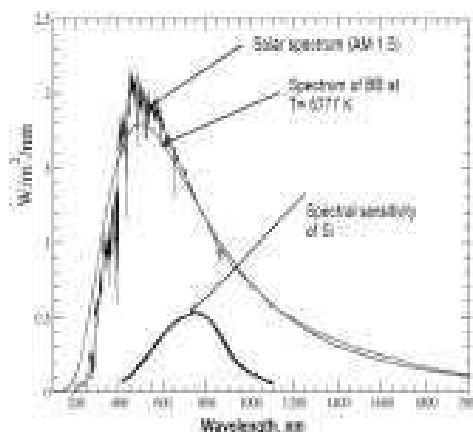


Fig. 1. Comparison of Sun spectrum, Spectrum of Black Body (BB) and Spectral sensitivity of Si.

- [1]. S. Chander & A. Purohit & A. Nehra. et al. Spectral Response and External Quantum Efficiency of Mono-Crystalline Silicon Solar Cell // International Journal of Renewable Energy Research-IJRER. – 2015. – V. 5. – N. 1. p.41–44.

Laser Diode Spectra and Intensity vs Temperature: Some Examples

S. Baschenko*, L. Marchenko, A. Negriyko,
I. Matsnev, V. Khodakovskiy

Institute of Physics, NASU, Kyiv, Ukraine

**Corresponding author: smbashchenko@gmail.com*

The dependences of the wavelength and the intensity of the radiation of laser diodes on their temperature are known from the general theory of semiconductor compounds of the type A_3B_5 . For laser diodes of different manufacturers, these dependencies may differ. Using the example of three high-power laser diodes (Northrop Grumman of the Silver Bullet type $P=20$ watts, Semiconductor Instruments Ltd ATC-Q $P=250$ watts and Jenoptik JPLD-x-QPNN $P=300$ watts), the dependences of the wavelength and radiation intensity on their temperature were simultaneously measured. The dependences obtained demonstrate the strict need to take them into account when designing pump modules. It is suggested to change (amplify) this dependence on the service life of high-power laser diodes.

Mie Scattering Correction for Fourier Transform Infrared Spectroscopy of Cells and Tissues

E. Gunko^{*1}, J.H. Solheim², D. Petersen³, F. Großerüschkamp³,
K. Gerwert³, A. Kohler², V. Skakun¹

¹ Faculty of Radiophysics and Computer Technologies, Department of System Analysis and Computer Modeling, Belarusian State University, Minsk, Belarus

² Norway Faculty of Science and Technology, Norwegian University of Life Sciences, Ås, Norway

³ Department of Biophysics and Protein Research Unit within Europe, Ruhr University Bochum, Bochum, Germany

**Corresponding author: eg.9393@gmail.com*

Strong scattering effects appear when the wavelength of the electromagnetic radiation used in a spectroscopic method matches the size of the measured sample. When the scatterer has a spherical shape, these scatter effects have been explained as Mie-type scattering [1], when parallel surfaces of materials are involved, so-called fringes are strongly distorting infrared spectra [2]. Scattering effects have been considered as a major obstacle for the interpretation and further use of spectra from infrared microscopy. In addition to scattering effects, other unwanted effects such as water and water vapor variations appear in the infrared spectroscopy of biological materials. During the recent years algorithms for separating and correcting Mie-type scattering in infrared microspectroscopy [3-6] were developed. These algorithms based on extensions of the Extended Multiplicative Signal Correction. Many of the current applications of infrared spectroscopy in biological sciences use imaging techniques. In infrared imaging, enormous amounts of spectral data are collected that must be corrected and analyzed.

- [1]. Mohlenhoff B, Romeo M, Wood BR, Diem M: Mie-type scattering and non-Beer–Lambert absorption behaviour of human cells in infrared micro-spectroscopy. *Biophys J* 2005, 88:3635–3640.
- [2]. Konevskikh T, Ponomosov A, Blumel R, Lukacs R, Kohler A: Fringes in FTIR spectroscopy revisited: understanding and modelling fringes in infrared spectroscopy of thin films. *Analyst* 2015, 140:3969-3980.
- [3]. Kohler A, Sule-Suso J, Sockalingum GD, Tobin M, Bahrami F, Yang Y, Pijanka J, Dumas P, Cotte M, van Pittius DG, et al: Estimating and correcting Mie scattering in synchrotron-based microscopic Fourier transform infrared spectra by extended multiplicative signal correction. *Applied Spectroscopy* 2008, 62:259-266.
- [4]. Bassan P, Kohler A, Martens H, Lee J, Byrne HJ, Dumas P, Gazi E, Brown M, Clarke N, Gardner P: Resonant Mie Scattering (RMieS) correction of infrared spectra from highly scattering biological samples. *Analyst* 2010, 135:268-277.
- [5]. Konevskikh T, Lukacs R, Blumel R, Ponomosov A, Kohler A: Mie scatter corrections in single cell infrared microspectroscopy. *Faraday Discussions* 2016, 187:235-257.
- [6]. Johanne Solheim, Evgeniy Gunko, Dennis Petersen, Frederik Groß erüschkamp, Klaus Gerwert, Achim Kohler “An open source code for Mie Extinction EMSC for infrared microscopy spectra of cells and tissues”, *Journal of Biophotonics* 2019-02-21.

The Combined Effect of Ultraviolet Radiation and Ozone in Disinfecting Pool Water

A.A. Semenov*¹, G.M. Kozhushko¹, T.V. Sakhno^{1,2}, I.V. Korotkova²

¹ Poltava University Economy and Trade, Poltava, Ukraine

² Poltava State Agrarian Academy, Poltava, Ukraine

**Corresponding author: a semen2015@gmail.com*

Operation of pools requires a complex of measures for filtering and disinfection of water [1, 2]. An extremely urgent task when disinfecting water in swimming pools is the use of UV-technologies, which completely eliminate pathogenic microflora and do not result in formation in the process of decontamination of toxic compounds. Bacteriological studies of water in the pool found that ultraviolet decontamination does not meet the requirements of the general microbiological number of CU/cm³, because no after effect radiation. Additional ozonation with the use of UV-disinfection technology can provide the necessary bacteriological purity of water in the pools of small volumes.

The device for the complex disinfection of water in pools by UV irradiation and with the use of ozone produced by low-pressure discharge lamps of this device is developed. [3].

The study of the effectiveness of bactericidal decontamination of water using the installation was carried out in a pool of 75 m³. This installation provides a dose of irradiation of water not less than 25 J/m² and additional ozonation with an amount of ozone of approximately 0.1 g/m³ of water. In order to ensure circulation of water, at least 4 times the exchange, two sets of capacity of 8 m³/h were installed per day. At additional ozonation, the microbiological number does not exceed 20 CFU/cm³. Additional ozonation (with a dose of 0.1 g/m³) using the UV technology of disinfection of water provides the necessary bacteriological purity of water in small pools, while the residual concentration of ozone in water does not exceed 0.015 mg/l.

- [1]. DIN 19643-1. Chemical preparation of water for swimming and bathing pools. Part 1: General Requirements
- [2]. SanPiN 2.1.2.568-96. Hygienic requirements for the device, operation and water quality of swimming pools. Sanitary rules and regulations.
- [3]. Semenov A., Kozhushko G., Sakhno T. Bactericidal disinfection of water in pools with complex action of ozone and UV radiation Scientific and technical collection // Urban management of cities. Series: Engineering Sciences and Architecture, 2018, 7 (146) 264-270.

The Near Resonant Spectral Line Shape of Pumped High Density Atomic Vapor Coupled with Two Laser Beams

A.S. Sizhuk*

Taras Shevchenko National University of Kyiv, Ukraine

**Corresponding author: andrii.sizhuk@gmail.com*

The absorption line shape for the system of strongly pumped interacting two-level atoms is discussed. Using the analytical expressions for the macroscopic absorption coefficient, previously derived in the kinetic limit, the probe absorption profiles were obtained for the model system. It was discovered the model of the vapor of sodium atoms pumped near resonant transition. Contribution from different effects is analyzed using the additivity of the corresponding absorption/reemission rates. It was shown for the quantum field induced long-range interaction, prevailing over short-range collisions, that the broadening, narrowing, and shifts of an absorption line shape can be explained in the terms of interaction integral, coupling the collective atomic polarization and population inversion. The existence of the threshold value (transition to the gain mode), the extreme value (maximum) of emission and the critical transit point from emission to absorption are theoretically explained. The built dependence of absorption coefficient on probe detuning and density of atoms allowed to interpret the experimentally observed gain threshold by means of the interaction integral and predict the qualitatively new behavior of pumped atomic vapor.

Design of the Device for Improving Vein Blood Circulation with Electrical Current and Mechanical Pressure

M.A. Terentyev

Physics Department, Taras Shevchenko National University of Kyiv, Ukraine

Corresponding author: teren.maxim@gmail.com

It is known that venous blood may move only due to a small difference in pressure between the venous environment and the right atrium. The movement of venous blood through the extremities is particularly difficult because it needs to move against the force of gravity. It turns out that a huge role in venous blood flow is played by the so-called reverse valves [1], which are located inside the veins. Thanks to them, venous blood, at any compression of the muscles, that is, the veins, moves only toward the heart. For initial research, we produced a simple device, similar to the "amplipulse" system [2], and investigated its effect on the limb muscles by applying a constant voltage to the electrodes located on different sides of the limb, in contrast to the "amplipulse" system, where they are located adjacent. Having conducted experimental research:

1) It is determined that the optimal voltage for an electric, painless limb effect is about $20 \pm \Delta U$ V, which varies depending on the thickness of the limb and the moisture of the skin, and should be prescribed individually for each person at the time of procedures.

2) It is known that when varicose veins expand, the reverse valves cannot fully fulfill their function, and therefore, in our view, the work of devices which perform one-site compression becomes ineffective because any action on the liquid is transmitted in both directions in the same way. So, in order to make the device effective in case of varicose veins is necessary to develop some mechanism replacing the operation of these valves.

To effectively change the action of venous valves, we decided to perform impulse feeding on a special scheme, the principle of which is based on multi-area wave extrusion of blood. Thus, even without the closure of venous valves, preservation of pre-compression does not allow displacement of venous blood in the reverse direction of the heart, which should significantly contribute to substantial acceleration of the flow of venous blood to the heart. To perform wave compressions, a "sleeve" was made with 4 pairs of electrodes, which are put along the limb where the voltage in rotation is given for a short time. The problem of impulse automation for long-term procedures was solved. After conducting theoretical research, we came to the conclusion that during breathing there is a compression of the muscles, and hence the veins, both in the chest and intraperitoneal organs. We came to the conclusion that the compression wave should be carried out during inspiration, and exhalation should take place in pauses between compressions, since it is during inspiration that favorable conditions for accelerating the blood flow through the veins occur [3].

[1]. Zlotnikov M.D., Venous System of Man // Brief Atlas. - 1947. - No. 2

[2]. Kutyina I.K., Orekhova E.M., Nesterov, N.I. Effects of Octagonal Transcranial Amplipulse-magnetotherapy on the State of Central Hemodynamics in Patients with Mild and Moderate Arterial Hypertension // Resorts, Physiotherapy and Exercise Therapy. -1997 -No. 6 - p. 9-11.

[3]. Pokrovsky V.M., Korotko G.F. Physiology of Human. - Chapter 7. - (Educational Literature for Students and Medical Universities) M.: Medicine 1997.

Transfiguration of the Properties of Water as a Solvent of the Products of Apitherapy

P. Vartik*, Yu. Myagchenko

Faculty of Physics, Taras Shevchenko National University of Kyiv, Ukraine

**Corresponding author: polinav19@ukr.net*

Bees create a protein that is included to honey, called defensin-1. It turned out that this protein can be used to treat burns and skin infections. Also, due to it, new drugs are being developed to combat antibiotic-resistant infections. The problem is the poor solubility of the products of apitherapy (propolis, wax moth) in water. So we tried to solve this problem.

Redox potential is a measure of the tendency of a chemical species to acquire from or lose electrons to an electrode and thereby be reduced or oxidised, respectively. Each species has its own intrinsic reduction potential; the more positive the potential, the greater the species affinity for electrons and tendency to be reduced. The measurement of redox potential is a common measurement for water quality.

We change the properties of water as a solvent - we convert water from Redox with the potential of "+ 200 mV" into water with Redox potential "- 600 mV". The method of comparing the efficiency of dissolution is the measurement of optical absorption spectra. While comparing absorption spectra of prepared and proprietary extracts, it was shown that the extraction efficiency is higher in a catholyte with value of redox potential - 650 mV and a temperature of 40 °C.

The extract prepared in a catholyte produced in an electrolyzer without diaphragm shows the best properties of extraction.

Our research opens the perspectives of finding new technologies for the extraction of flavonoids from hydrophobic substances.

Lasing of Rhodamine 6G in Waveguide Ultra-Thin Film

V.P. Yashchuk^{*1}, E.A. Tikhonov², G.M. Telbiz³, E.V. Leonenko³

¹ Physics Department, Taras Shevchenko National University of Kyiv, Ukraine

² Institute of Physics, NAS of Ukraine, Kyiv, Ukraine

³ L.V. Pisarzhevsky Institute of Physical Chemistry, NAS of Ukraine, Kyiv, Ukraine

Corresponding author: yavasil@ukr.net

Development of integrated optoelectronics needs light sources of minimum size. The most convenient for this purpose is a laser semiconductor diode, which uses waveguide lasing in a p - n junction layer with a thickness of 1 μm . But reduction of this thickness is difficult. Such possibility exists with usage of polymer film with lasing dyes which thickness may be much less. Although such laser needs external optical pumping but there are physical problems for which solution this is necessary or is not obstacle.

Fabrication of ultra-thin waveguide laser based on dyed polymer films requires solving two principal problems. The first one is ensuring of high concentration of molecules dyes to provide sufficient gain in the film without concentration quenching of luminescence. And the second one is to provide higher refractive index of the film to provide waveguide conditions at film/substrate interface. It is important because the indexes of classical polymers and glass substrates are nearly close.

The first problem has been solved by fabrication of hybrid polymer-inorganic mesostructured film with sol-gel technique. The fabricated film is dielectric matrix of about 200 nm thickness with nanopores of a diameter 12 nm, filled with dyed polymer solution. The film index is varied in the range 1.499–1.599 by changing of inorganic component and technological conditions. The second problem was solved by micelles formation in the nano-pores which prevent dye molecules aggregation that could reduce quantum yield of luminescence.

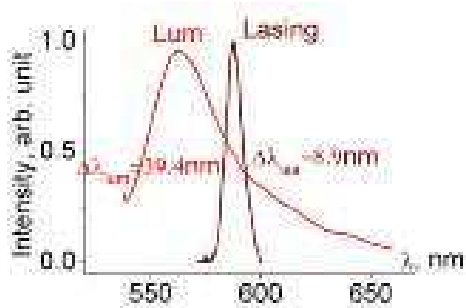


Fig. 1. Lasing and luminescence spectra of rhodamine 6G in hybrid nanoscale TiO_2 film.

Two films with SiO_2 and TiO_2 matrixes were fabricated and tested. Their radiation spectra were studied dependent on pump intensity (SH of YAG- Nd^{3+} Q-switched laser) focused on the strip $3 \times 0.5 \text{ mm}^2$. The SiO_2 film reveals regime of substrate radiative mode with radiation spectrum FWHM about 10 nm because proximity of the film and substrate indexes. The TiO_2 film with index $n=1.565$ forms the asymmetric waveguide with cut-off thickness of

180 nm and reveals waveguide lasing with radiation spectrum FWHM about 8.9 nm (Fig. 1). Threshold intensity of the lasing was about 0.4 MW/cm^2 , what is by order less than one of radiative mode in the first film.

General Regularities of Secondary Radiation of Dyes in Strong Scattering Media

V.P. Yashchuk^{*1}, E.A. Tikhonov², A.P. Smaliuk¹

¹ Physics Department, Taras Shevchenko National University of Kyiv, Ukraine

² Institute of Physics, NAS of Ukraine, Kyiv, Ukraine

**Corresponding author: yavasil@ukr.net*

In the presented work we have analyzed absorption (AS), luminescence (LS) and secondary radiation (SR) spectra of laser dyes in polymer vesicular films in dependence on dye concentration and on availability of multiple elastic scattering of light. These spectra were studied in dyed polymeric film of 15 mkm thickness in which multiple scattering may be produced by UV illumination that initiates formation of closely packed gaseous nitrogen vesicles of 1 mkm diameter. It was shown that dye concentration increase by two orders from 0.05 to 5 mM/l does not causes any changes of AS, that indicates absence of dye molecules aggregation. But the same change of the concentration causes strong spectral shift of LS which is strengthened by light multiple elastic scattering of vesicles (Fig. 1, spectra 3-5) due to boost of reemission of luminescence radiation in red wave region.

Under excitation intensity above 0.4 MW/cm^2 instead of luminescence secondary radiation arises which consist of random lasing (RL) and stimulated Raman scattering (SRS) at all Stokes lines which finding themselves in spectral range of RL. In concordance with this feature SR spectrum consist of continuous component of stimulated emission of RL and linear component of SRS. RL spectrum is localized in place of LS maximum in vesicular film.

SRS spectrum is localized within RL spectrum (Fig. 1, spectra 6, 7). SRS lines intensity is proportional to RL intensity at corresponding Stokes frequencies. So their intensity increases near RL spectrum maximum and decreases on its wings.

SRS lines do not arise beyond the RL spectrum. Therefore SRS lines observation needs manipulation with the film parameters (dye concentration and scattering efficiency) which shift RL spectrum towards to Stokes lines region or to change frequency of excitation radiation for shifting Stokes lines towards RL.

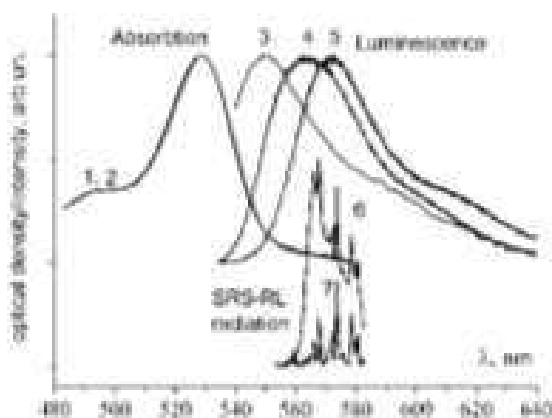


Fig. 1. Relative disposition of absorption (1), luminescence (3 – 5), SRS-RL (6) and it's SRS component (7). Shift of luminescence spectrum in dependence on dye concentration: 0.05 (3), 5 (4) mM/l, and on multiple scattering (vesicular film, 5 - mM/l)

Use of Water Catholytes to Reduce Environmental Load

L.E. Zhuk*, A.B. Hostieva*, Y.O. Myagchenko

Faculty of Physics, Taras Shevchenko National University of Kyiv, Kyiv, Ukraine

**Corresponding authors: lin.juck@gmail.com, gostevaanna0805@gmail.com*

For washing use substances that give water "alkaline" properties, that is, increase the pH and reduce the surface tension, that is, they increase the extraction of pollutants from tissues. Surfactants in these solutions, which enter the environment after washing, promote to the growth of blue-green algae. This leads to decrease in oxygen in water, which is necessary for aquatic organisms (fish, amphibians, etc.). We propose to find methods and devices that reduce the use of surfactants for washing by attracting catholytes instead of ordinary water. There can be two types of Catholics: "Ordinary" catholyte has a pH greater than 7. ORP - less than 0, mV (up to - "900 mV "Neutral" catholyte has a pH of 7. ORP - less than 0, mV (up to "-" 900 mV) To evaluate the efficiency of washing use spectrophotometric methods. We measured the transmission coefficients of light for solutions prepared in ordinary water and its catholytes using an RGB spectrometer. To do this, applied the same dyes on the same type of textile fabric. We prepare catholytes of various types and with different pH and ORP values. Than immersed the pre-painted tissue in a cuvette with ordinary water or in a cuvettes with different catholytes for a certain time (about 30 minutes). After that, we took the fabric from the cuvette and measured the light transmission coefficient for the colored solution in the cuvette. It is possible to measure the reflection coefficient of the light from the colored fabric before and after washing by RGB reflectometer. In this way, it is possible to compare the efficiency of washing in two ways: measuring the transmission of light after extraction of the dye in the solution, or measuring reflection of light from the tissue before and after washing.

- [1]. R..V. Kollar, V. Plichon. Spectrophotometric Determination of Phosphate// Anahtica Chimica acta.- 1970.-V.- 50.- p.- 457.
- [2]. Johnson K. S. Determination of Phosphate in Water // Anal. Chem.- 1982. – V. 54.- N. 7. - p. 1185.
- [3]. I.M. Piskaryov, N.A. Aristova, S.N. Tugolukov. "MIS-RT". - 2008. Issue № 46-2 (in Russian)

10
Index of Authors

A

Absanov, A. 38
Adamowicz, L. 30, 145, 165
Ahmadov, A.I. 189
Aleksandrov, M.A. 159
Amonov, A. 43
Androulidaki, M. 133, 143
Antonenko, O.I. 140
Arean, C.O. 11
Azhniuk, Yu.M. 64
Azovskyi, V. 207

B

Babiy, L.Yu. 104
Babkov, L.M. 66, 67
Babuka, T. 65
Babuka, T.Ya. 84
Babusca, D. 32, 33, 34, 160
Bairamova, D.B. 189
Balevicius, V. 105
Balijapalli, U.M. 52
Baran, J. 31, 66, 67, 75, 88, 96, 157
Barbash, V.A. 133
Baschenko, S. 208
Batyuk, L.V. 139
Bedarev, V.A. 62
Belykh, R. 49
Beregova, T.V. 152
Berest, V.P. 139
Berezovska, N.I. 142, 172, 178
Berezovskiy, M.M. 181
Bespalova, I. 134
Bezrodna, T.V. 66, 67, 71, 140, 157
Bezrodnyi, V.I. 140
Biliy, M.M. 201
Bliznjuk, O.N. 83, 141, 155
Blonskiy, I.V. 172, 178
Blonskyi, I. 58
Bobbink, F.D. 37
Bobrovnik, S.R. 106
Boiko, O. 95
Bondar, A.V. 89
Bondar, M.V. 12
Borodinova, T.I. 68
Borysiuk, V. 173
Boyko, V.V. 70

Bryndal, I. 57
Bublikova, K.I. 107
Buchatski, L.P. 112
Buchatsky, L.P. 152
Budianska, L.V. 103
Bugaychuk, S. 95
Bukivskii, A.P. 69, 89, 174
Bukivskii, P.M. 69, 174
Busko, T.O. 116

C

Calvez, L. 58
Charny, D.V. 159
Chechko, V.E. 27
Chegel, V.I. 116
Cheptea, C. 32
Chesnokov, E.D. 89
Chmeliov, J. 19
Choliy, Ya.V. 192
Chornii, V. 76
Chornii, V.P. 70
Chukova, O. 143, 163
Chumachenko, V. 156
Creanga, D. 160, 161
Curmei, N.D. 71

D

Dagys, L. 105
Datsenko, O.I. 175, 177
Davydova, N.A. 31
Demchenko, A.P. 13
Dementjev, A. 96, 108
Derhachov, M.P. 129
Dimitriu, D.G. 33, 34
Dmitrenko, O.P. 159
Dmitruk, I. 150
Dmitruk, I.M. 142, 172, 178
Dmytrenko, O.P. 116
Dmytruk, A. 58
Dmytruk, A.M. 142, 172, 178
Dorohoi, D. 161
Dorohoi, D.O. 32, 33, 34, 160
Doroshenko, I. 35, 42, 50, 51
Doroshenko, I.Yu. 196
Doroshenko, O. 35
Dotsenko, I.S. 201
Dovbeshko, G. 108, 158

Dovbeshko, G.I. 14, 119
Drigo, N. 37
Drozd, M. 31, 57, 75, 88, 96, 157
Dubey, I.Ya. 113, 122
Dubey, L.V. 122
Dubovik, O. 76
Dyson, P.J. 37
Dzhagan, V. 63

E

Eglitis, R. 72
Ermakov, V.N. 130, 144
Eshchanov, B. 36

F

Fakharuddin, A. 19
Fang, X. 37
Fediv, V.I. 121
Fei, Zh. 37
Fesenko, O.M. 182
Fesych, I.V. 174
Firsunin, S.N. 66
Franckevičius, M. 19, 176
Franckevicius, M. 37
Frigeri, P. 175, 177

G

Gabrusenoks, J. 72
Gamernyk, R.V. 69
Gavrilko, T. 96, 162
Gavrilko, T.A. 66, 67, 75, 88
Gegevičius, R. 19, 176
Gerasov, A.O. 44
Gerwert, K. 209
Gilinsky, A.M. 80
Glamazda, A.Yu. 122, 145
Glukhov, K. 60
Glukhov, K.E. 65, 84
Gnatchenko, S.L. 84
Gnatenko, Yu.P. 69, 89, 174
Gnatyuk, I. 96
Gnatyuk, I.I. 75, 88
Gnatyuk, O. 108
Gnatyuk, O.P. 14, 119
Golovynska, I. 175, 177
Golovynskiy, S. 175, 177
Golub, P. 93

Gomenyuk, O.V. 70
Gomonnai, O.O. 65
Gomory, A. 124
Gorban, Ya.K. 28
Gorkavenko, T.V. 73, 74
Goryuk, A.A. 99
Gotsulskiy, V.Ya. 27
Grančič, B. 87
Grazulevicius, J.V. 15, 52
Grechnev, G.E. 81
Großerüschkamp, F. 209
Grybauskaitė-Kaminskiene, G. 15
Grygorova, G.V. 109
Gubanov, V.O. 201
Gudim, I.A. 62
Gulbinas, V. 19, 37, 176
Gule, E.G. 121, 147
Gumenyuk, Ya.O. 114
Gunko, E. 209
Gutowska, M.U. 62

H

Haftel, M. 167
Hagan, D.J. 12
Hamamda, S. 133
Hanulia, T. 158
Hanulia, T.O. 119
Harahuts, I.I. 138
Harahuts, Iu. 156
Havryliuk, Ye. 63
Hizhnyi, Yu. 76, 173
Hizhnyi, Yu.A. 70
Holovina, N.A. 75
Honcharov, V.V. 179, 180
Hostieva, A.B. 216
Hrabovsky, E.S. 178
Hreb, V.M. 81
Huang, Zh. 37
Hubenko, K. 137
Hubenko, K.A. 146
Hushcha, T.O. 110

I

Ilchyshyn, I.P. 97
Isaieva, O.F. 121, 147
Ivaniuk, K. 15
Ivanov, A.Yu. 30
Ivanov, V.V. 191, 193

Ivashchenko, L.A. 182
Ivashchenko, V.I. 182

J

Jasiunas, R. 37
Juhymchyk, V. 136
Jumabaev, A. 38

K

Kachkovsky, O.D. 44
Kadan, V.M. 58
Kadashchuk, A. 16, 19
Kalugin, O.N. 191
Kamenskyi, D. 77
Kamenskyi, D.L. 78
Kanyuk, M.I. 116
Karachevtseva, A.V. 45
Karachevtsev, M.V. 131, 145, 148
Karachevtsev, V.A. 122, 131, 132,
145, 148, 165, 168
Karbivska, L.I. 149, 164
Karbivskyy, V.L. 149, 164
Karpicz, R. 96, 108
Karpova, O. 36
Kasian, N.A. 103
Kavok, N.S. 146
Kerita, O. 118
Kernazhitsky, L. 162
Keruckas, J. 15
Keruckiene, R. 15
Khalyavka, T. 162
Khalyavka, T.A. 154
Kharkhalis, L.Yu. 65
Khodakovskiy, V. 208
Khomenko, D.M. 203
Khropost, D. 39
Khrustalyov, V. 77
Kinder, M.M. 67
Klimavicius, V. 105
Klimenko, I.M. 107
Klimin, S.A. 79, 80, 90
Klishevich, G.V. 71, 157
Klochkov, V.K. 94, 109, 146
Knize, R.J. 167
Kobets, M.I. 62
Kobzar, I.P. 81
Kobzar, Ya. 115
Kohler, A. 209
Kohutych, A. 60
Kokhan, O.P. 64
Kolesnik, D. 108

Kolodka, R.S. 150
Konstantinov, V.A. 45
Korenyuk, P. 58
Kornienko, N.E. 28, 40, 190
Korniienko, O.N. 28, 190
Korniychuk, P. 98
Korolyuk, O.A. 59
Korotkova, I.V. 210
Kostetskyi, A.O. 111
Kosyanchuk, L.F. 140
Kovalchuk, A. 115
Kovalchuk, A.O. 121
Kovalenko, S.N. 191
Kovalevsky, A.V. 81
Kovaliuk, Z.D. 69
Kozachenko, V.V. 167
Kozak, A.O. 182
Kozhushko, G.M. 210
Kramar, V.M. 153
Kravchenko, V.M. 112, 113, 152
Kravets, V.G. 68
Kreminska, Yu.S. 113
Krivchikov, A.I. 59
Kruchinin, S.P. 194
Kryvoruchko, A.O. 180
Kryvoruchko, S.O. 180
Kudrya, V.Yu. 113, 114
Kuiliiev, B. 42
Kukhta, N. 15
Kulish, M.P. 116, 159
Kurioz, Yu. 98, 115
Kurnosov, N.V. 132, 168
Kushnirenko, V.I. 53
Kúš, P. 87
Kutko, K. 77
Kutko, K.V. 78
Kutsevol, N. 156
Kutsevol, N.V. 138, 151

L

Lampeka, R.D. 203
Lanova, M.A. 191
Lebedyeva, I.V. 23
Leitonas, K. 52
Lendel, V.V. 174, 186
Len, T. 166
Leonenko, E. 136
Leonenko, E.V. 214
Lesiuk, A.I. 116
Li, Baikui 175, 177
Lisetski, L.N. 17, 94, 103
Lis, T. 57

Litvinchuk, A. 63
 Liubachko, V. 60
 Lochbrunner, S. 135
 Loiseau, P. 79
 Lopatynskyi, A.M. 116
 Losytskyi, M.Yu. 23, 152
 Ludemann, M. 65
 Lutsiuk, Yu.V. 153
 Lutsyk, P.M. 111
 Lyogenkaya, A.A. 81
 Lysiuk, V.O. 82

M

Makarets, M.V. 192
 Makhlaichuk, V.N. 41
 Makhniy, V.P. 181
 Makowska-Janusik, M. 84
 Maksimchuk, P. 134
 Maksimchuk, P.O. 94, 137, 146
 Malevich, A.E. 29, 196
 Malin, T.V. 80
 Malomuzh, N.P. 27
 Malyukin, Yu. 134
 Malyukin, Yu.V. 109, 135, 137, 146
 Manuilov, E.V. 154
 Manzharova, V.S. 182
 Marchenko, A.A. 18
 Marchenko, L. 208
 Masalitina, N.Yu. 83, 141, 155
 Matsnev, I. 208
 Matzui, L. 166
 Mazur, N. 63
 Mchedlov-Petrosyan, N.O. 46
 Melnichenko, L.Yu. 186
 Melnichenko, M.M. 183
 Melnik, V.I. 71
 Melnyk, R.M. 194
 Melnyk, V.I. 157
 Melnyk, V.V. 181
 Mely, Y. 114
 Mensi, M. 37
 Merenkov, D.N. 62
 Meyliev, L. 42
 Mikhailenko, V.I. 99
 Minenko, S.S. 94
 Mishchenko, O.M. 172
 Moiseienko, V.N. 61

Morosanu, A.C. 32, 33, 34
 Morosanu, C. 161
 Mukhamedov, G. 36
 Murodov, G. 38, 43
 Myagchenko, Y. 39
 Myagchenko, Y.O. 107, 216
 Myagchenko, Yu. 213

N

Nadtoka, O.M. 151
 Naumenko, A. 156
 Naumenko, A.P. 44, 113, 114, 138, 151, 167, 201
 Naumova, D. 166
 Naumov, V. 162
 Naumov, V.V. 147
 Navozenko, O.M. 23
 Nazarenko, V. 115
 Nazeeruddin, M.K. 37
 Nedilko, S. 76, 173
 Nedilko, S.A. 143, 163
 Nedilko, S.G. 70, 133, 143, 163, 171
 Negriyko, A. 208
 Negriyko, A.M. 140
 Negrutska, V.V. 113
 Nesprava, V.V. 71, 140, 157
 Nesterenko, N.M. 78
 Nikolaieva, D.Y. 179
 Nikolenko, A. 158
 Novikova, N.N. 80
 Novikov, R. 49
 Nurmurodova, G. 43

O

Odarych, V.A. 184
 O'Donnell, R.M. 12
 Ogurtsov, A.N. 83, 141, 155
 Ohienko, O.V. 61
 Oleaga, A. 60
 Oleksienko, M. 39
 Olenchuk, M. 158
 Onanko, A.P. 159
 Onanko, Y.A. 159
 Orlovskaya, S.G. 185
 Ostapenko, N. 118
 Ostapenko, Yu. 118

Ostyakov, A.A. 29
Otajonov, Sh. 36
Ovcharenko, O.I. 89
Ovechko, V.S. 195
Ovsiienko, I. 166

P

Panfilov, A.S. 81
Papadopoulos, A. 133, 143
Pashayev, F.G. 189
Pashazadeh, R. 15
Pashchenko, V.O. 81
Pashynska, V.A. 124
Pathak, M. 52
Pavlenko, O.L. 40, 116
Pavlova, S. 58
Pavlov, I. 58
Perederii, O. 158
Permyakov, V.V. 154
Peschanskii, A.V. 84, 85
Pestsov, O. 49
Petersen, D. 209
Petranovski, V. 49
Pinchuk, A.O. 167
Pinchuk-Rugal, T.M. 116, 159
Piryatinski, Yu.P. 23, 111, 174
Piskach, L. 63
Pitsevich, G.A. 29, 196
Plokhotnichenko, A.M. 131, 145
Plyushchay, I.V. 73, 74
Plyushchay, O.I. 73
Podolska, V.I. 144
Pogodin, A. 60
Pogodin, A.I. 64, 87
Pogorelov, V. 51
Pogorelov, V.E. 196
Pogorielov, M.V. 172
Polovyi, I. 14, 108
Polovyi, I.O. 119
Ponezha, E.A. 31, 130
Ponomarov, V.K. 46
Poperenko, L.V. 184
Poperezhai, S. 77
Poperezhai, S.M. 78
Poperezhai, S.N. 62
Popescu, L. 160, 161
Popovskii, A.Yu. 99

Porada, O.K. 182
Posudievsky, O. 108
Pryhodiuk, O.A. 206
Pundyk, I.P. 116
Purans, J. 72
Pyaskovskaya, O. 108

Q

Qu, Junle 175, 177

R

Ramsay, A.J. 150
Rashevskaya, A.M. 120
Ratajczak, H. 57
Repetsky, S.P. 194
Revo, S.L. 133
Revyakin, V.P. 45
Reznichenko, V.Ya. 31
Roldán-Carmona, C. 37
Ropakova, I.Yu. 135
Roshchin, O.M. 140, 157
Roshchyn, O.M. 71
Rozouvan, S. 86
Rozouvan, S.G. 82
Rudko, G.Yu. 20, 121, 147
Rud, Yu.P. 112
Rusakova, N.V. 203
Rutkauskas, D. 202
Ryazanova, O.A. 122, 123
Rybak, A. 58

S

Sabov, M.M. 201
Sacarescu, L. 160
Sagan, V.V. 45
Sakhno, T.V. 210
Salazar, A. 60
Samoilov, A.N. 94
Sathiyarayanan, K. 52
Savchenko, D.A. 164
Scherbatskii, V.P. 133
Scrynsky, P.L. 182
Semenov, A.A. 210
Seminko, V. 134
Seravalli, L. 175, 177
Sereda, O.S. 107
Shapovalov, S.A. 46, 47
Sharifov, G. 38

Shaykevych, I.A. 186
 Shcherbakov, O.B. 152
 Shcherbakov, S.N. 154
 Shcherban, N. 96, 162
 Shcherban, N.D. 75, 88, 154
 Shekera, O. 115
 Sheludko, V.I. 70
 Shelyapina, M. 49
 Shevchenko, V. 115
 Shi, J. 12
 Shmeleva, L.V. 197
 Shpotyuk, O. 58
 Shymanovska, V. 162
 Shymanovska, V.V. 147, 154
 Siesler, H.W. 21
 Simokaitiene, J. 15, 52
 Sizhuk, A.S. 211
 Skakun, V. 209
 Sklyarchuk, V.M. 181
 Skuodis, E. 15
 Slepets, A. 143, 163
 Slobodyanyk, M.S. 70
 Slominskii, Yu.L. 167
 Slyotov, M.M. 181
 Smaliuk, A.P. 215
 Smola, S.S. 203
 Smolyak, S.S. 149, 164
 Snegir, S.V. 68
 Solheim, J.H. 209
 Solyanik, G. 108
 Sorokin, A.V. 135
 Sorokin, V.A. 125
 Stakhira, P. 15
 Stanovyi, O.P. 172
 Stashchuk, V. 86
 Stashchuk, V.S. 82
 Stepanenko, Ye.Yu. 112
 Stepanian, S.G. 30, 124, 145, 165
 Stepianiuk, D.S. 191
 Stratakis, E. 143
 Stryganyuk, G.B. 69
 Studenyak, I.P. 64, 87
 Studenyak, V.I. 87
 Stukalenko, V. 86
 Stukalenko, V.V. 82
 Styopkin, V. 95
 Styopkin, V.I. 68, 88
 Sugakov, V. 118
 Suprun, A.D. 197
 Svechnikova, O.S. 106
 Svezhentsova, K.V. 183
 Syetov, Y. 48

Syvolozhskiy, O. 166
 Szewczyk, A. 62

T

Tarakhan, L. 95
 Telbiz, G. 136
 Telbiz, G.M. 214
 Terebilenko, K.V. 70
 Terentieva, J.G. 120
 Terentyev, M.A. 212
 Teselko, P. 35
 Teselko, P.O. 133
 Thiyagarajan, M.D. 52
 Tikhonov, E.A. 97, 214, 215
 Tkachenko, I. 115
 Tofighi, S. 12
 Tokhadze, K.G. 43
 Tomchuk, A.V. 167
 Tomila, T.V. 182
 Tomkeviciene, A. 15
 Treideris, M. 176
 Tress, W. 19
 Trevisi, G. 175, 177
 Trostyanko, P.V. 191
 Tsyganenko, A. 49
 Tupitsyna, I. 76

U

Ulberg, Z.R. 144
 Usenko, E.L. 125

V

Valakh, M.Ya. 63
 Valeev, V.A. 125, 131
 Valkunas, L. 22
 Van Stryland, E.W. 12
 Vartik, P. 213
 Vashchenko, O.V. 103
 Vashchuk, D. 50
 Vasnetsov, M. 93
 Vasylechko, L.O. 81
 Vasylieva, A. 35, 50, 51
 Verbitsky, A.B. 111
 Vergun, L.Yu. 104, 106, 117, 204
 Vertegel, I.G. 89
 Vertegel, I.I. 89
 Vialtseva, A.A. 117
 Viduta, L. 95
 Viduta, L.V. 67
 Vikhrova, Y.A. 142
 Virych, P.A. 151
 Voitenko, T. 143, 163

Volnyanskij, M.D. 61
Voloshin, I.M. 122, 123, 168
Volyniuk, D. 15, 52
Vyshyvana, I.G. 194
Vysochanskii, Yu. 60
Vysochanskii, Yu.M. 84

W

Wolter, S. 135

X

Xia, R. 37
Xushvaktov, H.A. 38

Y

Yakovlev, V.A. 80
Yakubovskaya, G. 76
Yaremko, A.M. 121
Yashchenko, O.V. 133
Yashchuk, V. 207
Yashchuk, V.M. 23, 112, 114, 152
Yashchuk, V.P. 205, 206, 214, 215

Yaskovets, A.O. 140
Yefimova, S.L. 109, 135, 137, 146
Yeshchenko, O.A. 138, 167
Yukhymchuk, V. 63
Yurgelevych, I.V. 184

Z

Zabashta, Yu.F. 104, 117
Zahn, D.R.T. 64, 65
Zajarniuk, T. 62
Zakharchenko, B.V. 203
Zakharov, A.B. 193
Zaręba, J. 57
Zashivailo, T.V. 53
Zavalij, P.Y. 12
Zazhigalov, V.O. 179, 180
Zhao, P. 12
Zhuk, L.E. 216
Zhuravlev, K.S. 80
Zozulya, V.N. 123
Zuravskyi, M.V. 206
Zuy, O.N. 185
Zvyagin, A.A. 62